Proceedings of the I·R·E

A Journal of Communications and Electronic Engineering

(Including the WAVES AND ELECTRONS Section)

July, 1949

Volume 37 Number 7

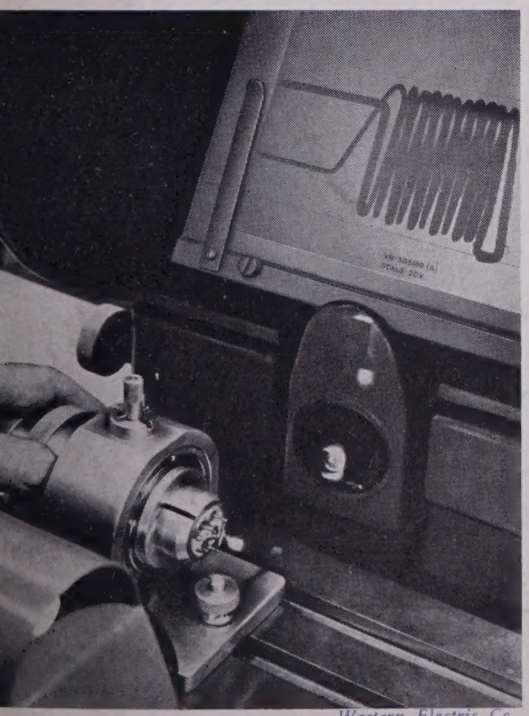

Western Electric Co.

"OPTICAL MICROMETER" FOR MICROWAVE TUBES

lio-relay systems utilize transmitting tubes of high precision trolled by observation of optical enlargements of tube ts.

PROCEEDINGS OF THE I.R.E.

Waves and Electrons Section

TABLE OF CONTENTS FOLLOWS PAGE 32A

The Institute of Radio Engineers

If your reserve tube is ready for active service in your THERMONIC equipment . . . it will pay you to put another tube on your shelf . . . the tube designed to our specifications, for your THERMONIC UNIT . . .

because we have been keeping an accurate check on tube performance life . . . and find that even though the manufacturer guarantees a minimum of 1,000 hours of operating life . . .

WE can safely extend that guarantee to **1500 HOURS!**

at a new LOWER PRICE!

. . . by purchasing your THERMONIC tube replacement through us, you now can be assured of

50% more

for your "efficient operation" dollar.

THER-MONIC
INDUCTION HEATING CORP. N.Y. U.S.A.

INDUCTION HEATING CORPORATION
181 WYTHE AVENUE • BROOKLYN 11, N. Y.

. . . More People Find That They Get MORE out of AMPEREX Electronic Tubes . . . Whatever the Application—it Will Pay You to . . .

Re-tube with AMPEREX

AMPEREX ELECTRONIC CORP.
25 WASHINGTON STREET, BROOKLYN 1, N. Y.
In Canada and Newfoundland: Rogers Majestic Limited

PROCEEDINGS OF THE I.R.E.

(Including the WAVES AND ELECTRONS Section)

Published Monthly by

The Institute of Radio Engineers, Inc.

VOLUME 37 — *July, 1949* — NUMBER 7

PROCEEDINGS OF THE I.R.E.

INSTITUTE NEWS AND RADIO NOTES SECTION

WAVES AND ELECTRONS SECTION

Responsibility for the contents of papers published in the PROCEEDINGS OF THE I.R.E. rests upon the authors. Statements made in papers are not binding on the Institute or its members.

Changes of address (with advance notice of fifteen days) and communications regarding subscriptions and payments should be mailed to the Secretary of the Institute, at 450 Ahnaip St., Menasha, Wisconsin, or 1 East 79 Street, New York 21, N. Y.

† Deceased

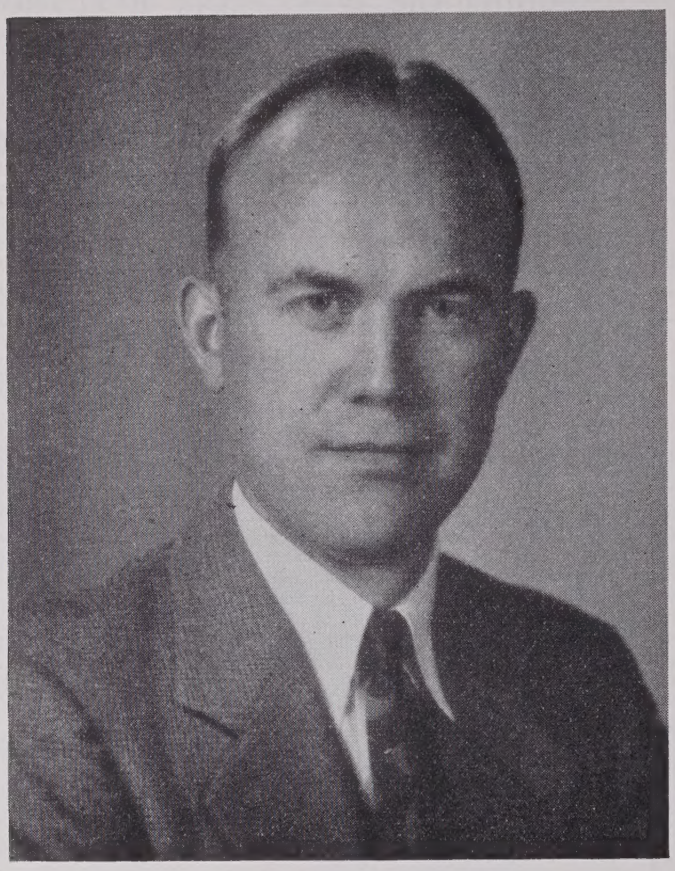

Murray G. Crosby

BOARD OF DIRECTORS, 1947–1949

Murray G. Crosby was born at Elroy, Wisconsin, in 1903. He received the B.S. degree from the University of Wisconsin in 1927, having joined the IRE as an Associate in 1925. In the latter year he became research engineer for the communications division of the RCA Laboratories, and there he specialized in frequency and phase modulation and point-to-point reception. He has written a number of technical articles in those fields, and has been issued 150 patents.

Mr. Crosby was transferred to IRE Member Grade in 1938, and two years later was awarded the Modern Pioneer Award from the National Association of Manufacturers for contributions which improved the American standard of living. Receiving the professional electrical engineering degree from the University of Wisconsin in 1943, he became a Senior Member of the Institute and subsequently was made a Fellow that same year for his "contributions to the development of high-frequency radio communications." In 1943 and 1944, while still associated with RCA, he served as expert technical consultant to the Secretary of War, and he also served on Panel Number One of the Radio Technical Planning Board.

Mr. Crosby left RCA in 1944, and joined the Paul Godley Co., consulting radio engineers, in 1945. Three years later he opened his own firm, Crosby Laboratories, in Mineola, Long Island, N. Y.

Mr. Crosby has been a member of a number of Institute Committees. Currently he is a member of the Executive, Policy Development, Editorial Administrative, Modulation Systems, and Standards Committees, as well as the Board of Editors; and Chairman of the IRE-RMA Problem Number Two Committee. He is on the Executive Committee of the Long Island Subsection. A fellow of the Radio Club of America, he is also a member of the AIEE.

An apparent fairy tale might be written, beginning: "Once upon a time, a group of farseeing engineers, scientists, teachers, and authors decided to form their own society having as its aim the advancement of the new wonder-art: radio. They planned to present in their meetings and journal not only thoughts of the moment, but guiding inspirations for the future."

And now a great pioneer and leader in radio and electronics has written the following guest editorial which adds to this tale almost these concluding words: "Fate smiled on their efforts. Their labors were crowned with unparalleled success, and they and their industry lived happily ever after."

But even if their happiness be clouded occasionally by doubt or confusion, they can still gain comfort, and mayhap some pride, from the thought that, in all essentials, they and their Institute have labored mightily and contributed essentially to the welfare of humanity.—*The Editor.*

Buried Treasure

W. C. WHITE

Recently I had occasion to refer to volume 2, 1914, of the PROCEEDINGS OF THE I.R.E. The reference completed, I found it fascinating to thumb through the papers in that volume. Without spending too many minutes, I found a number of statements therein which were quite prophetic, and would at that time have made a good starting point for a research or development that later turned out to have considerable interest and value. In deForest's paper on the audion, for instance, mention was made of the whistling sound on the telephone receiver connected in the plate circuit under certain conditions and, in the lively discussion that followed the meeting, there were some surmises as to the cause. In the same paper, mention was made of the luminous streaks in the audion bulb that varied with the signal, allowing one to read by eye the message received. There is also in that paper the suggestion that a vacuum tube as an amplifier could be operated right next to a microphone for certain possible applications. Some of our modern electronic devices now utilize certain of the ideas expressed, and they might have been arrived at earlier and by a different engineer, if work had been started on them soon after this paper was published.

In the same volume, a paper by John Stone Stone described the use of a cathode-ray tube for measurement work at radio frequencies. Apparently, however, its usefulness as a tool in the radio field was not appreciated until many years later.

Some material in the same volume intrigued me as possibly showing the beckoning finger of opportunity even today. There was, for instance, the paper on "The Influence of Alternating Currents on Certain Melted Metallic Salts." It described some experiments and results that appeared to its author to be mysterious. It is possible that even today the ideas expressed might represent the starting point for a profitable piece of research.

In volume 3, Dr. Alfred N. Goldsmith contributed a paper on various types of frequency changers having possible usefulness in the radio field and, to my surprise, found, even at that early date, that one of them was an electronic method.

Early descriptions of unexpected experimental results or chance observations may sometimes be explained by modern concepts. Also, new methods and new materials may enable a skilled engineer to produce a useful result therefrom.

Of course, our PROCEEDINGS over the years represent a tremendous accumulation of information in the radio and electronics field, and radio engineers are constantly digging into this mine of information for specific aids for some of their problems. Just to browse through some of the early volumes, however, is a most interesting experience, and, if followed up, may well reveal a "treasure" of considerable interest and value.

Electrical Network Analyzers for the Solution of Electromagnetic Field Problems*

K. SPANGENBERG†, FELLOW, IRE, G. WALTERS‡, STUDENT MEMBER, IRE, AND F. SCHOTT§, ASSOCIATE, IRE

Part I
THEORY, DESIGN AND CONSTRUCTION

Summary—**This is the first part of a paper on the design, construction, and operation of electrical network analyzers capable of obtaining solutions of the wave equation. There is discussed herein the design and construction of two network analyzers for solving the wave equation in both two-dimensional, axially symmetric, cylindrical co-ordinates and rectangular co-ordinates. The various design parameters are discussed and suitable solutions presented.**

I. Introduction

THIS PAPER will describe the design, construction, and testing of two network analyzers especially constructed to solve the wave equation and thus obtain the solution of various electromagnetic field problems.

It is well known that certain analogues may be used for the solution of differential equations. One of the best known analogues is the electrolytic tank, which provides solutions of the Laplace equation. It is also possible to construct electrical networks which will give solutions of the wave equation. An intimation of this was given in an early paper by Alford[1] but the complete details of this analogue were first enunciated by Kron and colleagues.[2–6]

The general principle involved is that solutions of ordinary and partial linear differential equations are closely approximated by solutions of corresponding difference equations which, in turn, have the same solution as the voltages and currents in properly constructed networks. In this paper there will be considered only the case of the wave equation in two-dimensional axially symmetric, cylindrical co-ordinates and rectangular co-ordinates. The networks to be described bear the same relation to the wave equation that the electrolytic tank bears to the Laplace equation.

II. General Theory

A. General Two-Dimensional Network Relations

In Fig. 1 is shown a two-dimensional electrical network. This network is two-dimensional in the sense that it will support the propagation of waves in two distinct co-ordinate directions. Essentially this network consists of two sets of interconnected artificial transmission lines made up of pi sections comprising series inductances and shunt capacitances. Waves may propagate in two component directions on such a network and thus be propagated at any angle. The particular network shown is represented as being in two-dimensional cylindrical co-ordinates, but the resulting network relations will be equally valid for two-dimensional rectangular co-ordinates if r is replaced by x and z is replaced by y.

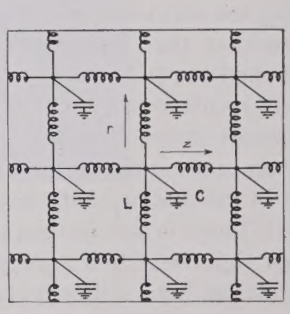

Fig. 1—General network configuration and notation.

The Kirchhoff's law relations for the network of Fig. 1 are approximately as follows:

$$\frac{\partial I_r}{\partial r} + \frac{\partial I_z}{\partial z} = - Y_\phi V_\phi \qquad (1)$$

$$\frac{\partial V_\phi}{\partial r} = - I_r Z_r \qquad (2)$$

$$\frac{\partial V_\phi}{\partial z} = - I_z Z_z. \qquad (3)$$

* Decimal classification: R143. Original manuscript received by the Institute, October 19, 1948; revised manuscript received, February 2, 1949. Presented, 1948 IRE National Convention, New York, N. Y., March 25, 1948. This paper reports work on a program sponsored by the Office of Naval Research under Contract N6onr-251, Task Order 7.

† Office of Naval Research, Washington, D. C.
‡ Dalmo Victor Co., San Carlos, Calif.
§ University of California, Los Angeles, Calif.

[1] A. Alford, "A method for calculating transmission properties of electrical networks consisting of a number of sections," PROC. I.R.E., vol. 21, pp. 1210–1220; August, 1933.
[2] G. Kron, "Numerical solution of ordinary and partial differential equations by means of equivalent circuits," *Jour. Appl. Phys.*, vol. 16, pp. 172–186; March, 1945.
[3] J. R. Whinnery and S. Ramo, "A new approach to the solution of high-frequency field problems," PROC. I.R.E., vol. 32, pp. 284–288; May, 1944.
[4] G. Kron, "Equivalent circuit of the field equations of Maxwell," PROC. I.R.E., vol. 32, pp. 289–299; May, 1944.
[5] J. R. Whinnery, C. Concordia, W. Ridgway, and G. Kron, "Network analyzers studies of electromagnetic cavity resonators," PROC. I.R.E., vol. 32, pp. 360–367; June, 1944.
[6] G. Kron, "Electric circuit models of partial differential equations," *Elec. Eng.*, vol. 67, pp. 672–684; July, 1948.

In the above equations, the symbols used have the following significance:

I_r = current in a radial element
I_z = current in a longitudinal element
V_ϕ = voltage across a shunt element, i.e., between a lattice junction and the ground plane
Z_r = impedance per unit length of a radial element in the $r-z$ lattice
Z_z = impedance per unit length of a longitudinal element in the $r-z$ lattice
Y_ϕ = shunt admittance per unit area.

B. Cylindrical Network-Field Relations

The general curl equations of Maxwell have the form

$$\text{curl } \overline{H} = \epsilon \frac{\partial \overline{E}}{\partial t} = j\omega E\epsilon \tag{4}$$

and

$$\text{curl } \overline{E} = -\mu \frac{\partial \overline{H}}{\partial t} = -j\omega H\mu \tag{5}$$

where all of the vector field components are assumed to have a time factor of the form $\epsilon^{j\omega t}$.

The corresponding components of the curl equations of Maxwell for a TM wave having only a ϕ component of magnetic field and no variation of any field component in the ϕ direction, i.e., $H_r=0$, $H_z=0$, $E_\phi=0$, are

$$\frac{\partial E_r}{\partial z} - \frac{\partial E_z}{\partial r} = \frac{-j\omega\mu}{r}(rH_\phi) \tag{6}$$

$$\frac{\partial (rH_\phi)}{\partial z} = -j\omega\epsilon r E_r \tag{7}$$

$$\frac{\partial (rH_\phi)}{\partial r} = j\omega\epsilon r E_z \tag{8}$$

in which the symbols have the usual significance for rationalized mks units.

From a comparison of the two sets of equations above, Table I shows the correspondence which is seen to exist between network and field quantities. The relations in Table I are valid for TEM and TM_0 waves only for problems in cylindrical co-ordinates having radial and axial variations of field only.

TABLE I
FIELD-NETWORK RELATIONS FOR CYLINDRICAL TM_0 AND TEM MODES

Field	*Network*
E_r	I_z
$-E_z$	I_r
rH_ϕ	V_ϕ
$j\omega\epsilon_r$	$Z_r=j\omega L$
$j\omega\epsilon_r$	$Z_z=j\omega L$
$\frac{j\omega\mu}{r}$	$Y_\phi=j\omega C$

Examination of the network-field relations for TM modes show that the radial and longitudinal series impedances are positive reactances whose magnitudes increase directly with frequency and radius. This indicates that the radial and longitudinal series-circuit elements are appropriately inductances which must increase linearly with the radius. Similarly, the shunt-circuit elements are capacitances whose magnitude varies inversely with the radial distance. This particular case, the one most commonly used with cylindrical co-ordinates, exhibits an inversion in the network-field analogy in that a magnetic field is represented by a voltage whereas an electric field is represented by a current.

For TE_0 modes in two-dimensional, axially symmetric, cylindrical co-ordinates, the correspondence between network and field quantities shown in Table II

TABLE II
FIELD-NETWORK RELATIONS FOR CYLINDRICAL TE_0 MODES

Field	*Network*
$-H_r$	I_z
H_z	I_r
rH_ϕ	V_ϕ
$j\omega\mu_r$	$Z_r=j\omega L$
$j\omega\mu_r$	$Z_z=j\omega L$
$\frac{j\omega\epsilon}{r}$	$Y_\phi=j\omega C$

holds. Here the analogy is direct; a magnetic-field component is represented by a current, an electric-field component by a voltage. It will be noted that, again, the required network elements are reactances, the series values having values directly proportional to frequency and to radial distance, whereas the shunt values are inversely proportional to frequency and directly proportional to radius. These conditions are easily met by using, for the series elements, inductances which increase with radius and, for the shunt elements, capacitances which vary inversely with the radius.

C. Rectangular Network-Field Relations

If one now writes the field curl equations for a two-dimensional rectangular TE mode, i.e., for $E_z=0$, $H_x=0$, $H_y=0$, the equations have the form:

$$\frac{\partial E_y}{\partial x} - \frac{\partial E_x}{\partial y} = -j\omega\mu H_z \tag{9}$$

$$\frac{\partial H_z}{\partial x} = -j\omega\epsilon E_y \tag{10}$$

$$\frac{\partial H_z}{\partial y} = j\omega\epsilon E_x. \tag{11}$$

When these equations are compared with the network equations (1), (2), and (3), with r replaced by x, and z replaced by y, it is seen that the network-field relations exist as shown in Table III. Here it is seen that the electric-field components are represented by current, and that the magnetic-field components are represented by voltages. It is also seen that the series elements may be

TABLE III
FIELD-NETWORK RELATIONS FOR RECTANGULAR *TE* MODES

Field	*Network*
E_y	I_x
$-E_x$	I_y
H_z	V_z
$j\omega\epsilon$	$Z_x=j\omega L$
$j\omega\epsilon$	$Z_y=j\omega L$
$j\omega\mu$	$Y_z=j\omega C$

inductances of constant value throughout the network, whereas the shunt elements may be capacitances, likewise of constant value throughout the network. This is the analogy which is used to represent the cutoff field in the cross section of an odd-shaped waveguide. The designations *TE* and *TM* for rectangular field problems as applied to resonators is somewhat arbitrary depending upon how the resonator is observed.

For *TM* modes in two-dimensional rectangular coordinates, the field-network relations are as shown in Table IV. The analogy in this case is seen to be direct,

TABLE IV
FIELD-NETWORK RELATIONS FOR RECTANGULAR *TM* MODES

Field	*Network*
H_x	I_y
$-H_y$	I_x
E_z	V_z
$j\omega\mu$	$Z_x=j\omega L$
$j\omega\mu$	$Z_y=j\omega L$
$j\omega\epsilon$	$Y_z=j\omega C$

in that electric-field components are represented by voltages, and magnetic-field components are represented by currents. Again, in this case, the proper network elements are inductances everywhere equal for the series elements, and capacitances everywhere equal for the shunt elements. This is the analogy used to study waveguide resonators with parallel upper and lower planes.

III. DESIGN CONSIDERATIONS

A. Two-Dimensional, Cylindrical-Co-ordinate Network

1. LC Product. A basic relation that is involved in all of the equivalent networks is

$$f_n = \frac{1}{N_\lambda \sqrt{LC}} \tag{12}$$

where

L = inductance per section at any point in the network
C = capacitance per section at a corresponding point in the network
f_n = network operating frequency
N_λ = number of elements per wavelength.

Actually, this is the low-frequency velocity relation for the equivalent filter made up of the tandem connection of the pi sections. If the cutoff frequency of the pi section is made sufficiently high relative to the operating frequency, the velocity will be substantially constant in the operating range.

2. Frequency of Operation. The selection of the operating frequency is an important one. For purposes of measurement, it would be desirable to have the operating frequency as low as possible. This would make possible the use of ordinary measuring instruments. However, a low operating frequency requires a large LC product, which, in turn, requires large values of inductance and capacitance. Large values of inductance are undesirable because in general, they have a low Q and a large bulk. Likewise, large capacitances are undesirable because of their bulk and difficulty of adjustment. From the standpoint of having network elements of convenient size, it would be desirable to operate at radio frequencies, where the inductances and capacitances could be quite small. However, operation at high radio frequencies is undesirable from the standpoint that an open network would radiate, and the coupling between elements would be quite high. Accordingly, a compromise between these requirements was made, and, in the network built at Stanford, operating frequencies in the range of 20 to 300 kc were selected. This range of operating frequencies has turned out to be a very desirable one. Stray field effects are just beginning to appear at the upper end of this frequency band, and yet the frequencies are high enough so that the circuit elements are reasonably small. At the same time, the operating frequency is low enough so that ordinary electronic instruments can be used in observing the circuit behavior. In the cylindrical network, an LC product of 16×10^{-14} (sections per second)$^{-2}$ was selected.

3. Range of Inductance Values. In the cylindrical network, the inductances are required to vary linearly with radius. This means that very small inductances are required close to the axis, while large inductances are required for large radial values. The smallest size inductor that can be used is determined by the smallest coil Q that can be tolerated. The largest inductor is determined by the physical size that can be used without inconvenience. The inductors were chosen to have a value of inductance equal to 200 microhenrys per radial section.

4. Range of Capacitance Values. As previously stated, the values of capacitance are required to vary inversely with radius for the cylindrical network. This means that very large capacitances are required near the axis, while small capacitances are needed for large radial values. In order to have capacitances which could be set with reasonable accuracy, it was decided to use ordinary mica trimmer capacitors. The largest size capacitor of this type commonly available is of the order of 1,000 $\mu\mu$f. Accordingly, the capacitance values were made equal to 800 $\mu\mu$f divided by the number of radial sections corresponding to the location. This choice was, in part, determined by the fact that the smallest capacitance used at the point most remote from the axis must still be fairly large compared to the input capacitance of any measuring device, such as a voltmeter, which may subsequently be used with the network. Since the net-

work had twelve radial sections, this meant that the outermost capacitors had a value of 67 $\mu\mu$f. It would be possible to use somewhat larger values of capacitance.

5. Allowable Coil Losses. Since the network-field relations which have been developed assumed perfect inductances, it is desirable to have Q's as large as possible. An idea of the allowable minimum coil Q can be obtained by examining the characteristics of an artificial transmission line having series inductances with finite coil Q's and perfect shunt capacitances. In such an artificial transmission line, the series impedance is given by

$$Z = R + j\omega L = j\omega L\left(1 - \frac{j}{Q}\right) \tag{13}$$

where $Q = \omega L/R$ and the admittance of the shunt element is given by

$$Y = j\omega C. \tag{14}$$

Using these values, the characteristic impedance of the line has a low-frequency value of

$$Z_0 = R_0 + jX_0 = \sqrt{\frac{Z}{Y}} = \sqrt{\frac{L}{C}\left(1 - \frac{j}{Q}\right)}. \tag{15}$$

Expanding this expression by the binomial theorem,

$$R_0 = \sqrt{\frac{L}{C}}\left(1 + \frac{1}{8Q^2} - \cdots\right) \tag{16}$$

$$X_0 = \frac{-1}{2Q}\sqrt{\frac{L}{C}}\left(1 - \frac{1}{8Q^2} + \cdots\right). \tag{17}$$

Likewise, the propagation constant is

$$\Gamma = \alpha + j\beta = \sqrt{ZY} = j\omega\sqrt{LC\left(1 - \frac{j}{Q}\right)}. \tag{18}$$

Expanding this by the binomial theorem,

$$\alpha = \frac{\omega\sqrt{LC}}{2Q}\left(1 - \frac{1}{8Q^2} + \cdots\right) \tag{19}$$

$$\beta = \omega\sqrt{LC}\left(1 + \frac{1}{8Q^2} - \cdots\right). \tag{20}$$

Examination of the above relations shows that the value of Q can be fairly low without destroying the basic relations demanded by the network for proper representation of the electromagnetic field. The minimum Q of the coarse section of the cylindrical network is 25, which corresponds to an attenuation of 1.09 db per wavelength or a voltage reduction of 10 per cent. For most of the coarse section, the Q's are of the order of 50, for which the voltage reduction is only 0.6 per cent per wavelength. Accordingly, the finite Q's of the coils are not a matter of serious concern.

6. Coil Data. Coils were wound with No. 7-41 Litz wire on a 5/16-inch bakelite rod. The coils were universally wound in the form of a small pi $\frac{1}{4}$ inch in width. The coils were so made that they could be plugged in and out of the circuit. This was accomplished by placing small contact rings on either end of the mounting rod of such size as to fit into a standard $\frac{3}{8}$-inch fuze clip. The maximum radius of a given winding was determined by the height of the mounting (approximately $\frac{1}{2}$ inch). For the large values of inductance, it was found necessary to use two and sometimes three such pi windings. The Litz wire was considered necessary to get a high Q at the operating frequency. Curves of inductance and corresponding coil Q as a function of the number of turns and the inductance, respectively, are shown in Figs. 2 and 3. As indicated in

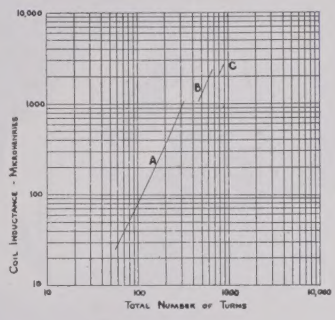

Fig. 2—Inductance versus turns of network-analyzer coils; coils pi-wound on 5/16-inch diameter fiber rod, all pi windings are wound on 11/16-inch centers, length of windings $\frac{1}{4}$ inch, wire No. 7-41 Litz, measurements made at 100 kc; (A) single-pi coils, (B) 2-pi coils, and (C) 3-pi coils.

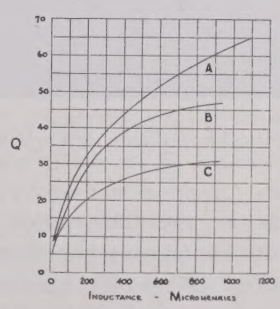

Fig. 3—Q versus inductance at 100 kc for network-analyzer coils pi-wound with No. 7-41 Litz wire on 5/16-inch diameter fiber rod, winding length $\frac{1}{4}$ inch; (A) free space (long-form coils); (B) rings only (short-form coils); and (C) rings and clips (short-form coils).

Fig. 3, the Q of the longer coils used in the coarse section were unaffected by either the contact rings or clips; whereas, the Q of the short coils used in the fine section was considerably reduced. The need of the fine section is explained in a later section. Coils were wound and inductance adjusted to the proper value within an accuracy of 0.5 per cent. The coils were wound on a Meissner coil winder, and the value of inductance was adjusted under conditions corresponding to mounting in the network, so that the effect of the rings and clips was properly accounted for.

7. Physical Form of the Network. The cylindrical network was constructed to have a radial dimension of one-half wavelength and an axial dimension of 1.5 wavelengths at the mean operating frequency of 100 kc. The major portion of the network was constructed with twenty-five elements per wavelength at the mean

operating frequency. There was, in addition, a fine section constructed in one corner of the network having fifty elements per wavelength at the mean operating frequency. The physical dimensions of the network are 4×12 feet. It is mounted on a $\frac{1}{4}$-inch Micarta panel, supported by a wooden framework. A picture of the network is shown in Fig. 4. An open-type structure was

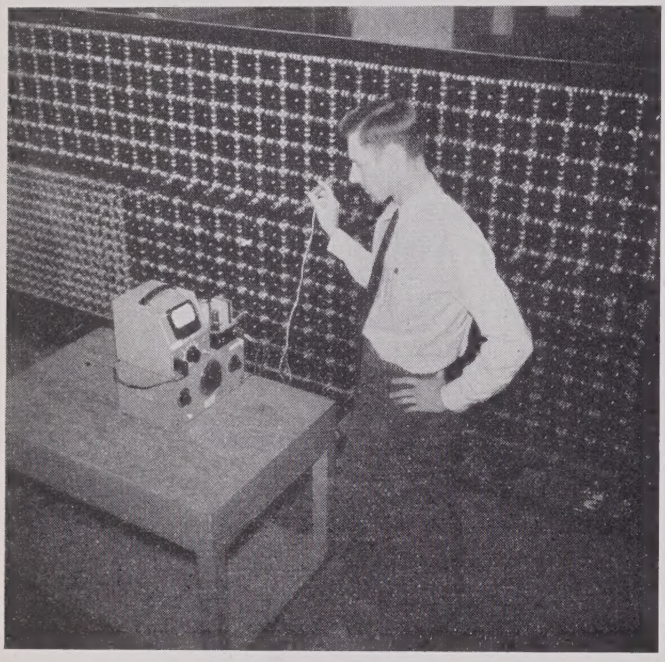

Fig. 4—Cylindrical-co-ordinate network in operation.

used, with posts at the inductance junctions. The trimmer capacitors comprising the shunt-reactance elements were located physically in the center of the squares made up of the inductors. A ground network was used on the back of the board to connect to the capacitors. The distance between junction posts was $3\frac{3}{4}$ inches. This gave a spacing of the inductors large enough to result in no observable mutual coupling between inductances at the operating frequencies.

8. Fine-Section Junction. In building the cylindrical co-ordinate network, it was considered desirable to have a portion of the network give more detail than the rest of the board. Accordingly, one-sixth of the network, the total dimensions of which were 0.5λ by 1.5λ, was constructed with fifty elements per wavelength at a mid-operating frequency of 100 kc, while the remaining five-sixths of the network was constructed with twenty-five elements per wavelength. Of the various arrangements possible to give greater detail than a network with a uniform construction of twenty-five elements per wavelength, this arrangement gives greatest detail for the smallest number of coils.

Although the use of a small fine section in conjunction with a larger coarse section results in economy of construction for a given detail, the problem of matching the fine to the coarse section does arise. The requirements of a junction are:

a. Time delays of an electrical wave must be proportional to the length of each section for propagation both normal and parallel to the junction.

b. The Z_0 of each section comprising the junction must be such that power will divide properly over the areas involved without reflection for waves both normal and parallel to the boundary. If the above conditions are realized, waves normal and parallel to the boundary will not be disturbed, nor will any wave crossing the boundary at an angle be disturbed. It is very difficult to meet all of the above conditions exactly. Of the various junction arrangements possible, one suggested by V. A. Westberg has been found to match the fine and coarse section so well the disturbance is hardly measurable. This junction configuration is shown in Fig. 5. In Fig. 5(a) are shown the impedance and delay values. In Fig. 5(b) these have

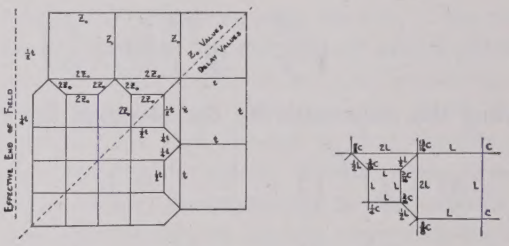

(a) (b)

Fig. 5—Junction configuration, (a) impedance and delay values, and (b) relative values of circuit parameters.

been translated into the proper relative inductance and capacitance values. For the cylindrical-co-ordinate network, the inductance values shown in Fig. 5(b) must be multiplied by radial distance, while the capacitance values must be divided by radial distance.

9. Cost of Construction. As analyzers go, networks of the type described here are relatively inexpensive devices. The first network built was the one for cylindrical co-ordinates. Coils for this network were wound in the Stanford laboratories by student assistants, and the entire construction was made, without recourse to external facilities, in a period of about one month. The cost of construction of this network, including materials, labor, and overhead is conservatively estimated at $6,500. The cost of the materials alone was approximately $2,000.

The second network was constructed for rectangular co-ordinates. Since the coils were all of the same size on this network, their fabrication was subcontracted. The rectangular co-ordinate network is estimated as having cost only $2,000. The reduction in cost resulted from a design without a fine section, which involved only half as many coils as in the first network at half the unit cost plus the reduction in time resulting from experience with the first network. The cost of the materials alone was under $1,000.

B. Rectangular-Co-ordinate Network

1. LC Product. The design problem encountered in constructing a network for two-dimensional rectangular co-ordinates is much simpler than that for cylindrical co-ordinates. A much greater tolerance in choice of values is permitted in this case because radial variation of circuit elements need not be considered. The *LC* product for the rectangular network was taken as about 2.8 times that used for the cylindrical-co-ordinate network. This gave a velocity of twenty-five elements per wavelength at 60 kc.

2. Values of Circuit Parameters. The coils for the rectangular-co-ordinate network were specified as having an inductance of 1,200 microhenries and a Q of 50 at 100 kc. The coils were of similar construction to those used in the coarse section of the cylindrical-co-ordinate network; however, it was found that sufficiently high Q was obtainable with No. 30 enameled solid-copper wire. The distributed capacitance of these coils was higher than that of the Litz-wire-wound coils, but still resulted in a natural resonant frequency of 2 Mc, well above the operating frequency. The capacitors for the rectangular network were 350 $\mu\mu$f trimmer capacitors. These could be set anywhere in the range of 50 to 500 $\mu\mu$f; the lower the value, the higher the operating frequency for a given number of electrical degrees per section. A compromise value of 370 $\mu\mu$f was chosen.

Operation of AM Broadcast Transmitters into Sharply Tuned Antenna Systems*

W. H. DOHERTY†, FELLOW, IRE

Summary—**The impedance of some broadcast antenna arrays varies so much over the transmitted band as to impair the performance of the radio transmitter. The impairment consists in clipping of sidebands and distortion of the envelope at high modulation frequencies. This paper reports on an experimental determination of the nature and magnitude of this impairment and on its substantial reduction by suitable coupling methods.**

Introduction

THE IMPEDANCE of a broadcast antenna, and particularly the common-point impedance of an array, often varies widely over the transmission band. When this is the case, the frequency response, amplitude linearity, and modulation capability of the broadcast transmitter can be adversely affected. Recognition of this difficulty by transmitter manufacturers has led to the formulation of an RMA specification for the "normal load" into which a transmitter should operate and meet its performance requirements. This is a load whose resistance does not depart more than 5 per cent from its midband or carrier-frequency value at ± 5 kc or 10 per cent at ± 10 kc, and whose reactance, which is zero at midband, does not exceed 18 per cent of the midband resistance at ± 5 kc or 35 per cent at ± 10 kc.

A study of the effect of frequency-sensitive loads from the viewpoint of the transmitter designer has been carried out by engineers of the broadcast transmitter development group of Bell Telephone Laboratories under the supervision of J. B. Bishop. Extensive data and oscillograms have been taken which indicate the extent of the impairment of transmitter performance under a variety of conditions, and the effectiveness of corrective methods which are to be described.

I. Monitoring Methods

The first phase of the study necessarily involved determination of proper monitoring conditions whereby actual sideband power, effective percentage modulation, and true distortion in the signal delivered to the antenna system can be measured. A preliminary discussion of the monitoring problem appeared in a previous publication,[1] in which it was shown that the appearance of the modulation envelope is greatly different at different points in a coupling circuit or at different points along a transmission line when the impedance of the termination at the side frequencies differs substantially from the impedance at the carrier frequency. This is illustrated by the oscillograms of Fig. 1, which show the voltage envelope for a modulation frequency of 7500 cps as observed at three points along a transmission line or coupling network whose termination, for example, is equivalent to a series-tuned circuit resonant at the carrier frequency. At the termination, or at points removed therefrom by an even number of quarter wavelengths, a fully modulated voltage wave may appear (Fig. 1(a)), and the amplitude of each of the two side-frequency voltages accordingly will be one-half the amplitude of the carrier voltage. But, because the impedance rises on either side of the carrier frequency (Fig. 1(d)), the side-

* Decimal classification: R355.131×R326.4. Original manuscript received by the Institute, September 28, 1948; revised manuscript received, January 3, 1949. Presented, 1948 IRE West Coast Convention, September 30, 1948, Los Angeles, Calif.

† Bell Telephone Laboratories, Inc., Murray Hill, N. J.

[1] W. H. Doherty, "Notes on modulation of AM transmitters," *The Oscillator*, p. 22, no. 5; October, 1946.

frequency *currents* will each be less than one-half the carrier current, and an inspection of the current envelope would show substantially less than 100 per cent modulation. On the other hand, at points removed from the termination by odd quarter wavelengths, the impedance will correspond to that of a parallel-tuned circuit (Fig. 1(f)), decreasing on either side of the carrier frequency; and, although the current envelope if observed would show a fully modulated wave, the voltage

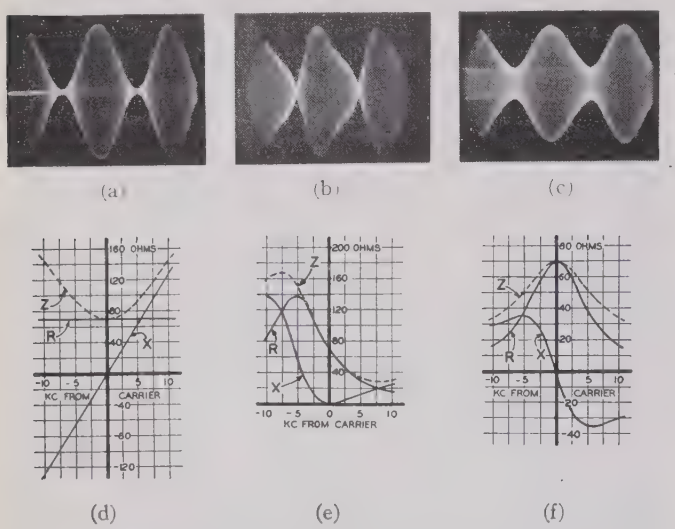

Fig. 1—Voltage envelopes and impedance versus frequency relations at three points in an output circuit or transmission line with narrow-band termination.

envelope (Fig. 1(c)) shows considerably less than 100 per cent modulation—in the case illustrated, only 60 per cent, since the impedance at the side frequencies is only 60 per cent of the impedance at the carrier frequency (the inverse of the situation of Fig. 1(d)). Finally, at odd eighth-wavelength points, where the impedance versus frequency curve is dissymmetrical (Fig. 1(e)), the voltage envelope has the distorted appearance indicated in Fig. 1(b). The current envelope at this point would also be badly distorted. A monitoring rectifier and conventional distortion-measuring instrument would register a high percentage of distortion for this wave, yet there are no extraneous side frequencies being radiated, the envelope distortion being entirely due to the inequality and phase dissymmetry of the two desired side-frequency voltages at this particular point in the line or coupling circuit. It is obvious that if, in addition, the operator were to raise the audio input level, endeavoring to bring about apparent full modulation at this point, much more severe distortion would be registered, because the wave at other points would then be over-modulated.

The impedance versus frequency relations indicated are those corresponding to a simple resonant circuit in which the ratio of reactive volt-amperes to watts at 550 kc, for example, is approximately fifty to one. The impedance curve of a simple resonant circuit appears on a Smith chart[2] as a circle. Fig. 2 shows impedance circles *D*, *E*, and *F* for points along a transmission line

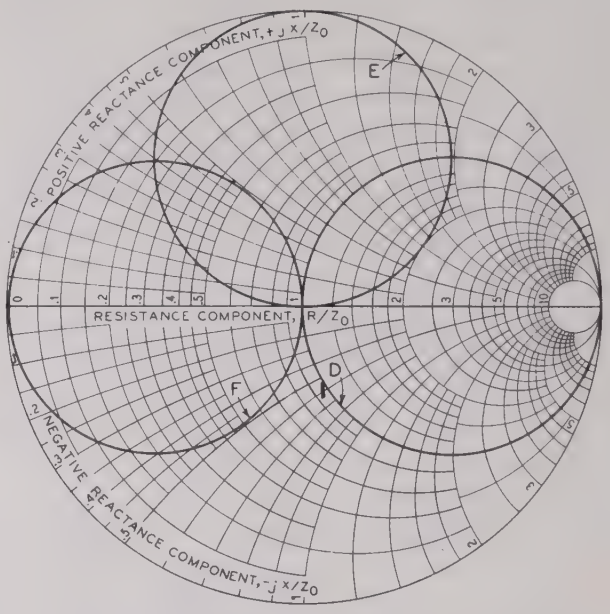

Fig. 2—Smith-chart impedance diagrams for a simple resonant circuit at points along a transmission line corresponding to *D*, *E*, and *F*, of Fig. 1.

or coupling circuit where the impedance versus frequency relations would correspond to *D*, *E*, and *F* of Fig. 1. The frequency dependence in the case shown is several times more severe than the RMA standard for artificial antennas for transmitter testing, but is comparable with that frequently found in actual broadcast installations.

Measurement of Effective Modulation and Distortion

If one wishes to determine actual delivered sideband power by measurement of a sample of the current envelope, it is necessary to make the inspection and measurement at a point in the circuit corresponding to Fig. 1(d), where the series resistance is independent of frequency over the band transmitted, since it is the current squared times the series resistance that determines power. We may refer to such points as *D* points for convenience. In order that the measurement may include true radiated distortion power, i.e., power in extraneous sidebands, the constancy should hold over a correspondingly wider band. Now, when measuring at such points, one should not try to adjust the audio input for 100 per cent modulation of the current envelope observed on the oscilloscope, but for a certain lower percentage—60 per cent, in the case considered in Fig. 1—since the voltage envelope (not being observed by the operator, but shown in Fig. 1(a)) will then have reached full modulation, and any further increase

[2] P. H. Smith, "An improved transmission line calculator," *Electronics*, vol. 17, pp. 130–134; January, 1944.

would necessarily entail severe distortion in both the voltage wave and the current wave.

If, on the other hand, it is the voltage envelope rather than the current envelope that is to be monitored, the point of measurement should be one where the *parallel* rather than the series resistance is constant over the transmitted band, since the power is the voltage squared divided by the parallel resistance. It can be shown[3] that this constancy will be found only at points corresponding to Fig. 1(f), one-quarter wavelength removed from D points. We may label these as F points. At these F points one must not look for a fully modulated wave, since the *current* wave (not being observed) will have reached full modulation, in the case considered, when the voltage wave, seen in Fig. 1(c), is only 60 per cent modulated.

Thus we have the curious situation that, with narrow-band antennas, and when modulating at high audio frequencies, only certain points D in the output circuit of the transmitter are suitable for determination of effective sideband power and distortion power when a sample of the current wave is being analyzed, and only certain other points F when a voltage sample is being analyzed; while the maximum permissible modulation of the wave being analyzed has to be set in the reverse manner, i.e., by inspection of the voltage envelope at points D or the current envelope at points F, or by calculation from the impedance versus frequency curve.

It should be noted that at D points, where the series resistance is independent of frequency, the parallel resistance is greater for the sidebands than for the carrier frequency, and a distortion measurement on the voltage envelope would be pessimistic since a given distortion power will be represented by a disproportionately high sideband voltage. Similarly, at F points, where the parallel resistance is independent of frequency but the series resistance is lower for the sidebands than for the carrier, a distortion measurement on the current envelope will be pessimistic. Thus the point where minimum distortion is registered is the correct monitoring point for the ideal case described, and will also, in general, afford the most reliable measure of distortion power in cases where the impedance diagram is irregular.

In order to permit the plotting of conventional curves of distortion versus modulation frequency for particular percentages of modulation, it is necessary to express the percentage modulation in terms of the quantity—current or voltage—which can be allowed to attain full modulation at the monitoring point, even though the true sideband power, with sharply tuned loads, does not correspond to full modulation. There is, moreover, justification for this in the fact that, when the maximum permissible modulation (without overmodulation) is reached, the power amplifier tubes are being required to deliver either full peak current or full peak voltage to the load, even if not both.

While it is only in certain types of programs that a broadcast transmitter is subjected to heavy modulation at high audio frequencies, the application of a test tone and measurement of harmonic distortion at such frequencies is a part of regular testing routine carried out with standard station equipment, and, when correctly done, provides valuable information both in the initial tune-up of a transmitter and in maintenance. However, an equally important application of the monitoring technique just described is in connection with the over-all frequency characteristic of the transmitter from audio input to sideband power output. This will be discussed in Section II. With the recent establishment by the Federal Communications Commission of a requirement for submission of performance data prior to renewal of licenses, it is important to be able to verify delivery of appropriate energy to the array from the transmitter for all modulation frequencies.

II. Operation of the Power Amplifier

With the impedance-versus-frequency characteristic varying widely from point to point in a coupling circuit, it is scarcely necessary to state that the characteristic as found at the particular point where the power-amplifier tubes are connected is of profound importance in the performance of the amplifier, regardless of the type of circuit or modulation method used. In particular, reverting to Fig. 1, if the impedance seen by the tubes were to vary with frequency in the manner given by Fig. 1(e), the tubes would *have* to impress on the circuit a voltage envelope resembling Fig. 1(b) in order that the voltage envelope at a proper voltage monitoring point (an F point) might be free of distortion. Indeed, since the impedance dissymmetry of Fig. 1(e) necessarily entails considerable phase modulation in the radio-frequency wave which does not show up in the oscillogram, it would be necessary for the tubes to introduce a corresponding phase modulation as well as to deliver a voltage envelope distorted in amplitude. Since one can ask only that a transmitter deliver to its load a voltage wave or a current wave free of phase modulation and having its envelope identical in shape to the audio input wave, it is apparent that, when the load is frequency-sensitive, only a point of impedance symmetry such as a D point or an F point is appropriate for making connection to the tubes. In the former case, when a high-frequency test tone is applied, the tubes will be asked to deliver full rated voltage and less than full rated current at the peak of the envelope; in the latter case, full rated current at less than full rated voltage. In either case, undistorted voltage and current envelopes are desired.

[3] The well-known impedance-inverting property of quarter-wave lines and their equivalent networks can be expressed in a form which shows, interestingly, that if one speaks of parallel components at one end and series components at the other end, the inversion holds for the resistances and also, *independently*, for the reactances; hence, the constant series resistance at D points necessarily means constant parallel resistance at points one-quarter wavelength therefrom, irrespective of reactance values.

Tests on several transmitters at powers from 1 to 10 kw, with very sharply tuned artificial antennas, have confirmed that when arrangements are made to connect the tubes to a *D* or *F* point the distortion at high modulation frequencies, when properly measured, differs very little from the distortion measured with a flat antenna, the slight increase observed being attributable to the effect of the sharp antenna on the width of the band over which negative feedback is effective. Fig. 3 shows the harmonic distortion in an experimental 10-kw broadcast transmitter at 95 per cent modulation with (1) a flat dummy antenna, and (2) a dummy

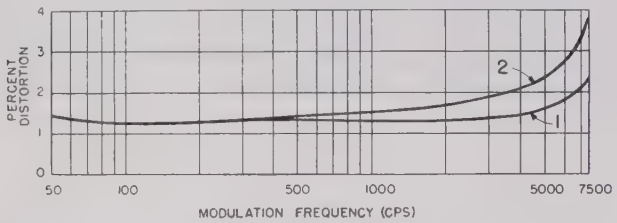

Fig. 3—Distortion curves for an experimental 10-kw transmitter at 95 per cent modulation with flat antenna (curve 1) and frequency-sensitive antenna (curve 2).

antenna having a ratio of kva to kw of 25 to 1 at 550 kc, giving an impedance-versus-frequency characteristic about half as severe as that of Fig. 1. The tubes were connected at an *F* point and the distortion and per cent modulation were determined in the manner described. In contrast, with the tubes connected at a point of impedance dissymmetry and the distortion and per cent modulation improperly monitored, apparent distortions as high as 20 and 30 per cent were recorded. Fig. 4 gives an example of the kind of envelope shape that was observed under such conditions. A distortion-measuring instrument registered 21 per cent for this wave.

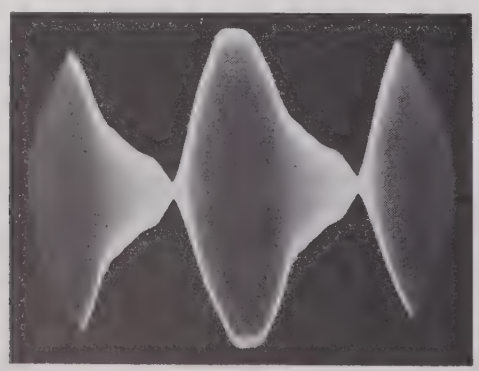

Fig. 4—Modulation envelope of a 10-kw transmitter for frequency-sensitive load as seen under improper operating and monitoring conditions.

The transmitter used for this test employed the high-efficiency circuit[4] devised by the author, with grid-bias modulation[5] of the final stage and employing "envelope" feedback, in which a sample of the radio-frequency output is detected and fed back to the audio input circuits.

From a distortion standpoint, the *D* and *F* connections are found to be about equally satisfactory. For transmitters employing envelope feedback, the *F* connection offers an important advantage in that it provides automatic compensation for the sideband-clipping tendency of the antenna. This comes about from the fact that with envelope feedback it is desirable for reasons of bandwidth to "pick off" a radio-frequency voltage sample directly at the plate of the final power tube; and if this point is an *F* point, the sample will then represent the voltage across a parallel resistance that is the same for the sidebands as for the carrier, and consequently the feedback will act to maintain a flat frequency characteristic in the radiated sideband power. When the impedance-versus-frequency characteristic of an antenna differs from that of a simple tuned circuit (i.e., exhibits in the transmitted band a curvature differing from that of the circles in Fig. 2), the corrective action of the feedback is less complete but still substantial. To achieve equivalent compensation for a narrow-band antenna characteristic by the use of high-kva coupling meshes in the output circuits would be unduly expensive in apparatus and would involve critical tuning and considerable radio-frequency power loss.

The potency of feedback derived from the radio-frequency envelope in bringing about delivery of the desired sideband energy to the antenna system is shown in Fig. 5, which pertains to the same 10-kw transmitter and the same types of loads to which the distortion curves of Fig. 3 apply. Curve 1 of Fig. 5 gives the overall frequency characteristic of the transmitter at 50 per cent modulation with no feedback when operating into a broad-band resistance load. The departures from flatness at the low and high ends arise mainly in the audio circuits in the transmitter. Curve 2, still without feed-

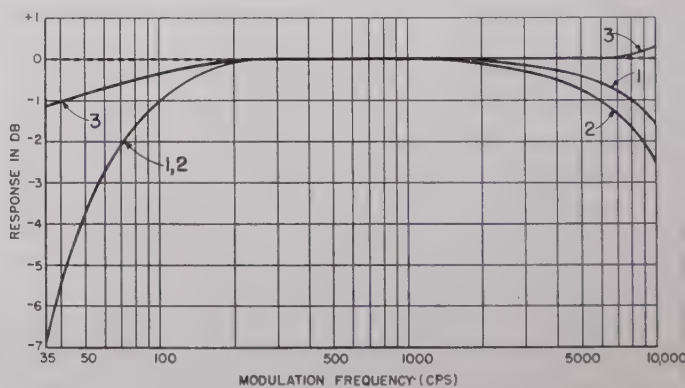

Fig. 5—Frequency characteristic curves for a 10-kw transmitter.

back, includes the additional loss at high modulation frequencies due to the frequency-sensitive load when the tubes are connected at an *F* point, the monitor being also connected at this point. But with envelope feedback applied, as derived from the voltage at this *F* point where the parallel resistance is constant over the band, the improved performance indicated by curve 3 is ob-

[4] U. S. Patent No. 2,210,028, W. H. Doherty.
[5] U. S. Patent No. 2,226,258, H. A. Reise and A. A. Skene.

ained. Fig. 6 shows, in contrast, corresponding curves or connection of the power amplifier tubes at a D point, where the parallel resistance is higher for the sidebands han for the carrier (but with the monitor still connected t an F point, since it is only here that a voltage-operted monitor will give a true indication of sideband power). The feedback in this case, being derived from

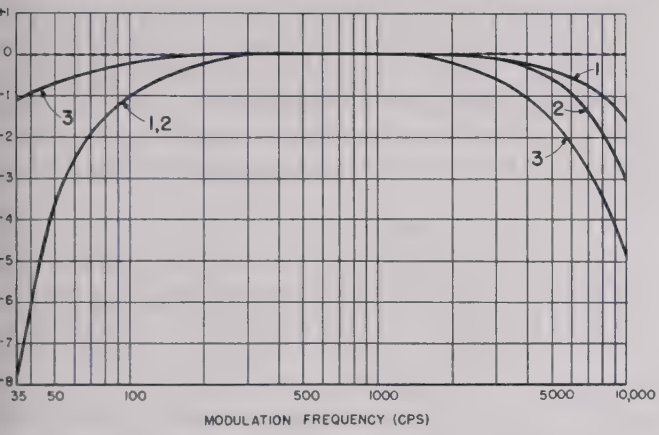

Fig. 6—Effect of unfavorable feedback connection on the frequency characteristic.

he voltage at the D point where the tubes are conected, actually aggravates the sideband-clipping ction of the sharp antenna, as seen in curve 3 of Fig. 6. This is because, while the power tubes tend to impress igher than normal sideband voltages on the circuit on ccount of higher impedance to sideband frequencies, nd thus partially compensate for the clipping action of he circuit, the feedback acts to prevent this compensaion.

III. Transmitter Output-Circuit Design

To incorporate in broadcast transmitters the facilities or reorientation of the impedance-versus-frequency haracteristic of any sharply tuned load that may be ncountered, a variable phase shifter is required, equivaent to a "line stretcher," with a total range approachng 180 degrees to cover all cases. Such a phase shifter, as built for the experimental 10-kw transmitter on which these tests were conducted, is shown in Fig. 7(a). With the recent commercial availability of variable vacuum capacitors of wide capacitance range, linear calibration, and high voltage rating, it was most practical to incorporate this phasing device in the high-impedance output circuit of the transmitter prior to transforming down to the transmission line. The transformation ratio of the phase shifter shown is unity, and the coils L_1 and L_2 have reactances equal to the terminating resistance R regardless of the phase shift desired. For the minimum phase shift of 90 degrees, capacitor C_2 likewise has a reactance of R ohms, and C_1 and C_3 have zero capacitance. For greater phase shifts, capacitor C_2 is increased, and capacitors C_1 and C_3 come into play. By proper choice of these three capacitances, the phase shift can be increased to any value up to 270 degrees (or more) with no change required in the inductances, the input impedance remaining a pure resistance of R ohms through-

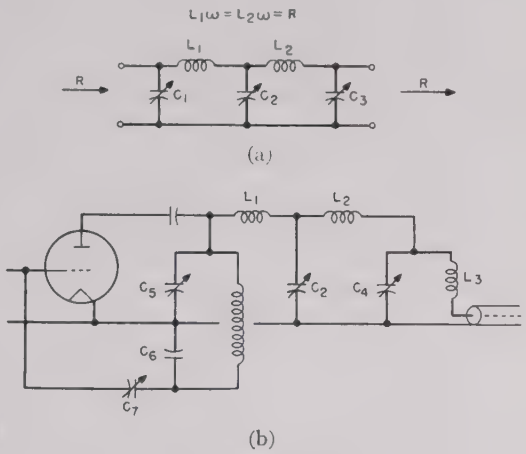

Fig. 7—Incorporation of a phase shifter in the transmitter output circuit.

out the range. The required admittances for these capacitances are:

$$C_1\omega = C_3\omega = \frac{1}{R}(1 - \cot \tfrac{1}{2}\Phi) \qquad (1)$$

$$C_2\omega = \frac{2}{R}(1 - \tfrac{1}{2}\sin \Phi) \qquad (2)$$

where Φ is the phase shift desired. These relations are shown in Fig. 8.

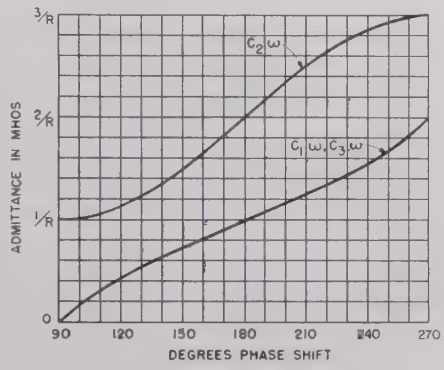

Fig. 8—Capacitive admittance required for the phase shifter of Fig. 7.

This phasing device is inserted, as shown in Fig. 7(b), between the radio-frequency plate terminal of the power amplifier and a load circuit consisting of C_4 and L_3, normally tuned to resonance and matching the amplifier to the transmission line. The built-out neutralizing circuit shown contains a "tank" capacitor C_5 with which the power tube is tuned in the conventional manner. With this arrangement, when a phase shift other than 90 degrees is required for improving performance with a frequency-sensitive antenna, the capacitances C_1 and C_3 of Fig. 7(a) are obtained by simply increasing the

values of C_4 and C_5, which, like C_2, are variable vacuum capacitors.

In stations whose radiation patterns are different for day and night operation, the daytime pattern usually involves a simpler excitation of the antenna array, giving a flatter impedance characteristic. The phase-shifter adjustment chosen would, accordingly, be that best fitted to the nighttime impedance curve.

In the 10-kw transmitter built for testing these principles, the tube shown in Fig. 7(b) was the No. 2 or "peak" tube of a high-efficiency amplifier operating at a plate potential of 10,000 volts. The desired load impedance for the amplifier was 720 ohms. Coils L_1 and L_2 were accordingly made 720 ohms each and coil L_3 was adjusted for 186 ohms to obtain, in combination with C_4 a transformation from the 51.5-ohm coaxial-line impedance to 720 ohms. Capacitor C_2 is made 720 ohms in all cases where the antenna presents no bandwidth problem. When a narrow-band antenna is encountered, the required phase shift for best operation is determined by plotting the impedance characteristic at the input terminals of the transmission line on a Smith chart with an added peripheral scale, as shown in Fig. 9. Recalling

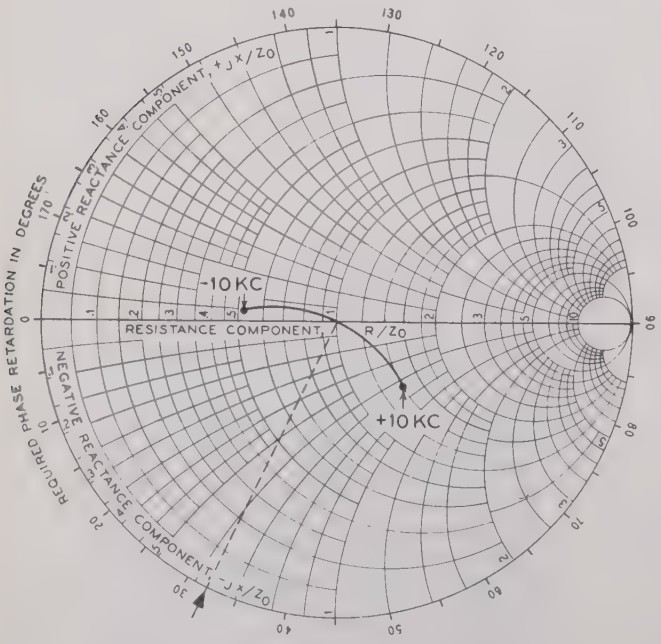

Fig. 9—Determination of the required phase shift in a typical case from the Smith chart.

that the desired orientation of the characteristic at the plate of the power-amplifier tube is that of circle F of Fig. 2, it is seen from Fig. 9 that the total phase retardation desired between the transmission line and the power tube for the case illustrated is either 32 degrees, or 180 plus 32 degrees. Since the phase retardation introduced by coil L_3 is $\tan^{-1}$ 186/51.5 or 75 degrees, it is necessary to adjust the phase shifter to 137 degrees to obtain the total of 212 degrees required orientation. Fig. 8 then gives the values of C_2 and for the increments to be made in C_4 and C_5 to constitute effectively the capacitances C_1 and C_3 of Fig. 7(a). The actual final adjustment of C_5 is, of course, that which gives a unity power-factor load at the amplifier tube.

The radio-frequency plate terminal, being an F point, is used as the source of energy for the feedback rectifier and monitoring rectifier, due consideration being given to the fact that with a narrow-band antenna the voltage envelope observed when modulation is applied at high audio frequencies will not indicate 100 per cent modulation when the current delivered by the tubes is fully modulated.

With some antenna arrays the impedance may vary so irregularly with frequency as to call for a compromise adjustment which is difficult of prediction from the impedance diagram. In such cases, experimental determination of optimum phase shift is desirable by direct observation of the envelope shape at the plates of the tubes. The type of phase shifter described is especially well adapted to this procedure because of the wide range of adjustment possible without removal of power and the constancy of carrier-frequency impedance as the phase shift is varied.

Because of the extra harmonic suppression provided by the phase-shifting network, the usual harmonic filter connected at the input to the transmission line and employing mica capacitors (due to the low impedance) is no longer required. In cases where an unusually high degree of suppression is needed for one harmonic, a small fixed vacuum capacitor paralleling L_3 will provide a substantial increase in suppression. The circuit described thus combines with its property of handling frequency-sensitive loads the features of high harmonic suppression and long-life components.

In most cases, a station with a new antenna and transmitter would operate initially with the phase shifter set for its minimum shift of 90 degrees. After the completion of all antenna adjustments and the establishment of the final radiation pattern, the transmission-line input impedance would be measured over a wide band, and the desirability of phase correction determined. By merely increasing the capacitances of three variable capacitors, any additional phase shift desired can then be introduced to permit optimum performance of the transmitter and provide a monitoring point where the most reliable measurements of this performance can be made.

Acknowledgment

The experimental transmitters used in the investigations reported were built by H. A. Reise and C. W. Norwood of Bell Telephone Laboratories, who were also responsible for all of the performance data obtained. The contributions of these engineers and their colleagues are gratefully acknowledged.

A Power-Equalizing Network for Antennas*

R. W. MASTERS†, ASSOCIATE, IRE

Summary—**A bridge type of network, which causes equal power to be delivered to two load impedances whose product is a predetermined real constant, is discussed. The input impedance of the bridge is found to be practically independent of suitably paired load-impedance values over a considerable band of frequencies.**

Immediate application to the design of television broadcast antennas is indicated, examples are given, and power loss is discussed.

I. Introduction

IT IS AN accepted fact that almost all of the various pattern-shape and power-gain requirements for a television broadcast antenna can be met by antennas falling into one general classification. These antennas are comprised of two separate parts which are equal in their impedance-versus-frequency characteristics in a common band of frequencies. The parts are energized with equal power at a relative phase of 90° at midband, and are located so that no mutual coupling exists.

The phasing of the parts is accomplished by using transmission lines which differ in length from a common driving point by one-quarter wavelength. Unless the lines are perfectly matched by their loads, their input impedances differ, and unequal power is delivered to the loads. Objectionable field-pattern distortion may result, and, if the lines are long, the pattern shape may fluctuate with frequency variations because of the cyclic change of the line input impedances. Reverberations sufficient to cause secondary images at a television receiver occur if the values of the voltage reflection coefficients of the antenna halves on their lines exceed 0.05 inside the channel. Moreover, transmitters operate least favorably into varying loads. The difficulty of matching antennas to their lines within the 0.05 reflection tolerance over the television channel probably explains why so few satisfactory designs exist.

This paper discusses a bridge network which greatly simplifies the design problem in regard to power division and impedance match for this large class of important antennas, as well as for a more general impedance group.

II. The Power Equalizer

A dissipationless coaxial-transmission-line version of the power-equalizing bridge is shown schematically in Fig. 1(a). K_1 and K_2 designate characteristic impedances of transmission lines, Z_L are equal loads of arbitrary complex value including zero and infinity, R is a pure resistor, and x indicates a line length. A generator of voltage V_3 is connected between points 0 and 3. All voltages are understood to be rms.

Let λ_0 represent the wavelength at the midfrequency of the band throughout which it is desired to equalize the power dissipation in the loads and eliminate reverberations. Let the lines K_2 feeding the loads differ in length by $\lambda_0/4$, and, temporarily, set

$$K_1 = K_2 = K = 2R. \tag{1}$$

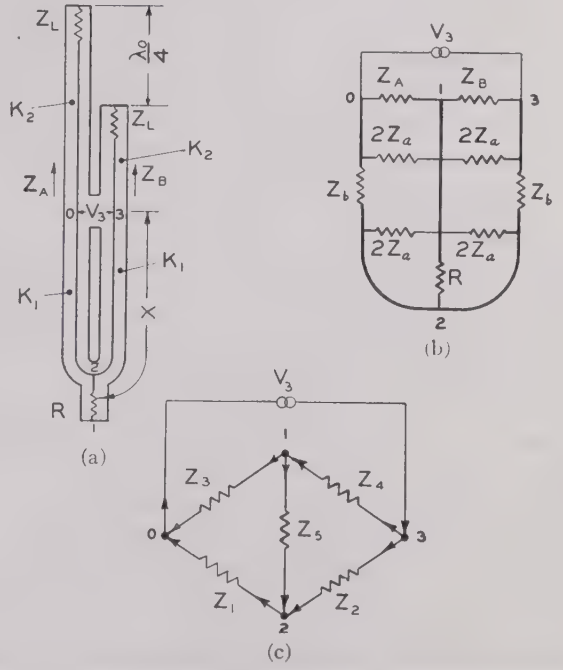

Fig. 1—Transformation from distributed- to lumped-constant bridge.

Except when $Z_L = K$, the loads will cause unequal impedances Z_A and Z_B to be presented in series across the generator. At λ_0, due to the odd quarter-wavelength line difference, these impedances obey the relationship,

$$Z_A Z_B = K^2, \tag{2}$$

which is fundamental in what is to follow. This relationship changes but slowly with frequency, so that (2) is approximately true for a considerable band of frequencies. Z_A and Z_B are the network loading, while the rest of the network, with the exception of R, is the bridge. A consideration of traveling waves in Fig. 1(a) leads intuitively to the following conclusions:

(a) All power dissipated in the loads at λ_0 is equally divided between them.

(b) The impedance presented to the generator at λ_0 is invariant with respect to variations in Z_L, and resistive if $x = \lambda_0/4$.

* Decimal classification: R221×R117.121. Original manuscript received by the Institute, August 26, 1948; revised manuscript received, February 23, 1949.

† RCA Victor Division, Radio Corporation of America, Camden, N. J.

(c) The generator and resistor may be interchanged if $R=2K$ and $x=\lambda_0/4$, without altering the salient network properties.

(d) Reflections at the loads are removed from the system by absorption in R.

(e) Small cumulative reflections due to imperfect junctions, elbows, and impedance matches throughout the lines K_2 are largely removed if the imperfections are equal and are located the same distance from the load in both lines.

(f) At λ_0, the ratio of power lost in R to the total input power is precisely the square of the absolute value of the voltage reflection coefficient q_v of the loads on K_2.

(g) The system is relatively wide-band with respect to frequency.

(h) If the loads are equal antenna halves, then the field pattern is remarkably stabilized with respect to frequency.

(i) The system permits considerable deviation from design perfection.

Waves initiated by V_3 at 0–3 of length λ_0 traveling toward Z_L are partially reflected at Z_L by a complex factor q_v times the incident voltage. Due to the quarter-wave difference in the two line lengths, the reflected waves return to the generator out of phase. They therefore ignore its presence, and instead continue along the lines K_1 to be absorbed in R, which matches the impedance of the parallel combination of lines K_1. These reflected waves are absorbed before they can react on the generator or reverberate. The impedance load presented to the generator is, therefore, $2K$ (the series sum of the characteristic impedances of lines K_2) in parallel with the reactances of the lines K_1, and the real power delivered to the two lines is equally divided. The power wasted is evidently $|q_v|^2$ times the input power, where q_v is the complex voltage reflection coefficient of Z_L on the lines K_2. It is important to note that R cannot absorb energy from initial waves traveling toward it from 0–3, since these waves arrive in the wrong phase at its terminals.

When the positions of the generator and resistor are interchanged, the reasoning proceeds along the same lines with about the same result. The only difference is that the generator load becomes $K/2$, x must be one quarter-wavelength long for perfect absorption of the reflected wave, and R must have a value equal to $2K$.

The network can likewise remove the small over-all reflections caused by imperfect transmission-line elements, such as elbows and transforming sections, as long as like elements are located at the same distance from the load in each line and the long line contains one perfect quarter-wavelength of line at the network terminals. This is obvious, since the imperfections combine with the loads to form new, equal loads.

Many antennas and loads are required to operate over a specified frequency range. In this case, the lines K_2 differ in electrical length by $\pi/2+\Delta$ radians, where

$$\Delta = \frac{\pi}{2}(\lambda_0/\lambda - 1). \tag{3}$$

Reflected waves returning to 0–3 from Z_L have a relative phase of $\pi+2\Delta$, and present a net voltage, between terminals 0–3, of

$$q_v'V_3 = (q_v \sin \Delta)V_3, \tag{4}$$

which assumes the role of a different-sized reflection as far as the generator is concerned. Only this component of the reflection can reverberate, since the rest of the wave is absorbed in R. It is the pseudo reflection coefficient q_v' which must be held to the 0.05 value required in television broadcast antennas. Since $\sin \Delta$ is less than 0.08 for any television channel, reverberation effects are almost completely eliminated, and the network loading seems practically constant to the generator, even for the absurd load values of zero or infinity.

The shunting effect of the lines K_1 will, of course, change with frequency, but their effect can be minimized. Assume that a two-wire balanced transmission line of impedance $2K$ supplies the terminals 0–3. A short-circuited length x of this line is then connected in parallel with the line $2K$ at a distance y from 0–3. By properly adjusting lengths x and y, both nearly equal to $\lambda_0/4$, the reflections on line $2K$ due to the shunt elements $2K$ and $2K_1$ (these elements are equal) may be made zero at any two frequencies in the band, especially picture and sound carriers in a television channel. If the input to the two-wire line be considered as the new driving point, it will be seen that the bridge is broad-banded. It is also broad-banded when the positions of the generator and the resistor R are interchanged, with R equal to $2K$.

Because of some imperfection in manufacture, it may be that R is not a perfect match to the system, but has a reflection coefficient $q_v'' \neq 0$ on the lines K_1. The pseudo reflection coefficient presented to the transmitter at λ becomes

$$q_v' = q_v^2 q_v'', \tag{5}$$

which is harmlessly small if q_v and q_v'' are both less than 0.50, for example. The power being radiated at λ_0 in the first reverberation by an antenna, namely,

$$P_t' = |q_v|^2 |q_v''|^2 (1 - |q_v|^2) P_t, \tag{6}$$

is likewise negligible under the same circumstances. It does not need to match the system very well in order to effect a great improvement in reverberation damping and power equalization.

Sometimes the loads Z_L are not equal, as is usually the case when one tries to make two antennas exactly alike. Small mechanical differences cause the impedances to differ. The pseudo reflection at the driving points can be minimized by using a small capacitor or inductor to alter the phase of the reflection coefficient

of one load to match that of the other. At λ_0, the pseudo reflection is then equal to the difference between the absolute magnitudes of the reflections from the two unequal loads, and the rest of the reflected energy is absorbed in R.

Equation (2) is sufficient to insure that the loads receive equal power, but not necessarily all the power, when they are connected to the bridge network. Accidental external coupling between Z_A and Z_B will upset this impedance relationship, so that the conclusions regarding the behavior of the network will no longer be strictly true. Nevertheless, considerable improvement may be obtained if such coupling is small, as may happen between poorly isolated antenna halves.

The configuration of Fig. 1(a) is representative of a group of several transmission networks able to perform the same general functions. All of them can be reduced to lumped-constant equivalent bridges through transformations similar to those of Fig. 1. Fig. 1(b) shows 1(a) after replacing the transmission lines K_1 by their equivalent π sections according to the well-known relations:

$$2Z_a = K_1 \coth \frac{\Gamma x}{2} = -jK_1 \frac{(1 + \cos \beta x)}{\sin \beta x} \tag{7}$$

$$Z_b = K_1 \sinh \Gamma x = jK_1 \sin \beta x \tag{8}$$

where $\Gamma = \alpha + j\beta$ is the complex propagation constant of the lines. The attenuation constant α has been assumed zero, leaving only the phase constant, β radians per meter. Fig. 1(c) shows the lumped bridge analogue after combining the elements of Fig. 1(b) in an obvious manner.

A more satisfactory proof of the performance of the bridge involves Fig. 1(c), in which the arrows indicate assumed directions of the currents. The network is solved for the voltages at the junctions relative to 0 in terms of V_3 by applying Kirchhoff's law concerning the sum of the currents at a junction. Knowing these voltages and letting an asterisk signify the complex conjugate of a quantity, the expressions are written for the complex power ψ_n delivered to each branch of the network; e.g.,

$$\psi_5 = \frac{(V_1 - V_2)(V_1 - V_2)^*}{Z_5^*}. \tag{9}$$

Assume that equations (1) and (2) are satisfied at all frequencies. The total complex power supplied to the network by V_3 is then found to be

$$\psi_t = \sum_{n=1}^{n=5} \psi_n = (1 + j \cot \beta x) \mid V_3 \mid^2 / 2K = \frac{V_3 V_3^*}{Z_{in}^*}, \tag{10}$$

the real part of which represents the power P_t delivered to the network. The input impedance Z_{in} of the network at the generator terminals is evidently

$$Z_{in} = 2K/(1 - j \cot \beta x). \tag{11}$$

If $x = \lambda_0/4$, the input impedance is $2K$. If the broad-banding stub is used as outlined above, the network presents an almost constant impedance to the generator over a wide range of frequencies.

The square of the absolute value of the reflection coefficient q_v is the power-loss factor, as is readily seen by taking the ratio of the real part of ψ_5 to that of ψ_t; thus,

$$\frac{Re\, \psi_5}{Re\, \psi_t} = \frac{Z_B - K_2}{Z_B + K_2}\Big|^2 = \mid q_v \mid^2.$$

The real parts of ψ_3 and ψ_4 are equal, showing that the dissipation in Z_A and Z_B is equally divided.

The reversible nature of the network is demonstrated by interchanging R and the generator and letting $K_1 = K_2 = K = R/2$. Using the same procedure, it turns out again that, if the broad-banding stub is used, the input impedance is practically constant, dissipation in the loads is equal and the power-loss factor is $\mid q_v \mid^2$.

K_1 need not equal K_2, but in order to match impedances it then becomes necessary to have $x = \lambda_0/4$ and $K_1 = \sqrt{2RK_2}$. The bridge works just as well at λ_0, but is not quite so broad-band as when $K_1 = K_2$, owing to the transforming action of the lines K_1. The bandwidth can be improved as before by using a broad-banding stub of impedance $2K_1$ on the line $2K_2$ supplying 0–3. The system is about equally broad-band in either of its reversible directions.

III. Examples of Use of the Power Equalizer

In connection with a certain antenna design, it was necessary to investigate the nature of the field patterns obtained from an array of equally energized radiators mounted on the four sides of a square tower. The opposite radiators were connected together in such a way that the currents in them were in time phase, but opposing each other in a peripheral sense around the tower. Two equal, uncoupled sets were thus formed, and, since it was desired to phase them in quadrature, the power equalizer was applicable.

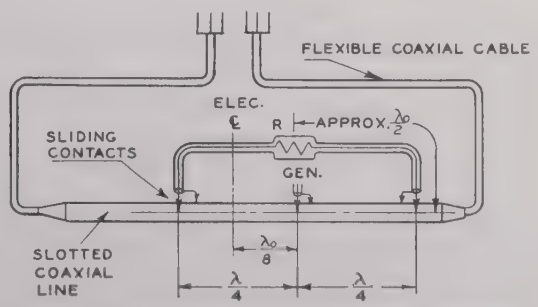

Fig. 2—A laboratory version of the power equalizer.

Ordinarily, in order to obtain good patterns from such an antenna over a wide range of frequencies and variations of tower size and spacing parameters, etc., a prohibitive amount of work would have had to be done

for each different variation to match impedances all the way to the generator on each line. With an adjustable laboratory version of the power equalizer, similar to that shown in Fig. 2, the work was made easy, and almost perfectly equalized patterns were always obtained. Fig. 3 compares two patterns taken on the same

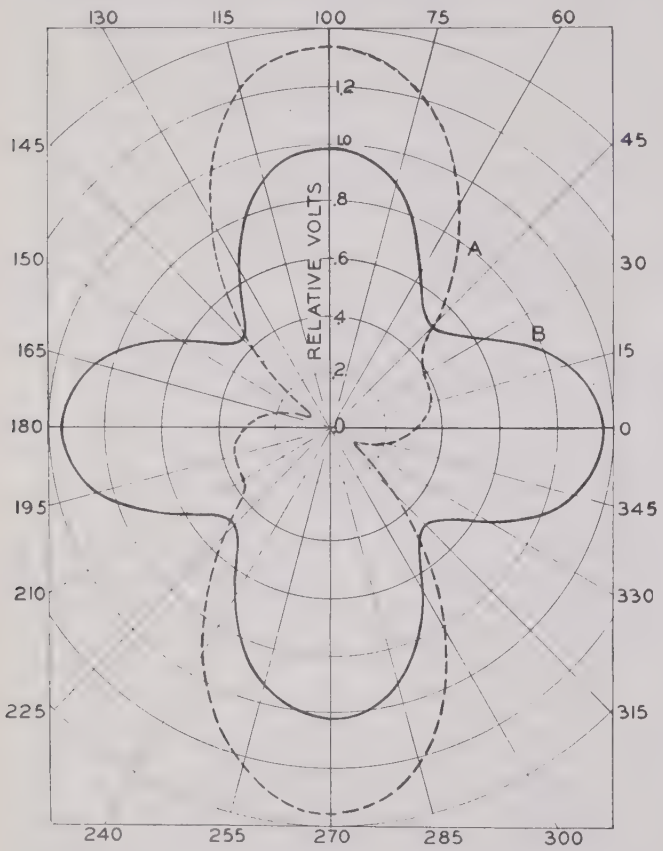

Fig. 3—Comparison of measured field patterns. Curve B with, and curve A without, the power equalizer connected.

antenna at the same frequency with and without the branch loop containing R in Fig. 2. Curve B illustrates how well the power equalizer equalized the radiation from the four tower faces. Much of the remaining asymmetry can be attributed to small differences between the opposite radiators and to variations in the cables.

The application of the power-equalizer principle to television antennas is not difficult. A bridge circuit[1] almost identical with Fig. 1(a) is already commonly used to diplex the picture and sound transmitters into an antenna which satisfies all requirements for the power equalizer. The picture transmitter drives terminals 0–3, while the sound transmitter drives terminals 1–2.

The necessary addition is a separation filter in the sound side which will divert the reflected energy of the picture transmitter, at and near its carrier into the resistor R without serious reflection. The filter must also prevent sound-power dissipation in the resistor. Such filters are well known.[2,3] The secret of satisfactory operation in this case is to match the antenna halves at the narrow sound-channel frequency, and then use the power equalizer to achieve broadband match for the picture frequencies. Another method is to use a separation filter to insert the sound energy into the picture side of the bridge. Both signals are then equalized, and only one line up the tower need be used if the bridge is located at the top. The cost of good transmission line is high.

IV. Conclusions

Since certain poorly matched antennas may be made to give excellent service at a negligible cost in lost power, it is felt that the power-equalizing bridge will definitely influence antenna designs. It is a powerful tool, applicable in any circumstance where the loading satisfies (2).

[1] L. J. Wolf, "Triplex antenna for television and F-M," *Electronics*, vol. 20, p. 88; July, 1947.
[2] See p. 91 of footnote reference 1.
[3] N. E. Lindenblad, "Antennas and transmission lines at the Empire State television station," *Communications*, vol. 20, pp. 13–18; May, 1949. Also vol. 21, pp. 10–26, April, 1941, and vol. 21, pp. 9–33, May, 1941; esp. May, 1941, p. 9.

Transmission-Line Characteristics of the Sectoral Horn*

HERBERT S. BENNETT†, SENIOR MEMBER, IRE

Summary—**The sectoral horn is analyzed from the engineering viewpoint in such a manner as to make it feasible to consider it as one component of an over-all microwave transmission system. Equivalent network functions are derived and graphed which are based on the consideration of the sectoral horn as a nonuniform transmission line. The resulting curves should be useful to those designing systems containing sectoral-horn components. The physical significance of the derived normalized functions is discussed, and the applicability of network philosophy is pointed out.**

* Decimal classification: R117.1. Original manuscript received by the Institute, September 16, 1948; revised manuscript received, January 20, 1949.
† Watson Laboratories, Red Bank, N. J.

I. Introduction

THE COMPLETE solution of Maxwell's equations for a given electromagnetic field problem is intimately connected with the geometry of the system. After setting up the differential equations of the

field in the appropriate co-ordinate system, the classical approach has been to treat each problem as a peculiar and individual entity. The solution of the equations, with appropriate boundary conditions, for the region under consideration has been the end objective. Under this approach, no co-ordinated attempt is made to apply the results to the solution of problems with similar geometries.

On the other hand, by borrowing a leaf from the procedures developed by the circuit designers who deal with the analysis of such iterative structures as filter networks and transmission lines, it can be seen that their techniques may be used with profit in the microwave regions where only the classical boundary-value "cavity" method of solving the Maxwell field equations had originally been used.

In this paper we will analyze the sectoral geometry, with the field vector orientation shown in Fig. 1, as one component of a microwave transmission system. This geometry is characterized by a uniformly increasing cross section in the plane perpendicular to the axis of symmetry. Thus we may expect the nonuniform trans-

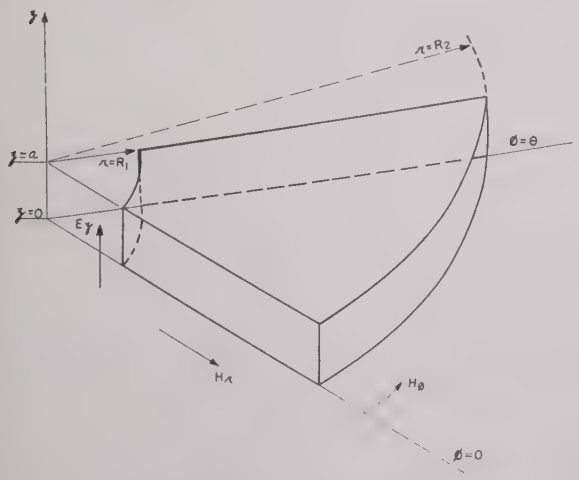

Fig. 1—Sectoral horn geometry in cylindrical co-ordinates (E type field shown).

mission-line formulation (or the "sectoral radial" transmission line, as we shall call it) to be applicable. In securing the solution, we shall attempt to mimic the uniform transmission-line representation. This will aid in the understanding of the physical significance of the various functions, and will require merely an extension of the concepts of the uniform transmission line which are more commonly used and understood.

The sectoral geometry being considered has wide application in the microwave field. Some of its applications are: (1) coupling section between two rectangular guides, (2) resonator, and (3) radiating horn antenna.

It should be noted that this paper applies the impedance and network concepts of Schelkunoff, Marcuvitz, and others. The sectoral-horn analysis contained herein makes use of the radial-transmission-line theory developed by Marcuvitz.[1]

II. Glossary

a = height of horn as defined in Fig. 1

$ctr\ (x, y)$ = sectoral-horn transmission functions (see (6))

$Ctr\ (x, y) = \dfrac{1}{Tnr\ (x, y)}$ sectoral-horn transmission functions (see (7))

E = electric field vector

H = magnetic field vector

$H_n^{(2)}(x)$ = Hankel function $= J_n(x) - jN_n(x)$

$$H_n^{(2)\prime}(x) = \frac{d}{dx}\left(H_n^{(2)}(x)\right)$$

$J_n(x)$ = Bessel function of first kind of order n and argument x

$$J_n'(x) = \frac{d}{dx}\left(J_n(x)\right)$$

$Kr(x, y)$ = sectoral-horn transmission functions (see (8))

$$k = \frac{2\pi}{\lambda}$$

$m = 1, 2, 3, 4, \cdots$ = the order of the mode for the field in the ϕ direction

$N_n(x)$ = Neumann function (or Bessel function of the second kind) of order n and argument x

$$N_n'(x) = \frac{d}{dx}\left(N_n(x)\right)$$

$$n = \frac{m\pi}{\theta}$$

$$n' = \sqrt{\frac{\epsilon}{\mu}}$$

r = cylindrical co-ordinate as defined in Figs. 1 and 3

$x = kR_1$ = input radius in wavelengths (see Fig. 3)

$y = kR_2$ = output radius in wavelengths (see Fig. 3)

$Y_{(x)}$ = admittance at a given cross section, x, i.e., the ratio of equivalent current to equivalent voltage at that cross section

$Y_{(x)}'$ = normalized input admittance

[1] C. G. Montgomery, "Principles of Microwave Circuits," vol. 8, Chapter 8, McGraw-Hill Book Company, Inc., New York, N. Y., 1948.

$$= \frac{Y_{(x)}}{Y_0'} \text{ (see (4))} = -\frac{H_\phi(x)}{n'E_z(x)}$$

$Y_{(y)}'$ = normalized output admittance

$$= \frac{Y_{(y)}}{Y_0'}$$

$Y_0' = \dfrac{n'r\theta}{a}$ = normalizing admittance factor (In the uniform case this reduces to the characteristic admittance)

z = cylindrical co-ordinate as defined in Figs. 1 and 3

λ = free-space wavelength

ϕ = cylindrical co-ordinate as defined in Figs. 1 and 3

θ = flare angle as defined in Figs. 1 and 3.

III. Relative Input Admittance Functions and Their Physical Significance

By solving the electromagnetic boundary value problem of Fig. 1 in cylindrical co-ordinates, assuming perfectly conducting walls with a perfect dielectric in between and E type field, (1), (2), and (3) may be secured:

$$E_z = [AJ_n(kr) + BN_n(kr)] \sin n\phi \tag{1}$$

$$H_r = \left[\frac{-n}{j\omega\mu r} AJ_n(kr) + BN_n(kr)\right] \cos n\phi \tag{2}$$

$$H_\phi = jn'[AJ_n'(kr) + BN_n'(kr)] \sin n\phi. \tag{3}$$

A and B are constants which are evaluated[2] from the boundary conditions. By proper manipulation of the equations one can achieve a relative or normalized input admittance $Y_{(x)}'$ similar to the one developed by Marcuvitz for the radial-line case, except that the component functions (6)–(8) are more complicated.

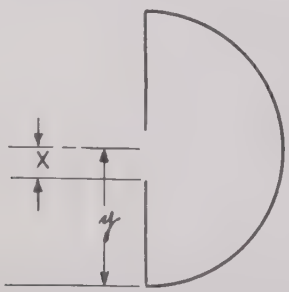

Fig. 2—Resonant cavity representation.

$$Y_{(x)}' = \frac{\text{input admittance at } x}{Y_0'} = \frac{j + Y_{(y)}' \operatorname{ctr}(x, y) K_r(x, y)}{Ctr(x, y) + jY_{(y)}' K_r(x, y)}. \tag{4}$$

[2] H. S. Bennett, "The electromagnetic transmission line characteristics of the sectoral horn geometry," thesis, Polytechnic Institute of Brooklyn, Brooklyn, N. Y., pp. 6–19; June, 1947.

This is analogous to the relative input admittance for the uniform transmission line.

$$Y_{(x)'\text{uniform}} = \frac{j + Y_{(y)}' \cot(y - x)}{\cot(y - x) + jY_{(y)}'}. \tag{5}$$

The various symbols used throughout are explained in Figs. 1 and 3 and in the glossary of symbols in Section

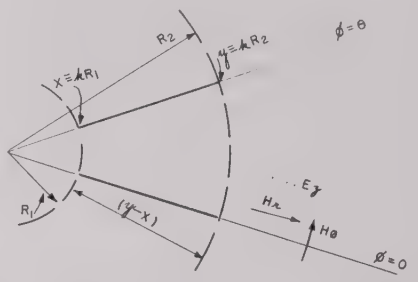

Fig. 3—Plan view of sectoral horn geometry (for reference with succeeding figures).

II. The component functions in (4) are new and defined as follows:

$$ctr(x, y) \equiv \frac{N_n'(x)J_n(y) - J_n'(x)N_n(y)}{J_n(x)N_n(y) - N_n(x)J_n(y)} \tag{6}$$

$$Ctr(x, y) \equiv \frac{1}{\operatorname{Tnr}(x, y)} \equiv \frac{J_n(x)N_n'(y) - N_n(x)J_n'(y)}{J_n'(x)N_n'(y) - N_n'(x)J_n'(y)} \tag{7}$$

$$Kr(x, y) \equiv \frac{J_n(x)N_n(y) - N_n(x)J_n(y)}{J_n'(x)N_n'(y) - N_n'(x)J_n'(y)}. \tag{8}$$

If y/x approaches 1 and $(y-x)$ remains finite it means, in effect, that we are considering a portion of the horn so far out that the flaring sides represented by $(y-x)$ appear to be parallel and in the limit when $y/x = 1$ they are parallel. Thus, in this limit, the relative input admittance functions for the sectoral case reduce to those applicable to uniform transmission lines. By employing the asymptotic expressions for Bessel and Neumann functions of large argument it can be shown that for $x, y \gg n$, (4) passes into (5). If we tabulate and plot these component functions of (4) as extensively as the ordinary trigonometric functions have been tabulated, we should find (4) just as useful for sectoral radial-line calculations as (5) is in the uniform-line case; and furthermore, if x and y are sufficiently large, the uniform-line formulas offer an excellent approximation. Component functions other than (6)–(8) could be evolved for the horn; but, as indicated below, our functions have very definite physical significance.

Consider the output end shorted, i.e., $Y_{(y)}' = \infty$. From (4) we get

$$Y_{(x)}' = -j \operatorname{ctr}(x, y). \tag{9}$$

[3] See pp. 21–22 of footnote reference 2.

n the limit of the uniform line where $y/x=1$, this be-omes

$$Y_{(x)}' = -j \cot (y - x). \tag{10}$$

For the output properly terminated to give $Y_{(y)}'=0$,

$$Y_{(x)}' = j \operatorname{Tnr} (x, y), \tag{11}$$

nd for the uniform line this becomes

$$Y_{(x)}' = j \tan (y - x). \tag{12}$$

The familiar formulas showing the fact that quarter-vave shorted uniform lines and half-wave open uniform nes both have zero admittance, etc., can be deduced rom the preceding statements; and we see that for alues of y/x not too far removed from unity the sec-oral radial line approaches this uniform line behavior. Graphs of the type shown in this paper will indicate or which values of y/x (in any given range of $(y-x)$) uch engineering approximations are valid.

It can be shown[4] that when the sectoral geometry is sed to connect two rectangular waveguides $1<y/x<2$. t can also be shown[4] that our graphs can be used for igher order modes by suitably adjusting the flare angle.

$$n = m\frac{\pi}{\theta} = 1 \times \frac{180°}{30°} = 2 \times \frac{180°}{60°}. \tag{13}$$

The data on the ctr function can be used in connec-on with the design of the sectoral geometry as a non-issipative resonant cavity. In order to have a true avity we must, in addition, have the "x" end shorted nd $y_{(y)}'=\infty$. If we can neglect the lumped circuit ntroduced by the discontinuity at the input, the esonant frequencies would be determined by the poles f the ctr curves. (Remember that $(y-x)$ is a function f frequency.) The quasicyclic nature (approximating he interval π) of the ctr function indicates that there ill be a series of resonant frequencies. It should be mphasized that the cycles are only similar, not identi-l, and therefore the resonant frequencies for a given ode order (e.g., $m=1$) are not just simple multiples f each other.

The case where $n=1$, $\theta=180°$ is of interest only as a esonant cavity (see Fig. 2) since the only type of rmination that is practical is $Y_{(y)}'=\infty$.

The data in Section IV may be used for calculating mpedance characteristic of a radiating horn. If the orn is considered as feeding into the impedance of ee space $=\sqrt{\mu_0/\epsilon_0}$, we can determine the input ad-ittance from (4) and the definition of the normalizing ctor, provided the horn is long enough, in which case can be shown[5] that (4) reduces to:

$$Y_{(x)}' = \frac{H_n^{(2)\prime}(x)}{H_n^{(2)}(x)}. \tag{14}$$

[4] See pp. 23–24 of footnote reference 2.
[5] See pp. 15–16 of footnote reference 2.

If the horn is not long enough to justify the use of (14) instead of (4), but the susceptance of the lumped circuit equivalent of the discontinuity at y is small compared with $\sqrt{\epsilon_0/\mu_0}$, then we get $Y_{(y)}'=a/r\theta$; otherwise $Y_{(y)}'$ must include the effect of the discontinuity.

It may happen that in any given design problem y/x and/or $(y-x)$ will fall outside the range of the curves in Section IV. This can be handled by breaking up the given sectoral geometry into two or more (usually two will be sufficient) sectoral radial lines in tandem. The output impedance of the first one is merely the input impedance of the second, and so forth. In this case there are no discontinuities at our assumed junction points. However, in most other practical cases a knowledge of the circuit elements equivalent to the discontinuities is necessary for the design of an over-all microwave transmission system.

IV. Discussion of Function Graphs

In this section are shown graphs of the functions (Figs. 4 through 12) for three values of flare angle; 180° (which is the limiting case of interest in the direction of large flare angle), 27.7°, and 51.4° are shown. These odd flare angles were made necessary because only multiples of half-order Bessel and Neumann function tables[6,7] were available. However, in the usual region of interest, which is between $\theta=20°$ and $\theta=65°$, the plotting of curves for multiples of half-order Bessel and Neumann functions should allow interpolations with engineering accuracy for θ values. For example, if $n=13/2$, and $m=1$, then $\theta=27.7°$; while for $n=11/2$, $m=1$; $\theta=32.7°$. At the higher end however, the interval is large. $n=7/2$ gives $\theta=51.4°$, while $n=5/2$ gives $\theta=71.9°$. The $n=3$ values ($\theta=60°$) would be very useful in this area.

The curves shown in this section were not intended as working curves. They were intended to illustrate the limiting ranges of usefulness. Thus, in some areas of the function graphs, the curves have relatively large slopes. These areas are not very useful for design purposes, since small changes in frequency or physical dimensions will cause very large changes in characteristics. Of course there are some design problems where such critical (resonant effect) response is desired. However, it is not advised that the very steep portions of the curves be used because the accuracy is not very good in these ranges. To aid somewhat in the use of these steep portions, the asymptotes to the curves are drawn as dash-dot vertical lines. (See Figs. 4 and 6.)

Two cycles were plotted for each curve to illustrate the repetitive nature of the functions. In general as we proceed out along the $(y-x)$ axis, the succeeding cycles become more "well behaved" over larger ranges of y/x and also, the curves, for adjacent values of y/x, form

[6] E. Jahnke and F. Emde, "Tables of functions," Dover Publications, New York, N. Y., 1945.
[7] Math. Tables Project, National Bureau of Standards, "Tables of Spherical Bessel Functions, Vol. I," Columbia University Press, New York, N. Y., 1947.

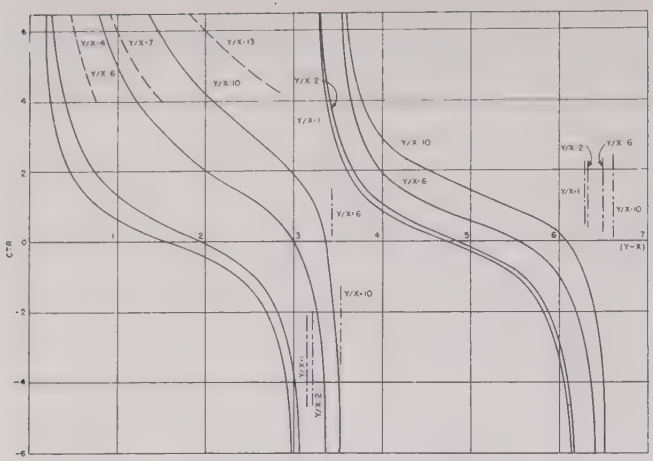

Fig. 4—*ctr* function
$n=1$ (dominant mode $\theta=180°$)
E type impressed field.

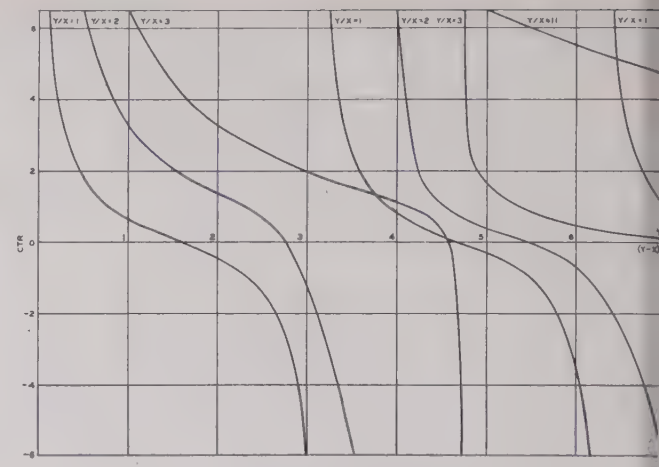

Fig. 7—*ctr* function
$n=7/2$ (dominant mode $\theta=51.4°$)
E type impressed field.

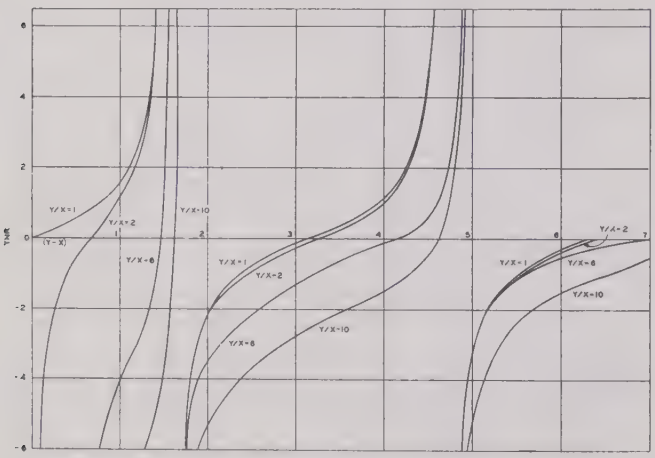

Fig. 5—*Tnr* function
$n=1$ (dominant mode $\theta=180°$)
E type impressed field.

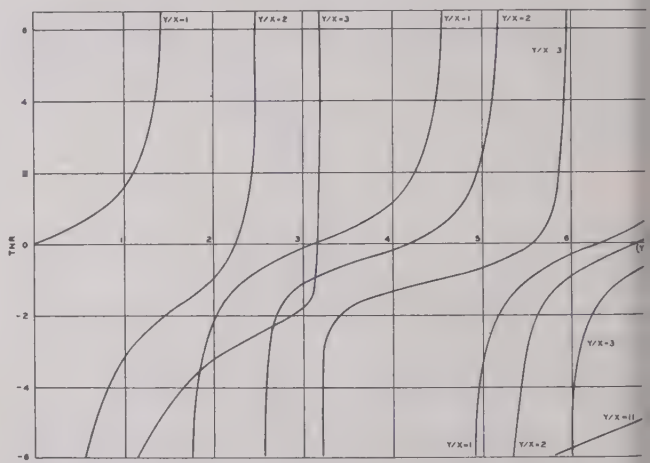

Fig. 8—*Tnr* function
$n=7/2$ (dominant mode $\theta=51.4°$)
E type impressed field.

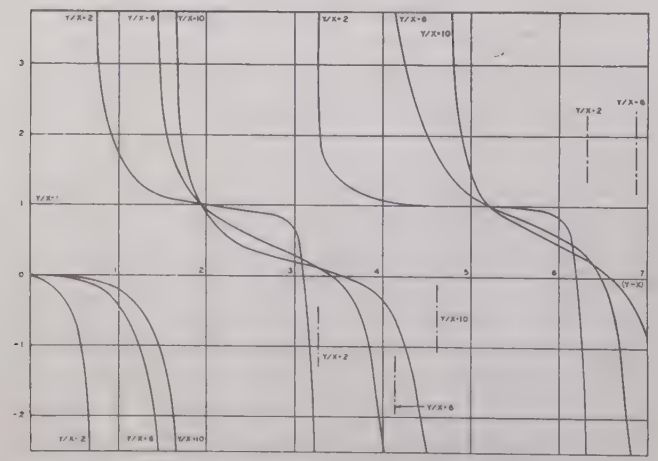

Fig. 6—*Kr* function
$n=1$ (dominant mode $\theta=180°$)
E type impressed field.

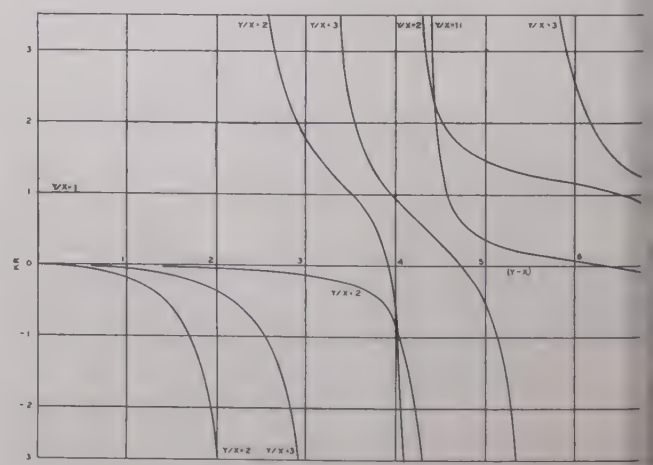

Fig. 9—*Kr* function
$n=7/2$ (dominant mode $\theta=51.4°$)
E type impressed field.

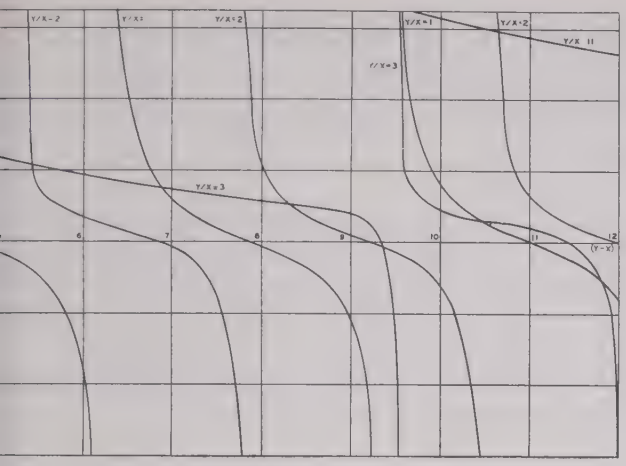

Fig. 10—*ctr* function
$n=13/2$ (dominant mode $\theta=27.7°$)
E type impressed field.

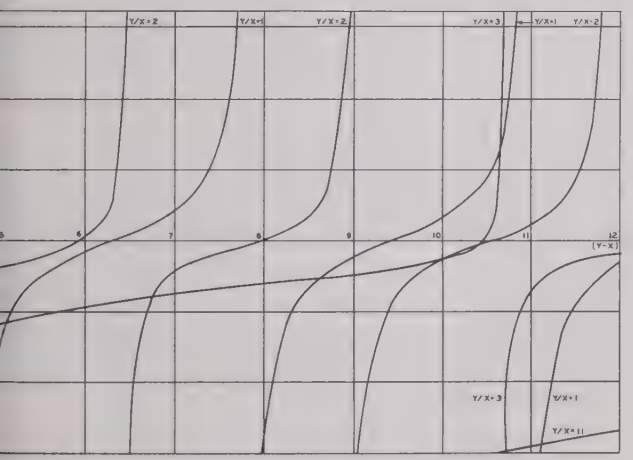

Fig. 11—*Tnr* function
$n=13/2$ (dominant mode $\theta=27.2°$)
E type impressed field.

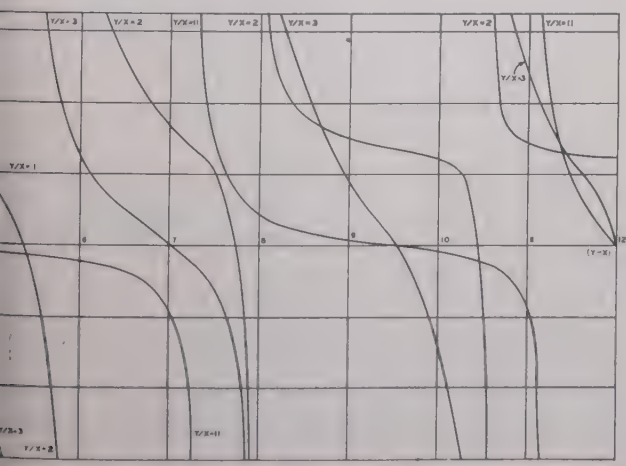

Fig. 12—*Kr* function
$n=13/2$ (dominant mode $\theta=27.7°$)
E type impressed field.

tighter envelopes. Whenever a family of curves in any given cycle of the *ctr* or *Tnr* functions start to cross each other, we have reached the upper limit of usefulness for the y/x parameter of that group insofar as engineering calculations are concerned, since it is not useful to interpolate between two curves which cross each other. The crossing is caused by the fact that the range in question requires x to be less than n, and it can be shown that $x<n$ defines the attenuation region.

It can be shown that when $x<n/(y/x)$

$$ctr = n/x \tag{15}$$

$$Tnr = -n/x \tag{16}$$

$$Kr = \left(\frac{-x}{n}\right)\left(\frac{J_n(y)}{J_n'(y)}\right). \tag{17}$$

In the appropriate ranges where $x<n/(y/x)$ we can use the relationships of (15) through (17) to secure very quickly additional graphs for intermediate values of y/x. This is illustrated in the *ctr* function graph for $n=1$ (Fig. 4) by the dotted line curves for $y/x=4$, $y/x=7$, and $y/x=13$. These curves aid greatly when a method of interpolation has to be decided upon, since they show the relative spacing as y/x varies.

It should be noted that, on the curves for $n=1$, the asymptotic values are indicated as dash-dotted lines. The values of zeros of the denominators for n half order were not available, so the asymptotic values are only shown on the curves for $n=1$. However, by studying the upper and lower lobes of the function as it goes to infinity one can estimate fairly well the $(y-x)$ values of the asymptote.

V. Conclusions

This paper has attempted to merely outline the steps leading to the resulting sectoral transmission functions drawn in Figs. 4 through 12. Since none of the modern calculating machines were available to the author, the calculation of the graphs was a very laborious chore. Therefore, only as many curves as were absolutely necessary to illustrate the point were actually plotted. Should these functions prove useful enough, it is believed that additional curves could be readily calculated by using one of the many large calculators now in existence. In the meantime, however, it is believed that the foregoing material should assist in the design of microwave transmission circuits employing the sectoral horn geometry.

VI. Acknowledgments

The author wishes to acknowledge gratefully the valuable assistance furnished by E. Weber and N. Marcuvitz of the Polytechnic Institute of Brooklyn in the preparation of the thesis upon which this material is based. Appreciation is also expressed to the USAF, Air Materiél Command, Watson Laboratories, and to the Polytechnic Institute of Brooklyn for granting permission to the author to submit this paper.

On the Theory of the Radiation Patterns of Electromagnetic Horns of Moderate Flare Angles*

C. W. HORTON†

Summary—A method attributed to Schelkunoff for the computation of radiation patterns is considered. For the case of transverse electric waves in a waveguide or horn of moderate flare angle, the problem of calculating the radiation pattern is reduced to that of evaluating two definite integrals. These integrals are evaluated for rectangular, circular, and semicircular horns for some common modes of vibration. A small amount of experimental data are presented to illustrate the agreement between theory and experiment.

I. Introduction

A METHOD of computing radiation patterns from electromagnetic horns that is easy to apply and which leads to patterns that agree well with experimental patterns has been developed by Schelkunoff.[1,2] Schelkunoff's theorems may be formulated in several different ways of which the following is selected for the present purpose. When an electromagnetic wave is radiated from the open end of a semi-infinite waveguide, the radiation pattern is the same as the pattern of a suitable distribution of surface electric currents J, and of surface magnetic currents M, over the aperture Σ of the waveguide. These current distributions are determined by

$$\vec{J} = \vec{n} \times \vec{H}^{\circ} \tag{1}$$

$$\vec{M} = -\vec{n} \times \vec{E}^{\circ}. \tag{2}$$

$\vec{n}$ is the normal to the aperture pointing out into the space away from the waveguide. $\vec{E}^{\circ}$ and $\vec{H}^{\circ}$ are the values of the electric and magnetic fields that would exist across Σ if the waveguide had not been terminated. When computing the radiation pattern of the current distributions, it is necessary to allow for the presence of the metallic waveguide which acts as a baffle. If the waveguide is large, its effect is secondary and may be neglected. This approximation is made in the following analysis.

It can be shown that the modes of vibration in sectoral and conical horns approach the corresponding modes of vibration in rectangular and circular waveguides as the limiting case when the flare angle ap proaches zero. This means that the radiation patter which are derived for an open waveguide may be appli directly to an electromagnetic horn, as long as the fla angle is not too large.

The values of $\vec{E}$ and $\vec{H}$ in the radiation field may computed from

$$\vec{E} = i\omega\mu\vec{A} - (1/i\omega\epsilon)\ \text{grad div}\ \vec{A} - \text{curl}\ \vec{F} \tag{3}$$

$$\vec{H} = i\omega\epsilon\vec{F} - (1/i\omega\mu)\ \text{grad div}\ \vec{F} + \text{curl}\ \vec{A} \tag{4}$$

where $\vec{A}$ and $\vec{F}$ are a magnetic and an electric vector p tential, respectively, which are given by

$$\vec{A} = (1/4\pi)\int_{\Sigma} (\vec{J}/r')\ \exp(ikr')d\Sigma \tag{5}$$

$$\vec{F} = (1/4\pi)\int_{\Sigma} (\vec{M}/r')\ \exp(ikr')d\Sigma. \tag{6}$$

Here r' is the distance from the surface element $d\Sigma$ the field point. These equations are in mks units and a true for periodic fields with the time factor $\exp(-i\omega$

In the next section the case of a transverse electr wave is considered, and (1) to (6) are reduced to a simp form suitable for the computation of the distant. Fraunhofer, diffraction pattern.

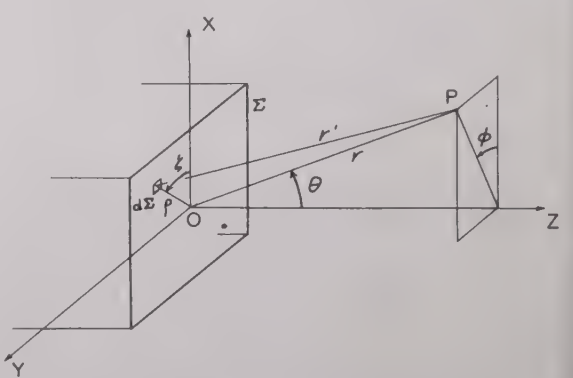

Fig. 1—The relations between the co-ordinate systems and the waveguide.

II. Application to the Transverse Electric Fiel

Consider the co-ordinate systems shown in Fig. The location of the field point P is given in spheri co-ordinates (r, θ, ϕ), while the location of the apertu element $d\Sigma$ is given in polar co-ordinates (ρ, ζ). One

$$r'^2 = \rho^2 + r^2 - 2r\rho\cos(\phi - \zeta)\sin\theta.$$

For large values of r, the ρ^2 may be neglected and binomial expansion may be applied to give

* Decimal classification: R118×R120. Original manuscript received by the Institute, September 10, 1948; revised manuscript received, January 24, 1949.

This work has been done under sponsorship of the Bureau of Ordnance, Navy Department, Contract NOrd-9195, at The University of Texas, and has been extracted from "On the Theory of the Radiation Patterns of Electromagnetic Horns," Bumblebee Report No. 86, Defense Research Laboratory, The University of Texas.

† Defense Research Laboratory, The University of Texas, Austin, Tex.

[1] S. A. Schelkunoff, "Some equivalence theorems of electromagnetics and their application to radiation problems," *Bell Sys. Tech. Jour.*, vol. 15, pp. 92–112; January, 1936.

[2] S. A. Schelkunoff, "On diffraction and radiation of electromagnetic waves," *Phys. Rev.*, vol. 56, pp. 308–316; August 15, 1939.

$$r' \cong r - \rho \cos(\phi - \zeta) \sin\theta. \quad (7)$$

he r' in the denominator of (5) and (6) may be re-aced directly by r, while the r' in the exponent must be placed by the more accurate form of (7). Thus (5) id (6) become

$$\vec{A} = \{\exp(ikr)/4\pi r\} \cdot \int_{\Sigma} \vec{J} \exp\{-ik\rho \cos(\phi - \zeta) \sin\theta\} d\Sigma \quad (8)$$

$$\vec{F} = \{\exp(ikr)/4\pi r\} \cdot \int_{\Sigma} \vec{M} \exp\{-ik\rho \cos(\phi - \zeta) \sin\theta\} d\Sigma. \quad (9)$$

lthough $\vec{A}$ and $\vec{F}$ are functions of θ and ϕ as well as r, we confine our attention to distant field points so that owers of $(1/r)$ greater than the first are negligible, en $\vec{A}$ and $\vec{F}$ may be treated as a constant vector times function of r in performing the vector operations indi-ted in (3) and (4).

A transverse electric wave in the waveguide may be presented by

$$\vec{E} = \{\vec{i} f(x, y) + \vec{j} g(x, y)\} \exp(ik'z - i\omega t) \quad (10)$$

here $k'(=2\pi/\lambda_{\text{guide}})$ need not equal the free-space lue k. The magnetic field $\vec{H}$ associated with $\vec{E}$ has com-nents given by

$$\left.\begin{aligned} H_x &= -(k'/\omega\mu) g(x, y) \exp(ik'z - i\omega t) \\ H_y &= (k'/\omega\mu) f(x, y) \exp(ik'z - i\omega t) \\ H_z &= (1/i\omega\mu)\{g_x(x, y) - f_y(x, y)\} \exp(ik'z - i\omega t) \end{aligned}\right\}. \quad (11)$$

When $\vec{E}$ is evaluated from (3), (8), (9), (10), and (11) d powers of $(1/r)$ higher than the first are neglected, e finds

$$\left.\begin{aligned} E_r &= 0 \\ E_\theta &= -i(k + k' \cos\theta)\{R_1(\theta, \phi) \cos\phi + R_2(\theta, \phi) \sin\phi\}(1/r) \exp(ikr - i\omega t) \\ E_\phi &= +i(k' + k \cos\theta)\{R_1(\theta, \phi) \sin\phi - R_2(\theta, \phi) \cos\phi\}(1/r) \exp(ikr - i\omega t) \end{aligned}\right\} \quad (12)$$

here

$$\begin{pmatrix} f(x, y) \\ g(x, y) \end{pmatrix} (\theta, \phi) = (1/4\pi) \int_{\Sigma} \begin{pmatrix} f(x, y) \\ g(x, y) \end{pmatrix} \cdot \exp\{-ik\rho \cos(\phi - \zeta) \sin\theta\} d\Sigma. \quad (13)$$

his derivation is given in the Appendix. Since $\vec{E}$ is a ansverse wave, the components of the magnetic field ay be found from the relationships

$$\left.\begin{aligned} H_r &= 0 \\ H_\theta &= -(k/\omega\mu) E_\phi \\ H_\phi &= +(k/\omega\mu) E_\theta \end{aligned}\right\}. \quad (14)$$

It might be pointed out that, normally, in spherical co-ordinates, θ is required to be positive, so that two values of ϕ (say, ϕ_0 and $\phi_0 + \pi$) are required to specify a full plane. However, it is equally permissible to specify a fixed value of ϕ and allow θ to take on both positive and negative values. This interpretation will be used in the discussion of patterns.

The problem of computing the radiation pattern of a semi-infinite waveguide for a transverse electric wave has been reduced to the problem of performing the integration of (13). This integration will be performed for various common waveguide sections.

III. Symmetry Considerations

It is possible to state certain general properties of the radiation pattern, provided the functions $f(x, y)$ and $g(x, y)$ are real. For example, the real parts of $R_1(\theta, \phi)$ and $R_2(\theta, \phi)$ are even functions of θ while the imaginary parts are odd functions of θ.

Consider the pattern in the plane $\phi = 0$. If the waveguide is symmetric about the x axis, and if $g(x, y)$ is an odd function of y, the component $E_\phi = 0$. Similarly, if $f(x, y)$ is an odd function of y, $E_\theta = 0$. On the other hand, if the waveguide is symmetric about the y axis, then $R_1(\theta, \phi)$ is pure real or imaginary according as $f(x, y)$ is an even or odd function of x. Likewise, $R_2(\theta, \phi)$ is even or odd according as $g(x, y)$ is an even or odd function of x.

Consider next the plane $\phi = 90°$. If the waveguide is symmetric about the y axis, and if $f(x, y)$ is an odd function of x, the component $E_\phi = 0$. Similarly, if $g(x, y)$ is an odd function of x, $E_\theta = 0$. On the other hand, if the waveguide is symmetric about the x axis, then $R_1(\theta, \phi)$ is pure real or imaginary according as $f(x, y)$ is an even or odd function of y. Likewise, $R_2(\theta, \phi)$ is even or odd according as $g(x, y)$ is an even or odd function of y.

IV. The Effect of a Perfectly Conducting Baffle

If the mouth of the waveguide or horn is mounted in a large, flat, perfectly conducting sheet, the pattern will be altered. The effect of these changes has been discussed by Schelkunoff.[3] When these changes are carried out, one has in place of (12)

$$\left.\begin{aligned} E_r &= 0 \\ E_\theta &= -2ik\{R_1(\theta, \phi) \cos\phi + R_2(\theta, \phi) \sin\phi\}(1/r) \exp(ikr - i\omega t) \\ E_\phi &= +2ik \cos\theta\{R_1(\theta, \phi) \sin\phi - R_2(\theta, \phi) \cos\phi\}(1/r) \exp(ikr - i\omega t) \end{aligned}\right\}. \quad (15)$$

V. Transverse Electric Waves in a Rectangular Waveguide

The radiation patterns of rectangular horns are well known,[4] and consequently they will be treated briefly

[3] See page 312 of footnote reference 2.

[4] S. A. Schelkunoff, "Electromagnetic Waves," p. 359, D. van Nostrand Co., New York, N. Y., 1945.

only in order to show the practicality of the present approach.

The transverse electric wave $TE_{m,n}$ has an electric field characterized by

$$f(x, y) = -(n\pi/b)\cos(m\pi/2 + m\pi x/a)\sin(n\pi/2 + n\pi y/b) \quad (16)$$

$$g(x, y) = +(m\pi/a)\sin(m\pi/2 + m\pi x/a)\cos(n\pi/2 + n\pi y/b) \quad (17)$$

where a is the dimension of the waveguide in the x direction and b is the dimension in the y direction.

In order to evaluate $R_1(\theta, \phi)$ and $R_2(\theta, \phi)$ simply, it is desirable to introduce two dimensionless parameters, α and β, defined as

$$\alpha = (ka/2)\cos\phi\sin\theta \quad (18)$$

$$\beta = (kb/2)\sin\phi\sin\theta. \quad (19)$$

Integration of (13) gives

$$R_1(\theta, \phi) = (\pi n^2 ab/8b)A\alpha/\{(m\pi/2)^2 - \alpha^2\}\{(n\pi/2)^2 - \beta^2\} \quad (20)$$

and

$$R_2(\theta, \phi) = -(m^2 b/n^2 a)R_1(\theta, \phi). \quad (21)$$

The constant A takes on the following four possible values:

m even, n even	$A = i\sin\alpha\sin\beta$
m even, n odd	$A = \sin\alpha\cos\beta$
m odd, n even	$A = \cos\alpha\sin\beta$
m odd, n odd	$A = -i\cos\alpha\cos\beta.$

In the particular case of the $TE_{0,1}$ mode the radiation patterns can be evaluated to give

$$\left.\begin{aligned} E_r &= 0 \\ E_\theta &= i(\pi a/8)(k + k'\cos\theta) \\ &\quad \cdot\cos\phi(\sin\alpha/\alpha)\cos\beta/\{(\pi/2)^2 - \beta^2\} \\ E_\phi &= -i(\pi a/8)(k' + k\cos\phi) \\ &\quad \cdot\sin\phi(\sin\alpha/\alpha)\cos\beta/\{(\pi/2)^2 - \beta^2\} \end{aligned}\right\}. \quad (22)$$

The spherical wave factor $(1/r)\exp(ikr - i\omega t)$ has been omitted in these and in the remainder of the equations. The various factors have simple physical explanations. In the $TE_{0,1}$ mode there is no variation in the electric field strength with the variable x. Thus there is no shading in the x direction, and the part of the pattern that results from integrating with respect to x is $(\sin\alpha/\alpha)$, which is the radiation pattern commonly associated with an unshaded rectangular opening. In the y direction the intensity of the electric vector varies cosinusoidally. This shading gives rise to the terms which are a function of β. The terms in ϕ represent the effects of the polarized source. The factors of the form $(1+\cos\theta)$ occur because of the flow of energy through the opening.

Figs. 2 and 3 show the experimental and theoretic patterns in the E and H planes, respectively, for a l sectoral horn. By the "E plane" is meant the plane cc taining the electric vector in the $TE_{0,1}$ mode. The mensions of the horn are $1.82\lambda_0$ in the H plane a $1.47\lambda_0$ in the E plane. It may be seen that the agr ment between theory and experiment is good.

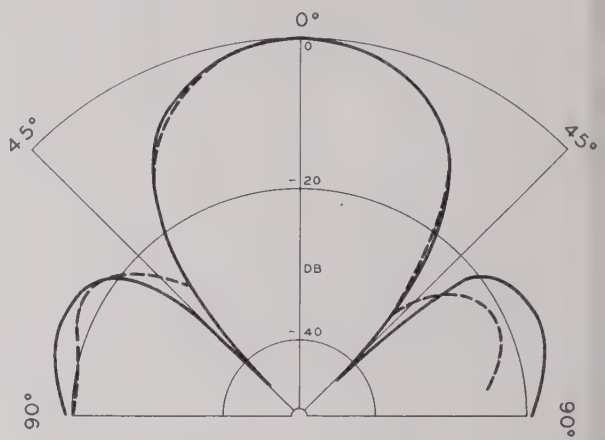

Fig. 2—The pattern in the E plane produced by a $TE_{0,1}$ wave i bisectoral horn of dimensions $1.47\lambda_0$ and $1.82\lambda_0$ in the E an planes, respectively. The solid line is theoretical and the das line is experimental.

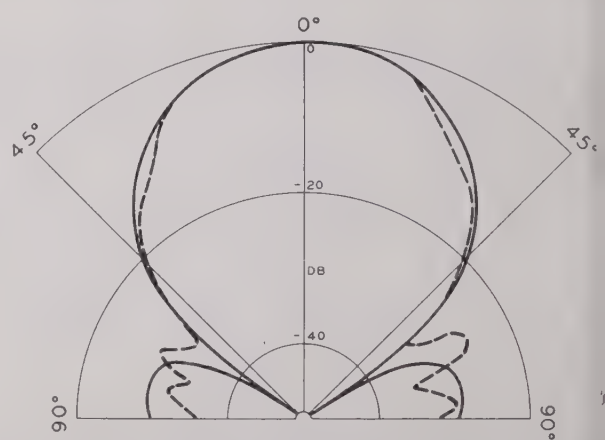

Fig. 3—The pattern in the H plane produced by a $TE_{0,1}$ wave i bisectoral horn of dimensions $1.47\lambda_0$ and $1.82\lambda_0$ in the E an planes, respectively. The solid line is theoretical and the das line is experimental.

VI. Transverse Waves in a Circular Waveguid

A. The $TE_{0,1}$ Mode of Vibration

The simplest mode of vibration in a circular wa guide is known as the $TE_{0,1}$ mode. For this mode, om ting an amplitude constant,

$$E_\rho = 0 \quad (23)$$

$$E_t = J_1(q\rho/a)\exp(ik'z - i\omega t) \quad (24)$$

where

a = radius of the guide

$q = 3.832$ = first positive root of $J_1(x) = 0$.

For this mode of vibration, the functions $f(x, y)$ a $g(x, y)$ defined in (10) become

$$f(x, y) = -J_1(q\rho/a) \sin \zeta \quad (25)$$

$$g(x, y) = +J_1(q\rho/a) \cos \zeta. \quad (26)$$

ence, one has

$$(\theta, \phi) = \mp (1/4\pi) \int_0^a \int_0^{2\pi} J_1(q\rho/a) \begin{matrix}\sin\\ \cos\end{matrix} \xi \cdot \exp\left\{-ik\rho \cos(\phi - \zeta) \sin\theta\right\} \rho d\rho d\zeta. \quad (27)$$

is can be integrated in a straightforward manner to ve

$$R_1(\theta, \phi) = \mp (ia^2 q J_0(q)/2) \begin{matrix}\sin\\ \cos\end{matrix} \phi J_1(\gamma)/(q^2 - \gamma^2) \quad (28)$$

ere

$$\gamma = ka \sin\theta. \quad (29)$$

us (12) gives

$$\left.\begin{aligned} &= 0\\ &= 0\\ &= (a^2 J_0(q)/2q)(k' + k\cos\theta) q^2 J_1(\gamma)/(q^2 - \gamma^2) \end{aligned}\right\} \quad (30)$$

the pattern of a circular waveguide excited in the $E_{0,1}$ mode.

The function $q^2 J_1(\gamma)/(q^2 - \gamma^2)$ is plotted in Fig. 4 as a nction of the dimensionless angle γ. This is the pattern at one would observe in any plane through the $0z$ axis.

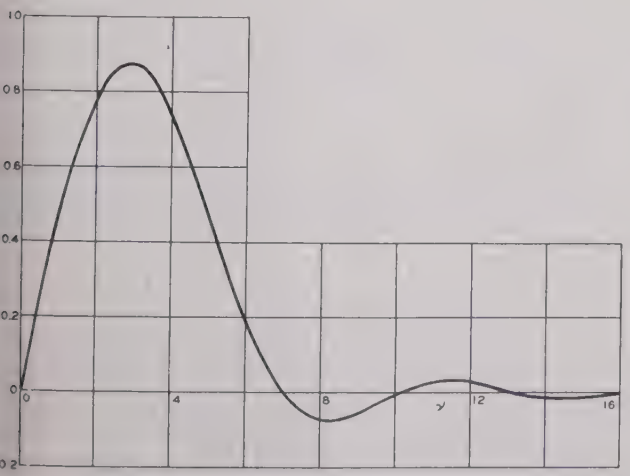

. 4—The pattern in any plane of a $TE_{0,1}$ wave in a circular waveguide versus the dimensionless angle γ.

The $TE_{1,1}$ Mode of Vibration

The next most simple mode of vibration in a circular veguide is known as the $TE_{1,1}$ mode in which the ctric field components are

$$E_\rho = (a/p\rho) J_1(p\rho/a) \cos\zeta \exp(ik'z - i\omega t) \quad (31)$$

$$E_\zeta = -J_1'(p\rho/a) \sin\zeta \exp(ik'z - i\omega t) \quad (32)$$

ere

a = radius of the waveguide

$p = 1.841$ = first positive root of $J_1'(x) = 0$.

Corresponding to these components, one has

$$f(x, y) = (a/p\rho) J_1(p\rho/a) \cos^2\zeta + J_1'(p\rho/a) \sin^2\zeta \quad (33)$$

$$g(x, y) = \left\{(a/p\rho) J_1(p\rho/a) - J_1'(p\rho/a)\right\} \sin\zeta \cos\zeta. \quad (34)$$

After some manipulation of Bessel functions, one arrives at the following expressions for the components of the electric field.

$$\left.\begin{aligned} E_r &= 0\\ E_\theta &= -i\left\{a^2 J_1(p)/4p\right\}(k + k'\cos\theta)\cos\phi P_1(\gamma)\\ E_\phi &= +i\left\{a^2 J_1(p)/4p\right\}(k' + k\cos\theta)\sin\phi P_2(\gamma) \end{aligned}\right\} \quad (35)$$

where

$$\gamma = ka \sin\theta \quad (29)$$

$$P_1(\gamma) = 2J_1(\gamma)/\gamma \quad (36)$$

$$P_2(\gamma) = 2p^2 J_1'(\gamma)/(p^2 - \gamma^2). \quad (37)$$

For the orientation under consideration, the planes $\phi = 0$ and $\phi = \pi/2$ will be denoted as the E and the H planes, respectively. Aside from the factor $(k + k'\cos\theta)$, $P_1(\gamma)$ is the pattern in the E plane of a circular waveguide or horn with $TE_{1,1}$ waves. Fig. 5 shows a plot of $P_1(\gamma)$ versus the dimensionless angle γ.

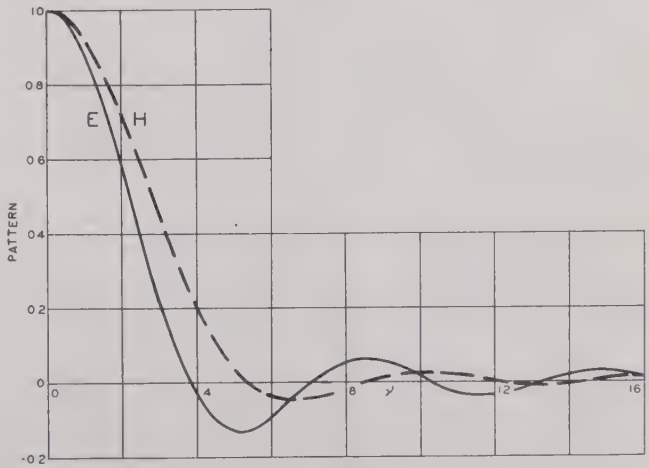

Fig. 5—The patterns in the E and H planes of a $TE_{1,1}$ wave in a circular horn versus the dimensionless angle γ. The solid curve E is a plot of $P_1(\gamma)$ of (36) and is the pattern in the E plane. The dashed curve H is a plot of $P_2(\gamma)$ of (37) and is the pattern in the H plane.

Aside from the factor $(k' + k\cos\theta)$, $P_2(\gamma)$ is the pattern in the H plane of a circular waveguide with $TE_{1,1}$ waves. Fig. 5 shows a plot of $P_2(\gamma)$ versus the dimensionless angle γ.

Figs. 6 and 7 show experimental and theoretical patterns in the E and H planes, respectively, for a circular horn whose diameter is $1.85\lambda_0$.

VII. The $TE_{1,1}$ Mode in a Semicircular Waveguide

The circular waveguide is frequently criticized because there is no physical restraint to prevent the rotation of the plane of the E vector. A possible solution of this difficulty would be to use a semicircular waveguide,

although the writer has not seen this discussed. The field components given by (31) and (32) will satisfy the boundary conditions in a semicircular waveguide bounded by the plane $\phi = \pm\pi/2$. The writer has not been able to effect the integration for $R(\theta, \phi)$ except for the two principal planes, $\phi = 0$ and 90°.

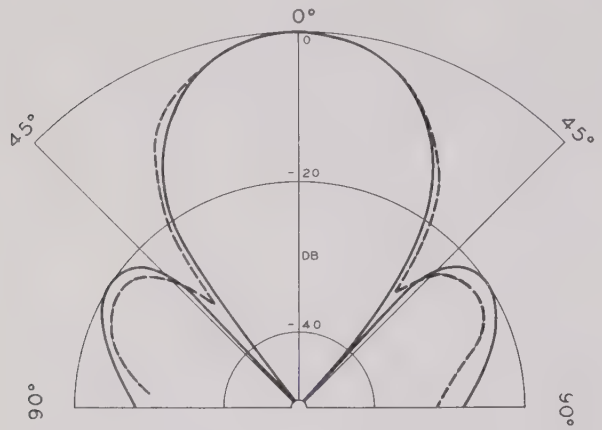

Fig. 6—The pattern in the E plane produced by a $TE_{1,1}$ wave in a conical horn whose largest diameter is $1.85\lambda_0$. The solid line is theoretical and the dashed line is experimental.

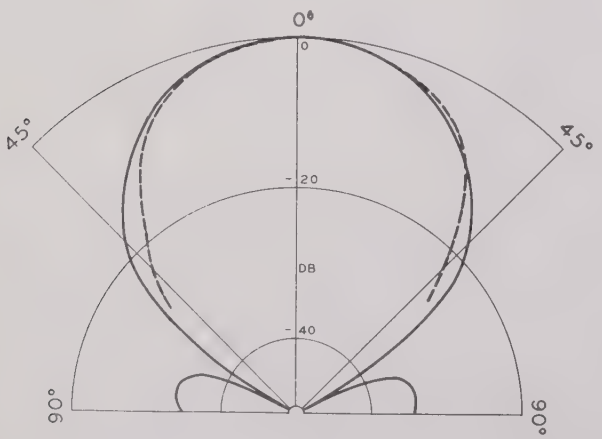

Fig. 7—The pattern in the H plane produced by a $TE_{1,1}$ wave in a conical horn whose largest diameter is $1.85\lambda_0$. The solid line is theoretical and the dashed line is experimental.

A. The Plane $\phi = 0$

It is possible to apply the arguments used in section III to show that $E_\phi = 0$; i.e., $R_2(\theta, 0) = 0$. After the integration with respect to ζ has been performed, one has

$$R_1(\theta, 0) = (a^2/8)\int_0^1 [J_0(ps)J_0(\gamma s) - J_2(ps)J_2(\gamma s)]sds$$

$$- i(a^2/4)\int_0^1 [J_1(ps)\boldsymbol{H}_0(\gamma s)/ps - J_2(ps)\boldsymbol{H}_1(\gamma s)/\gamma s]sds.$$

Obviously, the final pattern will be of the form $A(\gamma) - iB(\gamma)$, where $A(\gamma)$ is an even and $B(\gamma)$ is an odd function of γ. The integration can be performed to give the following pattern in the plane $\phi = 0$:

$$\left.\begin{aligned} E_r &= 0 \\ E_\theta &= -i\{a^2 J_1(p)/4p\}(k + k'\cos\theta)\{A(\gamma) - iB(\gamma)\} \\ E_\phi &= 0 \end{aligned}\right\} \quad (3$$

where

$$\left.\begin{aligned} A(\gamma) &= P_1(\gamma)/2 = J_1(\gamma)/\gamma \\ B(\gamma) &= \boldsymbol{H}_1(\gamma)/\gamma \end{aligned}\right\}, \quad (3$$

and

It will be noted that the real part of E_θ is equal to on half the value of E_θ for a circular waveguide given (35). That this must be true can be seen as follows. two semicircular waveguides are matched together form one circular waveguide, then the combined patte is

$$A(\gamma) - iB(\gamma) + A(\gamma) + iB(\gamma) = 2A(\gamma).$$

A plot of $2A(\gamma)$ is shown in Fig. 5. The graph of $B($ is shown in Fig. 8.

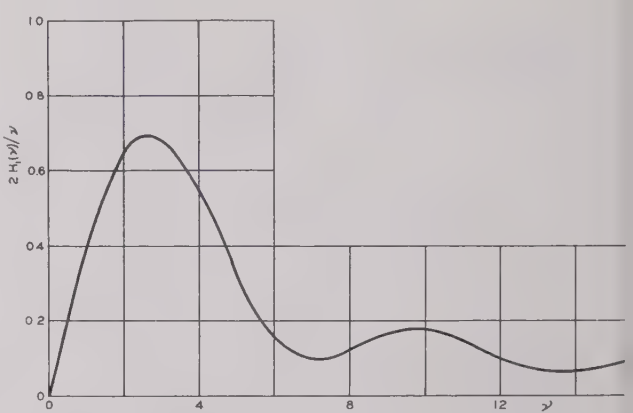

Fig. 8—A plot of the imaginary part of the pattern in the E plan a $TE_{1,1}$ wave in a semicircular waveguide versus the dimens less angle γ. A plot of twice the real part is given by the solid cu in Fig. 5.

B. The Plane $\phi = \pi/2$

It is obvious from considerations of symmetry t E_ϕ will have the same pattern in the case of the se circular waveguide as it does in the circular wavegui The exact expressions will differ by a factor 2 wh arises from the fact that the area is doubled in the cas the full waveguide. Therefore, the pattern of E_ϕ in present case is one-half of the value given in (35) plotted in Fig. 5.

E_θ is zero in the plane $\phi = \pi/2$ for the full circ waveguide, but it is not zero in the case of the se circular waveguide. When the integration with resp to θ is performed over the semicircle, one finds

$$R_2(\theta, \pi/2) = i(a^2/2\pi\gamma)\int_0^1 \{\cos(\gamma s) - \sin(\gamma s)/\gamma s\}$$

$$\cdot\{J_1(ps)/ps - J_1'(ps)$$

This can be integrated to give

$$R_2(\theta, \pi/2) = i(a^2/2\pi p^2)\{J_e(p, \gamma) + \cos\gamma J_0(p) - 1\}.$$

The function $J_s(p, x)$, which is defined as

$$J_s(p, x) = \int_0^x J_0(pu) \sin u du, \qquad (41)$$

has been extensively studied by Schwartz,[5] who tabulates the function $J_s(p, x)$ to 8D for $p=0.1$ (0.1) 1 and $x=0$ (0.1) 5. Unfortunately, this range of values is not suitable for the application to the diffraction patterns.

Thus the pattern in the plane $\phi=\pi/2$ becomes

$$E_r=0$$

$$E_\theta=-i(a^2/2\pi p^2)(k+k'\cos\theta)\{J_s(p,\gamma)+\cos\gamma J_0(p)-1\}$$

$$E_\phi=+i\{a^2J_1(p)/8p\}(k'+k\cos\theta)P_2(\gamma).$$

Figs. 9 and 10 show the patterns in the E and the H planes, respectively, of a semicircular horn whose diameter is $1.85\lambda_0$. The measurement in the H plane is for E_ϕ only.

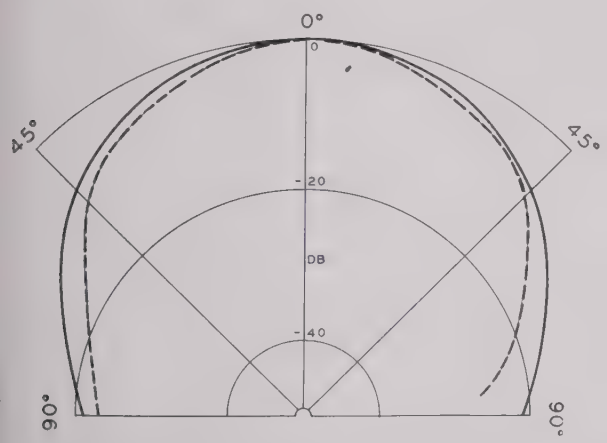

Fig. 9—The pattern in the E plane produced by a $TE_{1,1}$ wave in a semicircular horn whose largest diameter is 1.85 λ_0. The solid line is theoretical and the dashed line is experimental.

Acknowledgment

The writer wishes to thank R. B. Watson for the use of the experimental patterns that are shown in this paper.

Appendix

The derivation of (12) can best be done in two parts. First, let $g(x, y)\equiv 0$. Then

$$\vec{J}=\vec{n}\times\vec{H^0}=-\vec{i}\,(k'/\omega\mu)f(x, y)\exp(ik'z-i\omega t)$$

$$\vec{M}=-\vec{n}\times\vec{E^0}=-\vec{j}\,f(x, y)\exp(ik'z-i\omega t).$$

Neglecting powers of $(1/r)$ larger than the first, one has

$$\vec{A}=-\vec{i}\,(k'/\omega\mu r)R_1(\theta,\phi)\exp(ikr-i\omega t)$$

$$\vec{J}=-\vec{j}\,(1/r)R_1(\theta,\phi)\exp(ikr-i\omega t),$$

where $R_1(\theta, \phi)$ is defined in (13), and, consequently,

$$\operatorname{curl}\vec{F}=\vec{i}\,R_1(\theta,\phi)(ik/r)(\partial r/\partial z)\exp(ikr-i\omega t)$$
$$-\vec{k}\,R_1(\theta,\phi)(ik/r)(\partial r/\partial x)\exp(ikr-i\omega t)$$

and

$$\operatorname{grad}\operatorname{div}\vec{A}=\vec{r_0}R_1(\theta,\phi)(k'k^2/\omega\mu r)(x/r)\exp(ikr-i\omega t).$$

Upon converting $\vec{i}$, $\vec{k}$, and the cartesian components to polar form, one obtains

$$E_r=0$$

$$E_\theta=-i(k+k'\cos\theta)\cos\phi\cdot R_1(\theta,\phi)(1/r)\exp(ikr-i\omega t)$$

$$E_\phi=+i(k+k'\cos\theta)\sin\phi\cdot R_1(\theta,\phi)(1/r)\exp(ikr-i\omega t).$$

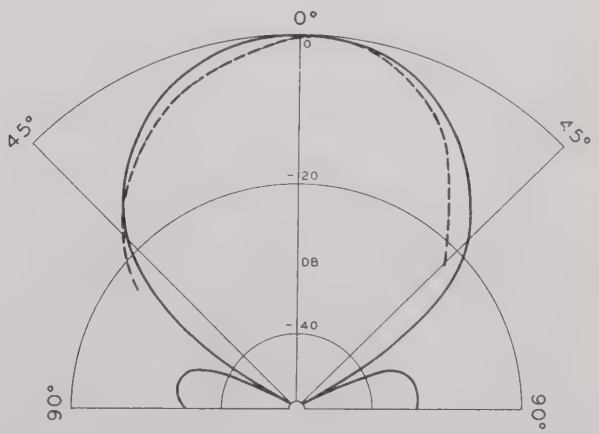

Fig. 10—The pattern in the H plane produced by a $TE_{1,1}$ wave in a semicircular horn whose largest diameter is 1.85 λ_0. The solid line is theoretical and the dashed line is experimental.

The second case of $f(x, y)\equiv 0$ can be derived as a special case of the preceding equations. If the electric vector in the waveguide is rotated 90° from $+\vec{i}$ to $+\vec{j}$, the electric and magnetic vectors in the radiation field must be rotated 90°. Hence the angle ϕ in the coefficients of the preceding equations must be replaced by $\phi-90°$, and $f(x, y)$ must be replaced by $g(x, y)$.

[5] L. Schwartz, "Investigations of some functions related to the cylindrical functions of zero order," *Luftfahrtforschung*, vol. 20, pp. 341–372; 1944. This paper has been translated by J. Lotsof for the Cornell Aeronautical Laboratory, May, 1946.

Piezoelectric Transducers*

WILFRED ROTH†, STUDENT, IRE

Summary—**A piezoelectric transducer operating in the thickness-vibration mode is represented as a six-terminal network. The mesh equations, electromechanical impedance matrix, and equivalent circuit valid for any general conditions of loading and frequency are obtained. Thus properties of the transducer can be determined once the crystal, the impedance of the loads, and the energy sources are specified. Equations for the electrical driving-point impedance and admittance are derived for all conditions of loading and frequency consistent with the original assumptions.**

I. Electromechanical Impedance Matrix

1. Introduction

THE USE OF piezoelectric transducers to produce ultrasonic energy for research and commercial purposes has increased rapidly in recent years. As a result, a theoretical analysis of the operation of such elements, which is capable of simplifying the work of the equipment designer, is extremely desirable. The analysis presented here was undertaken with this end in view.

Piezoelectric materials have the property of reacting mechanically to an applied electrical stimulus, and, reciprocally, of reacting electrically to an applied mechanical stimulus.[1,2] Such bilateral conversion of electrical to mechanical energy, and vice versa, is the function performed by the piezoelectric element in its various applications. Hence, any theoretical conclusions must be in a form equally convenient for use with either electrical or mechanical systems.

Although piezoelectric crystals are useful when operating in many varied modes, the mode principally in use for generation of the higher ultrasonic frequencies is that corresponding to X-cut quartz—the so-called thickness vibration. This mode is characterized by the collinearity of the mechanical strain and electric field-intensity vectors, and is the mode to be considered here.

2. Statement of Problem and Assumptions

Fig. 1 illustrates the problem to be considered. The crystal, its physical constants and geometry, and the loading acoustic media are specified, while the relations holding among the four mechanical and two electrical parameters are to be determined. The rationalized mks system of units is employed throughout to facilitate the joint use of mechanical and electrical parameters.[3]

To simplify the problem, the following assumptions are made:

(i) The crystal is an infinite slab with two plane, parallel surfaces perpendicular to the direction of propagation of the resulting acoustic disturbance.

(ii) The two plane surfaces are electric equipotentials.

(iii) The mechanical energy dissipated in the piezoelectric material is negligible.

(iv) The electrical or mechanical stresses either applied or produced are not sufficient to cause departure from a linear operating region.

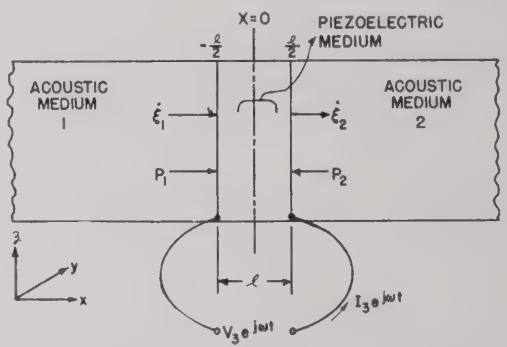

Fig. 1—The piezoelectrical medium terminated by two acoustic media and one electrical terminal pair.

These assumptions are not restrictive when applied to the type of transducer generally used for ultrasonic applications. In accordance with (i), the width of the crystal must be very much larger than its thickness. In practice, this ratio is frequently as large as 25 or 50 to 1, hence, this assumption is certainly valid. At very low frequencies, edge effects assume importance since the thickness may be in the order of the width, and a more elaborate theory is required.

Assumption (ii) restricts the analysis to widths small compared to the electrical wavelengths employed. This is always the case except for operation in the microwave region, where the wavelengths become comparable to the crystal dimensions.

Assumption (iii) is not at all restrictive unless the transducer is operating in a vacuum, in which case, all the mechanical energy is dissipated within the crystal. In most cases of practical importance, the dissipation in the acoustic material and supporting structure greatly exceeds that in the transducer, and no noticeable error is introduced by treating the dissipationless case.

* Decimal classification: R214.21×R265. Original manuscript received by the Institute, February 10, 1948; revised manuscript received, October 27, 1948. This work has been supported in part by the United States Signal Corps, the Air Materiel Command, and the Office of Naval Research.

† Formerly, Harvey Radio Laboratories, Inc., Cambridge, Mass.; now, Raytheon Manufacturing Corporation, Waltham, Mass.

[1] W. G. Cady, "Piezoelectricity," McGraw-Hill Book Co., Inc., New York, N. Y., 1946. An extremely complete, well-documented book on electromechanical phenomena in crystals. An excellent bibliography is included.

[2] W. P. Mason, "Electromechanical Transducers and Wave Filters," D. Van Nostrand Co., Inc., New York, N. Y., 1942; pp. 195–215. An equivalent circuit for a piezoelectric transducer is derived and used in several examples. Derivation of the piezoelectric equations is given in Appendix C.

[3] O. W. Eshbach, "Handbook of Engineering Fundamentals," John Wiley and Sons, New York, N. Y., 1936. Contains a useful table of conversion factors for various unit systems, pp. 1–130 to 1–14 and a discussion of existing systems, pp. 3–02 to 3–36.

In most applications, (iv) is not limiting. However, if henomena such as cavitation are encountered, the echanical loading becomes a function of the intensity id cannot be treated as a constant. In these cases, the resent treatment must be considered only as a first-der theory which indicates trends and approximate agnitudes rather than quantitative behavior.

Procedure

We shall regard the piezoelectric transducer as a cir-it element—either electrical or mechanical, depending on which terminals of the transducer are under exami-ation. By adopting this viewpoint, it becomes possible characterize the transducer completely by an electro-echanical impedance matrix relating electrical and echanical "currents" to the associated "voltages." More ll be said about the definition of these terms in a later ction.[4]

Since the mode we are considering has two opposing ystal surfaces from which ultrasonic energy is ra-ated, to represent this situation we can evidently in-oduce four mechanical terminals. To affect the crystal ectrically, it is necessary to attach electrodes to these ces. This also makes it possible to introduce two elec-ical terminals. In this manner, the transducer is con-dered as a six-terminal network and we seek the nesh" equations and the electromechanical impedance atrix which describes the interaction occurring among e variables specified for the respective terminal pairs.

As is the case with pure electrical networks, we must rst obtain the equations relating "voltages" and "cur-nts" at the six terminals. From this set of three "mesh" quations, the impedance matrix can be defined and enceforth used for design purposes. We shall see that l properties of the transducer can be determined from knowledge of this matrix and the boundary conditions the terminals.

The impedance matrix is developed in accordance ith the following procedure:

(i) Maxwell's equations and the constitutive relations tisfied by the piezoelectric crystal are introduced to btain the equations satisfied by the electrical parame-rs.

(ii) The piezoelectric equations which describe the in-rrelation among the electrical and mechanical varia-les for piezoelectric materials are used to develop pre-minary mesh equations in conjunction with the results (i).

(iii) Newton's first law is used to derive the wave quation satisfied by the mechanical displacement. After tegration, the result is employed to obtain the final esh equations in the desired form.

(iv) The impedance matrix follows directly from the mesh equations by proper definition of the operational process involved.

3.1. Introduction of Maxwell's Equations. In the rationalized mks system of units, Maxwell's equations are[5]

$$\nabla \times E + \frac{\partial B}{\partial t} = 0 \tag{1a}$$

$$\nabla \times H - \frac{\partial D}{\partial t} = J \tag{1b}$$

$$\nabla \cdot D = \rho \tag{1c}$$

$$\nabla \cdot B = 0. \tag{1d}$$

The constitutive relations for piezoelectric materials operating in the mode considered here are

$$B = \mu H \tag{1e}$$

$$D_x = \epsilon_x \left(E_x - h \frac{\partial \xi}{\partial x} \right) \tag{1f}$$

$$D_y = \epsilon_y E_y \tag{1g}$$

$$D_z = \epsilon_z E_z \tag{1h}$$

where

E = electric field intensity in volts per meter
B = flux density in webers per square meter
H = magnetic field intensity in ampere-turns per meter
D = dielectric displacement in coulombs per square meter
J = current density in amperes per square meter
ρ = charge density in coulombs per cubic meter
μ = permeability in henrys per meter
ϵ = inductive capacitance in farads per meter
h = piezoelectric constant in volts per meter
ξ = mechanical displacement in meters.

It is to be understood that all variables are functions of both space and time until proved otherwise.

In view of our original assumption of equipotential, parallel, plane surfaces, infinite in extent, it is evident that $E_y = E_z = 0$, and $\partial E_x/\partial y = \partial E_x/\partial z = 0$. From (1g) and (1h), we find that $D_y = D_z = 0$ and by expanding $\nabla \times E$ into its rectangular components, it is clear also that $\nabla \times E = 0$. From the former condition and (1c) we obtain

$$\frac{\partial D_x}{\partial x} = \rho, \tag{2a}$$

while the latter and (1a) result in

$$\frac{\partial B}{\partial t} = 0. \tag{2b}$$

From this result and (1e), it follows that B and H are independent of time. We know from physical considerations that, if a time-varying voltage is applied to the

[4] M. F. Gardner and J. L. Barnes, "Transients in Linear Systems," hn Wiley and Sons, New York, N. Y., 1942. Chap. II contains a scussion of the equations of electrical and mechanical systems both one and in combination.

[5] J. A. Stratton, "Electromagnetic Theory," McGraw-Hill Book Co., Inc., New York, N. Y., 1941; chap. I.

electrical terminals, E, D, and J must also vary with t in the same way. We found above that H, and, therefore $\nabla\times H$, is independent of t; hence, from (1b) we see that $\nabla\times H=0$. Since both $\nabla\times H$ and $\nabla\cdot H$ are zero, H itself must be a constant vector; and if no external sources of B are present, we are free to impose the conditions that

$$B = 0$$

and

$$H = 0. \tag{3}$$

The charge density ρ appearing in (1c) is real charge density, as opposed to polarization charge density, usually denoted by ρ'. As the crystal is a dielectric, ρ is zero except on the surfaces, whereas ρ' is certainly not necessarily zero. Thus, within the crystal we find that

$$\frac{\partial D_x}{\partial x} = 0; \tag{2c}$$

hence, D is independent of position—varying only with time. This is an important result and will be used in a later section.

We found above that $\nabla\times E=0$ and $E_y=E_z=0$. This permits us to set

$$E_x = -\frac{\partial\phi}{\partial x}$$

in the usual manner, where ϕ is a scalar potential function. By using the definition of voltage difference,

$$V_3 = \int_{\phi_1}^{\phi_2} d\phi,$$

it is immediately evident that

$$V_3 = -\int_{-l/2}^{l/2} E_x dx. \tag{4}$$

This result will be needed in the later development of the mesh equations.

As a result of the above, (1b) becomes

$$J_x = -\frac{\partial D_x}{\partial t}.$$

By remembering that $I=J\cdot A$, where A is the active area of the crystal, and by choosing the time variation of the impressed voltage to be $e^{j\omega t}$, we arrive at the expression for current

$$I_3 = -j\omega AD, \tag{5}$$

which is also required for the derivation of the mesh equations. It is no longer necessary to continue the use of subscripts, since we found a variation only with t, and x, y and z are no longer of concern.

It should be noted that an important result of the above discussion is that no electromagnetic radiation is produced by the transducer, since Poynting's vector, $E\times H$, is zero. This is a direct consequence of the assumptions concerning the shape of the crystal and the electrode arrangement, and only applies when these assumed conditions are valid.

3.2. Formulation of the Mesh Equations. The behavior of the piezoelectric medium for the mode considered here is described by the piezoelectric equations[6]

$$-P = C^D\frac{\partial\xi}{\partial x} + hD \tag{6a}$$

$$E = h\frac{\partial\xi}{\partial x} + SD. \tag{6b}$$

These correspond to the equivalent equations for normal elastic dielectric materials[7,8]

$$-P = \frac{Y(1-\sigma)}{(1+\sigma)(1-2\sigma)}\frac{\partial\xi}{\partial x} = C'\frac{\partial\xi}{\partial x} \tag{6c}$$

$$E = \frac{1}{\epsilon}D = S'D \tag{6d}$$

where

P = pressure in newtons per square meter
C^D = stress-to-strain ratio for infinite slab with $D=0$ in newtons per square meter
ξ = mechanical displacement of the meter
h = piezoelectric constant in newtons per coulomb or volts per meter
D = dielectric displacement in coulombs per square meter
E = electric field intensity in volts per meter
S = electric intensity to dielectric displacement ratio with $\partial\xi/\partial x=0$ in meters per farad (reciprocal of inductive capacitance)
Y = Young's modulus in newtons per square meter
σ = Poisson's ratio (dimensionless).

3.2.1. Mechanical Mesh Equations. From the first piezoelectric equation, (6a), and (5), we have

$$-P_1 = C^D\frac{\partial\xi_1}{\partial x} - \frac{h}{j\omega A}I_3 \tag{7a}$$

$$-P_2 = C^D\frac{\partial\xi_2}{\partial x} - \frac{h}{j\omega A}I_3, \tag{7b}$$

where the subscript 1 refers to $x=-l/2$, and 2 to $x=l/2$. In order to combine both mechanical and electrical variables in one equation, it is frequently convenient to consider velocity as the analogue of current, and force the analogue of voltage. It should be noted that this choice is not unique; other analogues are perfectly permissible.

[6] See footnote reference 2; p. 202, formulas 6.32. This set is converted to apply to the thickness vibration by changing the y subscript to x. Displacement is introduced rather than charge from the relation $Q=1/4\pi$ (Disp.), and the two sets become similar in form but not in units. This conversion is made if $C^D=y_0/10$, $h=3\cdot10^4D$ and $S=36\cdot10^9k$. Mason's values for the coefficients for different crystals can be used above if these changes are made.

[7] G. Joos, "Theoretical Physics," Stechert-Hafner, Inc., New York, N. Y., 1934, p. 165 (with $e_{22}=e_{33}=0$, $P_{11}=-P$ and $Y=E$).

[8] See footnote 5, p. 10.

[9] See footnote 4, pp. 60–64.

We shall follow this procedure here; but since pressure and not force is the parameter of interest, it is convenient to consider velocity analogous to current density, or surface area times velocity analogous to current.

In order to put (7a, b) in proper form, it is necessary to find the relation between $\partial\xi/\partial x$ and ξ since the latter is the desired variable. This can be done by integration of the wave equation which expresses ξ as a function of x and t. By application of Newton's first law to a small volume element of density ρ(in kg/m^3) as shown in Fig. 2, we can write

$$\rho dx dy dz \frac{\partial^2 \xi}{\partial t^2} = [P(x) - P(x + dx)]dydz.$$

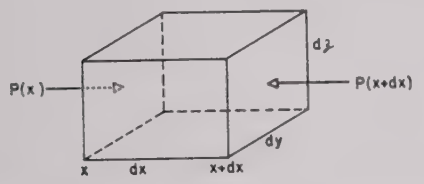

Fig. 2—Forces acting on a small volume element.

Since

$$P(x + dx) = P(x) + \frac{\partial P(x)}{\partial x} dx + \cdots,$$

we find, after neglecting higher-order terms,

$$\rho \frac{\partial^2 \xi}{\partial t^2} = - \frac{\partial P}{\partial x}.$$

Upon differentiation of (6a) and introduction in the above, we obtain

$$\rho \frac{\partial^2 \xi}{\partial t^2} = C^D \frac{\partial^2 \xi}{\partial x^2} + h \frac{\partial D}{\partial x}.$$

Recalling from (2c) that D is independent of x, we finally obtain the simple wave equation

$$\frac{\partial^2 \xi}{\partial x^2} = \frac{1}{c^2} \frac{\partial^2 \xi}{\partial t^2}, \tag{8a}$$

where

$$c = \sqrt{\frac{C^D}{\rho}} \tag{8b}$$

is the velocity of propagation of the elastic wave in the piezoelectric medium.

Assuming a time variation of the form $e^{j\omega t}$ as before, this integrates simply, and we have

$$\xi = [\xi_+ e^{-jkx} + \xi_- e^{jkx}]e^{j\omega t} \tag{9}$$

where

$$k = \frac{\omega}{c} = \frac{2\pi}{\lambda}.$$

This form of solution represents the mechanical displacement as the superposition of two traveling waves; one propagating in the positive x direction, and the other propagating in the negative x direction.

Upon differentiation, we find

$$\frac{\partial \xi_1}{\partial x} = jk\xi_+[-e^{j\theta} + \gamma e^{-j\theta}]e^{j\omega t} \tag{10a}$$

$$\frac{\partial \xi_2}{\partial x} = jk\xi_+[-e^{-j\theta} + \gamma e^{j\theta}]e^{j\omega t}, \tag{10b}$$

where

$$\theta = \frac{kl}{2}$$

$$\gamma = \frac{\xi_-}{\xi_+},$$

and

$$\dot{\xi}_1 = j\omega\xi_+[e^{j\theta} + \gamma e^{-j\theta}]e^{j\omega t} \tag{11a}$$

$$\dot{\xi}_2 = j\omega\xi_+[e^{-j\theta} + \gamma e^{j\theta}]e^{j\omega t}. \tag{11b}$$

Solving for ξ_+ in (11a), and substituting this in (10a), we obtain

$$\frac{\partial \xi_1}{\partial x} = \frac{k\dot{\xi}_1}{\omega}\left[\frac{\gamma e^{-j\theta} - e^{j\theta}}{\gamma e^{-j\theta} + e^{j\theta}}\right]. \tag{12a}$$

In a similar manner, by using (11b) and (10b), we have

$$\frac{\partial \xi_2}{\partial x} = \frac{k\dot{\xi}_2}{\omega}\left[\frac{\gamma e^{j\theta} - e^{-j\theta}}{\gamma e^{j\theta} + e^{-j\theta}}\right]. \tag{12b}$$

Recalling the fact that

$$\tanh x = \frac{e^x - e^{-x}}{e^x + e^{-x}},$$

if we define

$$\gamma = e^{2\psi}, \tag{13}$$

the above equations take the simple form

$$\frac{\partial \xi_1}{\partial x} = \frac{k\dot{\xi}_1}{\omega} \tanh (\psi - j\theta) \tag{14a}$$

$$\frac{\partial \xi_2}{\partial x} = \frac{k\dot{\xi}_2}{\omega} \tanh (\psi + j\theta). \tag{14b}$$

These two latter equations can now be substituted in (7a, b) to give the proper forms of mesh equations which describe the transducer from the mechanical terminals. By so doing, we obtain finally

$$P_1 = -\frac{\rho c}{A} \tanh (\psi - j\theta)A\dot{\xi}_1 + \frac{h}{j\omega A} I_3 \tag{15a}$$

$$P_2 = -\frac{\rho c}{A} \tanh (\psi + j\theta)A\dot{\xi}_2 + \frac{h}{j\omega A} I_3 \tag{15b}$$

where we have included the relation $C^D k/\omega = c^2\rho \cdot \omega/c \cdot 1/\omega = \rho c$. These equations have the desired form, but an ex-

pression for ψ in terms of the mechanical boundary conditions is required in order to make them more readily usable.

If the ratio of pressure to particle velocity is defined as acoustic impedance,[10] the boundary conditions at $x=-l/2$ and $x=l/2$ are specified by stating the acoustic impedances of the loading media. These are determining characteristics of materials, and in general, are both complex and functions of frequency. It should be remembered that the acoustic impedance for a wave traveling in the negative direction in a given medium equals the negative of the impedance for a wave traveling in the positive direction. This is simply seen physically from the fact that at a particular point of reference, the pressure is the same for both waves, but the velocities have opposite signs.

With this understood, the mechanical boundary conditions are imposed by stating

$$-z_1 = \frac{P_1}{\xi_1} \tag{16a}$$

$$z_2 = \frac{P_2}{\xi_2}. \tag{16b}$$

Employing (15a) and (16a), we find

$$-z_1\xi_1 = -\rho c \tanh(\psi - j\theta)\xi_1 + \frac{h}{j\omega A} I_3,$$

and similarly, from (15b) and (16b),

$$z_2\xi_2 = -\rho c \tanh(\psi + j\theta)\xi_2 + \frac{h}{j\omega A} I_3.$$

Reverting to the original exponential form for $\tanh x$ and (13), the defining relation for ψ, these become

$$z_1\xi_1 = \rho c \frac{\gamma e^{-j\theta} - e^{j\theta}}{\gamma e^{-j\theta} + e^{j\theta}} \xi_1 - \frac{h}{j\omega A} I_3 \tag{17a}$$

$$z_2\xi_2 = -\rho c \frac{\gamma e^{j\theta} - e^{-j\theta}}{\gamma e^{j\theta} + e^{-j\theta}} \xi_2 + \frac{h}{j\omega A} I_3. \tag{17b}$$

By introducing the expressions for ξ_1 and ξ_2 from (11a) and (11b), respectively, the two equations can be manipulated to solve for γ in terms of the boundary impedances and the constants of the crystal. The resulting expression is

$$\gamma = -\left[\frac{(\zeta_1 + 1)e^{j\theta} + (\zeta_2 - 1)e^{-j\theta}}{(\zeta_2 + 1)e^{j\theta} + (\zeta_1 - 1)e^{-j\theta}}\right] \tag{18}$$

where

$$\zeta_1 = \frac{z_1}{\rho c}$$

$$\zeta_2 = \frac{z_2}{\rho c}.$$

[10] P. M. Morse, "Vibration and Sound," McGraw-Hill Book Co., Inc., New York, N. Y., 1936; p. 191.

Finally, from (13), the expression for ψ, we obtain

$$\psi = \frac{1}{2} \ln\left[\left\{\frac{(\zeta_1 + 1)e^{j\theta} + (\zeta_2 - 1)e^{-j\theta}}{(\zeta_2 + 1)e^{j\theta} + (\zeta_1 - 1)e^{-j\theta}}\right\} e^{j\pi}\right]. \tag{19}$$

Having determined the value of ψ for any general conditions of loading, equations (15a, b) are complete. All the quantities are known with the exception of the three variables P, $A\xi$, and I. These, however, are just the quantities of interest, so that the remaining mesh equation describing the transducer from the electrical terminals must be derived. This will then give three equations and three unknowns from which the quantities of interest may be obtained.

3.2.2. Electrical Mesh Equations. By integrating the second piezoelectric equation (6b) with respect to x between the limits $-l/2$ and $l/2$ and then introducing (4) we find

$$-V_3 = h(\xi_2 - \xi_1) + SDl \tag{20}$$

where the subscripts have the same meaning as before.

Since $\xi = j\omega\xi$, (20) assumes the desired form

$$V_3 = \frac{1}{j\omega C_P} A\xi_1 - \frac{1}{j\omega C_P} A\xi_2 + \frac{1}{j\omega C_E} I_3 \tag{21}$$

where

$$C_P = \frac{A}{h}$$

$$C_E = \frac{A}{Sl}.$$

C_E is recognized as simply the electrostatic capacitance of the parallel-plate capacitor formed by the equipotential surfaces of the transducer separated by the dielectric material. C_P is defined here as the piezoelectric capacitance of the transducer as a matter of convenience, since it is so similar to C_E. This completes the derivation of the three mesh equations. We now proceed with the definition of the impedance matrix and a brief discussion of its use.

3.3. Electromechanical Impedance Matrix. The mesh equations obtained above are repeated here for convenience.

$$P_1 = -\frac{\rho c}{A} \tanh(\psi - j\theta)A\xi_1 + \frac{1}{j\omega C_P} I_3 \tag{15a'}$$

$$P_2 = -\frac{\rho c}{A} \tanh(\psi + j\theta)A\xi_2 + \frac{1}{j\omega C_P} I_3 \tag{15b'}$$

$$V_3 = \frac{1}{j\omega C_P} A\xi_1 - \frac{1}{j\omega C_P} A\xi_2 + \frac{1}{j\omega C_E} I_3. \tag{21'}$$

These were obtained for the polarity conditions shown in Fig. 3. Here all arrows point in the positive direction. The lack of symmetry made evident by the signs in (21') can be rectified by reversing the positive direction of ξ_2. This is shown in Fig. 4, where the symbol v has re

placed ξ to eliminate confusion. That is, $v_1 = \dot{\xi}_1$, but $v_2 = -\dot{\xi}_2$.

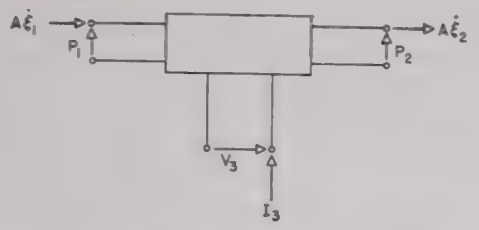

Fig. 3.—Six-terminal network with the original positive polarities.

We see by inspection of Fig. 4 that the six-terminal network is now completely symmetric; all currents are taken positive when feeding into the network at the particular terminals shown. The revised mesh equations become

$$P_1 = \frac{\rho c}{A} \tanh\left(-\psi + j\frac{\omega}{c}\frac{l}{2}\right) A v_1 + \frac{1}{j\omega C_P} I_3 \quad (22a)$$

$$P_2 = \frac{\rho c}{A} \tanh\left(\psi + j\frac{\omega}{c}\frac{l}{2}\right) A v_2 + \frac{1}{j\omega C_P} I_3 \quad (22b)$$

$$V_3 = \frac{1}{j\omega C_P} A v_1 + \frac{1}{j\omega C_P} A v_2 + \frac{1}{j\omega C_E} I_3. \quad (22c)$$

These can be written in matrix form if the usual rules of matrix multiplication are followed.[11]

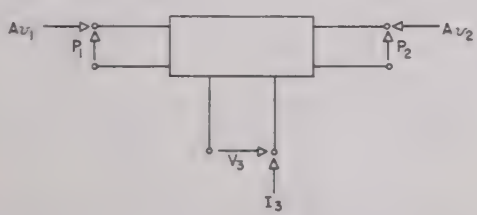

Fig. 4—Six-terminal network with the revised positive polarities.

Thus,

$$\begin{bmatrix} P_1 \\ P_2 \\ V_3 \end{bmatrix} = [Z] \times \begin{bmatrix} A v_1 \\ A v_2 \\ I_3 \end{bmatrix} \quad (23)$$

where the electromechanical impedance matrix $[Z]$ is

$$[Z] = \begin{bmatrix} \frac{\rho c}{A} \tanh\left(-\psi + j\frac{\omega}{c}\frac{l}{2}\right) & 0 & \frac{1}{j\omega C_P} \\ 0 & \frac{\rho c}{A} \tanh\left(\psi + j\frac{\omega}{c}\frac{l}{2}\right) & \frac{1}{j\omega C_P} \\ \frac{1}{j\omega C_P} & \frac{1}{j\omega C_P} & \frac{1}{j\omega C_E} \end{bmatrix}. \quad (24)$$

[11] E. A. Guillemin, "Communication Networks," vol. II, John Wiley and Sons, New York, N. Y., 1935; chap. IV. The application of matrix algebra to network analysis and the concept of an impedance matrix is discussed in considerable detail.

This matrix is seen to possess some very special properties. Since $Z_{13} = Z_{31}$, and $Z_{23} = Z_{32}$, the transducer obeys the reciprocity theorem if the proper precautions are taken as to the equality of the internal impedances of any power generating and indicating apparatus introduced.[12] This, of course, must always be the case when applying reciprocity tests. We see also that $Z_{13} = Z_{23}$ and $Z_{31} = Z_{32}$. This implies that the mechanical terminal pairs are equivalent so far as the electrical terminals are concerned. The third point of interest is that $Z_{12} = Z_{21} = 0$. This states that the velocity of one crystal face has no effect on the pressure at the other face. Only the current flowing into the electrical terminals and the velocity of the surface in question affects this pressure.

Finally, we recognize that the impedance elements comprising the matrix which are not only functions of frequency but also of acoustic loading once the crystal type and geometry are specified, are the two mechanical self-impedances, Z_{11} and Z_{22}. These are functions of loading since ψ is determined by the acoustic media at the two surfaces. If it were not for this complicating factor, the piezoelectric transducer would be a simpler element with which to work both theoretically and experimentally, since the remaining self- and mutual-impedances assume simple forms.

In the particular case of symmetric loading, we see from (19) that $\psi = j(\pi/2)$. Since

$$\tanh j\left(\frac{\omega}{c}\frac{l}{2} \pm \frac{\pi}{2}\right) = -j \cot\frac{\omega l}{c2},$$

we obtain the impedance matrix

$$[Z_s] = \begin{bmatrix} \frac{\rho c}{jA} \cot\left(\frac{\omega}{c}\frac{l}{2}\right) & 0 & \frac{1}{j\omega C_P} \\ 0 & \frac{\rho c}{jA} \cot\left(\frac{\omega}{c}\frac{l}{2}\right) & \frac{1}{j\omega C_P} \\ \frac{1}{j\omega C_P} & \frac{1}{j\omega C_P} & \frac{1}{j\omega C_E} \end{bmatrix} \quad (25)$$

which is only a function of frequency once the crystal is specified. Thus, the treatment of systems employing symmetrical acoustic loading is much simpler than that for the corresponding asymmetrical system.

By inspection of the general Z matrix, an equivalent circuit for the transducer which is valid for any operating conditions can immediately be determined. This is shown in Fig. 5.

4. Conclusions

The electromechanical impedance matrix, mesh equations, or equivalent circuit obtained above can be used to determine the operating characteristics of the transducer for any general conditions of driving or loading,

[12] See vol. 1, p. 152 of footnote reference 11.

regardless of the terminals in question. The procedure is identical to that used in connection with pure electrical networks whose impedance matrix is specified.

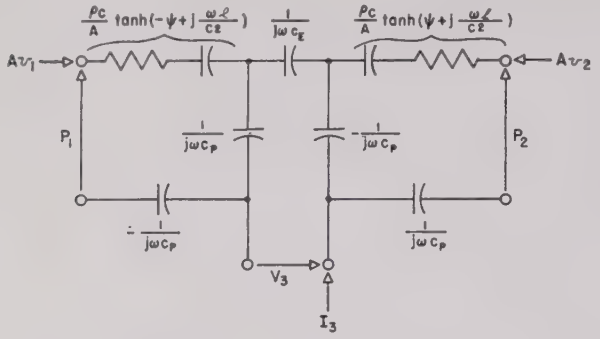

Fig. 5—Six-terminal equivalent circuit valid for any general terminating condition.

Once the boundary conditions satisfied by the respective terminal pairs are stated in terms of the actual values of loading impedances or energy sources, sufficient information is introduced to permit the solution of the set of linear equations for the unknown parameters. Because of the simple form of our final equations, these solutions can be obtained by any of the techniques for solving a set of three linear equations. The methods for solution of such a set of linear equations are numerous and varied, and hence, are beyond the scope of this paper.

As an example of the use of the above theory for the solution of a design problem, the properties of a piezoelectric transducer driven electrically and loaded acoustically in any arbitrary manner are investigated in Section II. General formulas of driving-point impedance and admittance are developed, and a summary of the principal operating characteristics is included. This information is of fundamental importance to the designer who is faced with the task of developing electrical apparatus capable of properly exciting a piezoelectric crystal when loaded by specified media.

II. Electrical Driving-Point Impedance and Admittance

1. Network Analysis of General Acoustic Loading

By use of (16) and the further relations introduced above, $\xi_1 = v_1$ and $\xi_2 = -v_2$, we specify the boundary conditions existing at the mechanical terminals in the general case by letting

$$z_1 = -\frac{P_1}{v_1} \tag{26a}$$

and

$$z_2 = -\frac{P_2}{v_2}. \tag{26b}$$

Incorporation of these conditions in the circuit of Fig. 5 leads to the circuit of Fig. 6. For problems dealing with reception of acoustic waves, the mechanical boundary conditions would be represented by pressure sources with suitable internal impedances and the electrical boundary condition would be represented by an electrical impedance. It is evident that many combinations of energy sources and sinks are possible, in accordance with the problem to be treated.

The method by which the minus signs in (26) are introduced in this circuit deserves particular comment. The pressure P has been considered a positive quantity in all the preceding work when the stress applied to a crystal face produces compression with the electrical terminals open-circuited; i.e., $I_3 = 0$. Hence, P denotes a pressure "rise" completely analogous to a voltage "rise" introduced when discussing a source of electromotive force.

In this sense, the arrows at the terminals of the circuit of Fig. 5 indicate directions of pressure and voltage rises. If we choose to keep both the same positive directions for current flow in the respective meshes as above and positive values for the terminating impedances, (26) shows that P is negative. Thus, the directions of pressure rises at the two mechanical terminal pairs must be opposite to those indicated in Fig. 5; or the pressure "drops" must be in the arrow directions. By following the velocity mesh currents in Fig. 6, it will be seen that this is indeed the case.

With this clearly in mind, it is evident that the complete solution of the asymmetrical transducer problem can be obtained from an analysis of the relatively simple three-mesh circuit of Fig. 6.

By solving this circuit for the driving-point impedance $Z = V_3/I_3$, we obtain the result

$$Z = \frac{1}{j\omega C_E}\left[1 - \frac{K^2}{j2\theta}S^*\right], \tag{27a}$$

where

$$S^* = \left[\frac{1}{\tanh(\psi+j\theta)+\zeta_2} + \frac{1}{\tanh(-\psi+j\theta)+\zeta_1}\right] \tag{27b}$$

in which $\zeta = Z/\rho c$, the normalized load impedance, and K^2 is as defined below.

By comparison of the piezoelectric equations (6) with those for a two-mesh electrical network, the simplification included above is achieved. For a two-mesh electrical network, the mesh equations can be written in the form[13]

$$V_1 = Z_{11}I_1 + Z_{12}I_2$$

$$V_2 = Z_{21}I_1 + Z_{22}I_2.$$

In the analysis of such systems, it is usually convenien

[13] See vol. II, p. 135 of footnote reference 11.

define the dimensionless quantity K known as the coupling coefficient," by the relation[14]

$$K^2 = \frac{Z_{12}Z_{21}}{Z_{11}Z_{22}}.$$

quations (6) have the same form as those above, and ere, too, it is convenient to define a dimensionless upling coefficient. In this instance, we obtain

$$K^2 = \frac{h^2}{C^D S}. \tag{28}$$

we recall from (21) that $C_P = A/h$ and $C_E = A/Sl$, nd from (8b), that $c = \sqrt{C^D/\rho}$, we find

$$K^2 = \frac{A}{C_P{}^2 \rho c} \times \frac{C_E 2\theta}{\omega}. \tag{29}$$

For applications in which the crystal and acoustic ads are specified, the solution is now complete, since l the parameters entering in the above expression for are known. However, we wish here to investigate the ehavior of this impedance as we vary the parameters; , unfortunately, a considerable amount of algebra is ecessary in order to convert (27) to a more useful rm. Our goal is to obtain expressions for the real and naginary parts of Z in terms of the system parameters: ystal constants, normalized load impedances, and fre- uency.

Substitution of the expression for γ (18) into those for nh$(\psi + j\theta)$ and tanh$(-\psi + j\theta)$ [cf. (12) and (14)], re- pectively leads to

$$\tanh(\psi + j\theta) = \frac{\zeta_2 + \zeta_1 \cos 2\theta + j \sin 2\theta}{\cos 2\theta - 1 + j\zeta_1 \sin 2\theta} \tag{30a}$$

$$\tanh(-\psi + j\theta) = \frac{\zeta_1 + \zeta_2 \cos 2\theta + j \sin 2\theta}{\cos 2\theta - 1 + j\zeta_2 \sin 2\theta}. \tag{30b}$$

sing these results for substitution in (27b), we have

$$S^* = \frac{2(\cos 2\theta - 1) + j(\zeta_1 + \zeta_2) \sin 2\theta}{(\zeta_1 + \zeta_2) \cos 2\theta + j(1 + \zeta_1\zeta_2) \sin 2\theta}. \tag{31}$$

Rationalization of this expression to obtain real and naginary parts results in

$$S^* = S_1 + jS_2 \tag{32a}$$

here

$$_1 = \frac{[\zeta_1+\zeta_2][2(1-\sec 2\theta)+(1+\zeta_1\zeta_2)\tan^2 2\theta]}{[\zeta_1+\zeta_2]^2+[1+\zeta_1\zeta_2]^2 \tan^2 2\theta} \tag{32b}$$

and

$$S_2 = \frac{[\tan 2\theta][(\zeta_1+\zeta_2)^2+2(1+\zeta_1\zeta_2)(\sec 2\theta-1)]}{[\zeta_1+\zeta_2]^2+[1+\zeta_1\zeta_2]^2 \tan^2 2\theta}. \tag{32c}$$

If we now consider the driving-point impedance as comprising a resistance R and reactance X in series, from (27a) and (32), we find

$$Z = R + jX \tag{33a}$$

where

$$R = \frac{K^2 S_1}{\omega C_E 2\theta}. \tag{33b}$$

and

$$X = \frac{K^2}{\omega C_E 2\theta}\left[S_2 - \frac{2\theta}{K^2}\right]. \tag{33c}$$

Although these are expressions for which we have been looking, they can be improved insofar as their applicability to a large range of design problems is concerned. It will be seen from the final equations that a crystal which is symmetrically vacuum-loaded, $\zeta_1 = \zeta_2 = 0$, has its first "resonance" for $\theta = \pi/2$. Since

$$\theta = \frac{\omega}{c}\frac{l}{2} = \frac{2\pi}{\lambda}\frac{l}{2},$$

if we define the quantity λ_0 from the condition that

$$\frac{2\pi}{\lambda_0}\frac{l}{2} = \frac{\pi}{2},$$

we have

$$\lambda_0 = 2l. \tag{34a}$$

Since the velocity of propagation within the crystal c is a constant of the piezoelectric material, we are able to define the quantity ω_0 by the equation

$$\omega_0 = \frac{2\pi c}{\lambda_0}. \tag{34b}$$

Finally, by defining the dimensionless parameter δ by

$$\delta = \frac{\omega}{\omega_0} = \frac{\lambda_0}{\lambda}, \tag{34c}$$

we find

$$\theta = \delta \frac{\pi}{2}. \tag{34d}$$

Upon introducing these relations in the expressions for the impedance, we obtain the final results:

$$Z = R + jX \tag{35a}$$

where

$$R = \frac{K^2}{\delta^2 \frac{\pi}{2} \omega_0 C_E}\left\{\frac{[\zeta_1 + \zeta_2][1 - \sec \delta\pi + \frac{1}{2}(1 + \zeta_1\zeta_2)\tan^2 \delta\pi]}{[\zeta_1 + \zeta_2]^2 + [1 + \zeta_1\zeta_2]^2 \tan^2 \delta\pi}\right\} \tag{35b}$$

[14] A lower-case letter is usually used, but to avoid confusion with k appearing in (9), the upper case will be used throughout.

and

$$X = \frac{K^2}{\delta^2 \frac{\pi}{2} \omega_0 C_E} \left\{ \frac{\tan \delta\pi \left[\frac{1}{2}(\zeta_1 + \zeta_2)^2 + (1 + \zeta_1\zeta_2)(\sec \delta\pi - 1)\right]}{[\zeta_1 + \zeta_2]^2 + [1 + \zeta_1\zeta_2]^2 \tan^2 \delta\pi} - \frac{\delta \frac{\pi}{2}}{K^2} \right\} \tag{35c}$$

The driving-point admittance is obtained very easily from these equations. Since the admittance Y is the sum of a conductance G and susceptance B in parallel, we have

$$Y = G + jB. \tag{36a}$$

By definition, $Y = 1/Z$; thus, from (35a) and (36a) it follows immediately that

$$G = \frac{R}{R^2 + X^2} \tag{36b}$$

and

$$B = -\frac{X}{R^2 + X^2}. \tag{36c}$$

Equations (35) and (36) are the general relations valid for all conditions of loading and frequency consistent with our original assumptions. The crystal constants, K, ω_0, and C_E, are only dependent upon the type of piezoelectric material used and its dimensions; whereas, the normalized load impedances, ζ_1 and ζ_2, are determined by the choice of crystal and the loading media. It must be remembered that, in general, ζ is complex, although in the majority of ultrasonic applications, ζ can be considered real.

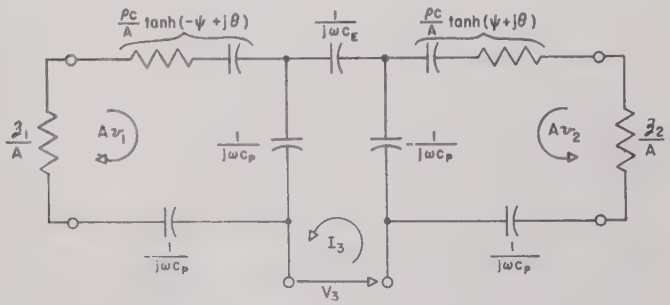

Fig. 6—Two-terminal equivalent circuit including two asymmetric mechanical terminations.

The two representations of the transducer driving its acoustic loads as electrical circuit elements are shown in Fig. 7. The series form is useful when the source of electrical energy has a high internal impedance, while the shunt form is useful for a source having a low internal impedance. These two limiting cases are usually approximated by constant current and constant voltage sources, respectively.

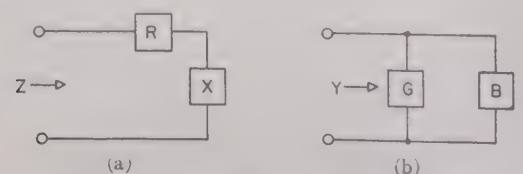

Fig. 7—(a) Two-terminal series equivalent circuit. (b) Two-terminal shunt equivalent circuit.

2. Summary of Important Characteristics

Detailed impedance and admittance curves, plotted as functions of frequency for several important loading conditions, are presented in an earlier report,[15] but for the sake of brevity are not repeated here. They give much information concerning the operating characteristics of piezoelectric transducers under varied conditions of loading and frequency. Although most of the details have been left to the actual curves, a listing of the important trends should be of considerable value in assisting the designer to comprehend the behavior of such elements. For verification of the items listed, reference to the curves and equations is required.

(i.) No power output is obtained at even harmonics of the fundamental frequency other than $f = 0$.

(ii.) Bandwidth increases when the load impedance increases. In most cases, this increase continues for load impedances greater than that of the crystal.

(iii.) Loading of both crystal surfaces leads to greater bandwidths than are obtained by keeping one surface unloaded.

(iv.) Maximum power output at resonance for a given driving source varies inversely with transducer bandwidth.

(v.) Operation at very low frequencies requires heavy loading of both surfaces and a source with a high internal impedance.

(vi.) Loading by materials having impedances greater than that of the transducer leads to doubly peaked resonance curves analogous to those obtained with over-coupled electrical circuits.

(vii.) With a high internal-impedance source, the resonance frequencies decrease with an increase in loading; but with a low internal-impedance source, the resonance frequencies remain very nearly constant.

(viii.) With a high internal-impedance source, the power output varies inversely with the square of the order of the harmonic of the fundamental frequency. With a low internal-impedance source and light loading this is also roughly the case; but with heavy loading the power output is very nearly independent of the order of the harmonic.

Acknowledgments

The author wishes to express his appreciation to Harold Mueller and J. A. Stratton for their interest in this problem, and for their helpful criticism and suggestions throughout the course of this work.

[15] W. Roth, "Piezoelectric Transducers," Research Laboratory of Electronics, Massachusetts Institute of Technology, Technical Report No. 43, July, 1947.

Broad-Band Power-Measuring Methods at Microwave Frequencies*

L. E. NORTON†

Summary—Two broad-band methods of measuring power at icrowave frequencies have been investigated. In both methods, the ormal load termination may remain connected to the microwave enerator while the power is being measured.

The first method makes use of the forces due to the electro-agnetic fields in a transmission system to cause displacements of diaphragm or membrane. This displacement is proportional to the uare of the actuating fields and is made to operate an indicating stem which gives output proportional to the microwave power.

In the second method, thin films on a skin-depth scale are in-rted in a microwave transmission system so as to cause only small scontinuities. A small fraction of the total power, usually 1/1800 1/200, is dissipated in the film. The indicator system measures e temperature rise of the film, ordinarily as a function of its re-stance change, and output is again proportional to the microwave wer.

Continuous characteristics have been measured from 1,000 to ,000 Mc, with additional isolated data at about 300 kc, 5 Mc, and 0 Mc. Both methods give a calibration flat to better than ±1 db etween 1,000 and 10,000 Mc with gradually reduced sensitivity at wer frequencies for the tellurium-zinc unit.

Introduction

WITH RAPID ADVANCES in the entire microwave field, and with ever-increasing use of this region of the frequency spectrum, improved easuring techniques of all kinds have become more and ore important. One of the quantities which must frequently be measured is power. While single-frequency ethods, and methods applicable to frequency bands nly a few per cent in width, have been used for many ears, little work has been reported on truly wide-band ethods—methods by which power could be measured ver frequency intervals of ten, and even approaching heoretically, at least) bands extending from very low equencies to the highest now obtainable in the microave spectrum.

Two broad-band methods of measuring power have een investigated. In each of these methods, the normal rmination may be connected to the system at all times. The two methods are basically different and will be escribed separately.

Method I

In the first method, use is made of the forces due to ectromagnetic fields in a microwave transmission system to produce deflections of a diaphragm. This diaragm is inserted in a transmission system so as to produce only a small discontinuity. Consequently, the fields are only slightly disturbed by the insertion of the diaphragm. The displacements of the diaphragm are then made to produce output from an indicator system, and the indicator output is proportional to the square of the fields at the diaphragm. For the case where the termination matches the transmission system and the standing-wave ratio is unity, the output is proportional to the power in the system. For any other termination which produces a standing-wave ratio other than unity, power may again be measured. In this case, an ordinary probe is incorporated in the transmission system near the diaphragm. By measuring both the standing-wave ratio and the value of the field at the diaphragm relative to either the maximum or minimum value, the power may again be calculated from the output indication. The field at the diaphragm is best determined $n\lambda/2$ distant from the diaphragm, where λ is the wavelength. However, for many applications, the normal termination produces a standing-wave ratio close to unity and the power may, therefore, be read directly.

The first experimental work was done with hollow transmission systems (waveguides) simply because the absence of an inner conductor made constructional work easier. However, in this case, the output indication is independent of frequency only so far as the fields are independent of frequency and, as is well known, in waveguides the fields have a frequency dependence. Therefore, a transmission system in which the fields are independent of frequency was later substituted for the waveguide. A coaxial line with a diameter small enough at the highest frequency so that only the principal mode is propagated is satisfactory to fulfill this condition.

One of the first factors to be considered was the magnitude of the force and diaphragm displacement for moderate powers in the transmission system.

For either waveguide or coaxial line, it should be pointed out that the force due to charges on the inner surface and the electric field terminated by the charge is opposite in sign to the force on the same surface due to the magnetic field and the field terminating current flowing on the surface. Fortunately, for any geometry of transmission which was investigated, these forces could always be made unequal and the resultant force was always approximately that of the larger force.

Orders of magnitude for component and resultant forces for waveguides and coaxial lines for specific powers are shown in Table I and Fig. 1. As indicated, for the best geometry for either waveguide or coaxial line, the maximum force for 10^{-3} watts in the transmission path is far from enormous. It is, in fact, about 10^{-6} dynes/cm^2 for 1 milliwatt.

* Decimal classification: R245. Original manuscript received by e Institute, March 14, 1948; revised manuscript received, January , 1949.

† Radio Corporation of America, RCA Laboratories Division, inceton, N. J.

TABLE I

Rectangular cross-section waveguide. Only $E_{1,0}$ mode propagated
Power 10^{-3} watts.
$\lambda = 3.22 \times 10^{-2} m$.
$a = 1.016 \times 10^{-2} m$.
$b = 2.286 \times 10^{-2} m$.
F_e, F_m, and $|F_r|$ are times 10^6 dynes/cm².

Waveguide height a				*Waveguide height a/10*			
Waveguide Width	F_e	F_m	$\|F_r\|$	Waveguide Width	F_e	F_m	$\|F_r\|$
b	0.204	0.101	0.103	b	2.04	1.01	1.03
				$8b/10$	3.80	0.86	2.94
				$3b/4$	5.52	0.68	4.84

These calculations are given in Appendix I and Appendix II. In a waveguide, both F_e, the force due to the electric component of field, and F_m, the force due to the magnetic component of field, vary inversely with the

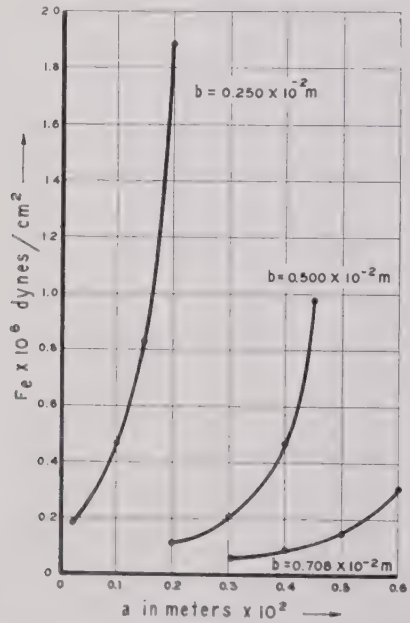

Fig. 1—Force F_e for several sizes of coaxial line.

small waveguide dimension a so the ratio F_e/F_m is independent of a. The important resultant quantity $|F_r|$, which is the difference between F_e and F_m, varies inversely with a. However, by reducing the large, or b, waveguide dimension, the F_e/F_m ratio is made large so that the resultant $|F_r|$ is reasonable and the indication is more sensitive.

In a coaxial line, $F_e = F_m$ so the resultant $|F_r|$ is zero. If there are gaps between the ends of the ribbon-type membrane and the main outer wall, the longitudinal current and associated F_m reduce nearly to zero and the resultant force $|F_r|$ is nearly equal to F_e.

If this method is to be used to measure power as small as several milliwatts, it is necessary to determine the signal-to-noise ratio for small actuating powers. The small magnitude of the force for small powers seemed to indicate that there was little point in attempting to use the deflected diaphragm in the equivalent of a dc system where the deflection would have to be measured from a zero reference which itself would be far from fixed in position due to the effects of other extraneous mechanical or acoustic forces which might be present.

Therefore, microwave energy impinging on the diaphragm was modulated completely and the over-all diaphragm and indicator system, with the diaphragm itself operating at its lowest resonant frequency, was made a narrow-band system. Modulation may be effected by direct modulation of the generator, a shutter placed anywhere in the path between generator and diaphragm, or by use of a switched parallel path with the diaphragm in one of the two parallel channels. It is most essential to choose the modulation rate of the microwave fields not so low that an additional and enormous "flicker effect" noise appears in the first tube, since it is then convenient to divide the total noise into only four contributing groups—the thermal noise of the grid-cathode circuit of the first tube following the diaphragm, the plate noise of the first tube, the thermal noise of the diaphragm, and the thermal noise of the air coupled to the diaphragm.

For a bandwidth of 10 cps at the modulation frequency of several kilocycles, the largest noise contribution is the thermal noise of the diaphragm. It seems unlikely that microwave powers smaller than about 1 milliwatt can be measured by this method since the computed signal-to-noise ratio at 1 milliwatt is only about 3. Experimental evidence appears to bear this out.

Any of several methods may be used to make use of the diaphragm displacement. A back plate may be placed immediately adjacent to the diaphragm so as to produce a capacitor. For use in an amplitude system, this capacitor is maintained at constant charge over the modulation cycle by a long-time-constant charging circuit. The resulting changing voltage across the capacitor is used as in a condenser microphone except that, in this case the following system is made narrow band. It was found necessary to use special cathode-follower coupling circuits between the diaphragm capacitor and the first amplifier tube when operating with only several milliwatts of microwave power. The small capacitor was also used to frequency-modulate a small line-controlled oscillator operating at a convenient frequency near 500 Mc. The ultimate limiting signal-to-noise ratio at low microwave power is about the same with the FM and AM systems. A metal-surfaced piezoelectric material with the inner metal surface replacing a section of metallic wall of the transmission system may also be used. The result is still another form of AM system. If desired, it is also possible to use optical methods for measuring the small diaphragm displacements.

The diaphragm arrangement applied to waveguide appears in Fig. 2. In adapting either piezoelectric crystals or metallic diaphragms to a coaxial-line system operating at wavelengths as short as 3 cm, to insure propagation of only the principal mode, the diameter must, of necessity, be small. To avoid serious geometric discont

nuities, it becomes impossible to incorporate a square or circular cross-section unit of 1 cm² dimension in the wall. Therefore, it is expedient to use long and narrow

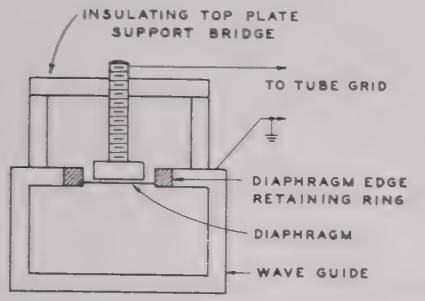

Fig. 2—Force-actuated diaphragm in a waveguide.

units with about the same over-all area to insure about the same acting force. A coaxial unit is shown in the photograph of Fig. 3.

Fig. 3—Force-actuated diaphragm in a coaxial line.

As has been indicated, the output potential of any of the force-operated units is proportional to the square of the electromagnetic fields. A calibration of the force unit against a standard thermistor wattmeter is shown in Fig. 4. It is also possible to calibrate the unit by another simple method. Since the microwave fields in the coaxial system are independent of frequency, the forces are likewise independent of frequency, and it is only necessary to substitute low-frequency fields (from the modulator, for example) as determined by voltmeters or ammeters and then to observe the relation between the known low-frequency fields and the output indicator.

If a standing wave of the form $\alpha = \alpha_0 \cos 2\pi L/\lambda$ exists along the diaphragm of length L, then Fig. 5 is a plot of the total force on the diaphragm as the length is increased, at constant frequency.

A plot of the output of the force unit at constant power input is shown in Fig. 6 for a wavelength range 3 to 30 cm.

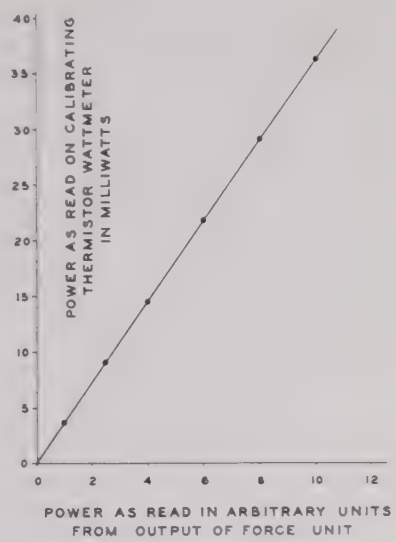

Fig. 4—Calibration of force-operated diaphragm unit versus a standard thermistor unit.

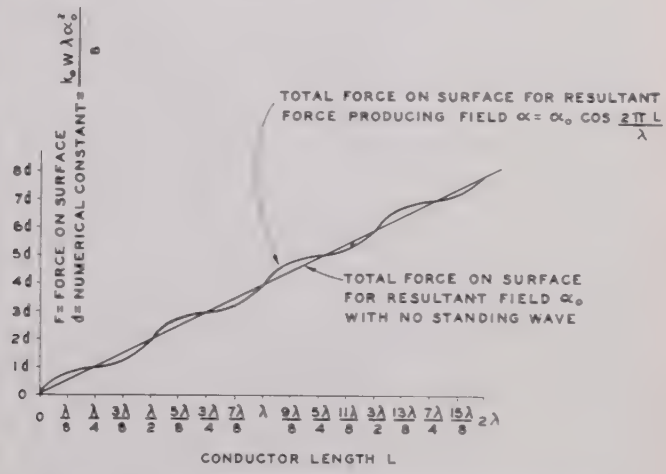

Fig. 5—Plot of total force on diaphragm versus length at constant frequency

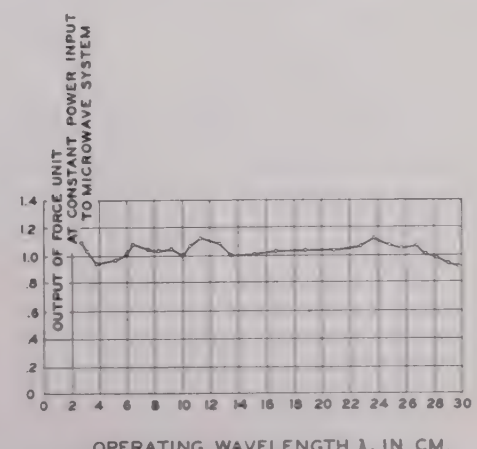

Fig. 6—Output of force-operated unit at constant power input for a wavelength range from 3 to 30 cm.

At power levels of the order of 10^{-3} watts, some care must be taken to isolate the diaphragm from extraneous noise excitation or acoustic excitation. If the minimum power is raised to 10×10^{-3} watts, the severity of the over-all problem is materially reduced.

As indicated in Fig. 4, the force-operated unit measures powers in the transmission system of the order of milliwatts. It is impossible to specify, in absolute fashion, the minimum power-measuring capabilities, since the result depends upon finally chosen minimum filter bandwidths and values of mechanical Q of the diaphragm. The result is modified further if, for example, instead of an integrating meter, a cathode-ray output device is used so as to utilize the selection and integrating properties of the eye in the presence of noise. However, for a diaphragm mechanical Q of about 3 in the presence of the closely spaced back plate near the diaphragm, and using a filter with an ultimate bandwidth of 1 cps at a resonance frequency of about 300 cps, the over-all signal-to-noise ratio is favorable for a driving force due to 1 milliwatt in the transmission system. Equally important, the output is independent of frequency.

Method II

This method uses a low-conductivity film, thin on a skin-depth scale, which is inserted in a transmission system so as to introduce small discontinuity into the system. A small fraction of the power is dissipated in the film. The fractions used have ranged from 1/1,800 to 1/200. The output indicating system provides a potential which is a function of the temperature rise of the film, and which is proportional to the square of the actuating electromagnetic field.

The thin film may be inserted in waveguide or coaxial line in either of several methods. Two general classifications may be made.

(a) Insertion of the thin film, with proper backing in a slot made by cutting away a section of waveguide wall, or of inner or outer conductor of coaxial line. Because of the difficulty of bringing out leads which would not disturb the microwave field configuration, no attempt was made to attach the thin film to a slot in the inner conductor.

(b) Insertion of the thin film in a plane normal to the direction of propagation in a waveguide or coaxial line. In the latter case, the plane of the thin film is, of course, also normal to the axes of the concentric conductors.

The first method is shown in Fig. 7. When a section of the wall of the transmission system is slotted and r placed by a strip of thin film, it is essential to place high-conductivity surface in back of, and close to, th film to prevent fields from appearing in the region b hind the film with resulting frequency-dependent radia tion. For this case of a thin film strip backed by a hig conductivity surface replacing a section of wall, to good approximation the total fields remain unchange from the original values.

However, the currents thus indicated are the tota currents flowing in the thin film and high-conductivit backing. Since only the fraction of the current flowin in the film contributes materially to its temperature ris it is necessary to determine the current division ratio This may be done as follows. The film and backing ar approximately in parallel for longitudinal current flo and the division ratio will depend on the equivalent im pedances of the two surfaces, each having a finite con ductivity.

The exponential decrease of fields through the thick ness of the thin film is small. Therefore, the entire physi cal volume of the thin film is exposed to the fields inde pendent of frequency so long as the film remains thin o a skin-depth scale. The current density in the thin fil does not change materially from its value at the surface The important result is that the equivalent impedanc of the thin film remains nearly constant as the frequenc is varied and is almost entirely real.

The situation is different in the thick, high-conductiv ity backing for the film. Here, because of the exponentia decrease of field intensity in the metal, more or less o the actual volume is exposed to the fields as the fre quency is changed. The result is that the equivalen resistance varies as the square root of the frequency Because the equivalent resistance of the thin film re mains constant with frequency while the equivalent re sistance of the thick backing varies as the square roo of the frequency, the power absorbed in the thin fil varies with the frequency.

This result is based on the assumption that a thin fil has only the properties of a scaled-down thin section o conductor. There is some experimental evidence, al though it is sketchy and incomplete, that evaporate thin films of certain metals exhibit either an equivalen series-inductance or shunt-capacitance effect which over a certain frequency interval, eliminated this powe

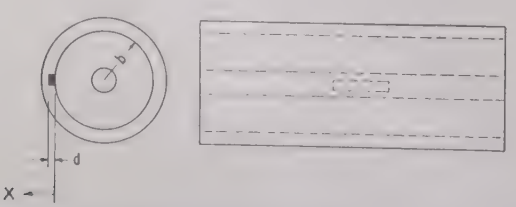

Fig. 7—Method of insertion of film and backing in a slot in the outer conductor of a coaxial line (shown schematically).

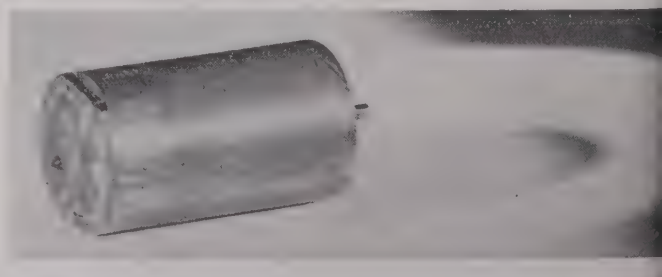

Fig. 8—Thin-film unit for insertion in a slot in a waveguide or coaxial line.

requency dependence. However, in general, the above esult holds and the configuration of Fig. 7 can never be nade very broad band.

A thin film unit suitable for insertion in a slot in a vaveguide or coaxial-line wall appears in Fig. 8.

Referring to the structure of Fig. 9 where the thin film s placed in a plane normal to the axes of the concentric onductors, a different situation exists. The thin film, vith some approximation, may be considered as a very hort section of line of complex characteristic imped- nce which is inserted between the other two sections f normal line.

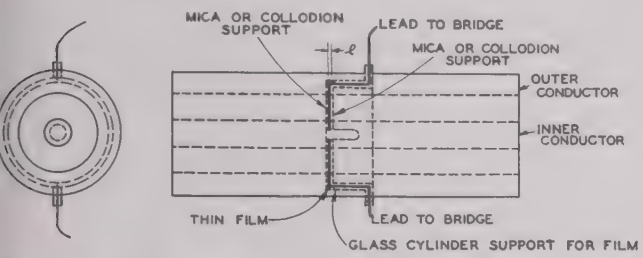

ig. 9—Method of inserting thin film in a plane normal to the axes of the concentric conductors of a coaxial line.

The conductivity of the tellurium-zinc thin-film ma- erial is 500 mhos per meter. For a maximum operating requency of 10^{10} cps and assuming (so as to obtain a lefinite number) that the maximum standing-wave ra- io introduced by the thin film should not exceed about .02 for all phases, the maximum permissible thickness f the film, l in Fig. 9, was calculated to be 3.2×10^{4} Angstrom units. For a film thickness equal to or less han this value, the discontinuity and reflection at the lm is slight provided the film is supported on a very hin base material like collodion or mica.

The leads from the thin film are brought out and con- ected as one arm of a four-element bridge. For a small nbalance, the unbalance current and potential are pro- ortional to the incremental resistance change. The in- remental resistance change for a small incremental emperature rise is proportional to the power in the ransmission system. Because of the nonlinear resist- nce-voltage characteristic of the tellurium-zinc films, lters with bandwidths narrow enough to eliminate har- nonics of the low-frequency potential applied to the ridge must be used with the amplifier and indicator sys- em following the bridge.

Initial calibration is effected by comparison with a alibrated wattmeter which is substituted for the nor- nal termination. Calibration was also made in another ay. A known amount of power was supplied to the ransmission system and the corresponding output read- ng noted. The incremental resistance change which was equired to give this output was determined by substi- uting known values of incremental resistance to give he same output reading. From the known resistance- emperature characteristic of the film material, the cor- responding temperature rise was computed. The power required to provide this temperature rise for a long, thin film was then calculated. This power, when compared with the power in the system, produced the ratio of power dissipated in the film to the power transmitted in the system.

Once this fraction is known, calibration is effected by switching in a known amount of power to the bridge at zero frequency as determined by a dc milliammeter, and noting the output of the indicator. The system gain is then always set to give the same output for the known value of calibrating dc power input.

For the case where a standing wave exists in the transmission system, the same procedure using a standing-wave detector, as described for the force-operated wattmeter, again permits power to be measured.

A calibration obtained by plotting output of the thin film against known powers in the transmission system is shown in Fig. 10. Although the sensitivity can be ex-

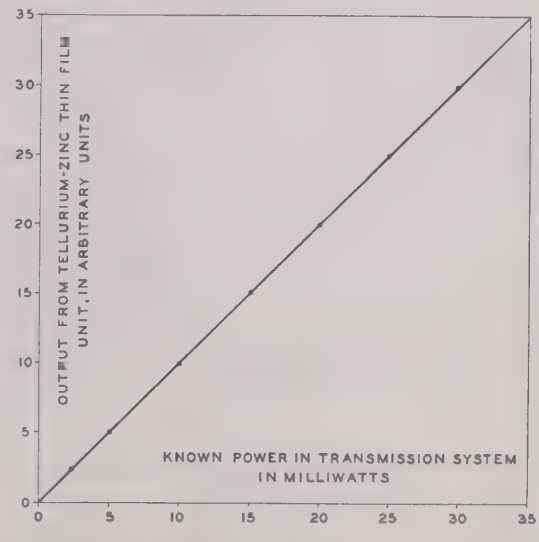

Fig. 10—Calibration of thin-film unit showing output versus known powers in the transmission system.

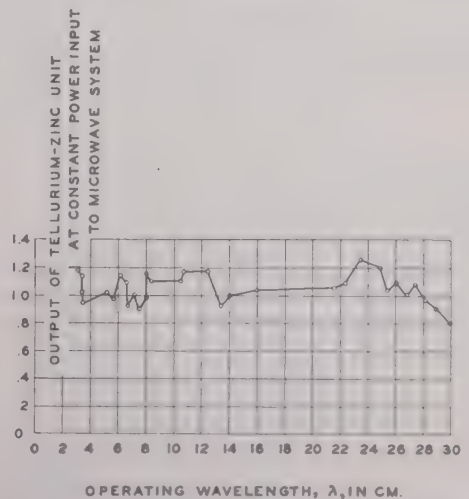

Fig. 11—Thin-film output versus frequency at constant microwave power

tended somewhat, because of the fact that only a small fraction of the power is dissipated in the film, many difficulties can be avoided if the minimum system power to be measured is made about 1 mw.

A plot of the indicator output against frequency at constant microwave power appears in Fig. 11. Most of the fluctuations are due to reflections at the various line couplings.

One of the thin film units for transverse insertion in a waveguide or coaxial line is shown in Fig. 12.

As in the case of the force-operated wattmeter, readings may be taken continuously with the normal termination always connected to the transmission system.

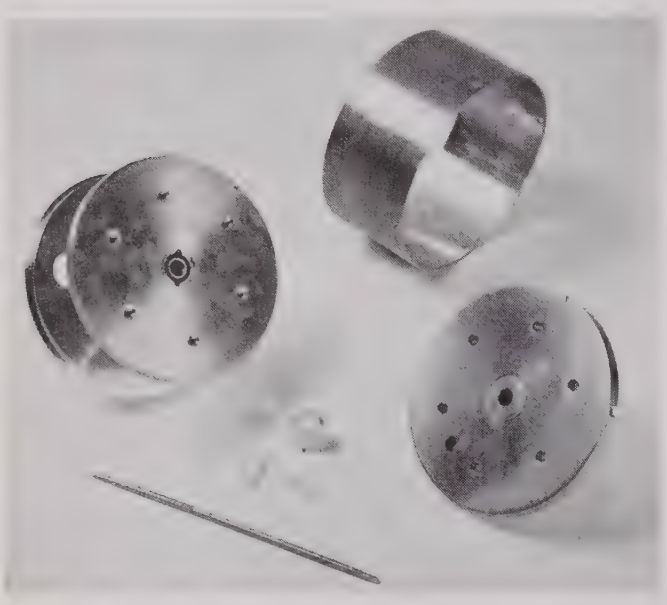

Fig. 12—Thin-film unit for insertion in a coaxial line or waveguide, plane normal to direction of propagation.

Appendix I

Force-Operated Unit and Waveguide Transmission Path

For the infinite conductivity, rectangular cross-section waveguide of Fig. 13, and with only the $E_{1,0}$ mode propagated, the following fields exist

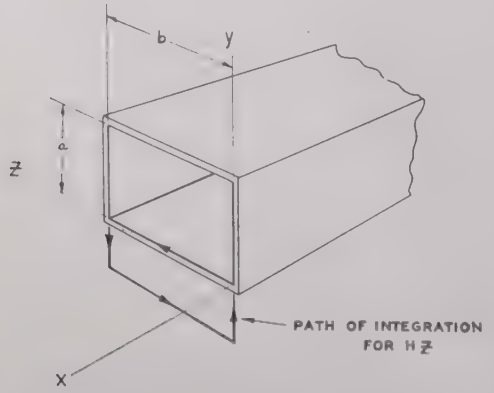

Fig. 13—Waveguide for discussion in Appendix I.

$$E_y = iA\omega\mu_0 \frac{b}{\pi} \sin\left(\frac{\pi z}{b}\right) e^{i(\omega t-\beta x)} \quad (7)$$

$$E_x = 0 \quad (7)$$

$$E_z = 0 \quad (7)$$

$$H_x = A \cos\left(\frac{\pi z}{b}\right) e^{i(\omega t-\beta x)} \quad (7)$$

$$H_y = 0 \quad (7)$$

$$H_z = iA \frac{b}{\pi} \sin\left(\frac{\pi z}{b}\right) e^{i(\omega t-\beta x)} \quad (7)$$

where

$$\beta = \left[\left(\frac{\omega}{c}\right)^2 - \left(\frac{\pi}{b}\right)^2\right]^{1/2}. \quad (7)$$

The following notation will be used:

a = small waveguide dimension
b = large waveguide dimension
$\mu_0 = 4\pi \times 10^{-7}$ henrys per meter
$\epsilon_0 = 10^{-9}/36\pi$ farads per meter
$c = 3 \times 10^8$ meters per second
$\lambda_0 = 2b$ = waveguide cutoff wavelength in meters
$f_0 = c/2b$ = waveguide cutoff frequency in cps
f = frequency in cps
S = power in watts.

The potential between top and bottom surfaces of th waveguide midway between the side walls ($z = b/2$) is

$$V = \int_0^a E_y dy = \frac{iA\omega\mu_0 ab}{\pi} \text{ volts} \quad (8)$$

and the total longitudinal current flowing along the to or bottom surfaces is expressed by the integral

$$I = \int_S H_z \cdot ds = \int_0^b H_z \cdot dz = i2A\beta\left(\frac{b}{\pi}\right)^2 \text{ amperes.} \quad (9)$$

Since it will be convenient to compute various quan tities on a unit power basis it is well to note that, fro the complex Poynting vector, the average power is

$$S = \int 1/2[E_y \times H_z^*]dA = \frac{A^2}{4}\omega\mu_0\beta\left(\frac{b}{\pi}\right)^2 ab \quad (10)$$

where the asterisk indicates the conjugate of H_z.

Defining a characteristic impedance on a power-cu rent basis,

$$Z_{SI} = \frac{S}{I_{\text{rms}}^2} \frac{\omega\mu_0\pi^2 a}{8\beta b} \quad (11)$$

and defining another characteristic impedance on a po tential-current basis

$$Z_{VI} = \frac{V}{I} = \frac{\omega\mu_0\pi a}{2\beta b}, \quad (12)$$

then from (8), (9), (10), (11), and (12) the rms potenti between top and bottom surfaces is

$$V_{\text{rms}} = \left[\frac{2\omega\mu_0 aS}{\beta b}\right]^{1/2} = \left[\frac{S\pi\omega a S \times 10^{-7}}{\beta b}\right]^{1/2} \text{ volts.} \quad (13)$$

The field E_y has no y dependence and so the field is simply

$$E_y = \frac{V}{a} = \left[\frac{S\pi\omega S \times 10^{-7}}{\beta b a}\right]^{1/2} \text{ volts/meter.} \quad (14)$$

The longitudinal rms current along either top or bottom of the waveguide for a power S is

$$I_{\text{rms}} = \left[\frac{8\beta b S}{\omega\mu_0\pi 2a}\right]^{1/2} \text{ amperes,} \quad (15)$$

and, since the longitudinal current in the z direction has a sin $\pi z/b$ distribution, the current per unit strip at the center where $z = b/2$ is

$$(I_x)_{z=b/2} = \frac{\pi}{2b}\left[\frac{8\beta b S}{\omega\mu_0\pi 2a}\right]^{1/2} = \left[\frac{\beta S \times 10^{7}}{2\omega\pi b a}\right]^{1/2} \text{ amperes.} \quad (16)$$

The force per unit area due to the electric component is directed along E_y and is

$$F_e = \frac{\epsilon_0 E^2}{2} = \frac{E^2}{72\pi} \times 10^{-4} \text{ dynes/meter}^2 \quad (17)$$

or

$$F_e = \frac{\omega S \times 10^{-11}}{9\beta b a} \text{ dynes/meter}^2 = \frac{S \times 10^{-3}}{3ab\left[1 - \left(\frac{\lambda}{2b}\right)^2\right]^{1/2}} \text{ dynes/meter}^2. \quad (18)$$

The force at the center of the bottom ($z = b/2$) conductor per strip of unit width and of unit length due to the magnetic field B and the field terminating longitudinal current is

$$F_m = (I_x)_{z=b/2} \times \frac{B_z}{2} \quad (19)$$

or

$$F_m = \mu_0 (I_x)_{z=b/2} \times \left(\frac{H_z}{2}\right)_{z=b/2} = \frac{\mu_0}{2}(I_x)^2_{z=b/2}$$
$$= 2\pi (I_x)^2_{z=b/2} \times 10^{-7} \text{ newtons}$$
$$= 2\pi (I_x)^2_{z=b/2} \times 10^{-2} \text{ dynes,} \quad (20)$$

all per unit width strip per unit length.

From (20) and (16), the force is

$$F_m = \frac{\beta S \times 10^5}{ba} \text{ dynes/meter}^2 = \frac{\left[1 - \left(\frac{\lambda}{2b}\right)^2\right]^{1/2} S \times 10^{-3}}{3ab} \text{ dynes/meter}^2. \quad (21)$$

The ratio F_e/F_m becomes

$$\frac{F_e}{F_m} = \frac{\frac{\omega S \times 10^{-11}}{9\beta b a}}{\frac{\beta S \times 10^5}{\omega b a}} = \frac{\omega^2 \times 10^{-16}}{9\beta^2} = \frac{1}{\left[1 - \left(\frac{\lambda}{2b}\right)^2\right]}. \quad (22)$$

The resultant force acting on a unit surface of top or bottom wall is

$$F_r = F_e + F_m \quad (23)$$

and, since F_e is directed in the positive y direction and F_m in the negative y direction,

$$|F_r| = F_e\left\{1 - \left[1 - \left(\frac{\lambda}{2b}\right)^2\right]\right\}$$

or

$$|F_r| = \left(\frac{\lambda}{2b}\right)^2 F_e. \quad (24)$$

Near cutoff, F_e becomes large, but of course, other considerations preclude the possibility of operating too near this critical wavelength. The resultant force F_r becomes very much larger as the cutoff wavelength is approached. In fact,

$$|F_r| \lim_{\lambda \to 2b} = \left(\frac{\lambda}{2b}\right)^2 \lim_{\lambda \to 2b} F_e = F_e. \quad (25)$$

Appendix II

Force-Operated Unit and Coaxial-Line Transmission Path

Referring to Fig. 14, the field conditions which exist are as follows:

$$E_r = \left[\frac{\mu_0}{\epsilon_0}\right]^{1/2} \frac{H_0}{r} e^{i(\omega t - \gamma z)} \quad (26)$$

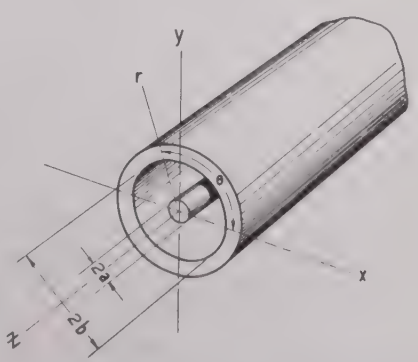

Fig. 14—Coaxial line for discussion in Appendix II.

$$E_\theta = 0 \tag{27}$$

$$E_z = 0 \tag{28}$$

$$H_r = 0 \tag{29}$$

$$H_\theta = \frac{H_0}{r} e^{i(\omega t - \gamma z)} \tag{30}$$

$$H_z = 0 \tag{31}$$

where

$$\gamma = \omega[\epsilon_0 \mu_0]^{1/2} = \frac{\omega}{c}, \tag{32}$$

and H_0 is a number.

The total voltage across the inner and outer conductors is

$$V = \int_a^b E_r \cdot d_r = \left[\frac{\mu_0}{\epsilon_0}\right]^{1/2} H_0 e^{i(\omega t - \gamma z)} \int_a^b \frac{dr}{r}$$

$$= \left[\frac{\mu_0}{\epsilon_0}\right]^{1/2} H_0 e^{i(\omega t - \gamma z)} \log b/a. \tag{33}$$

Combining (26) and (33),

$$V = rE_r \log b/a \tag{34}$$

or

$$E_r = \frac{V}{r \log b/a}. \tag{35}$$

The field at $r = b$ is

$$(E_r)_{r=b} = \frac{V}{b \log b/a}. \tag{36}$$

The total longitudinal current flowing on the inside surface of the outer conductor is

$$I = \int_0^{2\pi b} H_\theta \cdot da = 2\pi b H_\theta = 2\pi H_0 e^{i(\omega t - \gamma z)}. \tag{37}$$

The characteristic impedance of the line may be defined as

$$Z_0 = \frac{V}{I} = \frac{\left[\frac{\mu_0}{\epsilon_0}\right]^{1/2} H_0 e^{i(\omega t - \gamma z)} \log b/a}{2\pi H_0 e^{i(\omega t - \gamma z)}}$$

$$= \frac{\left[\frac{\mu_0}{\epsilon_0}\right]^{1/2}}{2\pi} \log b/a. \tag{38}$$

Since $\mu_0 = 4\pi \times 10^{-7}$ henrys/meter

$$\epsilon_0 = \frac{10^{-9}}{36\pi} \text{ farads/meter}$$

$$Z_0 = 60 \log b/a. \tag{39}$$

Computing the various quantities on a constant power basis,

$$S = \frac{V^2}{Z_0} = \frac{V^2}{60 \log b/a}, \tag{40}$$

so that (36) becomes

$$(E_r)_{r=b} = \left[\frac{60S}{b^2 \log b/a}\right]^{1/2}. \tag{41}$$

The force due to the field is, from (17),

$$F_e = \frac{(E_r)^2_{r=b} \times 10^{-4}}{72\pi} = \frac{5S \times 10^{-4}}{6\pi b^2 \log b/a}. \tag{42}$$

The longitudinal current per unit width strip on the inside surface of the outer conductor is

$$I_z = \int_0^1 H_\theta \cdot ds = H_\theta = \frac{H_0}{b} e^{i(\omega t - \gamma z)}. \tag{43}$$

$$I_z = \frac{V}{b\left[\frac{\mu_0}{\epsilon_0}\right]^{1/2} \log b/a}$$

$$= \left[\frac{60S}{b^2 \frac{\mu_0}{\epsilon_0} \log b/a}\right]^{1/2} \text{amperes/meter}. \tag{44}$$

The force per unit area due to the magnetic field H_θ and the field terminating current I_z is

$$F_m = I_z \times \frac{H_\theta}{2} = \mu_0 I_z \times \frac{H_\theta}{2}.$$

From (43) and (44)

$$F_m = \frac{5S \times 10^{-4}}{6\pi b^2 \log b/a} \text{ dynes/meter}^2. \tag{45}$$

The ratio of the two forces F_e and F_m is

$$\frac{F_e}{F_m} = 1. \tag{46}$$

The force $F_m = \mu_0 I_z \times H_\theta/2$ is, of course opposite in sign to the force $F_e = \epsilon_0 E^2/2$, so that the resultant force is zero, since

$$|F_r| = F_e - F_m = F_e - F_e = 0. \tag{47}$$

It is possible to make a ribbon membrane in a coaxial line almost entirely F_e operated by providing small gaps between the ends of the ribbon membrane and the main outer wall. The longitudinal current and corresponding F_m then reduce nearly to zero.

A Forward-Transmission Echo-Ranging System*

DONALD B. HARRIS†, SENIOR MEMBER, IRE

Summary—A new type of echo-ranging system is described in ich the receiver is located at a distance from the transmitter. It is own that, with a configuration of this type, the range of the target h respect to the receiving station is equal to the difference in path tween the direct and reflected waves divided by the versine of the gle of elevation of the receiving antenna ($\rho = \delta/1 - \cos\theta$). By mak- the radial writing speed proportional to this function, a PPI sentation system can be realized which shows a profile of the pagation path viewed from the side. This system has particular lication in detecting targets such as, for example, atmospheric ir- ularities, which have a low reflection coefficient at normal incident gles. The system, therefore, promises to be useful in the study of pagation problems.

Introduction

UHF PROPAGATION studies have revealed the undeniable existence of irregularities of some type in the propagation path, which result in ltipath transmission and variation in signal strength eived at distances considerably beyond the horizon. is phenomenon does not appear to be due to "ducts," ich produce a strong and fairly steady signal over a nsiderable period of time: the irregularities referred exist at times when ducts appear to be absent, and se extremely rapid fading. The appearance on the ording instruments is similar to that which would be sed by reflections from a multiplicity of reflecting jects moving at random in the propagation path.

Vertical radar soundings have been made[1] and have ccessfully located, directly overhead, air-mass bound- es of the type which may be responsible for the ob- ved results. It appears possible that similar sound- s taken horizontally, with grazing incidence and, con- quently, enhanced reflection response at the target face, might reveal numerous irregularities distributed roughout a considerable length of the propagation th.

This paper considers the possibility of developing an trumentation system, using radar techniques, cap- e of operating with small beam-to-target-surface gles, and of displaying, on a PPI indicator, a profile of least a portion of the propagation path, in order to ow the instantaneous shape, size, and location of ir- ularities located in the path at any time, and their tion over a period of time. The approach suggested d analyzed involves a pulsed transmitter at the trans- tting site, and a receiver at a distant receiving site apted to measure the difference in path between a ve received directly from the transmitter and waves lected from or refracted by irregularities at the same small angles encountered in propagation work; to indicate the angle of arrival of the reflected or refracted waves; and to apply the resultant information to a sweep circuit and PPI indicator in such a manner as to display the coordinates of the irregularities, with reference to a rectangular frame of reference in which the horizontal axis represents distance along the propagation path and the vertical axis represents elevation.

Form of the Display Control Functions

Fig. 1 shows a profile of the propagation path, viewed from the side. It is evident from the figure that the

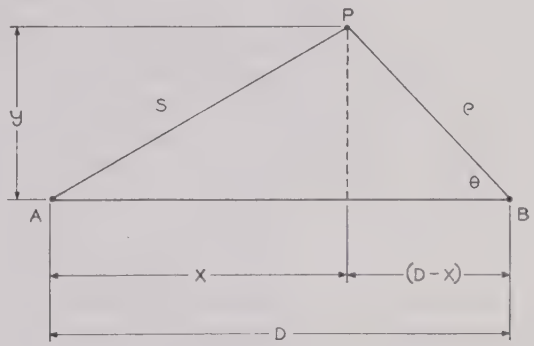

Fig. 1—Profile of propagation path between transmitter at A, and receiver at B, with target or irregularity at P.

range ρ may be determined from the following relationship:

$$S + \rho = D + \delta \tag{1}$$

where δ is the difference in path length between the direct and the reflected or refracted wave. We can eliminate S from this equation by employing the trigonometric relation

$$S = \sqrt{\rho^2 + D^2 + 2\rho D \cos\theta}, \tag{2}$$

which, when substituted in (1) gives, after expansion and collection of terms,

$$\rho = \frac{\delta(2D + \delta)}{2[D(1 - \cos\theta) + \delta]}. \tag{3}$$

If this equation were used directly to control the sweep voltage of a PPI-display system, some complication would result from the nonlinear dependence of ρ on δ. This disadvantage may be obviated by making the simplifying assumption that δ is small in comparison with $2D$ and with $D(1-\cos\theta)$. Under these conditions, (3) reduces to

$$\rho_a = \frac{\delta}{1 - \cos\theta}, \tag{4}$$

* Decimal classification: R537.1×R365.33. Original manuscript eived by the Institute, October 18, 1948; revised manuscript re- ved, March 9, 1949. Presented, 1949 IRE National Convention, w York, N. Y., March 9, 1949.

† Collins Radio Co., Cedar Rapids, Iowa.

[1] A. W. Friend, "Theory and practice of tropospheric sounding radar," PROC. I.R.E., vol. 37, pp. 116–138; February, 1949.

where ρ_a is the approximate range. This is an expression which can easily be used to control the sweep voltage along the scanning line.

Instrumentation

In practice, (4) would be applied to the control of the scanning voltage in the following manner: We first convert the independent variable of (4) from a distance to a time base, by substituting the relation

$$\delta = ct, \tag{5}$$

where c is the velocity of propagation, and t is the elapsed time between the reception of the direct wave and the reception of the reflected or refracted wave, to obtain

$$\rho_a = \frac{c}{1 - \cos\theta}\, t. \tag{6}$$

It is to be noted that this relationship is linear for any given value of the antenna elevation θ, but that it depends on this elevation. It is now evident that the displacement ρ_s of the spot across the face of the scope should be proportional to the range, or

$$\rho_s = k_1\rho_a = \frac{k_1 c}{1 - \cos\theta}\, t. \tag{7}$$

We attain this exact displacement by superimposing a sweep voltage

$$e_s = k_2\rho_s = \frac{k_1 k_2 c}{1 - \cos\theta}\, t \tag{8}$$

on the deflecting elements of the scope. Here k_2 is a constant depending on the characteristics of the tube. (k_2 is about 70 volts per inch in typical tubes.)

From (7), it is evident that the radial writing speed is

$$\frac{d\rho_s}{dt} = \frac{k_1 c}{1 - \cos\theta}. \tag{9}$$

As the elevation of the antenna changes, this radial writing speed is also varied by changing the time constants of the sweep circuits in accordance with information transmitted by synchros attached to the antenna elevation axis. The intensity of the spot is modulated by the echo signal received from the target, and, therefore, if such a signal is received at time t it will be displayed as a bright spot displaced along the scanning line by a distance $k_1\rho_a$ linearly proportional to the range of the target, as required.

The value of k_1 is, of course, determined by the range required and the size of the scope. If, for example, we wish to have the total length of the scanning line represent a distance of 0.5×10^6 feet (about 95 miles), and the scanning line is 4 inches, or 0.333 feet long, k_1 is 0.666×10^{-6}. Substituting this value, together with the velocity of light, in (9), we obtain for the writing speed in meters per second

$$\frac{d\rho_s}{dt} = \frac{0.666\times10^{-6}\times300\times10^6}{1 - \cos\theta} = \frac{200}{1 - \cos\theta}. \tag{10}$$

This quantity will actually vary between wide limits, depending upon the antenna elevation, as will be demonstrated later.

The synchronizing pulse for starting the sweep can probably best be transmitted over a separate channel.

Appraisal of Accuracy and Feasibility

The manner in which the approximate-range equation (4) deviates from the exact-range equation (3) at range values beyond $0.01D$ is shown by Fig. 2. It appears that, for our purposes, the discrepancy becomes unacceptable as the range exceeds $0.5D$, is probably tolerable between $0.5D$ and $0.1D$, and is negligible at a range of $0.1D$ or below.

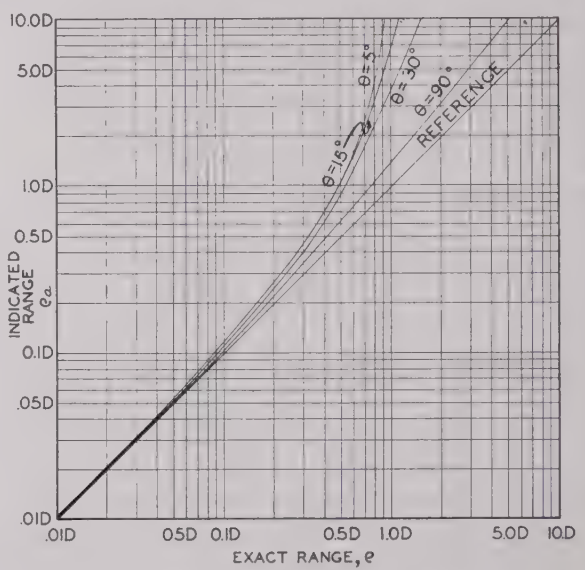

Fig. 2—Correct range ρ versus approximate range ρ_a for various elevation angles θ.

The pulse length required can be most easily determined by examining the actual path differences encountered at various altitudes and horizontal distances from the receiver. Since we are presumably interested in a horizontal layer of irregularities this procedure will be facilitated by the development of an equation relating the rectangular co-ordinates of the irregularity to the path difference. It can easily be shown that such an equation can be obtained from (1) by substituting the co-ordinate values of S and ρ. The result is

$$y = \frac{D}{2(p+1)}\sqrt{p(p+2)\left[p(p+2) - 4q^2 + 4q\right]} \tag{11}$$

where

$$p = \frac{\delta}{D} \tag{12}$$

$$q = \frac{x}{D}. \tag{13}$$

This is the equation of an ellipse in x and y. Thus, for ny given value of δ (or p), the irregularity may lie nywhere on an ellipse defined by (11), the foci of which e points A and B. Equation (11) is plotted in Fig. 3. is seen from this figure that if a base line of $D = 500{,}000$ et, or about 95 miles, be assumed, the delay ratio of an ject at $q = 0.90$, or at a distance of 50,000 feet from e receiver, and at an elevation of 2,500 feet, is somenat greater than 0.0001; a precise calculation employg (11) shows that the exact value is 0.000138, corsponding to a path difference of 69 feet or a time delay 0.0702 microsecond.

Since the irregularities involved may actually lie at elevation of 2,500 feet, it is concluded that extremely ort pulses of the order of 0.01 microsecond in length ll be required.

The range resolution realizable at a given elevation gle can be determined from the approximate range uation (6), which immediately gives, for the change range $\Delta\rho_a$ with change in time Δt,

$$\Delta\rho_a = \frac{c}{1 - \cos\theta}\,\Delta t. \tag{14}$$

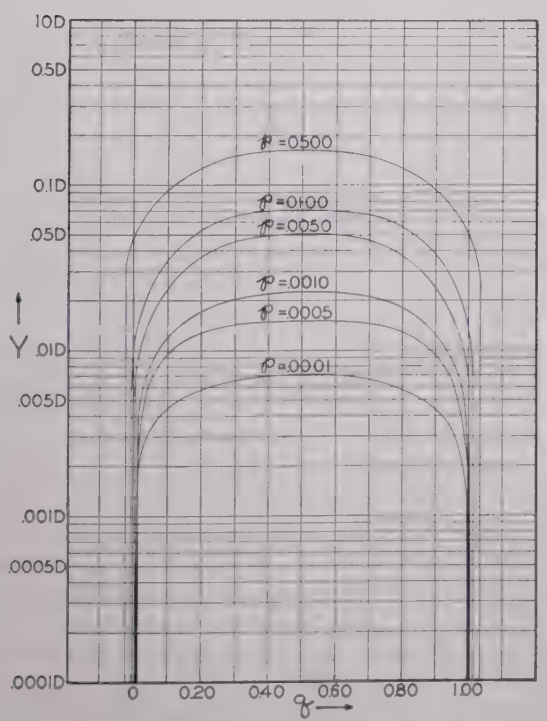

g. 3—Lines of constant delay ratio $p = \delta/D$, where δ is difference in path length between direct and reflected or refracted waves, and D is total length of path.

Now it is evident that, in order to obtain resolution, e time interval Δt between echoes from consecutive objects along the scanning line, must be at least equal to the pulse length T. Or,

$$\Delta\rho_{ar} = \frac{c}{1 - \cos\theta}\,T, \tag{15}$$

where $\Delta\rho_{ar}$ is the approximate range resolution.

The application of (10) and (15) to a surface at a constant elevation of 2,500 feet gives the following results at various horizontal distances from the receiver, assuming a base line of 500,000 feet, and a pulse length of 0.01 microsecond:

At a horizontal distance of 50,000 feet, corresponding to an antenna-elevation angle of 2.87°, the range resolution along the scanning line is 7,868 feet. The writing speed is 16.0 centimeters per microsecond.

At lower antenna-elevation angles, representing objects at a greater distance along the 2,500-foot constant-elevation surface, the range resolution will, of course, deteriorate, and the writing speed will also increase to a value attainable only with the greatest difficulty.

On the other hand, as the range decreases, the definition improves greatly, and the writing speed decreases to normal values. For example, for a target 2,500 feet high at a horizontal distance of 9,310 feet ($0.018D$) from the receiving site, corresponding to an elevation angle of 15°, the writing speed is 0.587 centimeter per microsecond, and the range resolution is about 290 feet.

With regard to the minimum range at which irregularities are observable, no data are available as to the maximum angle between the beam and the surface of the irregularity, beyond which the irregularity ceases to reflect or refract the beam. It seems safe to assume, however, that reflections will continue to be obtained up to an angle of arrival of 15°. It should, therefore, be possible to see irregularities lying at an elevation of 2,500 feet at horizontal distances from the receiving site not less than 9,310 feet.

This discussion of irregularities at minimum altitudes represents, of course, the worst condition. Irregularities lying at higher elevations will be readily detectable with improved definition.

Fig. 4 provides, for purposes of example, an over-all graphical summary of the specific propagation application proposed, involving a base line of 500,000 feet. In this figure the elevation y, in feet, is plotted against the horizontal co-ordinate x of the target, in feet, measured from the transmitter, for various constant values of the writing speed $d\rho_s/dt$, here designated as V_s, expressed in centimeters per microsecond, and of the resolution $\Delta\rho_{ar}$, in feet, employing the approximate equations (10) and (15).

Conclusion

Summarizing the analysis, it is indicated that it should be possible, using the proposed system, with a base line of 500,000 feet, to obtain valuable data regarding the nature of irregularities causing anomalous propagation phenomena, provided that the irregularities lie

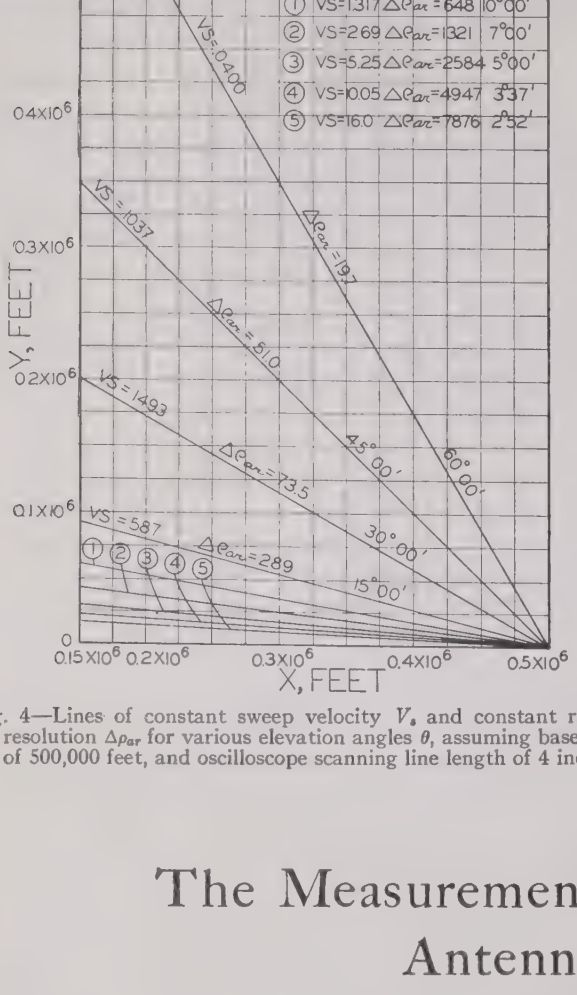

Fig. 4—Lines of constant sweep velocity V_s and constant range resolution $\Delta\rho_{ar}$ for various elevation angles θ, assuming base line of 500,000 feet, and oscilloscope scanning line length of 4 inches.

at elevations in excess of 2,500 feet. That portion of a hypothetical layer of irregularities at an elevation of 2,500 feet which extends along the propagation path between distances of $0.1D$, 50,000 feet, 9.48 miles, and $0.018D$, 9,310 feet, 1.76 miles, from the receiving site, should be presented with sufficiently good definition to permit detailed study. In order to achieve this result, it will be necessary to use equipment capable of detecting and displaying path differences as small as 69 feet, and time intervals as small as 0.07 microsecond, leading to the conclusion that a pulse length not greater than 0.01×10^{-6} seconds is required. A receiving antenna pattern 0.5° wide is required. Irregularities lying at higher elevations can be displayed with less difficulty and with improved definition.

In view of these requirements, it appears evident that the study should be made at microwave frequencies, probably in the X or K band.

Acknowledgment

The author gatefully acknowledges the assistance of his colleagues in the Collins Radio Co., J. W. Clark, W. W. Farley III, I. H. Gerks, J. P. Giacoletto, J. J. Livingood, D. O. McCoy, and W. W. Salisbury, and of F. W. Pierce of Rock Island, Ill., all of whom have read the original manuscript and made valuable suggestions.

The Measurement and Interpretation of Antenna Scattering*

D. D. KING†, MEMBER, IRE

Summary—**The significance of scattering cross section and back-scattering cross section in terms of antenna current distribution is considered. In particular, the influence of antenna load impedance on the magnitude and directional pattern of the scattered radiation is pointed out. A measuring scheme is described which utilizes the standing waves set up by energy reflected toward the transmitter from any receiving antenna or parasite. This method permits direct study of the back-scattering from loaded and unloaded antennas. Approximate scattering data for several types of antennas are included.**

I. Introduction

ALTHOUGH the concept of scattering and absorption cross sections is common to many branches of physics, its applications to antennas have been limited. This is reasonable, since the field pattern and input impedance suffice to specify antenna performance in a convenient fashion for practical use. An exception to this statement is the obvious application to radar of the back-scattering or radar cross section. The assigning of a radar cross section to a given target, whether it is an aircraft or a piece of "window," implies that this object functions as an antenna. The back-scattering cross section may therefore be interpreted as a measure of the antenna currents excited on such an object. The use of scattering data as a clue to the mechanism of antennas with complex shapes appears logical and the work described in the present paper was undertaken with this in mind.

The standing-wave method of measurement which was developed for the study of back-scattering furnishes information on the amplitude and phase of the scattered radiation relative to the incident beam. The image system used for the data to be presented also allows convenient variation of the antenna load. Of course, only antennas with a plane of symmetry are treated by image methods. The results obtained so far are of a preliminary nature and are presented to illustrate the possibilities and limitations of the method.

* Decimal classification: R221. Original manuscript received by the Institute, August 16, 1948; revised manuscript received, January 17, 1949. The research reported in this paper was made possible through support extended Cruft Laboratory, Harvard University, jointly by the Navy Department (Office of Naval Research) and the Signal Corps, U. S. Army, under Contract N5ori-76, T. O. I.

† Formerly, Cruft Laboratory, Harvard University, Cambridge, Mass.; now, Radiation Laboratory, Johns Hopkins University Baltimore, Md.

evertheless, certain conclusions may be drawn from
ie results presented which are not explicit in imped-
ıce and pattern data.

In the following sections some aspects of the scatter-
g concept are reviewed briefly. The experimental pro-
dure and results are discussed subsequently. Details
algebra are deferred to the Appendix for the con-
nience of the reader.

II. Basis of Scattering and Absorption Measurements on Antennas

Ordinarily, three cross sections or effective areas are
fined for an antenna. In these definitions the antenna
assumed to be illuminated by a substantially plane
ıve front.

sorption:

$$_0 = \frac{\text{power in load}}{\text{incident power density}}$$

attering:

$$_r = \frac{\text{power reradiated}}{\text{incident power density}}$$

ck scattering:

$$\sigma = 4\pi \frac{\text{power reflected toward the source/unit angle}}{\text{incident power density}}.$$

The absorption cross section may be derived from the
ld pattern by integrating the power received over the
tire solid angle. This summation of the power received
vided by the incident power density defines an average
sorption cross section equal to $\lambda^2/4\pi$ for any antenna
h matched load.[1] The product $(\lambda^2/4\pi)\cdot$(directivity)
en gives the absorption cross section in any particular
ection. Actually, the power received in the load is
luced by the amount of the losses in the antenna.[2]
An alternative definition of the absorption cross sec-
n is available in terms of the effective height h_e and
e input resistance R_a of an antenna.

$$A_0 = \frac{h_e^2}{R_a}\sqrt{\frac{\mu_0}{\epsilon_0}}. \tag{1}$$

e calculated value of A_0 given by (1) depends on the
rent distribution, and hence measurement of A_0
vides a test of calculated current distributions.[3]
The scattering cross section A_r is best considered in
terms of the equivalent circuit for the receiving antenna
drawn in Fig. 1.

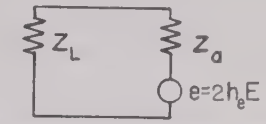

Fig. 1—Circuit of receiving antenna.

Here

Z_L = load impedance
Z_a = antenna input impedance
E = incident electric field
h_e = effective height of antenna for the particular angle of incidence.

Three values of the load impedance Z_L are now chosen in turn for the equivalent circuit:

1. $Z_L = Z_a^*$ where the asterisk means that the term is a complex conjugate. Then

$$P_L = P_a = e^2/4R_a. \tag{2}$$

Here P_L is the power dissipated in the load and P_a the power dissipated in the antenna; i.e., the power reradiated or scattered. Hence, for a matched load, absorption and scattering cross sections are equal.

2. $Z_L = 0$ Then.

$$P_a = e^2R_a/(R_a^2 + X_a^2). \tag{3}$$

The power scattered, and hence the scattering cross section, depends on the reactance X_a. In general, the scattering is small both far from resonance (X_a large) and at antiresonance (R_a large). At resonance, however, the scattering is four times as great with $Z_L = 0$ as with $Z_L = Z_a^*$. According to the equivalent circuit the phase of the scattered radiation relative to the incident wave varies from $-\pi/2$ for very short dipoles to $+\pi/2$ before antiresonance. However, the expression for the radiated field in terms of antenna current contains a factor $-j$ or exp. $(-j(\pi/2))$ which corresponds to a phase shift of $+\pi/2$. Therefore, the observed phase angle of the scattered radiation in the far zone should approach zero for short, unloaded dipoles; the observed phase angle should approach $\pi/2$ for $h = \lambda/4$ when $Z_L = 0$, and for all h when $Z_L = Z_a^*$,

3. $Z_L \to \infty$. With open-circuited terminals the equivalent circuit predicts zero scattering. This is correct in so far as the current distribution of the loaded or short-circuited antenna is concerned. However, an open circuit at the terminals of a complex antenna may permit other currents elsewhere in the antenna with appropriate scattering. An example of this is a dipole with a flat plate or a corner reflector.

[1] J. C. Slater, "Microwave Transmission," McGraw-Hill Book
, 1942, p, 264.
[2] C. G. Montgomery, "Techniques of Microwave Measure-
nts," McGraw-Hill Book Co., New York, N. Y., 1947, pp. 898–
[3] R. W. King, H. R. Mimno, and A. H. Wing, "Transmission
es, Antennas, and Wave Guides," McGraw-Hill Book Co., New
k, N. Y., 1945, pp. 164–173.

The back-scattering cross section σ is the product of the total scattering cross section A_r and the directivity. Actually, σ is proportional to the square of the directivity, since A_r involves the directivity and the energy is received and reradiated at the same angle. If the scatterer is operated with a matched load, the current distribution, and hence the directivity, is the same as for the antenna when used as a driven element. However, an unloaded scatterer, $Z_L=0$, may have a current distribution different from the loaded distribution.[4] Similarly, a more complicated structure involving parasitic elements may exhibit a scattering pattern different from its pattern as a driven or a receiving element. This is not contrary to reciprocal theorems since the scatterer then contains no load.

The dependence of the scattering pattern on the antenna load is generally small. However, the amplitude of the scattered radiation continues to be a function of the load impedance. This fact has been used in a scheme for antenna pattern measurements on aircraft models,[5] in which the load impedance of the receiving antenna in the model is varied at an audio rate and the resultant modulation of the back-scattering is detected in the transmitting horn.

Aside from furnishing a means of obtaining field patterns, scattering data provide information on the current distributions in complex antennas. Thus, the metal surfaces of aircraft, ships, or vehicles mounting antennas support parasitic currents. Considerable attention has lately been devoted to the study of such surface currents.[6]

In principle, the efficient utilization of the metallic surfaces of, say, an aircraft, as elements of a receiving antenna might be achieved as follows: First, locate regions of large surface current, and second, devise a scheme for efficient coupling of a transmission line and load to the surface currents. The success of such a scheme is measured in terms of input impedance and field pattern data. However, the choice of coupling depends on knowledge of the initial currents on the surfaces. These unloaded currents or "natural modes" are evidenced by corresponding maxima in the scattering cross section A_r. The back-scattering cross section σ is a more sensitive indicator of these "natural-mode" currents by virtue of the squared directivity factor involved. The effectiveness of coupling to the unloaded surface currents may be observed in terms of the ratio of unloaded to loaded scattering.

III. Standing-Wave Measurement of Back-Scattering

The determination of back-scattering by direct intensity measurements usually is hampered by the large attenuation from the inverse fourth-power term in the radar equation. Moreover, pulse techniques fail at sh ranges. An alternative approach to back-scatteri measurements is suggested by the analogy betwe wave transmission in free space and on a line. T application of transmission-line methods to the scatt ing problem yields formulas of practical value subj to certain mild restrictions.

The radiation field of an antenna is a traveling wa with propagation constant $\beta=2\pi/\lambda$, which is the sa as on a lossless line; the decline in amplitude is prop tional to $1/r$. An obstacle placed in the path of the traveling waves generates a reflected wave having certain fraction of the incident amplitude. The refl tion coefficient may be defined as usual in terms of t ratio of the sum and difference of incident and reflect waves. The resultant expression is more complicat than for a line since the standing-wave ratio is a fu tion of position. However, the formula as derived Appendix II involves no assumptions except that t field everywhere is of the form, constant $\cdot (e^{-i\beta r})/r$.

The formulas necessary to calculate the back-scatt ing cross section σ in terms of measured standing-wa ratios are derived in Appendix II. An application sample data is discussed in the following section. remains to analyze the actual distribution of the fields a function of the distance r from an antenna.

In case the antennas involved have dimensions mu greater than the wavelength, the situation may be d cussed in optical terms. The so-called Fresnel-Frau hofer boundary, defined as $R=D^2/\lambda$, (where D is t aperture diameter of the antennas and R their sepa tion) is the basic unit in this approach. At the distan $r=R$, the phase error is less than $\pi/4$ and the pow received is less than 5 per cent below the ideal valu This assumes a very small probe to test the field. Larg probes increase the distance R for the above limits error. In general, when the two antennas involved ha apertures D_1 and D_2, the minimum separation $R=(D_1+D_2)^2/\lambda$. From this, the minimum separati R may be expressed in terms of the distances R_s and calculated for the scatterer and probe separately.

$$R = R_s + R_p + 2\sqrt{R_s R_p}.$$

Details of the optical arguments are available in t literature.[2]

The situation when the antenna dimensions are the same magnitude as the wavelength is of grea interest in the present discussion. Under such con tions well-defined antenna resonances are to be pected. An exact analysis, of course, presumes a kno edge of the current distribution of the particular a tenna under test. However, an estimate of the distan involved is obtainable by assuming a dipole of app priate length with sinusoidal current distribution.

[4] See p. 165 of footnote reference 3.

[5] G. Sinclair, E. C. Jordan, and E. W. Vaughan, "The measurement of aircraft antenna patterns using models," Proc. I.R.E., vol. 35, pp. 1451–1467; December, 1947.

[6] J. V. N. Granger, "Low-Frequency Aircraft Antennas," Cr Laboratory Technical Report No. 25, December 30, 1947.

brief derivation of the necessary expression is given in Appendix I. Graphs of the results are shown in Fig. 2.

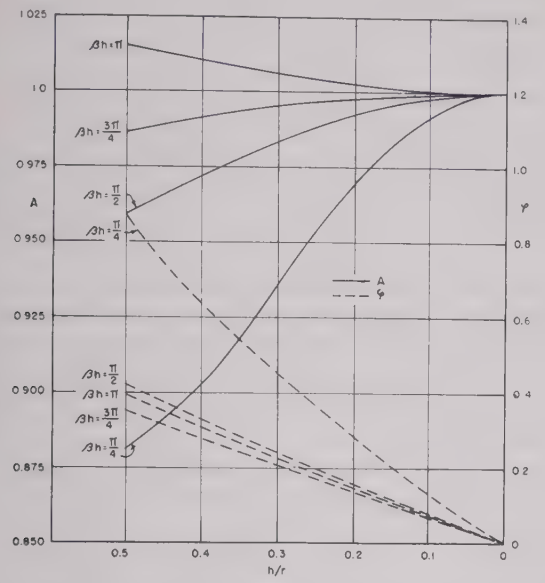

Fig. 2—Variation of amplitude A and phase ϕ of the field near a dipole. The abscissa is the ratio of dipole half-length to distance from the dipole.

Here, A represents the factor by which the ideal amplitude of E field must be multiplied to obtain the actual amplitude; ϕ is the phase shift from the ideal value.

The graph shows that errors in both amplitude and phase become small at relatively short distances from a dipole. These results are in agreement with those of Dunn and King[7] for the case of a dipole parallel to a conducting sheet. It appears that the radiation or far-zone field is a good approximation at points quite close to a dipole for all lengths $h \leqq \lambda/2$, i.e., as long as the gain, and hence the aperture remains small. Apparatus making use of this fact for the measurement of back-scattering at relatively short distances from antennas is described in the next section. Since a finite probe length is used, a somewhat larger separation, R, is required than Fig. 2 would indicate. By inserting in (4) separate readings from the graph for probe and scatterer, a good estimate of the new minimum separation may be obtained.

IV. An Apparatus for Back-Scattering Measurements

The standing-wave measurements proposed are to be made near the scatterer along the radius vector $\vec{r}$, between scatterer and source. The use of an image-plane system simplifies the design problem. This restricts the antennas under test to types with planes of symmetry, but there are many symmetrical structures which may be examined profitably. An image system eliminates the need of supports for the model under test and permits the use of a transmission-line probe protruding through a slot along $\vec{r}$ in the image plane. Furthermore, matching stubs and control equipment may be located directly behind the test position. These considerations favor the use of an image screen provided one of sufficient size and uniformity is available.

A large size is desirable for two reasons. First, reflections from the edges are thereby reduced to negligible proportions, and second, the transmitting antenna may be located very far from the region of measurement so that the incident beam approaches a plane wave. This effectively eliminates attenuation in the incident wave over the region in which measurements are made, and hence an inverse square relation replaces the inverse fourth power in the radar equation.

The standing-wave method is characterized by simplicity in the electronic apparatus required. The electronic equipment used for the present measurements is shown in Fig. 3. Monitors are provided for frequency and power. The latter consists of a directional coupler formed by two quarter-wave elements spaced a quarter-wavelength apart. The two cables from this array terminate in adjustable probes mounted on a slotted line matched at both ends. Crystals in the terminations at each end of this line give indications proportional to the incident and reflected power on the image screen. The incident-power output operates the monitor meter. Because of the critical adjustment required for a high front-to-back ratio, the reflected-power output of this type of directional coupler is not a satisfactory substitute for the standing-wave probe. In principle, the use of a directional coupler in the equivalent transmission line formed by the image screen appears feasible.

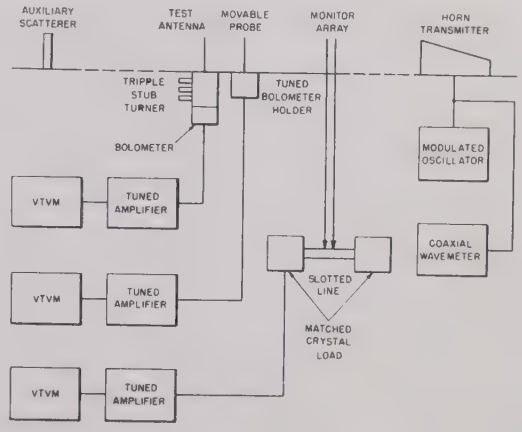

Fig. 3—Block diagram of the measuring system.

The antenna under test is mounted a short distance beyond the end of a slot cut in the image plane to accommodate a movable probe. The monitor is mounted at the opposite end of the slot, permitting the standing-

[7] B. C. Dunn, Jr., and Ronold King, "Currents excited on a conducting plane by a parallel dipole," Proc. I.R.E., vol. 36, pp. 221–229; February, 1948.

wave detector to travel over an interval of several wavelengths between monitor array and scatterer. To provide a matched load for certain measurements, a triple-stub tuner with bolometer load is used. The output of the bolometer amplifier furnishes the data for the determination of relative absorption cross sections, as mentioned earlier. Fig. 3 shows a block diagram of the system.

Intrinsic standing waves attributable to irregularities in the surface of the image screen proved to be an undesirable feature of the image-plane method. Here again the transmission-line analogy turned out to be useful: An auxiliary scatterer placed many wavelengths beyond the measuring position along the line can be adjusted to reduce substantially the intrinsic standing waves over the measuring interval. The remaining slight variations are compensated by the simple expedient of plotting the residual standing-wave pattern. Deviations from the mean value of the residual pattern are added to the observed maxima and minima or subtracted from them, according to the sign of the deviation.

V. Data and Results

A curve of the residual standing waves and the standing waves produced by a dipole slightly longer than $\lambda/4$, with $Z_L=0$, is shown in Fig. 4. The standing-wave ratios

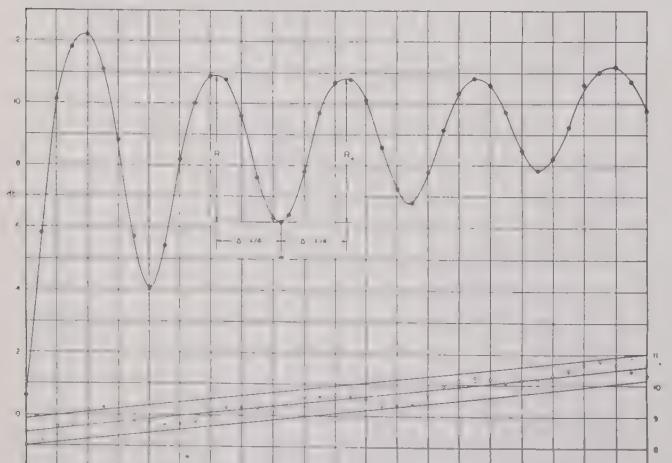

Fig. 4—Standing-wave data. The top curve was taken with a dipole scatterer; the lower curve shows residual standing waves.

relative to one of the minima are indicated. It is interesting to note that the mean slope of the intrinsic standing-wave pattern corresponds to an attenuation roughly double that calculated from the $1/r^2$ power attenuation from the distant source. Since here the distance r from the source is over 40λ, the discrepancy is presumably due to ohmic loss on the corroded surface of the screen, which is mounted on the outside wall of the laboratory.

Values of the reflection coefficient $b(\sigma=4\pi b^2)$, obtained for all values of the standing-wave ratio $R_\pm$ contained in the data of Fig. 4, are listed in Table I (The $\pm$ sign refers to ratios taken to the left and right as defined in Appendix II.)

TABLE I

ω	b_-	b_+	
43	3.79	3.94	
34.8	3.99	3.81	
26.5	3.57	3.69	($\bar{b}=3.78$)
18.0	3.74	3.69	

Values of σ plotted in Fig. 5 are calculated from th average of four values of b. Values of σ in Fig. 6 ar taken from one value of b only. Assignment of a probabl error of ± 5 per cent for the averaged values appear reasonable, except for small scattering when the stand ing-wave ratio is very low. A larger error is present i Fig. 6.

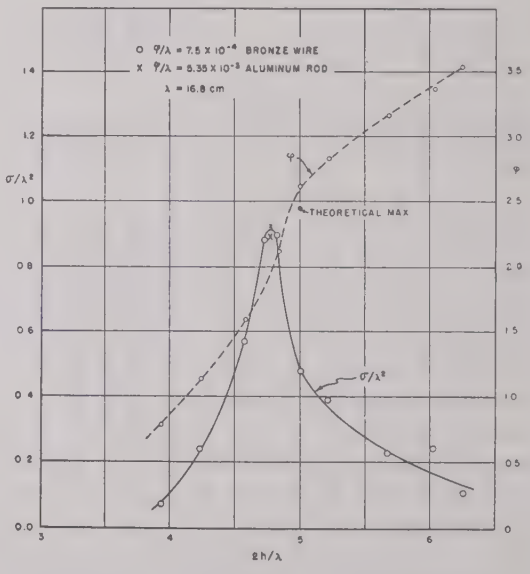

Fig. 5—Back-scattering from an unloaded dipole.

A systematic error arises from the position of th residual standing-wave pattern at the scattering an tenna. The values of σ are roughly 10 per cent lowe than they would be without residual standing waves o the image screen.

The correction for the deviation from the ideal radia tion field with $(ke^{-i\beta r})/r$ dependence is generally les than 10 per cent. Thus, assuming a probe length $h=\lambda/$ and a scatterer of length $h=\lambda/4$, the use of (4) and Fig 2 leads to a minimum distance $R\approx 2\lambda$ for an error o 4 per cent in amplitude and $\pi/8$ in phase. The actua probe length used is less than $\lambda/10$, but the minimun distance R is not reduced thereby. In standing-wav measurements, only the *change* in the deviation withi the interval $\Delta=\lambda/4$ between maximum and minimun contributes. Furthermore, the averaging of R_+ and R values should remove the error almost entirely, sinc

he deviations are in the opposite sense for the plus nd minus directions. No correction for the systematic rrors mentioned above is included in the results.

The dimensionless ratio σ/λ^2 and the phase angle ϕ f the scattered radiation are plotted in Fig. 6 for a thin ipole. The maximum value of σ/λ^2 agrees well with the heoretical and experimental data given by Van Vleck.[8] he theoretical resonant point is misplaced in Fig. 5, nd occurs at 0.475 in agreement with the data plotted.

The dependence of σ/λ^2 on the load Z_L is illustrated in ig. 6. The sharp resonance peak when $Z_L=0$ is absent or a matched load. The steady increase of σ/λ^2 with natched load is approximately twice as rapid as the ncrease in the absorption cross section A_0. This is to be xpected, since the directivity appears as a square in the ack-scattering. The phase of the scattered radiation is ndependent of antenna length for matched loads, but xhibits resonance behavior for the unloaded case.

A few results for a folded dipole and for the shunt-fed late or "flag-stub" described by Granger[9] are shown n Fig. 7. The presence of a load at the base of one edge f the metal plate results in a decrease in scattering; the arge scattering from the unloaded edge of the metal late is evidence of the antenna currents excited along he longitudinal edges.

No rapid changes in scattering and absorption appear s the width of the shunt-fed plate increased, nor does he length l of the coupling wire materially alter the results. However, any great reduction in the over-all length h causes a decline in both scattering and absorption. On the basis of these facts it seems reasonable to describe the operation of the shunt-fed plate in terms of resonant currents along both edges. Insertion of a coupling wire l produces a structure with similar currents to those in a folded dipole. An investigation of the impedance characteristics of the shunt-fed plate supports these conclusions.[10]

For the purpose of comparison, data for a quarter-wave dipole are included in Fig. 7: the length of the vertical lines represents the maximum spread of the four values used to obtain an average. The remaining curves in this figure represent similar averages, and hence only qualitative conclusions can be drawn from them.

Tests were also made on small aluminum hemispheres. The results obtained agree with the Rayleigh law within the probably error mentioned previously. In another trial, scattering from the flame of a small air-acetylene torch could not be detected for any flame length, even when the probe was within a half-wavelength of the flame.

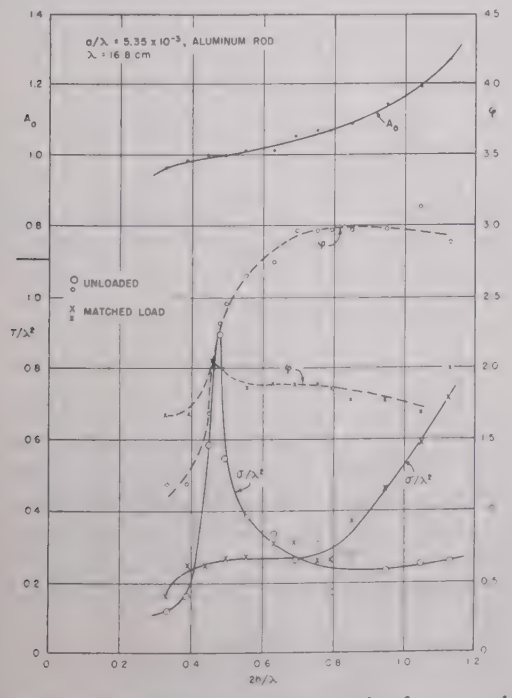

Fig. 6—Back-scattering and relative absorption from matched and from unloaded dipoles.

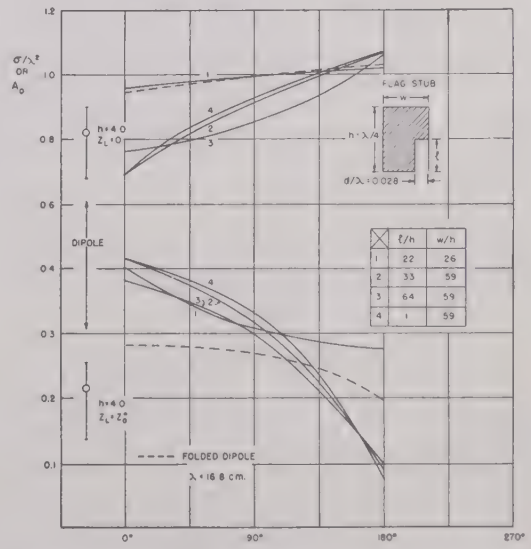

Fig. 7—Back-scattering (lower curves) and absorption from folded dipoles and stubs. The points at far left are for a dipole, $h=4$ cm.

VI. Conclusion

In spite of large experimental errors, the results presented are in good agreement with the expected scattering properties of the antennas tested. The inaccuracy of the present data is, in the opinion of the writer, largely a result of shortcomings in the image-screen used. Insufficient supports for the fine-mesh screening produced unstable ripples in the surface of the image plane. With some refinement, the standing-wave method of measurement may become a convenient tool in the determination of back-scattering. The results so ob-

[8] J. H. Van Vleck, F. Vloch, and M. Hamermesh, "Theory of adar reflection from wires and thin metal strips," *Jour. Appl. Phys.*, ol. 18, p. 280; March, 1947.

[9] See chapter 5 of footnote reference 6.

tained should, in turn, facilitate the design of aircraft antennas and the like where natural resonances are important in the operation of the antenna system as a whole.

Acknowledgments

Thanks are due to J. V. N. Granger and to Ronold King for reading the manuscript, and to Miss M. L. Richardson for numerical computations.

APPENDIX I

Deviation from the Radiation Field Pattern near a Linear Radiator

The component of the electric field parallel to the axis of a dipole with sinusoidal current distribution is given at all points in space by equation (5):[10]

$$E_z = -j30I_m\left\{\frac{e^{-j\beta R_2}}{R_1}+\frac{e^{-j\beta R_2}}{R_2}-\frac{2}{r}e^{-j\beta r}\cos\beta h\right\}. \quad (5)$$

Here R_1 and R_2 are radius vectors drawn from the ends of the antenna to the field points; r is drawn from the center of the antenna to the field point. The dipole half-length is h and $\beta=2\pi/\lambda$; I_m is the maximum value of the current amplitude.

For the present discussion, the field in the plane perpendicular to the antenna at its center is desired. Therefore,

$$R_1 = R_2 = R \quad (6)$$

$$R = \sqrt{r^2+h^2}. \quad (7)$$

In the expansion of (7), terms in $(h/r)^2$ are retained but fourth power terms are neglected.

$$R = r\left(1+\frac{1}{2}\left(\frac{h}{r}\right)^2\right). \quad (8)$$

Substitution in (5) and expansion of the exponential yields the following result:

$$E_z = -j60I_m\frac{e^{-j\beta r}}{r}\left\{\frac{1-j\beta\dfrac{r}{2}\left(\dfrac{h}{r}\right)^2}{1+\dfrac{1}{2}\left(\dfrac{h}{r}\right)^2}-\cos\beta h\right\}. \quad (9)$$

This formula may be simplified by expanding the term $(1+1/2(h/r)^2)$ in the denominator and by using a trigonometric identity for the quantity $(1-\cos\beta h)$.

$$E_z = -j60I_m\frac{e^{-j\beta r}}{r}\left\{2\sin^2\frac{\beta h}{2}-\frac{1}{2}\left(\frac{h}{r}\right)^2(j\beta r+1)\right\}. \quad (10)$$

Evidently the actual field differs in both amplitude and phase from the value predicted by the simple $1/r$ law. The correction factor is obtained by rearranging the formula.

$$E_z = \left[-j60I_m\frac{e^{-j\beta r}}{r}\cdot 2\sin^2\frac{\beta h}{2}\right]\cdot Ae^{-j\phi} \quad (11)$$

where

$$A = \sqrt{\left[1-\frac{\left(\dfrac{h}{r}\right)^2}{4\sin^2\dfrac{\beta h}{2}}\right]^2+\left[\frac{\beta h\left(\dfrac{h}{r}\right)}{4\sin^2\dfrac{\beta h}{2}}\right]^2} \quad (12)$$

$$\phi = \tan^{-1}\left\{\frac{\beta h\left(\dfrac{h}{r}\right)}{4\sin^2\dfrac{\beta h}{2}-\left(\dfrac{h}{r}\right)^2}\right\}. \quad (13)$$

The functions A and ϕ are plotted in Fig. 2.

APPENDIX II

Back Scattering or Radar Cross Section in Terms of Standing Waves

Let the source be located at $x=0$, and the scatterer a $x=l$. A movable probe occupies an intermediate positio x $(x<l)$, along the radius vector between source an scatterer. The signal received by the probe is propor tional to the electric field strength. The periodic maxim and minima which are received as the probe is move along the line xl serve to define a standing-wave rati in voltage. The usual definition in terms of incident an reflected waves is

$$VSWR = \frac{E_i+E_r}{E_i-E_r}. \quad (14)$$

For convenience, let $w=l-x$. Application of the in verse first-power dependence for the electric field yield the following values for E_i and E_r in terms of the refer ence potential E_0 near the source:

$$E_i = \frac{E_0}{x}; \qquad E_r = \frac{E_0 b}{lw}. \quad (15)$$

The coefficient b is a measure of the reflected amplitude A relation between b and the VSWR is obtained next

In order to define precisely the standing-wave ratio t be measured, let w_1 be the co-ordinate of the maximum and w_2 that of the minimum of the standing-wave pa tern. The expression for the VSWR may now be writte

$$VSWR = \frac{\dfrac{lw_1}{l-w_1}+b}{\dfrac{lw_2}{l-w_2}-b}\cdot\frac{w_2}{w_1}. \quad (16)$$

In order to eliminate w_1, let $w_1=w_2\pm\Delta$. Here it understood that $+\Delta$ corresponds to a maximum at in the direction of the source, and $-\Delta$ corresponds to

[10] Taken from unpublished notes of Prof. Ronold King; a similar result is found in J. A. Stratton, "Electromagnetic Theory," McGraw-Hill Book Co., New York, N. Y., p. 456; 1941.

maximum at w_1 in the direction of the scatterer. Accordingly, R_+ is taken to mean the ratio of maximum to minimum with $+\Delta$, i.e., the minimum nearest the scatterer, and R_- the ratio of maximum to minimum with $-\Delta$ i.e., the maximum nearest the scatterer. With these definitions a formula for the coefficient b may be obtained from (16).

$$b = \frac{lw_2}{l - w_2}\left\{\frac{R_\pm - \dfrac{1}{1 \pm \dfrac{\Delta}{l - w_2}}}{R_\pm + \dfrac{1}{1 \pm \dfrac{\Delta}{w_2}}}\right\}. \tag{17}$$

Since the source is usually far away, $l - w_2 \gg 1$, a slightly more convenient form is sufficiently accurate:

$$b = \frac{lw_2}{l - w_2}\left\{\frac{R_\pm \mp \dfrac{\Delta}{l - w_2} - 1}{R_\pm + \dfrac{1}{1 \pm \dfrac{\Delta}{w_2}}}\right\}. \tag{18}$$

The cross section σ is given by

$$\sigma = 4\pi b^2. \tag{19}$$

The phase shift ϕ at the scatterer is obtained from the relation

$$2\beta w + \phi = (2n + 1)\pi. \tag{20}$$

Discussion on "The Electron Wave Tube"*

ANDREW V. HAEFF

William B. Hebenstreit:[1] In one place in his theoretical treatment, Dr. Haeff has omitted a rather interesting point. In another place he has written two equations which are likely to give a misleading impression.

His equation (21) can be recast as follows:

$$\frac{1}{\left(\delta\frac{\omega}{v} + \gamma v\right)^2} + \frac{1}{\left(\delta\frac{\omega}{v} - \gamma v\right)^2} = \frac{1}{\omega_1^2}. \tag{1}$$

The question is, what happens when the current or the space-charge density gets very large? More precisely, what is the limiting gain as $\omega_1 \to \infty$? Setting the right-hand side of (1) equal to zero, we find the limiting value of the incremental propagation constant for the increasing wave to be

$$\gamma_\infty = j\left(\frac{\delta}{v}\right)\left(\frac{\omega}{v}\right). \tag{2}$$

Defining a beam wavelength λ_s, analogous to a guide wavelength in a waveguide,

$$\frac{2\pi}{\lambda_s} = \frac{\omega}{v}. \tag{3}$$

The number of wavelengths N in length l of a beam is

$$N = l/\lambda_s. \tag{4}$$

Further, if we call b the fractional velocity separation, then

$$\frac{\delta}{v} = \frac{b}{2}. \tag{5}$$

The limiting gain of a section N wavelengths long is, then,

$$G_\infty = 27.3Nb \text{ decibels}. \tag{6}$$

Equations (23) and (24) in Haeff's paper might give a misleading impression. Both equations are derived on the assumption that all four waves are started out at $t = 0$ and $z = 0$ with equal phases and amplitudes.

Since the four waves are independent, this is not, in general, true, but it may be true fortuitously. The relative phases and amplitudes with which the four waves start out depend upon the input boundary conditions.

* A. V. Haeff, "The electron wave tube—a novel method of generation and amplification of microwave energy," PROC. I.R.E., vol. 37, pp. 4–10; January, 1949.

[1] Hughes Aircraft Co., Culver City, Calif.

Andrew V. Haeff:[2] The expression for the limiting gain, as the space-charge density becomes very large, can be obtained quite directly from the equation (22) of my paper under the assumption that $\delta/v \cdot \omega/\omega_1 \ll 1$. Indeed,

$$\left|\gamma \frac{v}{\omega_1}\right|_{\omega_1 \to \infty} = \pm \sqrt{\left(\frac{\delta\omega}{v\omega_1}\right)^2 + 1 \pm \sqrt{4\left(\frac{\delta\omega}{v\omega_1}\right)^2 + 1}}$$

$$\approx \pm \sqrt{1 + \left(\frac{\delta\omega}{v\omega_1}\right)^2 \pm \left[1 + 2\left(\frac{\delta\omega}{v\omega_1}\right)^2\right]}$$

$$\approx \pm j \frac{\delta\omega}{v\omega_1} \cdot \tag{7}$$

Thus,

$$\gamma_{\omega_1 \to \infty} = j \frac{\delta\omega}{v \cdot v} = j\left(\frac{2\delta}{v}\right)\frac{\pi}{\lambda_g}, \tag{8}$$

and the gain

$$G = 20 \log_{10} e^{\gamma z} = 27.3\left(\frac{2\delta}{v}\right)\frac{z}{\lambda_g} \text{ decibels.} \tag{9}$$

This result is the same as was obtained by Mr. Hebenstreit (his equation (6)).

I may also point out that my formula (14) yields solutions quite readily in several other cases not specifically mentioned in my paper. Of particular interest is the case of two streams of electrons of equal charge densities moving in opposite directions. If the velocities of the two components of the stream are assumed to be $+v$ and $-v$, respectively, the expression for the propagation constant obtained from equation (14) is

$$\frac{\Gamma v}{\omega_1} = \pm \sqrt{-\left(1 + \frac{\omega^2}{\omega_1^2}\right) \pm \sqrt{1 + 4\frac{\omega^2}{\omega_1^2}}} \cdot \tag{10}$$

The above expression is of the same form as equation (22) of my paper. Therefore, the curve of Fig. 1 applies to this case, assuming that $x = \omega/\omega_1$. It is to be noted that space-charge waves propagate in either direction through electron plasma consisting of streams moving in opposite directions. Furthermore, since within a certain range of signal frequencies the propagation constant is real, such plasma is intrinsically unstable, and the amplitude of oscillations, once initiated in the plasma, will build up to saturation level, as was mentioned in my letter to the Editor of *The Physical Review*, November 15, 1948.

A somewhat similar situation holds for the case of uniform distribution of space charge over a range of velocities from $-v$ to $+v$. Such a condition can be taken as a rough approximation to quasistationary plasma in which electrons have Maxwellian distribution with th velocity $v = \sqrt{kT/2\pi m}$, where k is Boltzman's con stant; T is absolute temperature; and m is the mass o the particle. In this case, the integration of equatio (14) of my paper gives

$$1 = \int_{-v}^{+v} \frac{d\omega_1^2}{(\omega + j\Gamma v)^2} = \int_{-v}^{+v} \frac{c\,dv}{(\omega + j\Gamma v)^2} = \frac{2cv}{\omega^2 + \Gamma^2 v^2} \tag{11}$$

where

$$c = \frac{d\omega_1^2}{dv} = \left(\frac{e}{m\epsilon}\right) \cdot \frac{di}{vdv} = \left(\frac{e}{m\epsilon}\right) \cdot \frac{2i}{v^2} = \frac{\omega_1^2}{v},$$

i is the density of current in either direction, and $\omega_1^2 = 2(i/v) \cdot (e/m\epsilon)$.

The propagation constant in this case can be determined from the following expression:

$$\frac{\Gamma v}{\omega_1} = \pm \sqrt{2 - \frac{\omega^2}{\omega_1^2}} \cdot \tag{12}$$

Similarly to the previous case of two streams of discrete velocities $+v$ and $-v$, the plasma consisting of a uniform distribution of velocities $-v$ to $+v$ also exhibits negative attenuation for oscillations of all frequencies below $\omega = \sqrt{2}\omega_1$.

When the plasma density is very high, so that it can be assumed that $\omega/\omega_1 \ll 1$, the propagation constant approaches the values given below:

$$\Gamma_{\omega_1 \to \infty} \approx \frac{\omega}{v} \tag{13}$$

(discrete velocities),

$$\Gamma_{\omega_1 \to \infty} \approx \frac{\sqrt{2}\omega_1}{v} \tag{14}$$

(uniform charge versus density distribution), for the two cases, respectively. It may be mentioned that the injection of electron streams moving in the direction opposite to the main stream makes it possible to transmit space-charge waves in the backward direction (with respect to the motion of the main stream), and thus provides regenerative effects. The degree of regeneration can be controlled by regulating the amount of the injected current.

I appreciate Mr. Hebenstreit's comments (and comments received informally from R. G. E. Hutter, H. Krutter, and others) on the fact that the four solutions given by equation (22) are independent, so that, in general, the relative phases and amplitudes of the four possible waves are determined by the initial conditions of excitation.

[2] Naval Research Laboratory, Washington 20, D. C

Contributors to the Proceedings of the I.R.E.

Herbert S. Bennett (A'42–M'43–SM'44) s born on June 13, 1917, in New York, Y. He received the degree of bachelor of electrical engineering from the College of the City of New York in 1938, and the M.E.E. degree in 1939, from the same institution. From 1939 until 1942 he was employed by the U. S. Army Signal Corps as a radio engineer. In 1942 he was commissioned and served as a Technical Officer, first with the Signal Corps, and en with the United States Air Forces until 46. In 1946 he resumed his civilian employment as a research and development gineer with the U. S. Air Forces, at Watson boratories. He is now Chief, Program anning and Analysis Branch, at these boratories.

ERBERT S. BENNETT

In June, 1947, Mr. Bennett received the gree of master of science in physics from e Polytechnic Institute of Brooklyn, and at present engaged in research in the field electromagnetic diffraction in connection th his doctoral studies at that Institute.

Mr. Bennett is a member of Sigma Xi, e Scientific Research Association of nerica, the National Society of Professional Engineers, the American Institute of ectrical Engineers, Tau Beta Pi, and a Kappa Nu. He is now serving on e Admissions Committee of the IRE, and s an active member of the Technical Proam Committee for the 1947 IRE National nvention.

❖

W. H. Doherty (A'29–M'36–SM'43–44) was born in Cambridge, Mass., on gust 21, 1907. He received the S.B. degree in electric communication engineering in 1927, and the S.M. degree in 1928, both from Harvard University. In 1928 and 1929 he was associated with the radio section of the National Bureau of Standards. In 1929 he joined the Technical Staff of Bell Telephone Laboratories, Inc., at Whippany, N. J. Until 1940 work was mainly on high-power broadst transmitter design. In 1937 he received e Institute's Morris Liebmann Memorial ize for his development of a new high-ciency power-amplifier circuit.

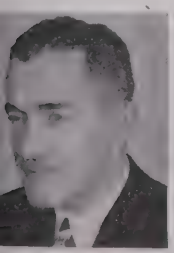

W. H. DOHERTY

During and since World War II, Mr. oherty has supervised Navy radar and fire-control projects, as well as the development of radio broadcasting equipment. He was recently transferred from Whippany to the Murray Hill laboratories as director of electronic and television research.

Mr. Doherty is a member of Tau Beta Pi and Sigma Xi.

❖

Donald B. Harris (SM'45) was born at Minneapolis, Minn., on February 10, 1901. He received the B.A. degree from Yale University in 1922, after completing a physics major. During the school year of 1922 to 1923, he occupied the position of master in physics and mathematics at the Adirondack-Florida School, Onchiota, N. Y. and Miami, Fla. In 1923 he became associated with the Cutting and Washington Radio Corp., Minneapolis, Minn. He joined the Northwestern Bell Telephone Co., in 1924, subsequently occupying various technical and administrative positions. During this period he independently developed a number of devices on which patents were granted, or are now pending.

DONALD B. HARRIS

In 1943 Mr. Harris became technical aide of Division 15 of the National Defense Research Committee stationed at Radio Research Laboratory, Harvard University, where he was responsible for the administration of contracts of Division 15 in the Cambridge, Mass., area. In 1947 he was a transmission and protection engineer of the Northwestern Bell Telephone Co., stationed at Des Moines, Iowa. At present, he is executive assistant to the director of research at the Collins Radio Co., Cedar Rapids, Iowa.

❖

C. W. Horton was born on September 23, 1915, at Cherryvale, Kan. He received the B.A. degree with honors in physics in 1935, and the M.A. degree in 1936, both from The Rice Institute, Houston, Tex. In 1945 he was awarded the Ph.D. degree from the University of Texas.

C. W. HORTON

Dr. Horton was a research associate at the Underwater Sound Laboratory, Harvard University, from 1943 to 1945. For this work he received a Development Award from the U. S. Navy Bureau of Ordnance, and a Certificate of Appreciation from the Office of Scientific Research and Development. Since 1945 he has been a research physicist at the Defence Research Laboratory and an assistant professor of physics at the University of Texas. He is a member of the American Physical Society, the American Geophysical Union, and the Society of Exploration Geophysicists.

❖

D. D. King (M'46) was born on August 7, 1919, at Rochester, N. Y. He received the A.B. degree in engineering sciences from Harvard College in 1942, and the Ph.D. degree in physics from Harvard University in 1946. He was a teaching fellow in physics and communication engineering in 1943, serving as a staff member of the pre-radar Officer's Training School at Cruft Laboratory, Harvard University. During 1945 he was a research associate at Cruft Laboratory. In 1946 he was appointed research fellow in electronics, and in 1947 assistant professor of applied physics at Harvard University.

D. D. KING

Since 1948 Dr. King has been an associate professor of physics in the Institute for Co-operative Research of The Johns Hopkins University. He is a member of Sigma Xi and the American Physical Society.

❖

R. Wayne Masters (S'40–A'43) was born on May 25, 1914, in Fort Wayne, Ind. He received the B.S. degree in electrical engineering from the University of Alabama in 1938, and the M.S. degree from the Ohio State University in 1941. In 1941 Mr. Masters became associated with the Victor Division of RCA, where he developed several antennas for radar equipments produced for the armed services. He is presently engaged there in research on television antennas and associated transmission equipment, and is credited with the invention and development of the RCA Super-Turnstile television antenna.

R. WAYNE MASTERS

Contributors to the Proceedings of the I.R.E

Mr. Masters recently completed a predoctoral course of study at the University of Pennsylvania. He is a member of Tau Beta Pi and Eta Kappa Nu.

❖

Lowell E. Norton was born on August 12, 1909, in Arlington, Minn. He received the B.S. degree in electrical engineering in 1932 and the M.S. degree in communications in 1935, both from the University of Minnesota.

LOWELL E. NORTON

He entered the services of the Research Division of RCA Manufacturing Co. at Camden, N. J., in 1935, and since 1942 has been at RCA Laboratories Division in Princeton, N. J.

Mr. Norton is a member of Sigma Xi.

❖

Wilfred Roth (S'43–A'45–S'46) was born on June 24, 1922, in New York, N. Y. He received the B.S. degree in electrical engineering from Columbia University in 1943, and the Ph.D. degree in physics from the Massachusetts Institute of Technology in 1948.

WILFRED ROTH

Dr. Roth was employed as a staff member of the MIT Radiation Laboratory from 1943 to 1946. His work consisted principally of development of electronic circuitry for specialized applications, with particular emphasis on the design of servomechanisms and computer systems.

Dr. Roth was a contributing author of the Radiation Laboratory Technical Series. In the years 1946 and 1947, he held an appointment as research associate in physics at MIT, where he conducted research on the propagation of ultrasonics in metals.

From January to August of 1948, Dr. Roth was associated with the Rieber Research Laboratory in New York, N. Y., as chief physicist, where he was concerned with the development of instruments for the geophysical and meteorological fields. In September, 1948, he became development group leader for the Harvey Radio Laboratories in Cambridge, Mass. He is engaged in the research and development of electronic aids to navigation.

Dr. Roth is a member of Tau Beta Pi, Sigma Xi, the American Physical Society, and the American Association for the Advancement of Science.

❖

Frederick William Schott (S'41–A'45) was born in Phoenix, Ariz., on October 2, 1919. In 1940, he received the degree of Bachelor of Arts (Honors) from San Diego State College. In 1941, he was awarded a university scholarship and began graduate work at Stanford University. The following year he continued under a Westinghouse Fellowship, and received the degree of electrical engineer in 1943. He resumed graduate study at Stanford University in 1947 and received the Ph.D. degree in 1948.

F. W. SCHOTT

He has held the following positions: junior engineer, San Diego Gas and Electric Co., San Diego, Calif., 1943 to 1944; ensign, United States Navy, 1944 to 1946; instructor in engineering and physics, San Diego State College, 1946 to 1947; acting instructor, Stanford University, summer, 1947; research associate, Stanford University, 1947 to 1948; and assistant professor, University of California at Los Angeles, 1948 to date.

Dr. Schott is a member of Tau Beta Pi, Sigma Xi, Sigma Pi Sigma, the American Association for the Advancement of Science, and the American Institute of Electrical Engineers, and is a registered electrical engineer in the State of California.

Karl R. Spangenberg (A'34–SM'4 F'49) was born at Cleveland, Ohio, on Apr 9, 1910. He received the B.S. degree i electrical engineerin in 1932, and the M.S degree in electric engineering in 193 both from the Cas School of Applie Science; and th Ph.D. degree fro Ohio State Univer sity in 1937.

K. R. SPANGENBERG

Since 1937, Dr Spangenberg ha been a member of th faculty of the elec trical engineering department of Stanfor University, as associate professor of elec trical engineering.

During the war, Dr. Spangenberg wa granted a leave of absence from Stanfor University to serve as consultant to th Signal Corps and to work at the Naval Re search Laboratory. He is presently head o the Electronics Branch of the Office o Naval Research.

❖

Glenn A. Walters (S'42) was born i Fresno, Calif. on March 31, 1920. He re ceived the B.S. degree in engineering at the University of Cali fornia at Berkeley Calif., in 1943. He then joined the Navy in its Flight Training Program. In 1945 he was assigned a Naval Liaison Office at the Radiation Laboratory at th Massachusetts Insti tute of Technology and later at Harvar University, where h worked on the development of microwav communication systems.

G. A. WALTERS

Upon his discharge in 1946, Mr. Walter accepted a position as research associate a Stanford University. He is at present en gaged in research and development of rada antenna systems at Dalmo Victor Co., San Carlos, Calif.

nstitute News and Radio Notes

MINATIONS—1950

At its May 4, 1949, meeting, the Board of ctors received the recommendations of Nominations Committee and the reports ie Regional Committees for officers and ctors for 1950. They are:

ident: Raymond F. Guy

-President: Sir Robert Watson-Watt

ctors-at-Large, 1949–1951 (two to be lected): Lloyd V. Berkner, Alois W. Graf, William R. Hewlett, James W. McRae

onal Directors, 1950–1951:
Region 1: Herbert J. Reich
Region 3: Ferdinand Hamburger, Jr., Walter C. Johnson
Region 5: Kenneth W. Jarvis, George Rappaport, John Reid
Region 7: Austin Eastman

According to Article VI, Section 1, of the stitution, nominations by petition for of the above offices may be made by r to the Board of Directors, setting forth ame of the proposed candidate and the e for which it is desired he be nominated. acceptance, a letter of petition must h the executive office before August 12, , and shall be signed by at least 100 ng members qualified to vote for the e of the candidate nominated.

CHNICAL COMMITTEE NOTES

The **Standards Committee** met on April The Master Index of Terms prepared by Definitions Co-ordinating Subcommit- under the Chairmanship of A. G. Jensen, been completed, and a list of the terms be distributed to the Chairmen of all Technical Committees, subcommit- and task groups. It can be made avail- on request to members of the IRE mittees, or to such persons as the Defi- ons Co-ordinating Subcommittee shall n proper. The Standards Committee plans to review the scope of all Tech- l Committees and to revise its Manual n early date. The proposed standard Radio Aids to Navigation, prepared by Committee of that name and presented ts Chairman, Henri Busignies, was ap- ed . . . . The initial meeting of the new **t IRE/AIEE Committee on Noise Defi- ons,** which reports to the Standards mittees of the IRE and AIEE, was on April 22. Since this Committee does stem from a Technical Committee, it organized as a full committee with the er to form subcommittees, task groups, ny other groups that might facilitate its c. T. A. Taylor is Chairman . . . . A ting of the **Industrial Electronics Com- ee** was held on April 20. This Committee joint activity of the IRE, AIEE, and MA, and is currently working in the field nduction and dielectric heating. There hree Subcommittees: Good Engineering ctice, which is concerned at the moment with the prevention of harmful radiation from industrial equipment; Definitions, which is drafting definitions of a number of terms used in this field; and the newly formed Measurements Group, which is studying the methods and instrumentation necessary to obtain the electrical characteristic of dielectric material at both room and elevated temperatures . . . . The **Video Techniques Committee** held a meeting during the IRE/RMA Spring Meeting in Philadelphia on April 27, at which the activities of the following Subcommittees were reported by their chairmen: V-1—Video Systems; V-3—Components and Signal Transmission, Definitions, and Symbols; V-2—Video Systems Components and Methods of Measurement and Test; and V-4—Video-Signal Transmission-Methods of Measurement and Test . . . . The **Committee on Electron Tubes and Solid State Devices** met at IRE headquarters on April 21 and plans to submit its work on definitions of terms for publication at an early date. The 1949 IRE Conference held June 20–21 at Princeton University, under the Chairmanship of Jack Morton, proved successful. Sessions on Microwave Tubes, Cathode-Ray and Storage Tubes, and Solid-State Devices were held. On the afternoon of the second day, several parallel "Rump Sessions" were held, at which informal discussion on various topics took place. C. M. Wheeler was appointed Chairman of the POHVT Subcommittee, and consideration was given to the forming of a Professional Group . . . . K. S. Van Dyke, Chairman of the **Piezoelectric Crystals Committee,** called the first meeting of this committee on May 9. The new Standards on Piezoelectric Crystals are expected to be available by the end of the summer . . . . The Joint Technical Advisory Committee convened at Headquarters on April 19 for its eighth meeting. It was decided that the JTAC will release in bound form at the end of the Committee's fiscal year, June 30, all official correspondence between the Committee and the FCC . . . . The first meeting of the **ASA Section Committee C-16 (Radio)** was held on April 29 at the American Standards Association Headquarters. Action was taken on thirteen IRE Standards and nine RMA Standards, in order to bring them up to date . . . . The Standards Co-ordinator, W. R. G. Baker, was host to a meeting of chairmen of the six organized **Professional Groups—Audio, Antenna and Wave Propagation, Broadcast Transmission Systems, Circuit Theory, Nuclear Science, and Vehicular and Railroad Radio Communications**—and promoters of potential IRE Groups at Syracuse on May 9, 1949. A Professional Group on Television had been considered, but at this meeting it was decided that the original Broadcast Engineers Group would change its scope to include television, AM, FM, Facsimile, etc. The Group was renamed the IRE Professional Group for Broadcast Transmission Systems . . . . The first meeting of the **Professional Group on Nuclear Science** was held at Washington on April 29 to discuss organization and future plans. Harner Selvidge was appointed Chairman, to succeed L. R. Hafstad. Immediate plans for the Group include the acquisition of papers on nuclear theory, heat transference, liquid metals, radiological instruments, new-type instrument controls, radio-isotopes, and radioactive materials in general. The Group decided to hold its annual meeting in the form of a Symposium sometime during the beginning of November. R. E. Lapp was named Chairman of the Planning Group of the 1949 IRE Nucleonics Symposium, which will emphasize biological tolerances. . . . The next **general meeting of Group Chairmen and Promoters** will be held in New York City in September.

Calendar of COMING EVENTS

AIEE Pacific General Meeting, San Francisco, Calif., August 23–26

1949 IRE West Coast Convention, San Francisco, Calif., August 30–September 2

1949 National Electronics Conference, Chicago, Ill., September 26–28

National Radio Exhibition, Olympia, London, England, September 28 to October 28

AIEE Midwest General Meeting, Cincinnati, Ohio, October 17–21

Radio Fall Meeting, Syracuse, N. Y., October 31, November 1–2

1950 IRE National Convention, New York, N. Y., March 6–9

PROCEEDINGS EDITOR ELECTED LIFE MEMBER OF AUSTRALIAN IRE

At the Annual General Meeting of the Institution of Radio Engineers, Australia, Alfred N. Goldsmith, Editor of the PROCEEDINGS OF THE I.R.E., was elected unanimously to honorary life membership of the Institution as of January 1, 1949.

The award was made in view of Dr. Goldsmith's "many years of successful contribution . . . to the development of radio science and in particular to the advancement of the technical well-being of those engaged in the art." It was also stated that the benefits of Dr. Goldsmith's efforts were regarded as world-wide, and that the Institution accordingly showed its appreciation by the grant of honorary life membership.

In his acceptance of the award, Dr. Goldsmith emphasized the present co-operative and friendly relationships that exist between the Institution of Radio Engineers,

Australia, and The Institute of Radio Engineers. He stressed the fact that these two organizations have demonstrated the essential unity of scientists and engineers working toward a common aim—namely, the advancement of their art.

IRE-URSI Met in May

The Institute of Radio Engineers and the International Scientific Radio Union (URSI) met jointly at the National Bureau of Standards in Washington, D. C., on May 2, 3, and 4. On the morning of May 2, J. H. Dellinger headed a session sponsored by URSI Commission 1—Radio Standards and Methods of Measurement. In the afternoon, Commission 7—Electronics, Including Properties of Matter—convened under the chairmanship of C. F. Metcalf.

The following day, J. C. Schelling (H. Norinder, Sweden, is the regular chairman) headed Commission 4's—Terrestrial Radio Noise—session in the morning, and L. C. Van Atta (B. van der Pol, Netherlands, is official chairman) took charge of the session on Radio Waves and Circuits, including General Theory and Antennas (Commission 6), which convened again in the afternoon. On May 4 there were organization meetings of Commissions 1 and 6 in the morning, and of Commissions 4 and 7 in the afternoon.

Distinguished Scientists to Speak at Electronics Conference

At the noon luncheon on the opening day, September 26, of the 1949 National Electronics Conference at the Edgewater Beach Hotel in Chicago, E. U. Condon, director of the National Bureau of Standards, will speak. F. Wheeler Loomis, President of the American Physical Society and head of the physics department of the University of Illinois, will be the speaker at the second noon luncheon of the three-day conference.

Cincinnati Section Held Spring Conference

The Cincinnati Section of the IRE held a Spring Technical Conference on Television on April 23, which drew an attendance of 345. J. F. Jordan headed a morning session at which E. W. Allen spoke on "The Propagation Characteristics of UHF Radiation," C. E. Nobles on "The Use of Stratovision in the UHF Band," O. M. Woodward, Jr., on "UHF Television Antennas and Matching Networks," and R. F. Romero on "UHF Tuners for Receiver and Converter Use." A buffet luncheon followed, during which time various exhibits relating to television were on view. The afternoon session, at which L. M. Clement was Chairman, featured papers by R. F. Wakeman, "UHF Converters for Use with Present Receivers"; J. D. Reid, "The Influence of UHF Allocations on Receiver, Design and Performance"; E. W. Commery, "The Psychophysiological Effects of Viewing Television"; and D. G. Fink, "Trends in Television Receiver Design."

In the evening a cocktail party preceded the official banquet, at which C. K. Gieringer, Section Chairman, presided. T. A. Hunter, Director of Region Five of the IRE, spoke on "Your Regional Director Looks at the IRE," and V. F. Cottrell delivered a speech on "Energy and Society." Inspection trips were held on the following day to the two television stations operating in Cincinnati (WKRC-TV and WLW-T).

Radiation Laboratory Reports Prove Commercial Success

The first instance of commercial publication of government reports has proved a success: early this year the McGraw-Hill Book Co. sent the U. S. Treasury a check for $24,250, a sum representing the royalties earned on 1948 sales of the partially published MIT Radiation Laboratory Series. Although the check is small, as payments into the U. S. Treasury go, it is one of the results of a transaction which saved the government close to $330,000.

In 1945 the wartime U. S. Office of Research and Development was confronted with the problem of publishing in report form the vast results of five years of intensive work on radar done at the Radiation Laboratory of MIT during the war. The laboratory was obligated by contract to supply the OSRD with 400 copies of the result of its work.

Under strict interpretation of Federal law, these reports would have to be produced by the Government Printing Office, but Vannevar Bush, director of the OSRD, believed that, if they were thus produced, they would be buried in government files. Accordingly, after prolonged debate it was decided that MIT would act as prime contractor and let a subcontract for commercial publication of the report. McGraw-Hill won the contract and, by the end of 1948, twenty-one volumes, averaging 600 pages each, had been produced. The remaining six are scheduled for publication in 1949. This not only saved the government the cost of printing, but, since 4,000 copies of each were printed, rather than 400, copies of the reports will be in the hands of thousands of scientists and engineers, where they will be useful for peacetime research in physics, biology, and other natural science, and will provide the engineering foundation for future industrial developments in television, communications, and electronics.

British Industries Fair Featured Radio Equipment

The most up-to-date equipment used in television transmitting and receiving, radio communications, aids to navigation, sound reproducing, and other branches of the radio and electronic engineering industries was shown at the British Industries Fair, held in both London and Birmingham from May 2 to May 13.

The world's first public demonstration of television on the 625-line system took place at Birmingham. Complete antenna systems were shown in three individual kits, comprising dipole, reflector, and cross-arm for different frequencies, eight- or twelve-foot masts, and different lashing kits and chimney brackets for the masts. A new high tensile light alloy was used in the manufacture of the elements and masts, reducing the weight of the antenna system by roughly one-third.

The increasing industrial applications of electronics were displayed, including methods of drying grass to ensure full nutritive value for livestock, a moisture meter for measuring the moisture content of grain and a portable PH meter which, by pushing an electrode into the soil, gives a direct reading of its acidity or alkalinity. A directly heated tetrode for use in mobile equipment, an electron microscope capable of magnifying an object one to one-hundred-thousand times, and the only controlled neon discharge lamp manufactured in England were also shown at Birmingham.

Shown at Olympia, London, was the first radio to incorporate the special double superheterodyne circuit, and which has band-spread tuning on the eight important short-wave bands. Also displayed was cloud and collision warning radar equipment designed to enable aircraft pilots to detect certain types of clouds associated with storm areas at a distance of forty miles. Other uses for this equipment include map pointing facilities, detecting other aircraft in the vicinity, and selecting a route through dangerous cloud formations at night or in poor visibility.

An automatic record changer displayed plays eight records of either size or mixed, which can be repeated or rejected by a pre-selecting button. Also exhibited was an electronic ionization voltage tester developed on a new principle to avoid damage to insulation under test.

NAB Studies Television Staffs

Television currently employs approximately ten per cent as many full-time persons as does the total AM-FM broadcasting industry, the National Association of Broadcasters announced, although television has only fifty-seven stations on the air. Approximately fifty per cent of television station staffs (aggregating 3,456 full-time persons) consist of technical personnel, eight per cent of film department personnel, twenty-two per cent of program personnel, sixteen per cent of administrative personnel, and four per cent of sales personnel.

ASA Held Company Member Conference

The American Standards Association held a Company Member Conference on May 19 and 20; the first day at the Benjamin Franklin Hotel in Philadelphia, Pa., the second at the Princeton Labs. of RCA. The Conference is the group in the ASA which gives companies an opportunity to exchange ideas, discuss standardization problems, and make recommendations for standard practices that will help to give better service to both producer and user groups.

MPE Offers est Films

The Society of Motion Picture Engineers d the Motion Picture Research Council ve developed a series of test films for use the standardization of practices and uipment in most pictures. These films are o applicable to television.

The 35-mm test films are: Visual, eater Sound, Multifrequency, Transmis-n, Buzz-Trade, Scanning-Beam Illumina-n, Sound Focusing, 3000-Cycle Flutter st, 1000-Cycle Balancing Test, and Multi-quency Warble.

The 16-mm test films are: Sound Projec-, Sound Service, Multifrequency, Buzz-ack, Scanning-Beam Illumination, Sound-cusing, 3000-Cycle Flutter, 400-Cycle gnal-Level, and Projector Lens Resolution rget.

Further information may be obtained m the SMPE, 342 Madison Ave., New rk 17, N. Y.

anel Inspects ceanographic Installations

The Panel on Oceanography of the Na-nal Military Establishment's Research d Development Board held a meeting at Jolla, Calif., at the end of April. At that ie they also inspected the military re-rch and development work carried on by Scripps Institute of Oceanography at Jolla, and the work in oceanographic earch of the U. S. Navy Electronics Lab-tory at San Diego. Created by the mmittee on Geophysics and Geography the Board, the Panel concerns itself with anographic studies and the mutual rela-ns existing between water, air, and the d adjacent to it as they affect the prob-ns of military research and development.

ritish Radio Council sues New Specification

A specification describing the general ditions and procedure for climactic rability testing of components for radio d other electronic equipment has been blished by the British Radio Industry uncil. The specification, No. RIC/11, is work of the RIC Technical Specifications mmittee in consultation with the British dio Equipment Manufacturers' Associa-n, the Radio Communication and Elec-nic Engineering Association, and the dio Component Manufacturers' Federa-n, and is the first produced by the Com-ttee.

The object of the Technical Specifica-ns Committee's work is to produce a ies of radio component specifications de-ned to ensure a high standard of reliabil-and performance for British components ring use, transit, and storage. The first ic need is to devise a standard series of ts for components, and RIC/11 is in-ded to fulfill that need.

Industrial Engineering Notes[1]

Report Estimates Radio Distribution Abroad

An eight-page mimeographed report detailing the distribution of radio receiving sets by countries and geographical regions throughout the world was issued this week by the International Broadcasting Division, U. S. Department of State. A total of 53,191,000 sets was estimated to be in use in Europe, with 35,292,000 capable of short-wave reception. It was stated that radio receivers behind the "Iron Curtain," which includes Russia and her satellites, number 9,534,000, of which 8,263,000 are equipped with short-wave facilities.

There are 1,785,240 receivers in the Middle East and Africa, and 1,626,015 of them are short-wave sets. Latin American republics have an estimated 6,495,500 radio sets with 3,677,200 capable of short-wave reception. Although a total of 11,808,000 radio receivers are estimated to be in use in the Far East, only 1,478,650 of them are short-wave sets.

OTS Puts Out Two New Indexes

A subject index to technological documents issued in Volume X (July–December, 1948) of the "Bibliography of Scientific and Industrial Reports," and a subject index and abstract collection of more than 1,000 unclassified scientific and technical reports dealing with European technology were published by the Office of Technical Services.

Copies of the first may be obtained from the OTS, Department of Commerce, Washington 25, D. C., at $1.00 per copy; and the second (PB 96941), which includes material on radar, communication devices, and tubes, may be secured from the same source.

FCC Chairman Heads U.S. Group at Paris Conference

FCC Chairman Wayne Coy was appointed by President Truman to head the U. S. Delegation to the International Administrative Telephone and Telegraph Conference of the International Telecommunication Union, which was held in Paris in May. Frances Colt De Wolf, chief of the Department of State's Telecommunications Division, and Paul A. Walker, FCC Commissioner, were named vice-chairman and delegate, respectively.

FCC Actions

The FCC adopted final rules (Mimeo. No. 32308) for the Citizens Radio Service. Designed primarily to afford a two-way short-range private communication service, the CRS is defined in its rules as "a fixed and mobile service intended for use for private or personal radio-communication, radio signalling, control of objects or devices by radio, and other purposes not specifically prohibited." In general, any U. S. citizen eighteen years of age or older will be eligible for a station license. Licenses will be valid for a period of five years, and the station license is normally the only authorization that will be required in order to operate a citizen's station. Two types of citizens stations may be authorized, with the distinctions based on technical and operating specifications, including input power of 10 watts for one type and 50 watts for the other type. All citizens operation will be in the 460- to 470-Mc band previously allocated to this service.

The FCC adopted a report and order (Mimeo. No. 33669) in Docket 9154, amending the Standards of Good Engineering Practice for AM broadcasting stations. The new rules concern ground-wave signals and were announced as proposed rules on October 1. . . . Restricted amateur radio operation in the band 1800 to 2000 kc on a shared basis with the Loran Service will be permitted, according to the FCC's amendment of its rules, subject to certain conditions and limitations.

The FCC has proposed a new over-all plan to "provide scope and direction for the immediate and long range development" of the Amateur Radio Service. The objectives of the scheme are to provide for the continued and directed improvement of the Amateur Service in its value to the public as a voluntary, noncommercial communications service; to extend the amateur's proven ability to contribute to the advancement of radio; to continue the improvement of the Amateur Service through a program which will encourage advancing skills in both the communication and technical phases of radio; and to provide a reservoir of trained operators, technicians, and electronics experts, both for the growing radio industry in peace-time and the greatly increased industrial and military demands in times of national emergency. The proposal (Mimeo. No. 33917) would reclassify amateur frequencies by usage within the service and create a new license classification comparatively easy to attain. Higher performance standards would also be adopted . . . . The FCC amended its rules governing the Aeronautical Services to provide for the assignment of very high frequencies in accordance with a chain system of allocation. The amendments (Mimeo. No. 33914) do not involve any change in the medium and high frequencies . . . . Mimeos. No. 32808, 33669, 33917, and 33914 may be obtained from the Secretary of the FCC, Washington 25, D. C. . . . The effective date of the Commission's amended rules and regulations regarding electric welding devices using radio frequencies was postponed to July 30, but the FCC denied a petition submitted by the Joint Industry Committee on High Frequency Stabilized Arc Welders and others, seeking further hearings on the new rules . . . . Extended use of mobile radio communications and the ever-increasing problem of finding spectrum space for these specialized services

[1] The data on which these NOTES are based were selected, by permission, from "Industry Reports," issues of April 22 and 29 and May 6 and 13, published by the Radio Manufacturers' Association, whose helpful attitude is gladly acknowledged.

were highlighted this week in a comprehensive FCC action making over-all revisions in the rules governing, and the frequencies utilized by, a multitude of mobile radio services. Rules and frequencies covering the operation of about 50,000 authorized stations and nearly 200,000 mobile units became effective July 1. Of importance to television is the notice taken by the FCC of possible effects the various services may have on nearby television channels in the 66–72 and 76–82 Mc bands. Fixed operations in the 72–76 Mc band will be permitted under the changed rules only if there is no interference to television. Text of the FCC Reprint and Order, which deals with assignments to services in the frequency bands 25–39, 30–44, 44–50, 72–76, 152–162, 450–460 Mc and certain portions of the government band, 162–174 Mc, were published in the May 6 issue of the "Federal Register," copies of which may be obtained from the Superintendent of Documents, Government Printing Office, Washington 25, D. C., for twenty cents.

Television News

FCC Chairman Wayne Coy has announced that the **"freeze" on television station grants will probably be lifted** within the year. After stating that the next significant phase of television development will be the addition of channels in the proposed uhf band, Mr. Coy added that modern television sets will probably not become obsolescent for a long time because the FCC plans to retain twelve channels in the uhf band; adaptors can readily be built for the present sets if the current 6-Mc black and white standards are employed in the uhf; and that most of the sets now in use are in cities having at least four authorized television stations—the few set-owners living in cities having fewer than four stations, and where uhf stations may some day be built, will be able to purchase converters to tune them in at a reasonable cost . . . . In the first ruling of its kind, the FCC granted a construction permit to NBC for the operation of an **experimental uhf television station** at Bridgeport, Conn., which will be operated as a satellite to station WNBT, New York, N. Y. WNBT'S programs will be picked up and rebroadcast by the experimental station, and will be received by a limited number of sets capable of receiving uhf broadcasts . . . . The **American Telephone and Telegraph Co. plans to extend its facilities in order to carry television network programs.** The new channels will enable stations in the Midwest to present a wider choice of programs coming from New York's television stages. Under present plans, the fourteen cities already on the Bell System's television network will be joined by Erie and Lancaster, Pa., and Wilmington, Del., during the summer. By fall it is expected that Providence, R. I., Rochester, N. Y., and Dayton, Columbus, and Cincinnati, Ohio will be linked . . . . Rapidly increasing sales of television sets have been accompanied by a rise in the job prospects in the television field, according to an "Occupational Outlook Handbook" prepared for the Veterans Administration by the Bureau of Labor Statistics, U. S. Department of Labor. The 454-page handbook, containing complete reports on 288 occupations, is available at $1.75 from the Superintendent of Documents, U. S. Government Printing Office, Washington 25, D. C. . . .

A special RMA Committee on television equipment for export met on March 23 in New York to develop a series of recommendations as to export standards. The committee believes that, ideally, a television system should be independent of power line frequencies, and that "in view of the current experience with 525-line, 60-field, 30-frame television systems, as set forth in the U. S. standards, and, in view of the flicker considerations, this committee feels that it should reaffirm these standards as representative of a practicably achievable ideal at this time." The committee's "suitable secondary recommendation" is a 625-line, 50-field, 25-frame system for use in areas where the power supply frequency is 50 cycles. An additional secondary recommendation was the adoption of a 525-line, 60-field, 30-frame system in areas where the power frequency is 60 cycles. In all other respects the committee recommends adherence to U. S. television standards.

There are sixty-one television stations on the air as well as sixty-one construction permits outstanding, and 323 applications to construct pending but "frozen." New stations on the air are: WKRC-TV, Cincinnati, WLWC, Columbus, WLWD, Dayton, Ohio, and WTVJ, Miami, Fla.

About two dozen applications to construct television broadcasting stations have been received by the Mexican Government, and, although no permits to operate television stations have been granted as yet, the first television station in that country is expected to be on the air before the end of the year. Arrangements have been completed for one station, and some sets are being assembled in Mexico City from parts imported from the United States. One experimental station (XEZA) has been certified by the Mexican Government to operate with 1-kw power in the 66 to 72-Mc band. Representatives of the Mexican Government are consulting the FCC with respect to their television standards.

FM Notes

According to the FM Association, a growing number of television sets are being equipped with FM sound reception facilities.

The number of FM stations on the air has reached 755, including 31 noncommercial educational outlets. New stations went on the air at Gainesville, Fla. (WDUN-FM); Berkeley, Calif. (KPFA); and Orlando, Fla. (WDBO-FM).

Television Set Production Rises as Radio Production Falls

Television set production by RMA member-manufacturers reached new records, both in March and during the first quarter of 1949. Radio receiver output continued at the reduced level to which it declined early this year.

In the first quarter, 422,537 television sets were manufactured and 182,361 sets were made in March. The quarterly output of television receivers was three and one-half times that of the first quarter of 1948.

FM-AM radio set production continued to decline, along with general radio receiver manufacturing, in the trend from radio to television. The total quarterly production was 317,918 FM and AM sets, just over half of the number manufactured during the first quarter of 1948.

Indicative of the sharp rise in television receiver production in 1948, sales of cathode-ray tubes during the year increased more than 361 per cent in number of units and over 142 per cent in value compared with 1947 sales. Cathode-ray receiving tube sales in 1948 numbered 1,265,472, valued at $31,985,461, compared with 274,008 tubes valued at $7,756,204 in 1947.

Books

Microwave Antenna Theory and Design, edited by Samuel Silver

Published (1949) by the McGraw-Hill Book Co., Inc., 330 W. 42 St., New York 18, N. Y. 613 pages +9-page index +xviii pages. 337 figures. 6¼ × 9¼. $8.00.

Microwave antennas bridge a transition region between the geometrical optics of light waves interacting with large objects, and the physical optics of light waves interacting with small objects. In the microwave region the apparatus used is neither very large nor very small with respect to the wavelength employed, and it is thus necessary in using either the geometrical or the physical method of treating an antenna problem to remember the limitations imposed by the other effects.

This volume covers the theoretical, practical, installation, and testing phases of microwave antenna design as developed by the MIT Radiation Laboratory and other similar agencies during the war. Because microwave antennas involve consideration of the effects listed above, many of the methods and much of the information will be found of value in the uhf and vhf regions. Although some of the basic theory of radio antennas is in a rather complicated and unsatisfactory state at present, the theory which has been given includes the most valuable approximations and the most general methods of use in the actual design and construction of antennas. Basic logic is used in the development of most of the material presented, and, where possible, the performance of various types of

ennas or antenna components is com-
ed in a way which is very helpful in de-
ing questions of design.

The book is complete and up to date,
h the exception of material which re-
ins unpublished for reasons of national
urity. Although the text was prepared by
umber of authors, the editor has done a
y good job of unifying the presentation
d preventing duplication among the vari-
s sections. The book connects the theory
h the practice in a very able manner.

RICHARD C. RAYMOND
Pennsylvania State College
State College, Pa.

herical Harmonics, by T. M. MacRobert

Published (1948) by Dover Publications, 1780
adway, New York 19, N. Y. 367 pages+4-page
ex+xv pages. 20 figures. 5½×8½. $4.50.

This is the revised edition of the book by
e present professor of mathematics in the
iversity of Glasgow which was written to
ovide a textbook on the theory of Fourier
ies, spherical harmonics, and Bessel Func-
ns. In this second edition, the restriction
integral values of the orders of the asso-
ted Legendre functions has been removed,
hough it still retains the original goal of
employing the method of contour inte-
tion. Two new chapters have been added;
apter Eight deals with some properties of
hypergeometric function and Chapter
ne deals with the associated Legendre
nctions of general real degree and order.
set of examples has been added to the
t.

The first three chapters deal with the
eory of Fourier Series and their applica-
n to conduction of heat and vibrations of
ings. Chapters Four to Seven are devoted
spherical harmonics, Legendre Coeffi-
nts, Legendre Functions, and the associ-
d Legendre Functions. In Chapters Eight
Twelve, expressions are obtained for the
vitational and electrostatic potentials of
dies bounded by circles, spheres, spher-
s, ellipsoids of revolutions, and eccentric
eres. Chapters Fourteen to Sixteen deal
h the Bessel Functions and their applica-
n to vibrations of membranes and con-
ction of heat.

For the engineer endeavoring to acquaint
nself with the mathematical tools supplied
the above functions, the book is difficult
ding because of the small amount of ex-
natory material on an engineering level.
r the student aided by accompanying lec-
es, however, and for the applied mathe-
tician, the book provides a useful, up-to-
e, and thorough treatment of the subject.

MILTON DISHAL
Federal Telecommunications Laboratories
Nutley 10, N. J.

ave Mechanics and Its Applications, by F. Mott and I. N. Sneddon

Published (1948) by the Oxford University Press,
Fifth Ave., New York 11, N. Y. 338 pages+2-
e name index and 3-page subject index+xii pages.
igures. 6¼×9¼. $10.00.

This book by Mott and Sneddon fills an
portant gap in the existing literature on
ve mechanics, the lack of a text which
uld cover more or less uniformly the
ire field of the present quantum theory and its application to various problems concerning the structure and properties of matter. There are excellent books presenting in complete form the mathematical foundations of wave mechanical theory, but treating its applications to various concrete problems only as examples of general theorems. Other books discuss in detail the theory of atomic and molecular structure (the field in which wave mechanics grew originally), but leave applications in other important fields, such as the theory of solids or nuclear physics, to special monographs on the subject.

In this book the authors make a successful attempt to describe the entire subject, showing the role of wave mechanical theory in the present development of the physics of matter. Extremely useful as a textbook for students beginning the study of theoretical physics, it will also appeal to experimentalists who would like to get acquainted with the wave mechanical interpretation of various classes of physical phenomena without getting into the deep waters of abstract considerations. For many years the reviewer was at a loss when asked to recommend a single good text for his classes in wave mechanics. With the appearance of this volume, the difficulty has been removed.

G. GAMOW
George Washington University
Washington, D. C.

Microwaves and Radar Electronics, by Ernest C. Pollard and Julian N. Sturtevant

Published (1948) by John Wiley and Sons, Inc., 440 Fourth Ave., New York 16, N. Y. 414 pages+11-page index+vii pages. 193 figures. 5½×8½. $5.00.

The authors' intention in this book is to present to the engineer, who has had little or no experience with microwaves, the basic fundamental and practical aspects of microwave and radar engineering. A sufficiently broad survey of the microwave field is given in order to enable the reader to continue intelligently with more detailed study of any particular phase which may be of interest to him. As a prerequisite, the reader requires only a working knowledge of physics, calculus, and electron tube theory and practice. The material of the book is primarily descriptive in nature, and the authors have avoided complex mathematical treatment, except as required for the proper presentation of specific subjects. To the engineer who has been in close contact with radar and microwaves, the book will appear far too brief and lacking in detail, but these factors will make the publication more attractive to those less experienced in the field.

The text is divided into three major sections of approximately equal length. In the first part the authors open their subject with a brief analysis of electromagnetic fields, the knowledge of which is essential for an intelligent understanding of the microwave circuit. The work then proceeds to a description and explanation of coaxial and waveguide lines and cavity resonators. Following this is a description of various microwave devices: low-level cw generators, magnetrons, crystal detectors, and measuring devices—including wavemeters, bolometers, and spectrum analyzers. Brief treatment is given to impedance matching in microwave lines, the basic fundamentals of antennas, and descriptive information on the more important waveguide and cavity elements, such as directional couplers, TR boxes, and "magic T."

The second section of the book covers the other electronic elements associated with radar systems. Included here are descriptions of various pulsing circuits for high and low levels, video amplifiers, cathode-ray tube indicators and their associated sweep and deflection circuits, amplifiers for low-level signals, and other radar receiver accessories. A brief chapter is devoted to servomechanisms and computer elements, and a final chapter of this section to miscellaneous circuits, such as regulated power supplies, multivibrators, and clamp circuits.

The concluding sections of the text give an explanation of the physical basis of radar, brief descriptions of typical radar systems, and the application of microwaves to physical research.

Obviously so broad a field can be covered only lightly in a single volume, but the coverage is singularly complete and sufficient references are included to facilitate further study if desired. The book is easy to read and the material is well presented. This is not a microwave reference book or handbook, nor is it intended as such. The engineer specializing in communications, power, or allied fields will find this volume a good introduction to the microwave art, since it presents a clear over-all picture without confusing detail.

R. J. PHILIPPS
Bell Telephone Laboratories
Whippany, N. J.

Exploring Electricity, by Hugh Hildreth Skilling

Published (1948) by the Ronald Press, 15 E. 26 St., New York 10, N. Y. 272 pages+5-page index +vii pages. 18 figures. 6×8½. $3.50.

Forty years ago a science writer in New York turned out a book entitled "What Is Electricity." With commendable candor the author began the book by stating, "We do not know what electricity is."

Professor Skilling in his new book, backed by what has come to light in the intervening decades of time, can with assurance say in the first sentence of his book, "There is a cliché that 'no one knows' [what electricity is]. This is absurd: pay no attention to it. Electricity is very well known. To know a thing is to know how it behaves, and few things are as well-known as electricity."

In full measure, "Exploring Electricity" fits in as an acceptable volume of the Humanizing Science Series, for Professor Skilling has done an excellent job in narrating a personalized history of electricity from the time of Thales forward to our own times. The "how to do it" type of technical book, popular thus far in the industrial age, may retain its usefulness indefinitely, but there is evidence that educators in science and engineering are increasingly attaching new importance to study which identifies scientific discoveries and inventions not only with the names of their respective discoverers and inventors, but with the conditions under which they worked and with their processes of thought. This has ever been the procedure in the study of political history: knowledge of

events has been closely linked with informative biographical material dealing with the life experiences of the outstanding participants. Emerson went the whole distance when he wrote, "Properly there is no history, only biography."

There are other histories of electricity, but, because of its clear treatment, readable style, and engaging sidelights, Professor Skilling's book could be made available in all engineering and science schools, elementary and advanced, as recommended reading. Purposeful students should derive inspiration from a reading acquaintance with the great men of science.

The reviewer regards the book as sufficiently complete to serve the author's purpose, and it is not, therefore, intended as adverse criticism, to note that there is no mention of the work of H. Abraham, A. C. Becquerel, and P. Langevin in France; O. J. Lodge in England; and C. F. Brackett, Robert Spice, Nikola Tesla, M. I. Pupin, John Trowbridge, and W. A. Rowland among the Americans.

DONALD MCNICOL
25 Beaver St.
New York, N. Y.

Industrial Electronics Reference Book, by Electronics Engineers of the Westinghouse Corp.

Published (1948) by John Wiley and Sons, Inc., 440 Fourth Ave., New York 16, N. Y. 669 pages+10-page index+x pages. 1135 figures. 8¼×11¼. $7.50.

The combined efforts of a group of electronics engineers of the Westinghouse Electric Corp. have produced a book which should find its way into the library of every industrial electronic engineer. The book proves, as did the distinguished MIT series, that, by proper co-ordination and editing, the work of several authors can present a unified and coherent story of a wide field, yet give in each chapter the authoritative treatment that comes only with the intensive knowledge of one aspect of the field.

Into the 669 large-sized pages, the thirty-seven authors have crammed an amount of information not found in any other book. While, as the title implies, the book is hardly meant to serve as a text in schools, yet the instructor will find much useful material, especially in the first four or five chapters which present an excellent explanation of the fundamental physical principles on which electron tubes operate.

To single out any one of the thirty-six chapters for particular praise would be an injustice to the rest; depending on his own interests, each reader will find some chapters of more interest than others. It should be noted here, however, that the sixty-seven pages of Chapter 24 on the timely subject of radio-frequency heating furnish formulas, graphs, and other data most useful to anybody engaged either in the design or operation of this type of apparatus.

Chapter 8, on industrial X-ray tubes, contains the description of as relatively recent developments as the betatron. The chapters on tuned circuits and filters, on transformers, and on rectifiers should also be mentioned for the completeness with which the material is treated.

Each chapter carries a list of references at the end which will be welcomed when further information on the subject is wanted. Happily the authors have completely avoided turning out a glorified catalogue of Westinghouse equipment and achievements; they have used freely charts and data from the work of others, giving credit in all instances.

Even with a book as complete as this, any reader could probably think of a few things that should have been included, in his opinion. Thus, the word "servomechanism" is not found among the chapter headings, or even in the index, although Chapter 30, entitled "Regulation," could almost as well have been called "Servomechanism Theory," since it deals with many features of the latter. Among oscillators, the *RC* tuned oscillator of the Wien-bridge type is not discussed. The multivibrator is mentioned a few times, but not much data pertaining to its design is given. Flip-flop, counting, and trigger circuits could also have been described in a little more detail. These things might have been included without increasing the size of the book by cutting down on the twenty-five page chapter on antennas, which seem to receive more attention than is justified in an industrial electronics book.

These are minor criticisms, however; the important fact is that the subjects included in the book are treated with authority, completeness, and skill, and for this reason the book can be wholeheartedly recommended.

WALTHER RICHTER
Allis-Chalmers Manufacturing Co.
Milwaukee 1, Wis.

Basic Electrical Engineering, by George F. Corcoran

Published (1949) by John Wiley and Sons, Inc., 440 Fourth Ave., New York 16, N. Y. 444 pages +5-page index+vii pages. 284 figures. 6×9¼. $4.50.

As the title implies, this book is a text designed primarily for introducing the field of electrical engineering to college undergraduates. Before courses in circuits, electrical machinery, electronics, and electronic circuits are taken, a certain background in basic material is required and this book is designed to fulfill that need.

The system of rationalized mks units is used throughout, after having been explained in the first chapter of the book. Concepts such as current, voltage, and power are skillfully introduced, and are followed by branch-current, mesh-current, and nodal methods of dc circuit analysis. The subjects of electric and magnetic fields, as well as magnetic circuits, are lucidly handled. This is followed by an introduction to the generation of electrical or mechanical power by means of rotating electrical machinery. Classical field theorems, like Gauss's Theorem, Ampere's Law, and the circuital law of magnetism, are discussed fully. Included also are such subjects as elementary transients, batteries, electrolysis, contact potential, and nonlinear circuit elements.

The book is very well written and the material excellently chosen. As a basic text, it covers material which is essential to both power and electronic engineering. Examples in both fields are given with a balance that is noteworthy. Especially good are the numerical examples which serve to illustrate the text. This book deserves the highest recommendation.

JOHN R. RAGAZZINI
Columbia University
New York 27, N. Y.

New Publications

The National Bureau of Standards has recently published three new pamphlets: **"Tables of the Confluent Hypergeometric Function $(n/2, \frac{1}{2}; x)$ and Related Functions,"** (NBS Applied Mathematics Series 3), **"Tables of Scattering Functions for Spherical Particles"** (NBS Applied Mathematics Series 4), and **"Medical X-Ray Protection up to Two Million Volts"** (NBS Handbook 41). The confluent hypergeometric function appears in the probability distribution of the statistics used in the analysis-of-variance tests when the hypothesis to be tested is not true, and a table of this function is also needed for the construction of the so-called *t*-test; moreover, statisticians will find this large-sized (eight-by-ten-inch), 73-page book of tables useful in connection with other tests . . . . The tables of intensities of light scattered by small spherical particles are based on Mie's theory on the scattering of light by particles with a radius comparable in magnitude with the wavelength of light, and will prove of interest to workers in many branches of physics, chemistry, and biology. In 119 eight-by-ten pages, the tables give the angulur distribution of intensity and the total light scattered by a small spherical particle in terms of size of particle and wavelength of the incident light, thus permitting both the concentration and diameter of spherical particles in suspension to be determined from measurements of the alternation of an incident beam due to scattering, providing the particles are of uniform size . . . . "Medical X-Ray Protection" supersedes Handbook 20 ("X-Ray Projects") and consists of 43 five-by-eight pages. The recommendations are intended primarily for the protection of the radiation worker and not for the patient . . . . All three of the publications mentioned may be obtained from the Superintendent of Documents, U. S. Government Printing Office, Washington 25, D. C., at 35, 45, and 25 cents per copy, respectively . . . . **"Radio Communication Transmitters,"** by J. J. Hubert, has been published by ATA Scientific Progress, Ltd., 76 Warwick Square, London, S. W. 1, England. Containing 286 pages and 167 illustrations, the book deals with the basic principles of radio transmitting equipment. Copies may be obtained for 30 shillings each, plus postage, from the publishers . . . . **"The Photofact Auto Radio Manual"** has been put out by Howard W. Sams and Co., Inc., 2924 E. Washington St., Indianapolis, Ind., from whom it may be obtained for $4.95. Large (eight and one-half by eleven inches) and profusely illustrated, the book contains 392 pages giving service information on more than 100 post-war automobile radio receivers, representing the products of 24 manufacturers. Standard notation schematics are used throughout.

Sections

Chairman		Secretary
H. I. Metz C.A.A. 84 Marietta St. N.W. Atlanta, Ga.	ATLANTA May 20–June 17	M. S. Alexander 2289 Memorial Dr., S.E. Atlanta, Ga.
G. P. Houston 3000 Manhatten Ave. Baltimore, Md.	BALTIMORE	J. W. Hammond 4 Alabama Ct. Baltimore 28, Md.
T. B. Lawrence 1833 Grand Beaumont, Texas	BEAUMONT—PORT ARTHUR	C. B. Trevey 2555 Pierce St. Beaumont, Tex.
R. W. Hickman Cruft Laboratory Harvard University Cambridge, Mass.	BOSTON	A. F. Coleman Mass. Inst. of Technology 77 Massachusetts Ave. Cambridge, Mass.
G. E. Van Spankeren San Martin 379 Buenos Aires, Arg.	BUENOS AIRES	A. C. Cambre San Martin 379 Buenos Aires, Arg.
J. F. Myers 249 Linwood Ave. Buffalo 9, N. Y.	BUFFALO-NIAGARA May 18–June 15	R. F. Blinzler 76 Woodward Ave. Buffalo 14, N. Y.
M. S. Smith 1701 10th St. Marion, Iowa	CEDAR RAPIDS	V. R. Hudek Collins Radio Co. Cedar Rapids, Iowa
K. W. Jarvis 6058 W. Fullerton Ave. Chicago 39, Ill.	CHICAGO May 20–June 17	Kipling Adams General Radio Co. 920 S. Michigan Ave. Chicago 5, Ill.
C. K. Gieringer 3016 Lischer Ave. Cincinnati, Ohio	CINCINNATI May 17–June 14	F. W. King RR 9 Box 263 College Hill Cincinnati 24, Ohio
F. B. Schramm 2403 Channing Way Cleveland 18, Ohio	CLEVELAND May 26–June 23	J. B. Epperson Box 228 Berea, Ohio
Warren Bauer 376 Crestview Rd. Columbus 2, Ohio	COLUMBUS May 13–June 10	George Mueller Electrical Eng. Dept. Ohio State University Columbus, Ohio
S. E. Warner Aircraft Electronics Assoc. 1031 New Britain Ave. Hartford 10, Conn.	CONNECTICUT VALLEY May 17–June 16	H. L. Krauss Dunham Laboratory Yale University New Haven, Conn.
A. S. Levelle 801 Telephone Bldg. Dallas 2, Texas	DALLAS-FT. WORTH	E. A. Hegar 802 Telephone Bldg. Dallas 2, Texas
George Rappaport 132 East Court Harshman Homes Dayton 3, Ohio	DAYTON May 12	C. J. Marshall 1 Twain Place Dayton 10, Ohio
T. G. Morrissey Radio Station KFEL Albany Hotel Denver, Colo.	DENVER	Hubert Sharp Box 960 Denver 1, Colo.
F. E. Bartlett Radio Station KSO Old Colony Bldg. Des Moines, Iowa	DES MOINES-AMES	O. A. Tennant 3515 Sixth Ave. Des Moines, Iowa
C. F. Kocher 17186 Sioux Rd. Detroit 24, Mich.	DETROIT May 20–June 17	P. L. Gundy 519 N. Wilson Royal Oak, Mich.
R. W. Slinkman Sylvania Electric Products Inc. Emporium, Pa.	EMPORIUM	T. M. Woodward 203 E. Fifth St. Emporium, Pa.
J. C. Ferguson Farnsworth Tel. & Radio Co. 3700 E. Pontiac St. Fort Wayne, Ind.	FORT WAYNE	S. I. Harris Farnsworth Tel. & Radio Co. 3702 E. Pontiac Fort Wayne, Ind.
W. H. Carter 1309 Marshall Ave. Houston 6, Texas	HOUSTON	J. C. Robinson 1422 San Jacinto St. Houston 2, Texas
R. E. McCormick 3466 Carrollton Ave. Indianapolis, Ind.	INDIANAPOLIS	Eugene Pulliam 931 N. Parker Ave. Indianapolis, Ind.
E. R. Toporeck Naval Ordnance Test Sta. Inyokern, Calif.	INYOKERN	R. W. Johnson 303 B. Langley China Lake, Calif.
C. F. Heister 838 U. S. Court House Kansas City 6, Mo.	KANSAS CITY	Mrs. G. L. Curtis 6005 El Monte Mission, Kan.
R. W. Wilton 71 Carling St. London, Ont., Canada	LONDON, ONTARIO	G. H. Hadden 35 Becher St. London, Ont., Canada
Berhard Walley Radio Corp. of America 420 So. San Pedro St. Los Angeles 13, Calif.	LOS ANGELES May 17–June 20	J. J. Fiske Westinghouse Electric Corp. 600 St. Paul Ave. Los Angeles 14, Calif.
D. C. Summerford Radio Station WKLO Henry Clay Hotel Louisville, Ky.	LOUISVILLE	R. B. McGregor 2100 Confederate Pl. Louisville, Ky.
F. J. Van Zeeland Milwaukee School of Eng. 1020 N. Broadway Milwaukee, Wis.	MILWAUKEE	H. F. Loeffler Wisconsin Telephone Co. 722 N. Broadway Milwaukee 1, Wis.
K. R. Patrick RCA Victor Div. 1001 Lenoir St. Montreal, Canada	MONTREAL, QUEBEC May 11–June 8	S. F. Knights Canadian Marconi Co. P.O. Box 1690 Montreal, P. Q., Canada
L. A. Hopkins, Jr. 1711 17th Loop Sandia Base Branch Albuquerque, N. M.	NEW MEXICO	T. S. Church 3079-Q-34th Street Sandia Base Branch Albuquerque, N. M.
J. W. McRae Bell Telephone Labs. Murray Hill, N. J.	NEW YORK May 4–June 1	R. D. Chipp DuMont Telev. Lab. 515 Madison Ave. New York, N. Y.
J. T. Orth 4101 Fort Ave. Lynchburg, Va.	NORTH CAROLINA-VIRGINIA	C. E. Hastings 117 Hampton Rds. Hampton, Va.
W. L. Haney 117 Bourque St. Hull, P. Q.	OTTAWA, ONTARIO May 19–June 16	G. A. Davis 78 Holland Ave. Ottawa, Canada
M. W. Bullock Capital Broadcasting Co. 501 Federal Securities Bldg. Lincoln 8, Nebr.	OMAHA-LINCOLN	B. L. Dunbar Radio Station WOW Omaha, Nebr.
A. N. Curtiss Radio Corp. of America Camden, N. J.	PHILADELPHIA May 5–June 2	C. A. Gunther Radio Corp. of America Front & Cooper Sts. Camden, N. J.
M. A. Schultz 635 Cascade Rd. Forest Hills Borough Pittsburgh, Pa.	PITTSBURGH May 9–June 13	E. W. Marlowe Union Switch & Sig. Co. Swissvale P.O. Pittsburgh 18, Pa.
A. E. Richmond Box 441 Portland 7, Ore.	PORTLAND	Henry Sturtevant Rt. 6, Box 1160 Portland 1, Ore.
A. V. Bedford RCA Laboratories Princeton, N. J.	PRINCETON	L. J. Giacoletto 9 Villa Pl. Eatontown, N. J.
K. J. Gardner 111 East Ave. Rochester 4, N. Y.	ROCHESTER May 19	Gerrard Mountjoy Stromberg-Carlson Co. 100 Carlton Rd. Rochester, N. Y.
E. S. Naschke 1073-57 St. Sacramento 16, Calif.	SACRAMENTO	W. F. Koch 1340 33rd St. Sacramento 14, Calif.
G. M. Cummings 7200 Delta Ave. Richmond Height 17, Mo.	ST. LOUIS	C. E. Harrison 818 S. Kings Highway Blvd. St. Louis 10, Mo.
O. C. Haycock Dept. of Elec. Eng. University of Utah Salt Lake City, Utah	SALT LAKE	M. E. Van Valkenburg Dept. of Elec. Eng. University of Utah Salt Lake City, Utah
C. L. Jeffers Radio Station WOAI 1031 Navarro St. San Antonio, Texas	SAN ANTONIO	L. K. Jonas 267 E. Mayfield Blvd. San Antonio, Texas
L. G. Trolese U. S. Navy Elect. Lab. San Diego 52, Calif.	SAN DIEGO May 3–June 7	Jack Jacoby U. S. Navy Elect. Lab. Point Loma, Calif.
F. R. Brace 955 Jones St. San Francisco 9, Calif.	SAN FRANCISCO	R. A. Isberg Radio Station KRON 901 Mission St. San Francisco 19, Calif.
J. M. Paterson 2009 Nipsic Bremerton Wash.	SEATTLE May 12–June 9	J. E. Hogg General Electric Co. 710 Second Ave. Seattle 1, Wash.

Sections

	Chairman	Secretary
Syracuse	F. M. Deerhake 600 Oakwood St. Fayetteville, N. Y.	S. E. Clements Dept. of Electrical Eng. Syracuse University Syracuse 10, N. Y.
Toledo	A. R. Bitter 4292 Monroe St. Toledo 6, Ohio	J. K. Beins 435 Kenilworth Ave. Toledo 10, Ohio
Toronto, Ontario	C. Graydon Lloyd Canadian General Electric Co., Ltd. 212 King St., W. Toronto, Ont., Canada	Walter Ward Canadian General Electric Co., Ltd. 212 King St., W. Toronto, Ont., Canada
Twin Cities	D. A. Murray Fed. Comm. Comm. 208 Uptown P.O. & Federal Cts. Bldg. Saint Paul, Minn.	C. I. Rice Northwest Airlines, Inc. Holman Field Saint Paul 1, Minn.
Washington	T. J. Carroll National Bureau of Stand. Washington, D. C.	P. DeF. McKeel 9203 Sligo Creek Parkway Silver Spring, Md.
Williamsport	J. C. Starks Box 307 Sunbury, Pa.	R. G. Petts Sylvania Electric Products Inc. 1004 Cherry St. Montoursville, Pa.

SUBSECTIONS

	Chairman	Secretary
Akron (Cleveland Subsection)	H. R. Hegbar 2145 12th St. Cuyahoga Falls, Ohio	H. G. Shively 736 Garfield St. Akron, Ohio
Amarillo-Lubbock (Dallas-Ft. Worth Subsection)	H. W. Harris 711 Kentucky St. Amarillo, Tex.	E. N. Luddy Station KFDA Amarillo, Tex.
Centre County (Emporium Subsection)	F. T. Hall Dept. of Elec. Engr. Pennsylvania St. College State College, Pa.	J. H. Staten Dept. of Eng. Research Pennsylvania St. College State College, Pa.
Hamilton (Toronto Subsection)	E. Olson 162 Haddon Ave., N Hamilton, Ont., Canada	E. Ruse 195 Ferguson Ave., Hamilton, Ont., Canada
(Lancaster Philadelphia Subsection)	R. B. Ayer RCA Victor Division New Holland Pike Lancaster, Pa.	J. L. Quinn RCA Victor Division New Holland Pike Lancaster, Pa.
Long Island (New York Subsection)	H. A. Wheeler Wheeler Laboratories 259-09 Northern Blvd. Great Neck, L. I., N. Y.	M. Lebenbaum Airborne Inst. Lab. 160 Old Country Rd. Box 111 Mineola, L. I., N. Y.
Monmouth (New York Subsection)	L. E. Hunt Bell Telephone Labs. Deal, N. J.	G. E. Reynolds, Jr. Electronics Associates, Inc. Long Branch, N. J.
Northern N. J. (New York Subsection)	J. B. Minter Box 1 Boonton, N. J.	A. W. Parkes, Jr. 47 Cobb Rd. Mountain Lakes, N. J.
South Bend (Chicago Subsection) January 20	A. R. Kahn Electro-Voice, Inc. Buchanan, Mich.	A. M. Wiggins Electro-Voice, Inc. Buchanan, Mich.
Urbana (Chicago Subsection)	R. M. Wainwright Elec. Eng. Department University of Illinois Urbana, Ill.	M. H. Crothers Elec. Eng. Department University of Illinois Urbana, Ill.
Winnipeg (Toronto Subsection)	S. S. Stevens Trans Canada Airlines Box 2973 Winnipeg, Manit., Canada	S. G. L. Horner Hudson's Bay Co. Brandon Ave. Winnipeg, Manit., Canada

IRE People

Hans W. Kohler (A'34–VA'39), formerly a staff member of the U. S. Army Signal Corps, research laboratories, was appointed to the staff of the National Bureau of Standards, where he will engage in theoretical work in the electronics division. Dr. Kohler has conducted extensive investigations in the vhf range, including antennas, wave propagation, transmitter, and measurement problems.

Born in Thun, Switzerland, Dr. Kohler received the electrical engineering degree in 1925 from the Federal Polytechnic Institute in Zurich. From 1926 to 1932 he was employed by the American Telephone and Telegraph Co.'s department of development and research.

He taught at the Cruft Laboratory, Harvard University, from 1925 to 1936, and was awarded the Sc.D. degree in the latter year. In 1937 he joined the staff of the Radiomarine Corporation of America's transmitter laboratory, leaving the same year to work for the Naval Research Laboratory, where from 1937 to 1942 he did theoretical and laboratory work on superfrequencies.

In 1942 he joined the radio development section of the Civil Aeronautics Administration, where he engaged in theoretical studies and field work on very-high-frequency radio ranges and localizers and on interference problems. He is the author of several papers published in the PROCEEDINGS.

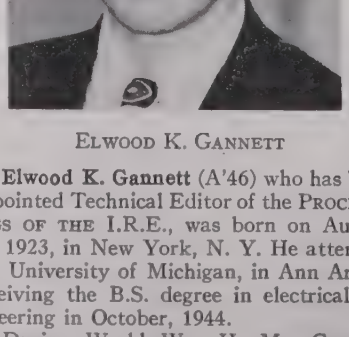

ELWOOD K. GANNETT

Elwood K. Gannett (A'46) who has been appointed Technical Editor of the PROCEEDINGS OF THE I.R.E., was born on August 26, 1923, in New York, N. Y. He attended the University of Michigan, in Ann Arbor, receiving the B.S. degree in electrical engineering in October, 1944.

During World War II, Mr. Gannett served in the United States Navy as an ensign. He attended Pre-Radar School at Bowdoin College and Radar School at the Massachusetts Institute of Technology. Subsequently he was assigned to duty as the electronics officer on a seaplane tender operating in the ports of Hongkong and Shanghai.

Mr. Gannett joined the administrative staff of the Institute in August, 1946, as assistant to the Executive Secretary. In December, 1947, he became the Assistant Secretary of the IRE. He has served as Chairman of the Institute Activities Committee for the 1947 National IRE Convention, and Chairman of the Facilities Committee for the 1948 and 1949 Conventions.

As Assistant Secretary, Mr. Gannett's duties were chiefly concerned with Student Branch activities, Sections, and PROCEEDINGS circulation.

❖

Thomas A. Elder (SM'45), formerly section engineer in the tube division of the General Electric Co.'s electronics department, has been named designing engineer for transmitting tubes in the industrial and transmitting tube division.

Born in Kenton, Ohio, he attended Ohio University and was graduated in 1930 with the B.S. degree in electrical engineering. He then joined the General Electric Co. as a student engineer, and, after leaving the test course, was employed in the vacuum-tube engineering department until 1931, when he was promoted to assistant section engineer in the tube division.

Robert Delavergne Avery (J'29–A'33–SM'44), chief engineer of J. H. Bunnell and Co., Brooklyn, N. Y., died recently.

Mr. Avery was born in Canon City, Colo., on June 4, 1911. He was educated at the Jefferson High School in Roanoke, Va., from which he was graduated in 1928. In that year he joined radio station WDRJ as chief operator; in that capacity he designed the first broadcasting studio equipment for the Virginia Polytechnic Institute, and designed and supervised the construction of the 250-watt radio station WLNA at Lynchburg, Va.

From 1931 to 1938 he was chief engineer of radio station WDBJ, where he was in complete charge of the technical operation of the station and where he designed a new broadcasting plant. In 1938 he was appointed chief engineer of the Commonwealth of Virginia. There he designed, supervised, constructed, and took charge of the operation of the state police communications system.

In 1943 he started work on a confidential research project under Columbia University's contract with the OSRD at the Airborne Instrument Laboratory, leaving in 1944 to join the Bunnell Co.

From 1946 to 1948 Mr. Avery was a member of the Institute's Admissions Committee.

Wilbur S. Hinman, Jr. (SM'46), deputy ief of the National Bureau of Standards' rdnance development laboratory, has been ppointed assistant chief of the Bureau's ectronics division. In his new capacity he ill, besides continuing to act as chief of the rdnance electronics section, aid in the direcon of research and development of elecronic apparatus, instruments, controls, cirits, tubes, and ordnance devices.

Born in Washington, D. C., Mr. Hinman ttended the Virginia Military Institute, om which he received the bachelor of sci ce degree in electrical engineering in 1926. that year he joined the Westinghouse lectric and Manufacturing Co. as a student ngineer, later becoming a radio engineer.

In 1928 Mr. Hinman joined the staff of e National Bureau of Standards as a mem r of the radio section. From 1941 to 1948 e was chief of the Bureau's fuze develop ent section, chief of the special projects roup for the production of a new electronic omb director, and consultant to division ur of the National Defense Research Com ittee. As deputy chief of the ordnance deelopment laboratory, Mr. Hinman is reponsible for research and development in e field of proximity fuzes for bombs, rocks, mortars, and guided missiles.

Mr. Hinman has achieved recognition as authority on the radio proximity fuze and dio meteorography. A co-inventor with the te Harry Diamond (see page 1011 of the ugust, 1948, issue of the PROCEEDINGS) of basic design utilized in the radio proximity fuze, radiosonde, and the automatic weather station, Mr. Hinman has also conducted extensive research in upper-air wind measuring equipment, direction finders, automatic-volume control for aircraft radio receivers, radio compasses, and blind landing aids.

In recognition of his original contributions to the nation during the war, Mr. Hinman has received the Presidential Certificate of Merit, the Ordnance Development Award, the Army's citation for exceptional service, and the Department of Commerce Medal for meritorious service. The author of numerous technical papers, some of which have appeared in the PROCEEDINGS, he is a member of the American Ordnance Association.

Arnold E. Bowen (SM'46) microwave research worker on the Bell Telephone Laboratories' technical staff, died this year.

Mr. Bowen was born in Massasachusetts on October 31, 1900. He received the Ph.D. degree in 1921 from the Sheffield Scientific School of Yale University, after which he served as an instructor in the Yale Graduate School until 1924. During the summer sessions he worked as an engineer for the American Telephone and Telegraph Co., and in 1924 he became a full-time member of their development and research department, where he specialized in inductive co-ordination of power and telephone systems.

In 1934 Mr. Bowen transferred to the technical staff of the Bell Telephone Laboratories, where he did research in field and waveguides and microwave electronics. In 1942 he became technical consultant on airborne radar to the U. S. AAF, but returned to Bell the following year to act as consultant on microwave communication systems for the Signal Corps and to investigate microwave propagation.

From 1943 to 1945 he was chief of the U. S. AAF's airborne radar section, where he was concerned with the characteristics, requirements, operational use, etc., of all airborne radar equipment. In 1945 he returned to Bell Laboratories to do research in the microwave field.

William R. Patton (A'36–VA'39) has joined the Lenkurt Electric Co. at San Carlos, Calif., as a field engineer in the carrier-equipment division.

A graduate of Oregon State College with the communications engineering degree, Mr. Patton is an active radio amateur (W6CCR). After finishing school, he was employed by the U. S. Naval Research Laboratory at Anacostia, Washington, D. C., and then took charge of radio communication systems for the Oregon State Highway Commission.

During World War II, Mr. Patton was on the staff of the OWI, working on the operation and construction of high-power broadcast and short-wave radio transmitters. Subsequently, he was assistant superintendent of communications for Africa and the Middle East with Trans-World Airlines at Cairo Egypt, after which he joined the staff of United Airlines.

❖

Frank E. Norton (A'31–M'40–SM'43) was appointed chief engineer of the Bendix Aviation Corp.'s Television and Broadcast Division.

Mr. Norton received the B.S. degree from the University of California, and later earned the A.M. degree in physics from Columbia University. In 1937 the University of California awarded him a degree in electrical engineering.

After engaging in development work for the Bell Telephone Laboratories, where he specialized in television transmission and synchronization circuits, broad-band amplifiers, and cathode-ray tube equipment, Mr. Norton joined the development division of the Curtiss-Wright Corp. as senior development engineer in charge of the electronic laboratory development of radar devices and flight trainers.

Mr. Norton holds original patents on television sweep circuits, and he did some of the pioneer development work in color television for the Bendix Radio Division. He is a senior member of the Society of Motion Picture Engineers.

Joseph Willard Milnor (A'16–M'26–SM'43), retired consulting engineer, died recently. Born October 25, 1889, in Williamsport, Pa., Mr. Milnor was graduated from Lehigh University in 1912, with first honors in mathematics. After serving for a year with the General Electric Co. of Pittsfield, he entered the engineering department of the Western Union Telegraph Co. in 1913. Nine years later he was promoted to research engineer, and in 1936 became transmission engineer. Appointed consulting engineer in 1943, Mr. Milnor retired from active work the following year.

During his thirty-one years with Western Union, Mr. Milnor engaged in a variety of problems in the field of telegraph transmission and the design of communications equipment. He made many important contributions to methods for reducing interference from power and other sources into telegraph circuits, and to telegraph signal transmission, submarine cables, and carrier current telegraphy.

The author of many papers, Mr. Milnor held a large number of patents in the fields of interference suppression, submarine cable, and carrier current telegraphy. He was a member of the American Association for the Advancement of Science, the American Museum of Natural History, Tau Beta Pi, and the Wire Club of New York.

IRE SECTION CHAIRMAN

Kenneth W. Jarvis

CHICAGO SECTION

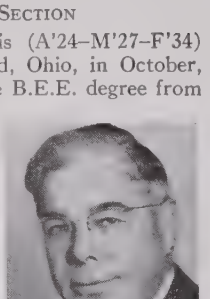

Kenneth W. Jarvis (A'24–M'27–F'34) was born in Mansfield, Ohio, in October, 1901, and received the B.E.E. degree from Ohio State University in 1923. In that year he entered the employment of the Westinghouse Electric and Manufacturing Co., leaving in 1925. For the next nine years he worked as a radio engineer with various manufacturers, and entered private development and consulting engineering in 1934. At present he is manager of the electronics division of the Automatic Electric Co., president of the Jarvis Electronics Corp., and a lecturer in the graduate school of Northwestern University.

George Rappaport

DAYTON SECTION

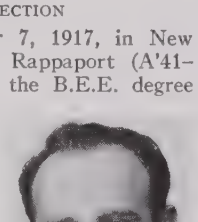

Born on December 7, 1917, in New York, N. Y., George Rappaport (A'41–M'49–SM'46) received the B.E.E. degree from the College of the City of New York in 1940. After graduation he joined the General Electric Co., leaving in 1941 to work on microwave instrument landing systems for the Aircraft Radio Laboratory at Wright Field. In 1942 he was transferred to Washington, D. C. Later he was sent back to Wright Field to become assistant chief engineer of the Air Matériel Command's special projects laboratory. In 1946 he was promoted to chief engineer in charge of advanced development at the Aircraft Radiation Laboratory. In 1947 he received the M.S. degree from Ohio State University.

Thomas G. Morrissey

DENVER SECTION

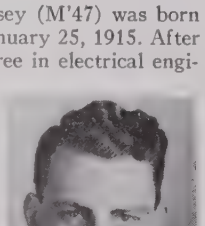

Thomas G. Morrissey (M'47) was born in Denver, Col., on January 25, 1915. After receiving the B.S. degree in electrical engineering from the University of Colorado in 1936, he became a member of the Bell Telephone Laboratories' radio research staff. In 1942 he transferred to the long lines department of A.T. & T., and was assigned to Denver as a transmission engineer on the transcontinental buried cable project. Returning to private industry in 1946, Mr. Morrissey became chief engineer of station KFEL in Denver, where he established KFEL-FM, and now directs the experimental television station WXEL.

F. E. Bartlett

DES MOINES-AMES

Born in Marshalltown, Iowa, on October 16, 1906, F. E. Bartlett (A'45) worked as a railroad telegraph operator after finishing school; then became interested in amateur radio work, which contributed to his becoming associated with radio broadcast operation. He worked for various radio stations in the Midwest, beginning as an announcer and later turning to the engineering aspect of the field. In 1944 he joined the staff of the Murphy Broadcasting Co. as chief engineer for radio station KSO in Des Moines, his present position.

Mr. Bartlett was active in the organization of the Des Moines-Ames section of the IRE in 1947.

Charles F. Kocher

DETROIT SECTION

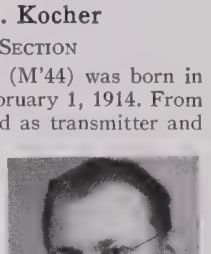

Charles F. Kocher (M'44) was born in Detroit, Mich., on February 1, 1914. From 1933 to 1939 he served as transmitter and studio operator at radio stations WEXL, WJBK, and WWJ, Detroit, while attending the Lawrence Institute of Technology, from which he graduated in 1939 with the B.E.E. degree. Upon graduation he became transmitter engineer at NBC's Chicago radio station WMAQ. In 1940 he joined the FCC's field staff and, after various assignments throughout the country, he was placed in charge of the Cleveland Field Office in 1942. Two years later he became chief engineer of radio station WXYZ in Detroit.

Raymond E. McCormick

INDIANAPOLIS SECTION

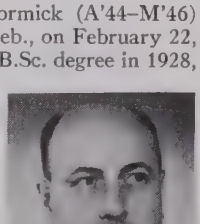

Raymond E. McCormick (A'44–M'46) was born in Lincoln, Neb., on February 22, 1905. He received the B.Sc. degree in 1928, and the M.S. degree in 1932, both from the University of Nebraska. After teaching at Northeastern State College in Oklahoma, Mr. McCormick became an instructor at an electronics training school for military service men in Omaha, Neb., in 1942. A year later he joined the Military Intelligence Division Laboratories of the War Department at Arlington, Va. In 1945 he became associated with the Radio Development Division of the CAA Experimental Station at Indianapolis, Ind.

Mark W. Bullock

OMAHA-LINCOLN SECTION

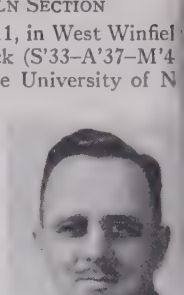

Born August 20, 1911, in West Winfiel N. Y., Mark W. Bullock (S'33–A'37–M'4 was graduated from the University of N braska in 1934 with the B.S.E.E. degree, and became transmitter supervisor for radio station KOIL, Omaha. In 1938 he was appointed chief engineer for radio stations KFAB and KFOR in Lincoln, as well as for KOIL. In 1943 he took charge of the construction of the OWI's internation broadcast station at Mason, Ohio. This cor pleted, he became principal radio engine in the OWI's Washington bureau of cor munications facilities. After returning KFAB, he left in 1948 to become technic director of the Capital Broadcasting Co.

Obed C. Haycock

SALT LAKE SECTION

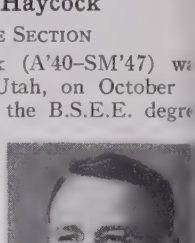

Obed C. Haycock (A'40–SM'47) w born in Panguitch, Utah, on October 1901. After receiving the B.S.E.E. degr from the University of Utah in 1925, he joined the graduate student program at the Westinghouse Electric and Manufacturing Co. In 1926 he returned to the University of Utah and he has remained there, except for several leaves, including one to receive the M.S.E.E. from Purdu University in 1931, and one during the wa to work on jungle acoustics in Panama. Pr fessor Haycock is currently associate dire tor of an Army research project at the Un versity of Utah.

Donald A. Murray

TWIN CITIES SECTION

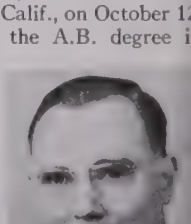

Donald A. Murray (A'35–VA'39–M'4 was born in Redlands, Calif., on October 1 1905. After receiving the A.B. degree i electrical engineering from Stanford University in 1928, he went to Germany on an exchange scholarship, returning to Stanford and receiving the E.E. degree in 1932. From then until 1937 he worked for the Mackay Radio and Telegraph Co., and for Heintz and Kaufman, Ltd., leavin in the latter year to join the FCC's enginee ing department. From 1941 to 1945 he w inspector in charge of the FCC's Fifteen Radio District at Denver; then he was tran ferred to the FCC's Sixteenth Radio Distric in St. Paul, where he is engineer in charge

Geiger Counter Tubes*

HERBERT FRIEDMAN†, ASSOCIATE, IRE

Summary—The following are some of the many rocesses that contribute to the mechanism of the scharge in Geiger counters: formation of the pri-ary ion pairs; ion multiplication within the gas by ownsend avalanche formation; spreading of the valanches through photoelectric absorption of ultra-olet quanta in the gas; transfer of ionization energy om positive ions of the rare gases to the polyatomic olecules of the "quenching" admixture; release of condary electrons at the cathode by positive ions d metastable atoms; de-excitation of metastable oms of the rare gases by collisions with atoms of lmixed foreign gases; and decomposition of poly-omic molecules by electron impacts and photon ab-rption. Present theories provide a qualitative un-erstanding of the fundamental roles played by all of ese processes, but their combined effects are too mplex to predict the wide variation in characteris-cs of tubes obtained with slightly altered practices construction or choices of gases. This paper is a re-ew of existing theories and methods of constructing bes to obtain maximum counting efficiencies and her desirable characteristics, such as low threshold ltage, thermal insensitivity, long life, high resolu-on, and low background.

SINCE THE FIRST demonstration of the tube counter by Geiger and Muller in July 1928,[1] the unusual sensitivity such counters has found widespread ap-lications in the detection of high-speed par-cles and energetic photons. The extensive terature on Geiger counters is not only in-cative of their manifold uses, but is also a easure of the divergence of theories de-sed to explain their mechanism and the merous recipes prescribed for the prepara-on of good counters. In the last ten years, owever, a consistent and relatively com-ete theory of counter-tube operation has een developing,[2–8] together with a know-ow for their construction, which now per-its production of large numbers of reliable bes with identical characteristics. This pa-er is a review of current theories of the echanism of the Geiger-counter discharge d a survey of the many different types of unters designed for specialized applica-ons.

A Geiger counter is a gas-filled diode op-ated in the region of the unstable corona discharge. There are two types of counters, characterized by their filling gases. One uses simple monatomic or diatomic gases, such as hydrogen, air, the rare gases, or mixtures of these, and is known as the nonself-quenching type. The second category includes mixtures of simple gases and small percentages of "quenching" admixtures, which are usually polyatomic organic molecules. In general, the firing characteristics of both types of fillings are very much alike, but the subsequent stages of the discharge and the deionization processes are distinctly different. The emphasis in this paper will be devoted almost entirely to a description of the self-quenching type of tube, which is now used almost universally in preference to the simple gas type. The condition for starting a discharge is that at least one low-energy electron be produced within the counter gas. This electron kindles an avalanche discharge which spreads rapidly throughout the length of the tube and lasts for a few microseconds. Within a fraction of a millisecond after the triggering event, all ions and electrons are cleared out of the interelectrode space, and the tube is ready to respond again to the passage of another ionizing particle. A single electron is capable of triggering a discharge which can be easily detected with little or no amplification. In this respect, the Geiger counter comes close to fulfilling the requirements of a perfect detector.

The electrode system of a Geiger counter usually consists of a fine wire and coaxial cylinder. Most tubes are filled with a rare gas combined with a trace of a polyatomic vapor such as alcohol, ether, amyl acetate, and many others. At low voltages, the tube behaves as an ionization chamber with an internal amplification factor of unity. A relatively small potential difference prevents recombination losses, and is sufficient to draw a saturation current from the tube, supplied entirely by the primary ionization. Raising the voltage brings on gas multiplication by impact ionization of the gas molecules in the manner of the familiar Townsend avalanche. The multiplication factor increases with increase in voltage, and the current delivered by the tube is proportional to the primary ionization up to multiplications of 10^5 or 10^6. Throughout this range, the discharges are single Townsend avalanches, each avalanche originating from a primary ion pair and localized within a fraction of a millimeter along the length of the wire. At still higher voltages, every avalanche breeds new avalanches, spreading the discharge along the full length of the tube, through the medium of the very-short-wavelength ultraviolet rays generated in each Townsend avalanche. The discharge continues to burn until a critical space-charge density of positive ions is reached. The amplification factor then becomes independent of the amount of primary ionization, and all discharge pulses attain equal amplitudes. This condition characterizes the operation of the Geiger counter. The Geiger-counting threshold is usually determined experimentally by observing, with an oscilloscope cou-

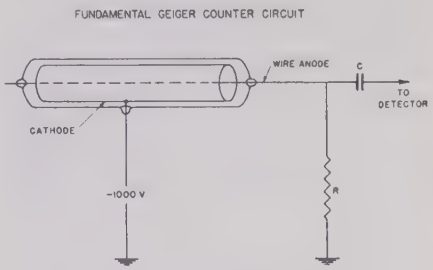

Fig. 1—Fundamental Geiger-tube circuit.

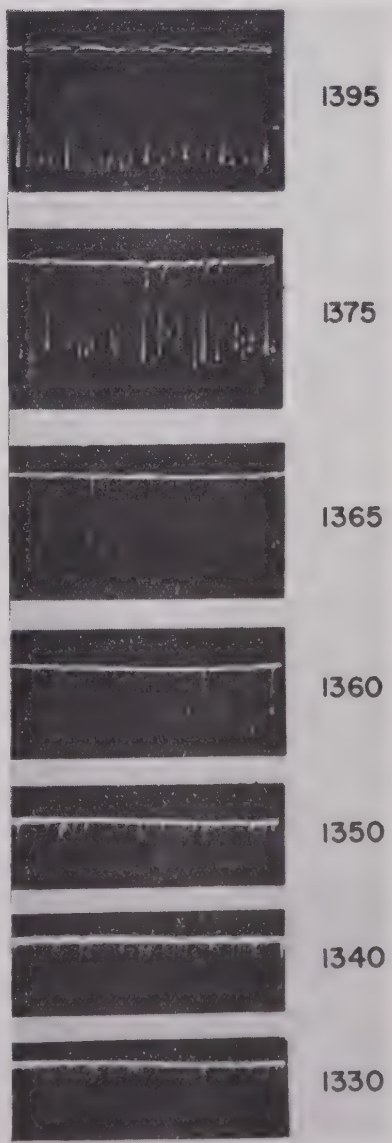

Fig. 2—Approach to uniform pulse amplitudes near Geiger-counting threshold. Counter-tube dimensions are 10, 1.0, and 0.0125 cm. Argon-ammonia filling.

* Decimal classification: 621.375.2. Original manuscript received by the Institute, March 7, 1949.
† Naval Research Laboratory, Washington 20, D. C.

[1] H. Geiger and W. Muller, "Technical considerations concerning the electron counting tube," *Phys. Zeit.*, vol. 29, pp. 839–841; November, 1928. Also, vol. 29, pp. 489–493; August, 1929.
[2] A. Trost, "The addition of saturated vapors to G-M tubes," *Zeit. für Phys.*, vol. 105, pp. 399–444; May, 1937.
[3] C. G. Montgomery and D. D. Montgomery, "Discharge mechanism of the G-M counter," *Phys. Rev.*, vol. 57, pp. 1030–1040; June, 1940.
[4] W. E. Ramsey, "Measurements of discharge characteristics of G-M counters," *Phys. Rev.*, vol. 57, pp. 1022–1029; June, 1940.
[5] H. G. Stever, "The discharge mechanism of fast G-M counters from the dead time experiment," *Phys. Rev.*, vol. 61, pp. 38–52; January, 1942.
[6] S. A. Korff and R. D. Present, "The role of polyatomic gases in fast counters," *Phys. Rev.*, vol. 65, pp. 274–282; May, 1944.
[7] A. Nawijn, "The mechanism of the G-M counter," *Physica*, vol. 9, pp. 481–493; May, 1942.
[8] A. G. M. Van Gemert, H. Den Hartog, and F. A. Muller, "Measurements on self-quenching G-M counters," Parts I and II, *Physica*, vol. 9, pp. 556–564 and pp. 648–664; June and July, 1942.

pled to the simple circuit of Fig. 1, the lowest voltage at which all pulses become equal in size. As threshold is approached, statistical fluctuations in the breeding of new avalanches from preceding avalanches may interrupt the chain before the discharge has filled the entire length of the tube. The transition to Geiger counting is ordinarily very sharply defined, as is illustrated in Fig. 2, which shows the rapid transition from incomplete growth of the discharge characterized by nonuniform pulse heights, to the threshold where each discharge has spread throughout the tube. The number of discharges is directly related to the number of primary particles striking the tube, and does not depend appreciably on the applied potential over a range of a few hundred volts known as the "plateau." At higher voltages, the condition of a self-sustained corona is reached, and the discharge maintains itself until the potential is removed. Sufficiently high potentials bring on the transition to a glow discharge in which the current rises very rapidly and the voltage across the electrodes falls to a low stable value. The complete voltage characteristic of the cylindrical ionization tube is illustrated in Fig. 3.

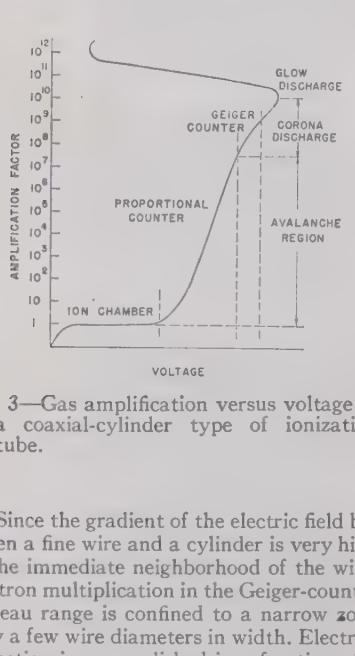

Fig. 3—Gas amplification versus voltage in a coaxial-cylinder type of ionization tube.

Since the gradient of the electric field between a fine wire and a cylinder is very high in the immediate neighborhood of the wire, electron multiplication in the Geiger-counter plateau range is confined to a narrow zone only a few wire diameters in width. Electron collection is accomplished in a fraction of a microsecond, during which the positive ions form a virtually stationary sheath about the wire. The eventual severing of the chain of electron avalanches is attributable to the electrostatic shielding effect of this positive-ion sheath. Subsequently, the ion sheath must be neutralized without reigniting the discharge. This constitutes the major problem in obtaining successful counter-tube performance.

At first glance, the structure and mechanism of the Geiger counter appear to be deceptively simple. The complete Geiger-counter mechanism is rather complex and involves (1) the Townsend avalanche, (2) the spreading of the discharge, (3) the motion of the ion sheath and growth of the pulse, (4) the deionization process, and (5) all the effects involved in suppression of spurious pulses. This last category includes ionization transfer from positive ions of the rare gas to polyatomic vapor molecules, suppression of secondary emission at the cathode, quenching of metastable states, and photodecomposition of the polyatomic gas.

The performance of any particular Geiger counter is described by its threshold voltage, the length and slope of its plateau, its efficiency, pulse characteristics, maximum counting rate, temperature dependence, and useful life. No single type of counter exhibits all of the ideal characteristics, but some tubes meet the requirements of specialized applications almost to perfection.

The Townsend Avalanche

The electric field strength between coaxial cylinders is given by

$$E(r) = \frac{V}{r \log \frac{b}{a}} \qquad (1)$$

where $E(r)$ is the field at distance r from the axis, V is the applied potential difference, and b and a are the cathode and anode radii, respectively. Consider a typical counter, operating with an applied potential difference of 1,000 volts. The field strength at the surface of the wire is about 40,000 volts per cm. It falls inversely as the distance from the wire and is less than a few hundred volts per centimeter at distances greater than $b/2$ from the anode. Immediately after the passage of an ionizing particle, the secondary electrons which it produced are accelerated radially toward the wire. Each electron gains energy, which it loses through inelastic collisions leading to excitation or ionization of the gas. Every inelastic collision brings the electron to rest, after which it starts to travel its next free path in the direction of the field. The excited molecules may radiate their energy or be de-excited by subsequent collisions. If, for example, the counter is filled with hydrogen to a pressure of 100 mm Hg, the electron mean free path is about 10^{-3} cm, and sufficient energy for impact ionization cannot be gained in one mean free path until the electron reaches the high-field region very close to the wire. The potential fall per mean free path at the cathode is as little as 0.2 volts, but rises to about 20 volts at the surface of the wire. This energy gained per mean free path first reaches the ionization potential of the hydrogen molecule, 16 ev, at a distance of four free paths, which is slightly less than one wire radius from the surface of the wire. Beyond the immediate neighborhood of the wire, the energy for ionization can be acquired only over several mean free paths.

Increasing the voltage across the counter toward the threshold for Geiger counting expands the multiplication zone in the gas over an increasing number of mean free paths. More and more electrons are added to the avalanche, together with photons radiated from excited states of higher energy which are capable of photoionizing the gas or photoelectrically releasing electrons from the cathode. These photoelectrons are in turn accelerated toward the wire, where they contribute new avalanches. Geiger-counting threshold is marked by the release of a sufficient number of photons per avalanche to guarantee the generation of a succeeding avalanche by photoelectric effect in the ga or at the cathode.

The properties of the single Townsen avalanche can generally be summarized a follows: At threshold the multiplication fac tor in the avalanche is about 10^8; each ava lanche is quite discrete, and the lateral ex tension along the length of the wire arisin from diffusion of the electrons in the ava lanche is about 0.1 mm; the duration of th single avalanche is less than 10^{-9} secon measured from the beginning of the multi plication process.

The threshold voltage for the corona dis charge depends for the most part on the na ture of the gas as characterized by the firs Townsend coefficient η, which is defined a the ionization produced by an electron pe volt of potential difference. The coefficient depends on the energy gained by an electron per mean free path, which is a function of the ratio of field strength E to pressure p. The threshold requirement that each avalanch release a sufficient number of quanta to pho toelectrically trigger another avalanche i expressed in terms of a second coefficient, γ as

$$\gamma n = 1 \qquad (2$$

where γ is the number of photoelectrons ejected per ion pair formed in the gas and n is the number of ion pairs per Townsend avalanche. Experimentally, it is observed that γ for the simple gases does not vary markedly with different cathode materials, but that the nature of the gas, its pressure, and the electrode geometry, as reflected in η, are the quantities which are mainly responsible for establishing the threshold voltage.

Among the diatomic and inert gases, equal values of η are achieved at widely different values of E/p. The rare gases—helium, neon, argon, krypton, and xenon—produce higher threshold voltages in the order of increasing atomic number. Hydrogen requires a higher starting voltage than argon, and that of air or nitrogen is still higher. Traces of impurities have a pronounced effect on the starting voltage of the corona, as will be shown in a later section. Most present-day counter tubes include a small percentage of a polyatomic "quenching" gas in addition to the rare gas which is usually the major constituent. Although the ionization potential of this polyatomic constituent is always lower than that of the rare gas, its presence almost invaraibly raises the threshold voltage. This is so, because a large portion of the electron energy is dissipated in exciting molecular vibrations at each impact, rather than ionizing. Polyatomic molecules with absorption bands in the near infrared portion of the spectrum can absorb energies amounting to a fraction of an electron volt, or less than the energy acquired by an electron per mean free path even in the neighborhood of the cathode. Inelastic collisions can, therefore, bring the electron to rest every time it encounters a polyatomic molecule. In contrast to the simple gas fillings, an electron is much less likely then to acquire ionization energy over several free paths. As a result, the zone of ionization contracts with addition of the polyatomic gas, and the minimum field strength for a corona discharge increases. Argon with alcohol admixture is one of the most commonly used

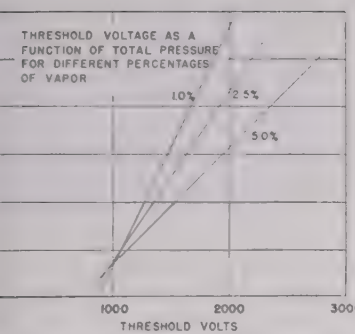

4—Variation of threshold voltage with omposition and pressure of a self-quench-ng gas mixture. (After Trost in footnote eference 2.)

er-counter fillings. Fig. 4 illustrates the t of argon pressure, percentage of alco-dmixture, and the size of the electrodes he threshold voltage.

Spread of the Discharge and Formation of the Ion Sheath

ove the threshold of Geiger counting, sands of Townsend avalanches per cen-ter of length of the tube are ignited ugh the emission and absorption of ul-olet light. Neutral gas molecules are ed by electron impacts in the avalanche ess and, in returning to the ground state, ultraviolet quanta with energies below onization potential of the gas. If the ter tube is filled with simple gases, the violet photons generate new avalanches eleasing photoelectrons at the cathode. rate of spread of the discharge is then ndent only on the lifetime of excited s or molecules and on the photon tran-me.

f a polyatomic vapor admixture such as ol is included with the simple gas, the on mechanism is very much altered. In xture of argon and alcohol, the highest ed states of argon at about 11.6 ev ex-the energy required to ionize an alcohol cule, 11.3 ev. Energetically, therefore, possible for the ultraviolet photon ra-d by an argon atom to ionize a mole-of alcohol, and thereby release an elec-which may trigger a new avalanche. efficiency of such absorption processes great that the number of quanta arriv-t the cathode is insufficient to provide significant number of photoelectrons. In ion to the absorption of ultraviolet ta by the polyatomic gas, there is evi-e for absorption processes in the rare tself, although their mechanism at pres-s not well understood.

Many investigations have been at-ted with the object of identifying the re of the ultraviolet radiation and its es of production and absorption within gas mixtures used in counters. Among arliest of these experiments was that of ner,[9] who studied counters filled with en, hydrogen, or air. The experiment sted of mounting two counters inside the same envelope, with their cylinders open to each other and their anodes separated by about 1 centimeter. From measurements of the number of counts which spread from one counter to the other at different pressures, Greiner computed absorption coefficients for the different gases. To prove that the spread, ing was accomplished by the passage of ultraviolet radiation across the gap between the counters, he inserted light filters between the tubes. Only the thinnest nitrocellulose films, about twenty-thousandths of a micron in thickness, which were transparent to ultraviolet radiation below 1,000 Å, permitted the discharge to spread from one tube to the other.

Greiner's experiment was performed with simple gases, in which the ultraviolet radiation regenerated Townsend avalanches by a cathode photoelectric effect. In another version of this type of experiment, Ramsey[10] showed that two counters would trigger each other in coincidence when filled with monatomic or diatomic gases, but that the introduction of a small amount of polyatomic admixture caused the counters to fire at random with respect to each other. Furthermore, by plotting coincidence rate versus resolving time of the coincidence circuit, it was found that the photoemission was confined to a period of approximately 1 microsecond, even though the pulse on the counter wire required from 1 to 20 microseconds to attain one-half its peak amplitude.

The mean free path of the ultraviolet radiation responsible for spreading the discharge in counters with polyatomic constituents has been evaluated by a number of experimenters. Stever[4] obtained an interesting picture of the process by using divided cathodes and beaded anodes. In the latter type of counter, glass beads were sealed on to the wire at equal intervals along its length. From observations of pulse size, it was established that the discharge jumped the obstacle of the glass bead only if the beads had less than a minimum diameter, or what is equivalent, if the ratio of field strength to pressure E/p exceeded a critical value. Further[11] studies showed that, besides the obstructing effect of the glass bead for ultraviolet light, the field intensity was reduced about the glass bead. The photons were all absorbed in the immediate neighborhood of the bead where the field was too low to develop a complete avalanche.

Attempts to clarify the details of the emission and absorption processes have not been entirely successful. Alder[12] and his coworkers recently performed a variation of the Greiner type of split-counter experiment to determine the absorption coefficient of an alcohol vapor admixture for the ultraviolet photons emitted in the discharge. The two counters were mounted in a common envelope at a fixed separation of 11 centimeters. At first, the counters were filled with a mixture of simple gases, argon plus air, which gave satisfactory counting characteristics. With this filling, every count in one tube triggered the companion tube coincidentally. Contaminating the simple gas mixture with only a few tenths of a millimeter Hg of alcohol sufficed to reduce the number of spreading discharges to a vanishingly small figure. The absorption coefficient computed from this experiment was 640 cm^{-1} (at atmospheric pressure). With an admixture of 15 mm Hg of alcohol, the number of photons fell to $1/e$ of its initial value in 0.8 mm. In obtaining this result it was assumed that introducing alcohol in these low concentrations did not affect the number of photons per discharge nearly so much as it did the absorption of photons.

Still another experiment of this type, reported by Liebson,[13] attempted to avoid the possibility of confusing a decrease in photon emission with an increase in absorption coefficient. All conditions of the discharge were held constant and only the gas path which the photons were required to traverse was altered, by an expanding bellows connection between the counters. The magnitudes of the total absorption coefficients for the rare gases, with the alcohol or methylene bromide admixtures which he used, were comparable to those computed by Alder and his coworkers, but Liebson found that constant coefficients per unit pressure were obtained only if the absorption were attributed entirely to the rare gas.

The qualitative conclusion to be drawn from these experiments is that, in gases containing polyatomic admixtures, the absorption of ultraviolet quanta by photoionization of the gas is very effective in confining the spreading mechanism to the immediate neighborhood of the wire. The ultraviolet radiation may be composed of a number of wavelengths, some of which may reach the cathode and contribute a photoelectric effect. Experiments with split-cathode counters,[14,15] filled with the typical operating mixtures, showed a small but measurable spreading of the discharge by ultraviolet radiation absorbed in the gas at distances of many centimeters, which could not be attributed to the same photons which propagate the discharge along the wire. These less-abundant photons were also capable of ejecting an appreciable number of cathode photoelectrons as part of the mechanism of spreading the discharge. In any combination of gas mixtures and cathode surfaces, it may be expected that all of these processes of photon emission and absorption in the gas and photoelectric emission at the cathode play a role, but their relative importance may differ considerably. There is a need for still more refined measurements of the production of photons and the cross sections of photon absorption between 600 Å and 1,200 Å before the Geiger-counter mechanism can be quantitatively described.

If Alder's value of about 1 millimeter for the mean free path of the quanta is accepted, it is immediately apparent that the dis-

. Greiner, "On the spreading of the discharge in r tubes," *Zeit. Phys.*, vol. 81, pp. 543–555; , 1933.

[10] W. E. Ramsey, "Period of photon emission in a counter discharge," *Phys. Rev.*, vol. 58, pp. 476–477; September 1, 1940.

[11] M. H. Wilkening and W. R. Kanne, "Localization of the discharge in G-M counters," *Phys. Rev.*, vol. 62, pp. 534–537; December, 1942.

[12] F. Alder, E. Baldinger, P. Huber, and F. Metzger, "On the growth of the discharge in counter tubes with alcohol vapor admixtures," *Helv. Phys. Acta.*, vol. 20, pp. 73–95; Issue I, 1947.

[13] S. H. Liebson, "The discharge mechanism of self-quenching G-M counters," *Phys. Rev.*, vol. 72, pp. 602–608; October, 1947.

[14] J. D. Craggs and A. A. Jaffe, "Discharge spread in Geiger counters," *Phys. Rev.*, vol. 72, pp. 784–792; November, 1947.

[15] C. Balakrishnan, J. D. Craggs, and A. A. Jaffe, "Discharge spread in Geiger counters with methane and methane-argon fillings," *Phys. Rev.*, vol. 74, pp. 410–414; August, 1948.

charge in a counter with a polyatomic admixture will spread with a smaller velocity than in a simple gas counter. The original avalanche will radiate quanta in all directions and breed new avalanches, whose number will fall exponentially with distance from the parent avalanche. The first generation of avalanches will initiate succeeding generations and the discharge will spread step-wise along the length of the wire, producing thousands of avalanches per centimeter. Since the duration of a single step can not be much less than 10^{-8} second, the velocity of spread may be as slow as 10^6 to 10^7 centimeters per second.

The relation between the velocity of spread and the overvoltage is almost linear.[16] By lowering the noble-gas pressure without altering the quenching-gas pressure, the spread velocity is increased. This behavior could be explained by a decrease in the duration of a single avalanche because of increased electron mobility in the avalanche. The velocity of propagation furthermore depends on the nature of the noble gas, all other factors being constant. For example, the discharge spreads about three times as fast in helium as in argon. Here, again, the explanation may be in the higher electron mobility in helium compared to argon, which would be expected to decrease the duration of the individual avalanche.

Growth of the Pulse

Because of the enormously greater mobility of the electrons compared to the positive ions (about 1,000/1), the positive ions at the wire move only a few thousandths of a centimeter before the completion of the electron avalanche. As the discharge continues, the positive-ion space-charge sheath builds up, until the field strength near the wire is lowered beyond that required to maintain gas multiplication.

For small overvoltages, the charge generated per unit length of counter depends almost linearly on the overvoltage $V-V_s$, which is the difference between operating voltage and threshold. At higher overvoltages the slope of the curve of charge per pulse versus overvoltage falls to about half its initial value. At a given overvoltage the charge per pulse is almost independent of the pressure and depends only on the geometry. These characteristics are illustrated by the curves of Fig. 5 for alcohol-argon mixtures. The capacitance of a typical counter ($=1$ cm, $a=0.01$ cm) supports a charge of about 1.2×10^{-13} coulombs per cm of length per volt of potential difference. In most counters of average size, the charge per pulse lies between 10^{-11} and 10^{-13} coulomb per cm of length at threshold, and may be 100 times as great at the end of the plateau.

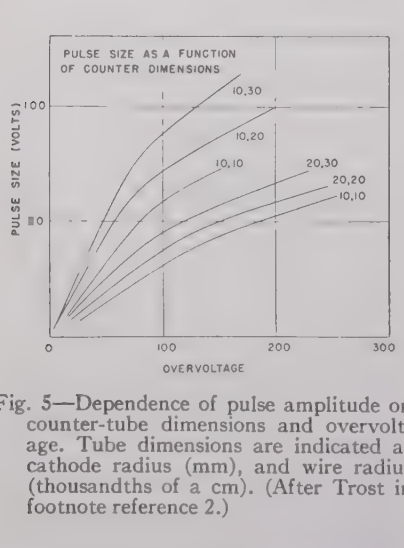

Fig. 5—Dependence of pulse amplitude on counter-tube dimensions and overvoltage. Tube dimensions are indicated as cathode radius (mm), and wire radius (thousandths of a cm). (After Trost in footnote reference 2.)

The voltage pulse on the wire can be attributed entirely to the motion of the positive ions. The electrons are held on the wire by the image force field of the positive ions. Initially, with the sheath almost in contact with the wire, nearly all the electrons are bound to the wire. As the sheath expands radially, the image charge decreases and the electrons flow away from the anode, giving rise to a voltage pulse on the grid of the amplifier coupled to the wire of the counter. The rate of release of electrons at the wire depends on the rate of drift of the ion sheath, which, in turn, varies with the radius of the sheath. The radial velocity of the sheath is approximately proportional to the field or inversely proportional to the radial distance from the wire. At the start, the shape of the pulse is affected by the time required to propagate the discharge throughout the length of the tube. Since the d
charge may spread at the rate of about 10
per microsecond in a self-quenched count
it may require of the order of a microseco
for the entire ion sheath to mature in a lo
counter, during which time the voltage pu
can rise to a few tenths of its peak val
(without differentiation). The rate of r
increases until the time at which the i
sheath is completed. After the sheath is co
pleted, the rate of rise of the pulse decreas
It may attain one-half its peak value in 1
2 microseconds, and thereafter increase ve
slowly. With infinite series resistance in t
fundamental circuit (no RC differentiatio
the pulse would reach its final and maximu
value in the time required for the positiv
ion sheath to traverse the tube, about 1(
to 10^{-3} second. Decreasing the series resi
ance allows the applied potential to be
stored on the wire in accordance with t
time constant given by the product of t
wire system capacitance and the series
sistance. The appearance of the differe
tiated pulse for different values of the ser
resistance is shown in Fig. 6.

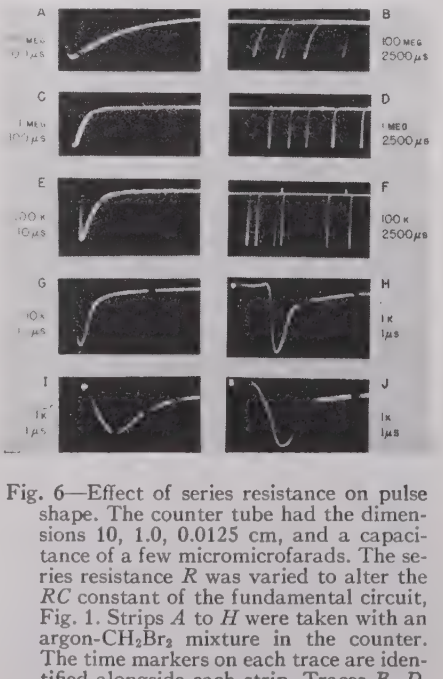

Fig. 6—Effect of series resistance on pulse shape. The counter tube had the dimensions 10, 1.0, 0.0125 cm, and a capacitance of a few micromicrofarads. The series resistance R was varied to alter the RC constant of the fundamental circuit, Fig. 1. Strips A to H were taken with an argon-CH_2Br_2 mixture in the counter. The time markers on each trace are identified alongside each strip. Traces B, D, and F were photographed with a recurrent sweep. All of the others are triggered sweep patterns. Strips I and J illustrate the effect of overvoltage on the rise time of the pulse in a neon-argon-chlorine mixture with a threshold of 550 volts. Trace I was taken at an overvoltage of 50 volts, trace J at 300 volts. All photographs were made with a DuMont Type 248 oscilloscope.

The Dead Time and Recovery Time

As the positive-ion sheath moves ou
ward towards the cathode, the field near t
wire returns to normal. The time requir
for the positive ions to reach the critical d
tance from the wire corresponding to thres
old field defines the dead time of the counte
During this period the counter is insensiti
to the passage of further ionizing particle
The additional time required for the ions
reach the cathode is called the "recove
time," and the size of any pulse occurri
within this time is determined by the tir
elapsed since the initial discharge, a pulse
the end of the recovery time being of t
same size as the initial pulse.

Figs. 7(a) and 7(b) show a trigger
sweep pattern of the type first used b
Stever[5] to illustrate the dead-time and r
covery-time characteristics for a self-quenc
ing tube. Following the trigger pulse, t
sweep shows no pulses until the dead-tim
interval is passed, at which time small puls
begin to appear. These grow in amplitu
with elapsed time from the triggering of t
sweep. The envelope of these pulses trac
the shape of the recovery curve of the ele
tric field near the anode wire, as shown
Fig. 7(c). From studies of the recove
curve, it is possible to obtain considerab
information about ion mobilities in differe
gases and at various field strengths. Mar
interesting observations have already bee
made. For example, it is possible to identi
the ions making up the sheath in mixtur
of polyatomic gases, such as, for exampl
alcohol and methane, where the recover
time was found to be characteristic of th
drift time of alcohol ions.[17] In many gas
the observed mobilities are identified wit
fragment ions, rather than the parent mol
cules.[18] The drift time of the ions in a hydr

[16] J. M. Hill and J. V. Dunworth, "Rate of spread of discharge along the wire of a Geiger counter," *Nature*, vol. 158, pp. 833–834; December 7, 1946.

[17] S. C. Curran and E. R. Rae, "Analysis of t
impulses from Geiger-Mueller tubes," *Rev. Sci. Inst*
vol. 18, pp. 871–877; December, 1947.

[18] P. B. Weisz, "Radiation chemistry of the Geige
Muller counter discharge," *Jour. Phys. and Colloi
Chem.*, vol. 52, pp. 578–585; March, 1948.

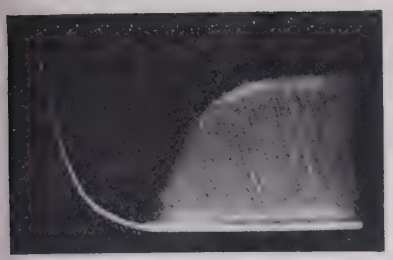

(a)

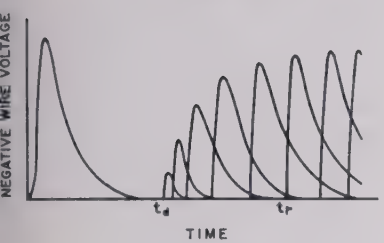

(b)

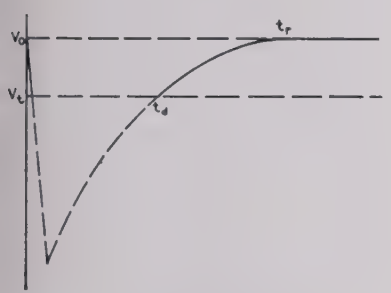

(c)

Fig. 7—(a) Dead-time pattern photographed on triggered sweep.
(b) Schematic representation of a dead-time pattern, indicating dead time t_d at the foot of the envelope of pulses triggered during the recovery interval from t_d to t_r.
(c) Variation of electric field at the anode surface during the period of ion-sheath transport from anode to cathode.

en-alcohol mixture, surprisingly enough, vas found to be longer than in oxygen-alcohol, indicating that the mobilities of these ons in the high fields of counters may be onsiderably different from those measured t small field strengths.[17]

The dead time and recovery time in a ube of ordinary dimensions are roughly qual to each other, and of the order of a few undred microseconds. The critical distance o which the ions must move before the field t the wire recovers to threshold is about alf the counter radius. This critical radius $_e$ is related to the overvoltage $V-V_0$, the ylinder radius b, and the charge q, per unit ength of the ion sheath by

$$r_c = be^{-V-V_0/2q}. \quad (3)$$

The dead time therefore decreases with increasing overvoltage, and is shorter in a tube f smaller dimensions and larger ratio of node to cathode diameter. Dead times as hort as 5 microseconds have been obtained n tubes having cathode and anode diameers of 0.25 inch and 0.15 inch, respectively.

The Role of the Quenching Admixture

The treatment of the Geiger-counter mechanism up to this point provides a picture of the growth of the discharge and the shape of the pulse. Upon the subsequent arrival of the positive-ion sheath at the cathode, the electric field within the counter tube is fully restored. This introduces the possibility of rekindling the discharge by secondary electron emission. Suppose, for example, that the sheath consists of argon ions whose ionization potential is in excess of twice the work function of the cathode surface. An argon ion can first draw an electron out of the cathode and become neutralized. The energy difference between the ionized argon and the work function appears as recombination radiation with an energy in excess of the photoelectric threshold energy. The recombination photon can then eject an electron from the cathode and initiate a new avalanche. In a nonself-quenching counter it is, therefore, necessary to quench the discharge by the use of either a large series resistance or an electronic quenching circuit, which prevents recovery of the threshold counting field until deionization of the gas is complete.

Self-quenching counters are usually produced by admixing a small amount of polyatomic organic vapor to the nonself-quenching gas. Almost any molecule, inorganic as well as organic, containing three or more atoms, will contribute the quenching mechanism. Self-quenched counters have been made with triatomic gases, such as sulphur dioxide and nitrous oxide. Among the diatomic molecules, only the halogens have been found to quench properly. The primary requirement for quenching is that no excited or ionized molecules capable of inducing secondary emission shall reach the cathode surface. In a typical mixture of ten parts of argon to one of alcohol at a total pressure of 10 cm Hg, an argon ion formed in the discharge must make about 10^5 collisions with gas molecules in traversing the anode-to-cathode distance. Because of this large number of collisions, the chances are very favorable for the transfer of ionization from argon ions to molecules of alcohol.[19] Energetically, all that is required is that the ionization potential of the quenching gas be lower than that of argon. This condition is fulfilled by alcohol in argon, and is satisfied by almost all polyatomic molecules in combination with helium, neon, or argon. The ionization potential usually decreases with increasing complexity of the molecule. In the experience of this laboratory alone, over thirty different admixtures were investigated which produced usable self-quenching counters. When krypton or xenon are the vehicular gases, their ionization potentials are lower than those of many of the commonly used quenching gases, and it becomes much more difficult to select admixtures which satisfy the requirements of the transfer process.

In transferring ionization energy to the polyatomic molecule, the neutralized argon ion emits recombination radiation. This radiation may be absorbed by another polyatomic molecule, which then photodissociates into two or more neutral molecules or radicals, with emission of still-longer-wavelength photons. The degradation of the original photon through many processes of this type amounts to a "red shift" of the photon spectrum beyond the photoelectric threshold of the cathode. The positive ions of the polyatomic molecules and dissociation fragment ions migrate to the cathode, where they are neutralized by drawing electrons out of the metal surface. After neutralization, the molecule is left in an excited state from which it may radiate a photon or predissociate without radiating. Radiation is very unlikely to occur because the lifetime against radiation is about 10^{-8} second, which is much greater than the time required for the neutralized atom to travel the remaining distance to the cathode. The quenching process can be completed successfully, then, if (1) the excitation energy left with the neutralized molecule is less than the photoelectric threshold of the cathode, in which case no secondary electrons can be ejected, or (2) the excitation energy is dissipated in predissociation before the molecule collides with the metal wall.

It is possible that the first process, which requires the ionization energy E_i of the quenching admixture to be less than twice the work function ϕ of the metal cathode, may be largely responsible for the excellent quenching properties of the halogens, and perhaps the halogenated hydrocarbons, such as methylene bromide. In experiments conducted here, tubes filled with these admixtures were equipped with quartz windows but produced no photocathode response to the shortest U.V. transmitted by quartz, about 1,850 Å or 6.5 ev. The cathodes used in these tubes were iron or copper, which in vacuum photocells are known to have work functions of 4 to 5 ev. However, it is also well known that in the presence of even the less active gases, the photoelectric threshold of these metals may be considerably shifted, so that it would not be surprising if the halogens were capable of increasing the threshold energies well beyond the limit of 6.5 ev observed in the quartz window tubes. Since E_i of Cl_2 is 13.2 ev and of Br_2 is 12.8 ev, it is apparent that the condition for secondary emission, $E_i > 2\theta$, is not fulfilled.

The second process, in which the molecule predissociates before radiating, becomes more and more probable, the greater the complexity of the polyatomic molecule. Neutralization of a polyatomic ion occurs by field emission[20] which is effective at a distance of about 10^{-7} cm from a metal surface whose work function is about 4 or 5 ev. After neutralization, the excited molecule ($E_{exc} = E_i - \phi$) must approach within about 10^{-8} cm, of the surface before secondary electron emission is possible.[21] At the thermal velocities with which the positive ions approach the cathode, 10^{-7} cm is traversed in about 10^{-12} second. To avoid secondary emission, the molecule must predissociate in less than

[19] H. Kallmann and B. Rosen, "Elementary processes in collisions of ions and electrons," *Zeit. für Phys.*, vol. 61, pp. 61–86; March, 1930.

[20] M. L. E. Oliphant and P. B. Moon, "The liberation of electrons from metal surfaces by positive ions," *Proc. Roy. Soc. A.*, vol. 127; pp. 386 et seq; 1930.

[21] H. S. W. Massey, "The theory of the extraction of electrons from metals by positive ions and metastable atoms," *Proc. Camb. Phil. Soc.*, vol. 26, pp. 386-401, part III; 1930.

10^{-13} second. The lifetime against predissociation in polyatomic molecules is closer to 10^{-13} second, about the time of one interatomic vibration. Spectroscopically, this property of predissociation in polyatomic molecules can be detected by the appearance of continuous absorption at wavelengths equal to $(E_i-\phi)$. Using alcohol ($E_i=11.3$ ev) and copper ($\phi=4.0$ ev) for illustration, the difference $(E_i-\phi)$ is 7.3 ev, which remains with the molecule as excitation energy, equivalent to absorption of a quantum of 1,700 Å wavelength. The alcohol spectrum shows continuous absorption below 2,000 Å accompanied by photodecomposition, indicating that the neutralized but excited molecules should predissociate in about 10^{-13} second and satisfy the quenching requirement.

The Influence of Metastable Atoms

A metastable atom produced in the discharge remains in that state until its energy is radiated or dissipated in a collision of the second kind. If the metastable atom, which is electrically neutral, drifts to the cathode wall, the probability of ejecting an electron there may be as high as 50 per cent. Although the average lifetime of metastable states in neon before radiation is about 10^{-4} second, Paetow[22] found a measurable current caused by metastable atoms in neon persisting for as long as a second after terminating a discharge between parallel plates.

The highly purified rare gases, taken by themselves, are unsuited for use in counters because their metastable states are so readily excited by electron impacts. Ejection of electrons by these metastables, after the positive-ion sheath has spread beyond the critical dead-time radius, reignites the discharge and leads to trains of multiple counts, or continuous discharge. A counter tube filled with rare gas is, therefore, unusable unless a foreign gas is admixed which de-excites the metastable atoms on colliding with them. Hydrogen is effective in quenching the metastable states of argon and neon, and has been used with those rare gases to make permanent gas mixtures for nonself-quenching tubes. The effect of mixing hydrogen with argon or neon on the performance of a counter operated with an external quenching circuit is illustrated by the plateau curves of Fig. 8. Less than 10 per cent of hydrogen in neon does not provide enough collisions between hydrogen atoms and metastable neon atoms to de-excite completely the metastables before they radiate or reach the cathode. Adding more than 10 per cent of H_2 produces a plateau almost as long as is obtained in pure hydrogen. Argon requires a much greater admixture of hydrogen to produce a satisfactory plateau. The ionization energies E_i, and metastable energies E_m, listed in Table I, show that it is energetically possible that metastable neon can be quenched by ionizing hydrogen, but that argon can be quenched only by exciting hydrogen ($E_{exc}=11.5$ ev).

Much more striking effects attributable to the quenching of metastable states were

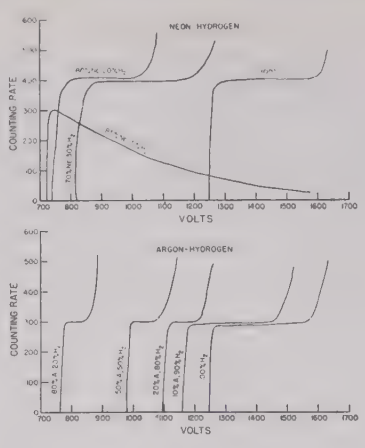

Fig. 8—Plateau curves for mixtures of neon-hydrogen and argon-hydrogen obtained with a Neher-Harper electronic quenching circuit.

discovered by Penning[23] and his coworkers in their studies of breakdown voltages V_B in rare gas discharges. Great differences appeared in the measured V_B which could only be attributed to minute traces of impurities. For example, baking a tube filled with pure neon dropped its V_B by 100 volts, but a subsequent glow-discharge treatment raised it again. A high-frequency electrodeless discharge sometimes raised and sometimes lowered V_B. Only after prolonged glow discharging, which is known to clean up many impurity gases, would V_B reach a stable upper value. By deliberately contaminating neon with traces of argon, mercury, and krypton in concentrations as low as 0.0001 per cent, Pennings obtained remarkable reductions in V_B.

TABLE I

Vehicular gas	Admix. Per cent	E_i	pd	V_B	V_B'
None $E_m=16.6$ ev	0.02 K_r	13.3	20	350	170
	0.01 H_2	16.1	18	350	260
	0.05 H_2	16.1	18	340	210
	0.01 N_2	16–17	18	350	200
	0.05 N_2	16–17	18	340	160
Argon $E_m=11.6$ ev	0.03 K_r	13.3	15	500	500
	0.03 Xe	11.5	14	520	530
	0.05 CO_2	15	14	460	470
	0.05 CO_2	14	14	480	500
	0.05 NO	9	14	470	480

NO was the only exception to the rule that V_B is reduced if $E_i<E_m$. Penning suggested that the neutral NO molecule had many states above the ionization limit of 9 volts which were closer to the 11.6 ev of metastable argon, making excitation to those levels more probable than ionization.

It was impossible to explain these results by hypothesizing that, since the admixed gas had a lower ionization potential than the main gas, it was therefore more readily ionized, resulting in a lowering of V_B. The relative contribution of the mercury admixture to ionization, for the case of Hg contamination in neon, was computed to be about 0.0005, entirely too small to be significant. An explanation of the reduced V_B, based on the transfer of excitation energy of neon to ionization energy of the admixture, was more plausible. In pure neon there is no

mechanism for converting excitation ener to ionization, but neon atoms excited metastable states in the discharge cou have a relatively great efficiency for ioniz tion of a trace admixture if the energy co dition $E_m>E_i$ is fulfilled. Many collisio are made during the life of the metastab atom, and, consequently, the chance of eventual collision with an admixture ato is great. To materially influence the brea down voltage, these collisions should occ within a few microseconds of the first av lanche. At the pressures ordinarily used counter tubes, a metastable atom may mak between 10^4 and 10^5 molecular collisions p microsecond. A concentration of quenchir admixture as low as 10^{-4} to 10^{-5} would, there fore, effectively remove almost all the meta table atoms within a few microseconds, every collision between a metastable and a admixture molecule had a high probabilit of de-exciting the metastable.

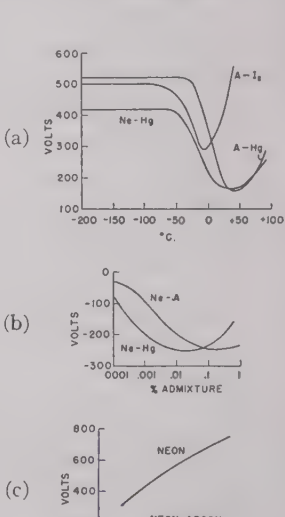

Fig. 9—Effects of impurity gases on th breakdown characteristics of the rar gases. (After Penning in footnote refer ence 23.) Fig. 9(a) shows the effect of dif ferent concentrations of iodine and mer cury in argon and neon on the break down voltage of the discharge betwee parallel plates about 1 cm apart. The ar gon pressure was 15 mm, neon pressur was 21 mm, and the admixture concen tration was controlled by its vapor pres sure at different temperatures. Fig. 9(b is a semilogarithmic plot of the Ne-H data in percentage of admixture versu decrease in V_B. A similar curve is show for neon with small percentages of argo admixture. The data of Fig. 9(c) wer obtained by starting with 0.06 per cen argon in 10.1 mm of neon, which gave V_B of 159 volts, and then diluting th mixture with neon up to a maximu pressure of 112 mm, which raised V_B t only 185 volts.

Fig. 9 and Table I summarize the result of Penning and his coworkers. The column of Table I list: E_i, the ionization potential o the admixture; pd, the product of pressur and distance between electrodes; V_B, th breakdown voltage of the pure rare gas; V_B

[22] H. Paetow, "Spontaneous electron emission and field emission following gas discharge bombardment of thin insulating layers," *Zeit. für. Phys.*, vol. 111, pp. 770–790; March, 1939.

[23] F. M. Penning, "The influence of very minute admixtures on the striking voltage of the rare gases," *Zeit. für Phys.*, vol. 46, pp. 335–348; January, 1927.

ie breakdown voltage with the admixed im-
urity gases. The most pronounced effects
ere obtained with an admixture of argon in
eon, where as little as 0.005 per cent argon
112 mm Hg of neon reduced the striking
oltage from 770 volts to 185 volts between
arallel plates, 7.5 millimeters apart (Fig.
(c)).

Low-Voltage Counters

The condition that E_m of the rare-gas
oms be higher than E_i of the admixture
satisfied by a great many of the polyatomic
uenching gases commonly used in counters.
he tendency to reduce the striking voltage
y converting metastable energy to ioniza-
on energy, however, is opposed by the
ndency toward inelastic electron impacts
ith the polyatomic molecules. These im-
acts keep the electron energies below E_m
nd E_i of the rare gas and suppress the
owth of Townsend avalanches, thereby
ising the threshold-voltage requirement.
n normal counter mixtures, the concentra-
on of polyatomic constituent needed to
uench adequately the discharge and pro-
uce a satisfactory life is so high that the
rocess of holding down the distribution of
ectron energies in the avalanche through
elastic impacts with polyatomic molecules
more important than the ionization of
etastables. The most notable exception
bserved here thus far was methylene
romide in argon, where the amount of ad-
ixture could be reduced to a few tenths of
per cent without destroying the quenching
roperties of the mixture. Such tubes,
perating at 250 volts, exhibited plateaus
bout 100 volts long and had useful lives of
10^7 counts. Weisz[24] observed the effect of
iluting hydrocarbon admixtures in argon to
ery low concentrations. The threshold
oltage was markedly reduced in every case
atisfying $E_m > E_i$, although no examples
ere observed which promised practical use-
lness in the sense of satisfactory plateaus
nd long counting life.

Recent attempts to produce low-voltage
resholds in counters, with the neon-argon
ixture and others described in Table I
bove, have been very successful. Previously
ie lowest operating voltages had been ob-
ined by reducing the gas pressure, decreas-
g the anode and cathode radii, or introduc-
g a grid. None of these techniques pro-
uced low voltage thresholds without sacri-
cing other desirable features, such as high
fficiency and fast recovery times. The
eory of operation of counters filled with
ermanent gases having high threshold
oltages and utilizing electronic quenching,
pplies equally well to mixtures of the Ne-A
ype with their characteristically low values
f V_B. Simpson[25] prepared counters filled
ith 5 cm Hg of neon and 0.01 per cent
rgon, which operated in a Neher-Harper
uenching circuit with thresholds at 120 to
35 volts. Self-quenching counters having
w threshold voltages were prepared by
dding fractions of a mm Hg pressure of
polyatomic vapors to the neon-argon mix-
ture. At the lowest threshold voltages, ob-
tained by using the minimum amounts of
vapor, such counters were temperature-
sensitive, short-lived, and required some
electronic circuitry to assist the quenching.
Using somewhat higher pressures, i.e., 1 mm
Hg of ethylacetate and 50 cm Hg of Ne-A
fast counters were made in this Laboratory
with thresholds of 350 volts and plateaus of
100 to 150 volts. These counters had useful
lives of about 10^7 counts.

Counters employing traces of the halogen
gases with neon or argon[26] have low threshold
voltages combined with many other desir-
able properties. They cannot be damaged by
excessive counting rates or running over the
upper voltage limit of the plateau. When
chlorine or bromine is used, the tubes are in-
sensitive to temperature variations over a
wide range. As was indicated in Penning's
experiments, a halogen admixture is also
capable of reducing the corona breakdown
voltage, when the energetic requirement
$E_i > E_m$ is satisfied. Fig. 9 shows that a
trace of iodine ($E_i = 9.7$ ev), in argon
($E_m = 11.6$ ev) was as effective in reducing
V_B as was Hg. In a similar manner, chlorine
($E_i = 13.8$ ev) and bromine ($E_i = 12.8$ ev)
should ionize metastables in neon ($E_m = 15.6$
ev). At higher concentrations of halogen
admixture, the halogen acts predominantly
as an electron trap and raises the break-
down voltage. As the halogen concentration
is reduced, however, ionization of the halo-
gen molecules upon impact with metastable
rare gas atoms becomes more probable than
electron attachment, and the starting volt-
age is lowered. Fortunately, relatively small
concentrations of halogen are required to
satisfy all the Geiger-counter quenching
requirements. It has been pointed[27] out that,
in theory, the halogens possess the properties
required in quenching that are otherwise
found only in polyatomic molecules.

A major difficulty in the use of halogen
admixtures is the clean-up of the small
amount of halogen, originally present, by
chemical reactions within the tube. Tubes
constructed with electrodes of brass, copper,
silver, aquadag, and various plated surfaces
failed very quickly when filled with a rare
gas plus a halogen admixture. Satisfactory
results have thus far been obtained with the
use of tantalum and of chrome-iron, and
bromine appears to be much less reactive
than chlorine. If the efficiency of the counter
for ionizing events need not be greater than
90 per cent, higher concentrations of the
halogens may be used, and a slow clean-up
then produces a correspondingly slower de-
terioration. Both the inefficiency and oper-
ating voltage rise rapidly with increasing
halogen admixture, however, and it is much
more desirable to seek to eliminate the
chemical clean-up process from the begin-
ning, rather than to resort to higher con-
centrations of the halogen.

The pulse characteristics in low-voltage
counters differ only to a minor degree from
those of the more common higher-voltage
counters. The lower the operating voltage,
the longer is the rise time of the pulse. At
the lowest voltages, the time to reach peak
amplitude may be ten times as long as in
similar "high"-voltage counters. The charge
per pulse is also considerably greater. Dead
times are not appreciably different, and gen-
erally center about 200 microseconds for
tubes of ordinary dimensions.

The Plateau Characteristic and Spurious Counts

The plateau of a Geiger counter may be
defined as the voltage range over which the
counting rate at a constant intensity of ir-
radiation is substantially independent of
voltage. If the term "counting range" is
taken to mean the difference in voltage be-
tween threshold and the inception of a
self-sustained corona discharge, then the
plateau is always much shorter than the
counting range. No Geiger counter exhibits
an ideally flat plateau characteristic for any
considerable range above the threshold
voltage. An increase in counting rate with
overvoltage is always observed which may
be as high as 0.1 per cent per volt in counters
that are still considered satisfactory for
many applications.

A portion of the slope can be attributed
to a real increase in sensitivity, but the re-
mainder arises from increasing numbers of
spurious counts at high overvoltages. The
former effect is largely explained as an in-
crease in volume of the counter through the
growth of the electrostatic field at its ends.
Of course, any misalignment of the elec-
trodes, such as the wire being cocked at an
angle to the axis of the cylinder, will in-
crease the sensitivity with increasing over-
voltage by causing different portions of the
counter to exhibit different threshold volt-
ages. Finally, any inefficiency from failure
to mature a complete discharge would be
lessened by an increase in overvoltage, since
the number of photons per discharge in-
creases with overvoltage and improves the
probability of spreading the discharge com-
pletely. The electrostatic effects can be
minimized, in general, by carefully aligning
the electrodes, making the length-to-diam-
eter ratio as large as convenient, polishing
the anode to remove sharp points, and
shielding the ends of the wire with insulating
sleeves so as to limit the expansion of the
sensitive volume beyond the ends of the
cylinder. In the preparation of most count-
ers these precautions are more or less routine,
so that spurious pulses generated by the
discharge itself are usually the major con-
tributors to plateau slope.

The most serious source of plateau slope
in Geiger counters is a type of spurious
counts that appear in the form of "after-
discharges" or trains of counts following a
valid count. In some counters these multiples
appear almost immediately above thresh-
old; in all counters they appear at suffi-
iently high overvoltages. The voltage region
in which these trains of multiple counts be-
gin to appear in appreciable numbers marks
the limit of the useful plateau range. Cer-
tain fillings, such as argon and alcohol,
which show no spurious pulses at overvolt-
ages of 100 to 200 volts, produce very flat
plateaus. If the argon is of spectroscopic
purity (99.9 per cent) and the alcohol is
free of air and water, a plateau slope less

[24] P. B. Weisz, "Starting potential of the Geiger-Mueller counter discharge," *Phys. Rev.*, vol. 74, pp. 1807–1812; December, 1948.
[25] J. A. Simpson, "The theory and properties of low-voltage radiation counters," MDDC report 870, declassified, 1947.
[26] S. H. Liebson and H. Friedman, "Self-quenching halogen-filled counters," *Rev. Sci. Instr.*, vol. 19, pp. 303–307; May, 1948.
[27] R. D. Present, "On self-quenching halogen counters," *Phys. Rev.*, vol. 72, pp. 243–244; August, 1947.

than 0.01 per cent per volt may be obtained. A commercial grade of argon (98 per cent), on the other hand, produced slopes from 0.05 to 0.15 per cent per volt, and contamination with air increased the slopes proportionately.[28] An optimum concentration of quenching admixture was also observed which was about 5 per cent for alcohol. Larger concentrations increased the slope. This behavior could be explained by failure of an increased number of discharges to develop fully because of the suppression of photon emission in the avalanches. A mixture of 20 per cent of alcohol in argon increased the slope to 0.05 per cent per volt. The behavior of alcohol-argon is also typical of helium and neon and many of the more commonly used hydrocarbon quenching admixtures, such as ether, ethyl acetate, amyl acetate, and ethylene. In contrast, many spurious counts were observed[17] when alcohol was used with O_2, N_2, or H_2. For a mixture of hydrogen and alcohol, 27 per cent of the counts observed in the middle of the plateau were spurious; in oxygen and alcohol the fraction of spurious counts was 10 per cent.

Although a counter may initially exhibit a very flat plateau, the slope invariably increases with use. The rate at which this proceeds initially and over longer periods of use varies with the particular gas mixture. In argon, with alcohol admixture, the slope may increase considerably at first, then remain relatively unchanged for a major portion of the useful life, and finally deteriorate very rapidly. Some mixtures show a tendency to recover when not in use. All of these effects reflect the contamination of the gas mixture by decomposition products of the discharge and the correlated loss of the optimum concentration of quenching constituent.

The process responsible for the major portion of the spurious pulses observed in counter tubes is positive-ion bombardment of the cathode. As the overvoltage is raised, the number of positive ions per discharge increases. Since the emission of secondary electrons is directly proportional to the number of ions arriving at the cathode, the number of spurious counts should increase with overvoltage. Because of the well-defined time require for the positive-ion sheath to traverse the interelectrode space, spurious pulses arising from secondary emission are readily recognized. On an oscilloscope screen, trains of spurious pulses at high overvoltage have the appearance of relaxation oscillations. The successive pulses in a train are uniformly spaced in accordance with the nature and pressure of the vehicular gas and the overvoltage, as predicted by the dependence of ion mobility on pressure and field strength. Figs. 10, 11, and 12 illustrate the increasing length of the trains of multiple pulses with increasing overvoltage or decreasing concentration of quenching admixture; the increase in spacing of multiples as the mobility of the positive ions is reduced by increased pressure; and the dependence of the mobility, as reflected by the spacing of pulses, on the collision cross sections of the rare-gas atoms. Before arriving at the condition of continuous corona discharge, the number of pulses in individual trains may reach thousands without destroying the perfect spacing between pulses.

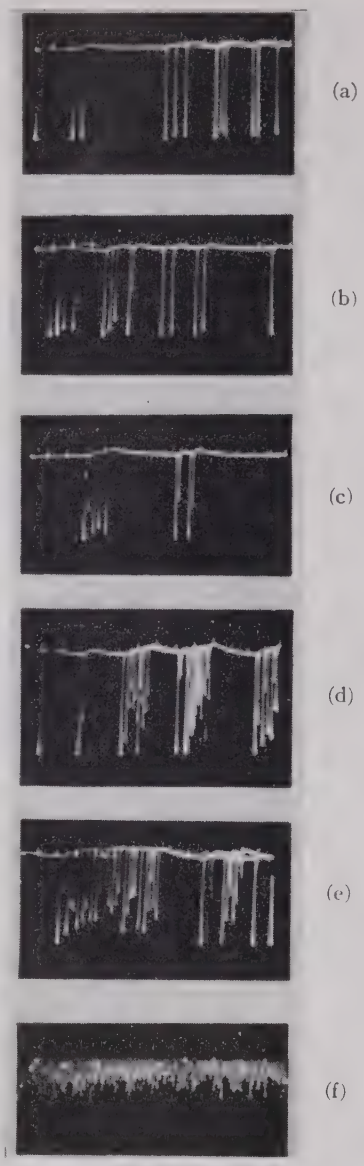

Fig. 10—Appearance of multiple pulses with insufficient admixture of quenching vapor. All traces were photographed at an overvoltage of 100 volts. Initial filling was argon, 20 cm Hg, plus CH_2Br_2, 0.5 mm Hg, which showed single pulses (trace A). Successive dilutions of the CH_2Br_2 were made by pumping the mixture to 10 cm Hg and restoring 10 cm of pure argon. Traces B to F illustrate the appearance of increasing numbers of spurious counts with removal of the quenching agent.

The idea behind most procedures for treating counter tubes prior to filling is to produce a high work function at the cathode surface, and thereby reduce spurious pulses due to secondary emission. In many instances the effect of adsorbed polyatomic molecules on the metal surface is to increase its work function more markedly than most of th treatments to oxidize, or make the surfac passive, which have so often been recom mended in the literature. Measurements o the photosensitivity of an alcohol-argo counter with a clean copper cathode sho that the photoelectric threshold is depresse toward the ultraviolet as more alcohol i admixed with the argon. During use, the dis charge decomposes the alcohol and th threshold climbs steadily back toward th visible. When using low-work-function-elec trode materials, such as aluminum or mag nesium, the work function must be consider

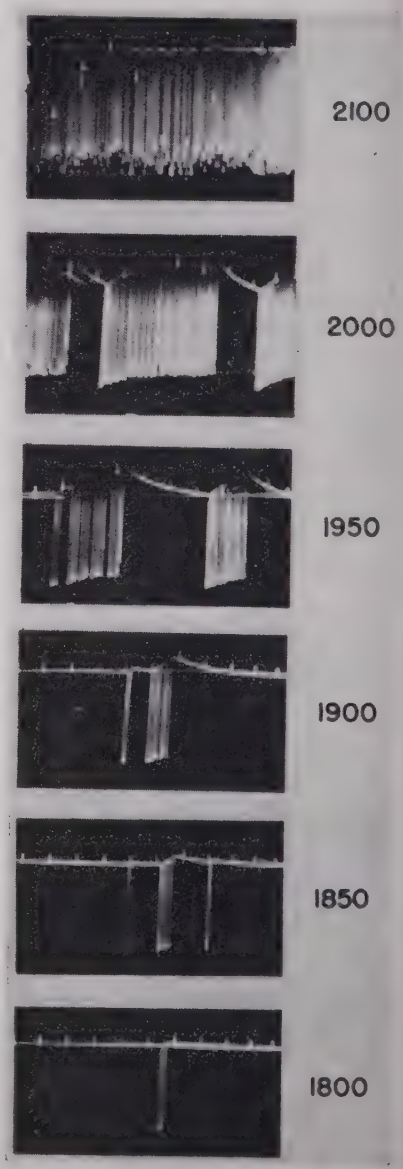

Fig. 11—Development of spurious pulses at high overvoltages. The filling was 20 cm Hg of argon plus 10 mm Hg of CH_2Br_2. Threshold was 1,500 volts. At overvoltages in excess of 300 volts, multiple pulses, appear with uniform spacings characteristic of secondary emission due to positive ion bombardment of cathode. Higher overvoltages increase the average length of the trains of pulses and their frequency of occurrence. Marker pulses are 2,500 microseconds apart.

[28] S. A. Korff, W. B. Spartz, and J. A. Simpson, "Summary report on neutron counter work," MDDC Report 1704.

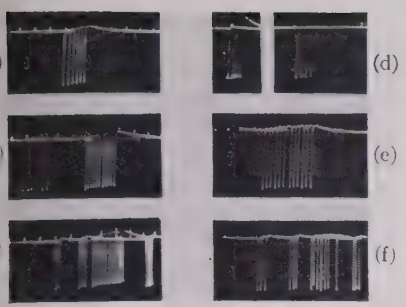

Fig. 12—Effect of gas mixture on spacings between multiple pulses. Traces (a), (b), and (c) were made with 75, 35, and 15 cm Hg of argon respectively and a constant admixture of 10 mm Hg of CH_2Br_2. As the pressure of the argon was reduced, the mobility of the positive ions increased, and the intervals between pulses became shorter. Trace (d) illustrates the greater mobility in helium as compared to argon. All markers are spaced 2,500 microseconds apart, but the right-hand portion of trace (d) is expanded. Traces (e) and (f) show the opposite trend toward decreasing mobility in a heavier gas such as Xe.

ably increased by chemical treatment or by deposition of a very thin layer of a more suitable surface, such as copper, before satisfactory counting can be obtained. Glow discharging in an active gas, before filling is often effective in subsequently preventing spurious counts. Several more extreme treatments have been described, such as mechanically coating the cathode with a very thin layer of a high-work-function surface; for example, a coating of lacquer. The influence of such a coating can be judged from its effect on the photoelectric threshold. Because the lower-energy photoelectrons released at threshold cannot penetrate the thin coating, the photoelectric limit appears to be shifted toward the ultraviolet.

A less-important class of spurious counts are those attributable to the charging of particles or thin layers of insulating material on the cathode. During the discharge, positive ions may remain bound to these insulating surfaces, or the particles may acquire charge as a result of photoelectric emission. Subsequently, spurious counts may be triggered by electrons released in the neighborhood of these charged spots. Experiments with plane-parallel electrodes[29] demonstrated the presence of an electron current decreasing roughly exponentially with time, following the termination of a glow discharge. A measurable current was observed for fully 15 minutes with nickel electrodes coated with collodial graphite and magnesium oxide. After prolonged baking to remove the oxide, this after-discharge current almost entirely disappeared. The effect of irradiation was demonstrated by an experiment[30] in which parts of a counter tube were exposed to intense X rays and the counter subsequently reassembled. A much higher background was then observed, which decayed slowly with time. Many counters go over into an unbroken chain of counts when the overvoltage exceeds the limit of the plateau and do not recover when returned to what was previously normal operating voltage. The applied voltage must then be dropped below threshold for at least a few seconds before such tubes recover. This general behavior closely resembles the phenomena observed in the aforementioned experiments with MgO coatings and irradiated electrodes.

[29] A. Guntherschulze, "Electron velocity in insulators at high field strengths and its relation to the theory of electric penetration," *Zeit. Phys.*, vol. 86, pp. 778–786; December 7, 1942.

[30] Mr. Roggen and Mr. Scherrer, "An After-effect of X-ray irradiation on counter tube performance," *Helv. Phys. Acta*, vol. 15, pp. 497–499; 1942.

Life of Self-Quenching Counters

Most self-quenching counters exhibit similar symptoms of aging. The threshold voltage rises, the plateau slope increases, and multiple pulses appear at progressively lower voltages. Many tubes become increasingly photosensitive. Some counters may be brought into self-sustained discharge above the plateau, yet recover immediately when returned to operating voltage; whereas others are permanently destroyed if brought into continuous discharge, even momentarily. Most of these observations are understandable in terms of the decomposition of the quenching admixture in the course of the discharge. A typical counter initially contains approximately 10^{20} polyatomic molecules. About 10^{10} of these molecules are ionized in each discharge, and dissociate when they reach the cathode wall. It seems necessary, therefore, to accept an upper limit of about 10^{10} counts for the maximum life of a self-quenching Geiger counter containing polyatomic molecules. A simple demonstration of the breakdown of the polyatomic constituent is obtained by attaching a sensitive manometer to a counter tube under life test. The increase in total pressure contributed by the partial pressures of the end products of the discharge is readily observed. It is now believed that the aging may generally be attributed to a combination of two processes: (1) an alteration in the optimum gas composition resulting from decomposition of the quenching vapor, and (2) the deposition on the electrodes of polymerization products manufactured as a result of the discharge. The former process is sufficient to account for most of the deterioration of ethyl alcohol and ethyl acetate fillings. The latter process has been identified with the short-lived performance of methane fillings.

The primary decomposition products[31] are neutral radicals and fragment ions. Mass-spectrometer research in recent years has revealed an abundance of fragment ions formed in electron bombardment of complex molecules, compared to the number of ions of the parent molecules. In some molecules, such as tetramethyllead,[18] the parent ion is not observed at all. Some of the dissociated fragments may combine to form other organic molecules, which may or may not be quenching molecules. It may be reasoned that, starting with a large molecule, a relatively greater portion of the products of the discharge may again have quenching properties. This seems to be generally true. The lifetime of a counter using amyl acetate, for example, is about ten times as long as that obtained with ethyl-alcohol admixture. Eventually, all the larger molecules must be broken down into the lighter fractions, including nonself-quenching gases such as hydrogen and oxygen.

In the case of methane, tubes are found to fail at between 10^7 and 10^8 counts, which is insufficient to account for decomposition of enough of the original admixture to spoil the tube. It has been shown[32] that the decomposition of methane yields hydrogen along with saturated and unsaturated hydrocarbons, and a deposit on the cathode cylinder which can be identified as a polymerization product formed from the unsaturated hydrocarbons. This polymerization process is known to occur quite readily in an electrical discharge at the surface of a metal electrode. The failure of counters using propane and butane also appears to be tracable largely to the deposition of dielectric polymers on the cathode surface. Such tubes cannot be restored to operation by refilling with a fresh gas mixture, unless the electrodes are washed with a solvent capable of removing the deposits.

[31] S. S. Friedland, "On the life of self-quenching counters," *Phys. Rev.*, vol. 74, pp. 898–901; October 15, 1948.

Short Time Delays in the Firing of Geiger Counters

Coincidence counting is one of the most powerful tools available for the analysis of nuclear-disintegration schemes and cosmic-ray phenomena. In all cases, it is advantageous to reduce the coincidence resolving time to as short an interval as possible, if merely to reduce the number of accidental coincidences which statistically occur in direct proportion to the resolving time. In determining the decay scheme of a nucleus which undergoes a series of radioactive transitions in rapid succession, observations of delayed coincidences can reveal the time relationships in the chain of nuclear radiations. If two transitions follow each other in less than 10^{-8} second, it is experimentally impossible to distinguish the spacing between them with Geiger counters. If, however, the second transition in a sequence follows the first after an average time interval greater than 10^{-8} second, it becomes possible to detect the deviation from simultaneity by delaying the count produced by the first transition long enough to bring it into coincidence with the second. To apply this type of measurement to timing events separated by as little as tenths of a microsecond requires experimental resolution times of a few hundredths of a microsecond. In attempting to decrease the resolving time much below a microsecond, however, many experimenters found inherent uncertainties in the firing times of counters of the order of a tenth of a microsecond,[33] which were entirely distinct from the occasional longer delays of 10 to 100 microseconds resulting from electron attachment to form negative ions.

[32] E. C. Farmer and S. C. Brown, "A study of the deterioration of methane-filled Geiger-Mueller counters," *Phys. Rev.*, vol. 74, pp. 902–905; October 15, 1948.

[33] C. W. Sherwin, "Short time delays in Geiger counters," *Rev. Sci. Instr.*, vol. 19, pp. 111–116; February, 1948.

The maximum resolution achieved with any coincidence arrangement using a pair of Geiger counters depends on the rate of growth of the pulse in each counter following the passage of the ionizing photon or particle. Experimentally, it is observed that, even when a pair of counters of average dimensions are fired by the same high-speed particle, there occurs a relative randomness in firing times with an average difference of as much as 0.2 microsecond. Short time delays in firing of a counter may be attributed to two sources: (1) the electron-transit time in the avalanche; (2) the time required to develop the initial part of the ion sheath after the first electron avalanche reaches the wire. The former delay arising from electron-transit time is essentially independent of overvoltage, whereas the latter delay, involving growth of the ion sheath, decreases with increasing overvoltage. As was mentioned earlier, the elementary process of avalanche production, beginning at a distance of a few wire diameters from the anode, requires about 10^{-9} second. The collection time for the triggering electron and single Townsend avalanche which it creates, will obviously depend on the radial distance at which the primary electron is produced. To compute this time it is necessary to know the velocity of the electron at all distances from the wire. However, since an electron starting at the cathode must traverse the first half of the radial distance to the wire at nearly thermal velocities, its motion in the outer $r/2$ portion of its path counts for almost all of the collection time. The average energy acquired per mean free path over the first half radius from the cathode is about 1/4 ev., which corresponds to an average velocity of about 3×10^{7} cm/sec. The maximum possible transit time in a tube of one centimeter radius will therefore be somewhat greater than 3×10^{-8} second.[34] For an electron starting at intermediate radial distances, the transit time is roughly proportional to the square of the distance. In counters of larger diameters, transit times can, therefore, reach values in excess of a microsecond. Measurements[35] on a tube 7 cm in diameter revealed transit time delays of 0.3 to 2 microseconds.

The portion of the delay attributable to the rate of growth of the ion sheath depends on the sensitivity of the detector amplifier, the position along the length of the tube at which the sheath starts to develop, and the overvoltage. During the first tenth of a microsecond required for the sheath to spread a distance of a few millimeters, the rate of rise of the pulse on the wire may be less than one volt per tenth of a microsecond. Obviously, a wide-band, high-sensitivity amplifier would be required to detect the pulse within this time interval. The rate of rise increases rapidly after the first 10^{-7} second, depending somewhat on whether the counter is triggered at the center or near one end. At the center, the discharge may spread in both directions; whereas, at either end of the tube, the discharge can propagate only in the direction of the opposite end. The slope of the pulse during the spread of the discharge is roughly twice as steep in the former case. The behavior with change in overvoltage is also readily understandable, since the discharge is matured by photon emission and absorption, and the abundance of photons per avalanche increases with higher overvoltage.

It is clearly indicated, then, what steps may be taken to achieve the fastest possible coincidence resolving times. The smallest diameters and lowest filling pressures consistent with other experimental requirements should be selected to minimize transit time fluctuations. A sensitive wide-band amplifier and operation at high overvoltage will make it possible to detect the pulse in the earliest stage of its growth. Resolving times as low as 0.035 microsecond without coincidence losses due to random time delays were obtained in experiments by Mandeville and Scherb,[36] with argon-ethyl ether fillings and a fast coincidence circuit.

Cosmic-Ray Efficiency

In the majority of Geiger-counter-tube types, it may be safely assumed that a single ion pair formed anywhere within the volume of the Geiger counter will trigger a discharge. In detecting the passage of an ionizing particle, such as a cosmic-ray meson, the efficiency can ordinarily be made greater than 99.5 per cent by selecting a heavy gas and filling to a relatively high pressure. The rare gases, except for helium, yield many ions per centimeter of path when traversed by a high-speed cosmic-ray particle. The values of the specific ionization (ions per cm per atmosphere) in neon, argon, and xenon are 12, 29, and 44, respectively, but the values for helium and hydrogen are no greater than about 6. Since the number of ions produced per centimeter of path fluctuates statistically, there is always a chance that the particle may traverse the counter without producing an ion pair. The average number of electrons N left behind by a meson if it traverses a path length d in the counter is npd, where n is the specific ionization, and p is the fraction of atmospheric pressure. The probability of not producing an electron is, therefore, e^{-N} and the efficiency ϵ is given by

$$\epsilon = 1 - e^{-N}. \qquad (4)$$

For example, when the gas in the counter is argon at 1/10 atmospheric pressure, and the track length through the tube is 2 cm, 6 ions per meson are produced, on the average, and the efficiency is 99.8 per cent. If, now, the particle penetrates the counter close to the wall, traversing about 1/6 centimeter, N becomes equal to 1, and the efficiency is only 63 per cent. In the same way, one finds that the efficiency for small counters and for counters filled with hydrogen or helium is considerably lower. For 90 per cent efficiency in a 2-cm path, it is necessary to use about 15 cm Hg pressure of hydrogen or helium, as compared to 3 of argon.

In certain cosmic-ray experiments, low efficiencies are deliberately sought so as to distinguish, for example, between heavily ionizing mesons and electrons. Counters are prepared for such experiments by filling with a lower pressure of hydrogen or with three or four centimeters of helium, to which is added the minimum amount of a light polyatomic vapor sufficient to produce a self-quenching counter with a usable plateau.

There is another type of inefficiency associated with electron attachment which was first demonstrated[37] in studies of coincidence counting, with cosmic-ray telescope arrangements. In the region near the cathode, the combined effects of low field strength and production of relatively few ion pairs makes electron capture to form negative ions sufficiently probable to have a marked effect on efficiency. The heavy negative ions drift slowly into the high-field region, where the negative charge may detach and initiate a delayed discharge, or the ion may retain its charge and not produce an avalanche at all. By varying the resolving time[38] of the coincidence circuit used with an oxygen-filled counter from 0.2 to 70 microseconds, the efficiency of coincidence counting was altered from 50 to 80 per cent. When the oxygen was diluted to 6 per cent of an oxygen-argon mixture, the efficiency remained about 96 per cent from 0.2 to 600 microseconds. The portion of the inefficiency which disappeared with increasing resolving time represented delayed counts originating from negative ions which gave up their electrons near the wire from 10 to 100 microseconds after their attachment. The inefficiency which is unaffected by resolving time represents the fraction of primary ionizing events which do not mature into counts. Although this inefficiency is only barely detectable in argon plus 6 per cent oxygen, it is very pronounced in tubes containing admixtures of the halogens, halogenated hydro-

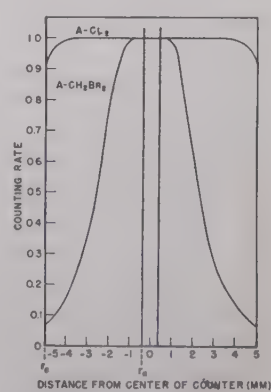

Fig. 13—Variation of counting rate with radial distance from the anode. The counter tube was scanned with a fine pencil of X-rays traveling parallel to the anode. (After Friedman and Birks, in footnote reference 39.)

[34] S. A. Korff, "On the rise of the wire potential in counters," *Phys. Rev.*, vol. 72, pp. 477–481; September, 1947.
[35] H. Den Hartog, F. A. Muller, and N. F. Verster, "Time lags in Geiger-Muller counters," *Physica*, vol. 13, pp. 251–264; May, 1947.
[36] C. E. Mandeville and M. V. Scherb, "Disintegration schemes and the coincidence method," *Nucleonics*, vol. 3, pp. 2–12; October, 1948.
[37] J. C. Street and R. H. Woodward, "Counter calibration and cosmic ray intensity," *Phys. Rev.*, vol. 46, pp. 1029–1034; December, 1934.
[38] M. E. Rose and W. E. Ramsey, "On time lags in coincident discharges of Geiger-Muller counters, *Phys. Rev.*, vol. 59, pp. 616–617; April, 1941.

rbons, ammonia, or sulphur dioxide. Fig. 3 shows the response to a collimated beam X-rays passing axially down an end-indow counter tube at various radial stances from the cathode.[39] With a filling argon plus methylene-bromide admixture, ie efficiency decreased from close to 100 er cent near the wire, to only a few per nt at the cathode. Exposed to cosmic rays is tube showed an over-all efficiency of out 15 per cent. Corresponding measure-ents are shown for chlorine and argon.

Soft X-ray Counters

A counter tube for detection of soft X-ys can be designed so as to produce a unt for virtually every quantum which ters the tube. In early work with X-ray unters, relatively low pressures of filling ses were used, and ionization of the gas ayed a minor role in triggering the count-s. The X-ray beam was usually directed at ie cathode cylinder, and released photo-ectrons which initiated the counts. The -ray photoelectric yield of any element aches a maximum on the short-wavelength de of its X-ray critical-absorption limit. or wavelengths longer than those associ-ed with the critical absorption, the ab-rber is relatively transparent, yielding w photoelectrons. By selecting for the thode a material whose K absorption limit ll at a slightly longer wavelength than the diation being measured, it was possible to tect about 15 per cent of the quanta hich struck the cathode,[40] as in the the se of a zirconium cathode used to measure rays generated at 30 kev ($\lambda_{max}=0.6$ Å).

The form of counter tube best suited to e measurement of soft X-ray beams is the d-window type, filled with a gas capable of sorbing a large fraction of the radiation lmitted in the direction of the axis of the be. The absorption of X rays of wave-ngths softer than 0.5 Å is almost entirely photoelectric process in heavy gases such argon, krypton, and xenon. It is, there-re, permissible to assume that the per-ntage of an X-ray beam absorbed in the unter-tube gas represents the quantum unting efficiency, provided that each ected photoelectron triggers a discharge. argon is the vehicular gas, it strongly sorbs the K-series radiations of elements to about Zn (30). Krypton (36) whose itical X-ray absorption falls at 0.9 Å, is efficient absorber of wavelengths shorter an this limit, and also matches the ab-rption in argon at the longer wavelengths. enon (54) absorbs strongly throughout this tire region of the spectrum. Fig. 14 illus-ates the absorption characteristics of these ree gases in the wavelength range from 4 to 2.4 Å.[39] It is apparent that efficiencies proaching 100 per cent are attainable er a large portion of this spectral range, if e proper gas is used at sufficiently high essure or if a long-enough gas path is pro-ded to absorb the X-ray beam.

The most transparent, yet vacuum-ght, windows for X-ray counters are in-

[39] H. Friedman and L. S. Birks, "Geiger counter ectrometer for X-ray fluorescence analysis," *Rev. i. Instr.*, vol. 19, pp. 323–331; May, 1948.
[40] H. M. Sullivan "Quantum efficiency of Geiger-üller counters for X-ray intensity measurements," *v. Sci. Instr.*, vol. 11, pp. 356–362; November, 1940.

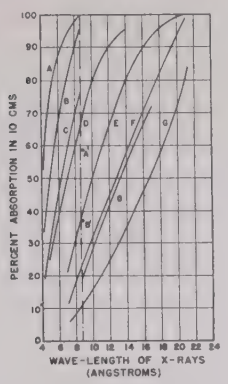

Fig. 14—Absorption of soft X rays in 10 centimeters of the rare gases at various pressures. A—krypton, 76 cm Hg; B—krypton, 40 cm Hg; C—krypton, 20 cm Hg; D—xenon 20 cm Hg; E—argon, 76 cm Hg; F—argon, 40 cm Hg; G—argon, 20 cm Hg; A′—continuation of A; B′—continuation of B. (See footnote reference 39.)

blown glass bubbles, mica, beryllium, and Lindemann glass (consisting mainly of lithium tetraborate). Glass-bubble windows of thicknesses between 0.5 mg/cm² and 1.0 mg/cm², with apertures 2 centimeters in diameter, are strong enough to support atmospheric pressure on the concave side and still transmit, 1,000 ev X rays. Table II indicates the X-ray transparencies of mica, beryllium, and Lindemann glass at a few wavelengths in the soft X-ray region.

TABLE II

Window	Transmission (per cent) CrK_α (2.27 Å)	FeK_α (1.94 Å)	CuK_α (1.54 Å)
0.020 inch Lindemann	4.5	14	38
0.010 inch Lindemann	22	37	61
0.001 inch Aluminum	37	53	71
0.001 inch Mica	40	56	74
0.0005 inch Mica	64	75	86
0.020 inch Beryllium	65	76	86

At MoK_α (0.74Å) all the windows listed above transmit in excess of 90 per cent of the X rays.

Typical tube constructions are illustrated in Fig. 15. With glass or mica windows, the active counting region can be brought up close to the window. Beryllium, and aluminum windows are highly transparent, but introduce the difficulty of insulating the window from the cathode, or

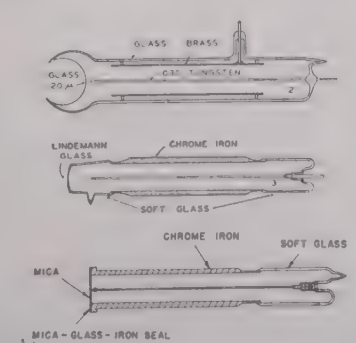

Fig. 15—End-window constructions for soft X-ray counters.

retracting the anode to eliminate discharging to the window. The resultant dead space immediately behind the window somewhat reduces the efficiency of the counter.

A beryllium window is particularly useful when it is necessary to measure soft X rays in the presence of beta rays. For example, 5-year Fe^{55} decays by K-electron capture into Mn^{55}, which then emits 5.9 kev X rays. Fe^{59} has a 47-day half life, and emits beta rays with a maximum energy of 0.46 Mev and hard gamma rays. An argon counter with a beryllium window, 0.4 mm thick, detects about 50 per cent of the soft X rays of Fe^{55} but less than 2 per cent of the Fe^{59} betas. The ratio of sensitivities can then be inverted by using a thin mica window and helium, which will respond to every beta particle entering the tube, but cannot absorb the X rays.

Gamma-Ray Counters

As the frequency of the electromagnetic radiation increases beyond the soft X-ray region, the photoelectric absorption in the gas assumes an insignificant role. Most gases used in counter tubes do not appreciably absorb photons whose energies exceed 60,000 or 70,000 electron volts, and direct ionization of the gas is negligibly small. Hard X rays or gamma rays are detected by virtue of the ionization of the counter gas by secondary photoelectrons, Compton recoil electrons, and electron-positron pairs produced within the cathode material. For the lighter elements and higher frequencies of gamma rays, the absorption is almost entirely the result of Compton scattering. At the other extreme of higher atomic numbers and softer radiation, photoelectric absorption becomes most important. Electron-positron pairs do not appear below 1.02 Mev, the sum of the mass energies of the two particles. The cross section for pair production increases slowly with the excess of energy above this threshold, and is proportional to atomic number. The photoelectric absorption coefficient is approximately proportional to the cube of the atomic number, and decreases rapidly with increasing frequency. At 1 Mev, the photoelectric absorption coefficient in copper is already reduced to roughly 2 per cent of the Compton scattering coefficient. In the very heavy elements, however, the photoelectric effect remains relatively important up to much higher energies. At 2.6 Mev, the photo-effect in lead is still about 15 per cent of the Compton scattering. Pair production becomes comparable to Compton effect at much higher energies. In lead, gamma rays of 5 Mev produce about one positron for every three Compton recoil electrons. The same ratio is reached in copper at closer to 10 Mev, and in aluminum at about 15 Mev. The combined effect of all three processes contributing secondary electrons is to make the counting efficiency roughly proportional to gamma-ray energy, if the counter is constructed of a light element such as copper. Cathodes of heavier elements—lead, bismuth, or gold—raise the efficiencies to a pronounced degree at both the low and high energy extremes.

In many nuclear experiments, such as the determination of reaction yields, it is necessary to know the absolute counting

efficiency at particular wavelengths. In order to compute what percentage of gamma-ray quanta of a given energy incident on a Geiger counter will trigger counts, it is essential to understand how the number of secondaries injected into the gas of the counter depends upon the thickness and material of the cathode. If, for example, the thickness of the cathode wall is much less than the range of the secondaries, almost all the secondaries will enter the gas and produce counts; but, by the same token, the fraction of the primary beam converted to secondaries will be small. On the other hand, when the thickness is much greater than the range of the secondaries, the absorption of primary radiation may be relatively great, but the secondaries produced at depths from the inner wall surface greater than the maximum recoil-electron range cannot emerge to contribute counts. This behavior is illustrated in Fig. 16, computed for 2-Mev gamma rays entering aluminum. An optimum thickness exists which produces the maximum number of secondaries per primary quantum. This thickness is of the order of the maximum range of the secondaries in the cathode material.

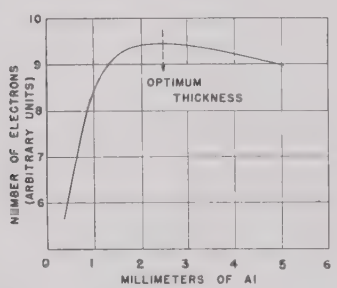

Fig. 16—Ratio of secondary electrons to primary gamma rays (2 Mev) emerging from aluminum absorbers of different thicknesses.

The Compton electrons exhibit a roughly exponential absorption as a consequence of multiple scattering and the dependence of recoil energy on angle. Let an absorption coefficient μ_2 be assigned to the recoil electrons, and let μ_1 represent the linear absorption coefficient for gamma rays. It then can be shown that, for cathode thicknesses equal to or greater than the optimum, the ratio R of the number of secondaries emerging from the cathode to the number of primary quanta transmitted is, approximately,

$$R = \frac{\mu_1}{\mu_2 + \mu_1}. \qquad (5)$$

This ratio is very nearly the efficiency of the counter. For example, a 2-Mev gamma ray, whose absorption coefficient in Al is about 0.12, produces Compton recoil electrons having an absorption coefficient of about 20. The efficiency according to (5), should be about 0.6 per cent. At 1.0 Mev, μ_1 is 0.17, and μ_2 about 55, which should reduce the efficiency to about 0.3 per cent. It is approximately true for lighter elements, such as Al and Cu, that the efficiency in the gamma-ray region from 0.2 to 3 Mev is proportional to the energy, and increases at the rate of about 1 per cent per Mev.

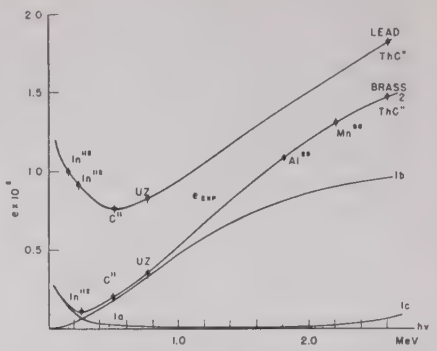

Fig. 17—Efficiencies of gamma-ray counters with brass or lead cathodes in the spectral range from 0.1 to 2.6 Mev. Curves 1(a), 1(b), and 1(c) are the theoretical contributions from photoelectric effect, Compton scattering and pair production in brass. Curve 2 for brass and that for lead are experimental. (See H. Bradt *et al.*, footnote reference 44.)

The wavelength dependence of the contributions to counting efficiency[41] for each of the three absorption processes is shown in Fig. 17 for a copper cathode. The major contribution to the efficiency comes from Compton scattering. When the cathode is made of a heavier element, the efficiency is higher because of the more important contributions from photoelectric absorption and pair production. Fig. 17 also shows the total efficiency curve for lead. Since the Compton effect is independent of atomic number, the difference between the Pb and Cu curves represents the enhanced photoelectric contribution at lower frequencies and pair production at higher frequencies.

Considerable numbers of Geiger-counter survey instruments are being used to monitor radioactive contaminations in atomic-energy activities and X-ray laboratories, and in many cases the meter readings are calibrated in roentgens. It is interesting to apply some of the above data on efficiency to the problem of the ratio of counting rate to roentgen dose at various wavelengths. If, for example, the counting rate per milliroentgen per hour is assumed to be 100 cps at 1 Mev, then a copper-cathode counter will deliver about 135 cps and a lead counter 106 cps at 2 Mev, for the same dose rate. This ratio of counts to roentgens has a minimum somewhere between 0.1 and 05. Mev. On the low-frequency side of the minimum, the counting rate and roentgen dosage rate diverge widely.

Several years ago, Trost[42] attempted to apply counters to roentgen dose measurements under 0.5 Mev in connection with stray radiation from X-ray apparatus. Using a typical metal-in-glass counter tube, he found it possible to keep the ratio of counts to roentgens constant within ±12 per cent between 60 and 120 kv. When a filter combination consisting of 1 mm of tin plus mm of brass was interposed between th source and the tube, the curve of count versus roentgens was flat to ±10 per cen from 120 to 300 kv. To include the very sof radiation under 60 kv, he constructed a tub with a plexiglass wall, 1 mm thick, an operated it slightly below Geiger threshol in the region of limited proportionality. Fo energies in excess of 35 kev, the current de livered by this tube paralleled an "air wall ionization-chamber response within ±1 per cent. These results are illustrated i Fig. 18 reproduced from the literature.[43]

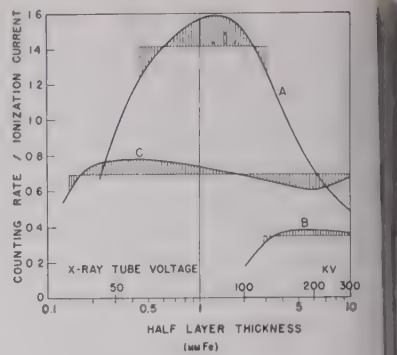

Fig. 18—Ratio of ionization-chamber cu rent to output of a Geiger counter: (A Unfiltered; (B) filtered; and a propo tional counter (C) made of plexiglas (See Trost, footnote reference 42.)

Methods of Improving the Gamma-Ray Efficiency

Any construction which increases the are of cathode surface per unit volume of the counter will increase the number of secondary electrons injected into the gas, and thereby increase the efficiency. The exposed inner surface of a cylindrical cathode may be increased by a factor of $\sqrt{2}$ over that of a smooth surface by cutting 45-degree threads on the inside or by a factor of $\pi/2$ by employing a closely wound helix of 16- or 20-gauge wire as the cathode. The greatest advantage was gained by the substitution of a wire-mesh screen for the solid-wall cathode.[43] The optimum mesh was found to be about 100 wires per inch, and gave about a 50 per cent improvement in efficiency over a smooth-walled cathode of similar material. Part of this gain was attributed to the ability of the electric field to penetrate the apertures in the mesh and draw in electrons formed on the outside.

Bundling large numbers of smaller-diameter tubes within the volume of a single large tube is another simple method of increasing efficiency, particularly when dealing with a collimated beam of radiation. Since perhaps 99 per cent of the gamma-ray beam is transmitted through the walls of the first cylinder, the second cylinder in the path of the rays has almost as much chance of producing a count as the first. Ten

[41] H. Bradt, P. C. Gugelot, O. Huber, H. Medicus, P. Preiswerk, and P. Scherrer, "Sensitivity of counter tubes with lead, brass, and aluminum cathodes for gamma rays in the energy interval 0.1 Mev-3Mev," *Helv. Phys. Acta*, vol. 19, pp. 77–90; Sec. II, 1946.

[42] A. Trost, "Application of counter tubes to nondestructive testing," VDI—*Zeitschrif*, vol. 85, pp. 829–833; October, 1941.

[43] R. D. Evans, and R. A. Mugele, "Increased gamma ray sensitivity of tube counters and the measurement of the thorium content of ordinary materials," *Rev. Sci. Instr.*, vol. 7, pp. 441–449; December 1936.

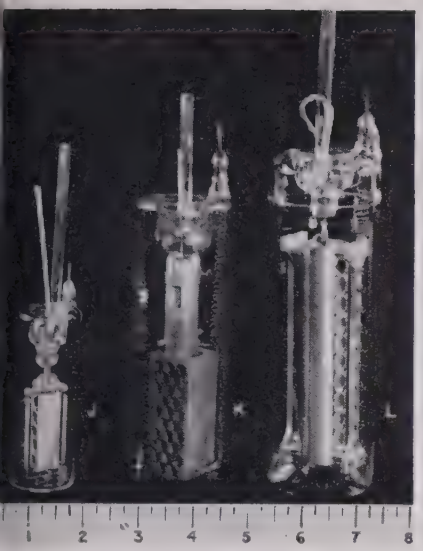

ig. 19—Multiple counter tubes in parallel combinations.

ounter cylinders in line may, therefore, ield about nine times as many counts as a ngle counter placed in the path of a parallel undle of rays. The counters shown in Fig. 9 were intended for use in this way. If, owever, a number of smaller-diameter ylinders are bundled in place of a single rge tube of comparable over-all dimenons, the gain in efficiency for detection of n isotropic flux of radiation is not very reat unless a very large number of tubes is sed. The relative efficiencies of the bundle tubes and the equivalent simple tube are iven by the ratio of the sum of the dimeters of the individual tubes to the iameter of the simple large tube. For a undle of seven tubes, the ratio is 7/3; for ineteen tubes, the improvement in effiency is only 19/7.

Perhaps the most successful multi-eleent tubes designed to increase efficiency ere described by Hare in a series of patnts[44] filed in 1941–1943. It is not necessary retain the coaxial-cylinder arrangement order to obtain a Geiger-counting plaau. Because of the concentration of the eld near the wire, the plateau is relatively sensitive to the shape of the cathode. For xample, a plane electrode may be substiuted for the cathode cylinder (Fig. 20(a)). his configuration may be expanded in ne dimension, as shown in Fig. 20(b), and nally in two dimensions to form a multiicity of both plates and wires, as in Fig. 0(c). The efficiency of such an assembly is pproximately equal to the number of ates, even when as many as ten plates are sed, and does not depend very much on rientation. Theoretically, the limit to the ficiency obtainable with such structures ay approach 30 to 40 per cent. Practical strictions on the number of plates emoyed would be governed by the mechanical nitations on the closest spacings. Hare ated that spacings between plates of 2 illimeters were successfully employed.

[44] U. S. Patent Numbers 2,397,073 and 2,397,071 D. G. C. Hare, 1946.

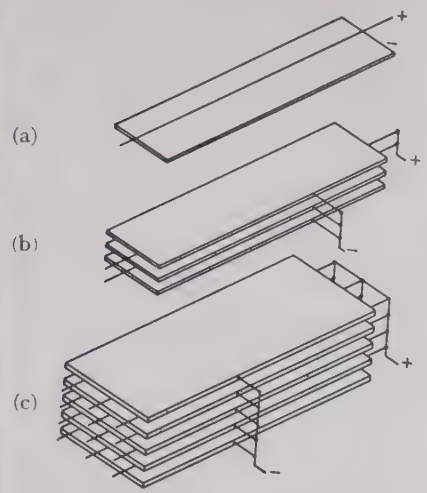

Fig. 20—Multiple plate and wire construction of a gamma-ray counter.

The extent to which the geometry of the counter may deviate from the simple coaxial cylinders, and still retain full volume sensitivity, depends on the nature of the gas in the counter. With the more commonly used "100 per cent efficient" mixtures, such as argon-alcohol, a considerable assymetry is tolerable. However, with halogen admixtures, halogenated hydrocarbons, and other electronegative gases, the loss of sensitivity in the weak-field regions near the corners of a box counter of rectangular cross section, for example, would leave most of that part of the counter volume insensitive to radiation. Recently, Curran and Reid[45] investigated the behavior of box-shaped cathodes with various numbers of parallel-wire anodes, and determined the effects of assymetries in anode positions relative to cathode walls and of anode spacings relative to each other.

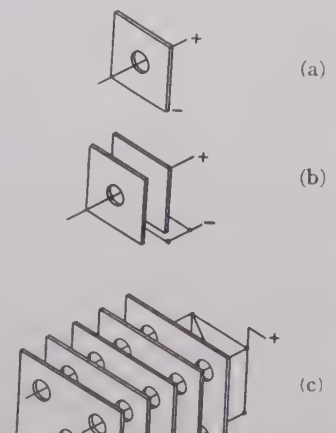

Fig. 21—Perforated disk-type of contruction for a high-sensitivity gamma-ray counter.

[45] S. C. Curran and J. M. Reid, "Properties of some new types of counters," *Rev. Sci. Instr.*, vol. 19, pp. 67–76; February, 1948.

Fig. 22—Photograph of a multiple-disk counter.

Many other arrangements to increase the cathode surface have been suggested. The construction shown in Fig. 21(a) consisting of a wire anode passed perpendicularly through a hole in a plate, will function as a Geiger counter. The sensitive volume of such a configuration extends out considerably farther than the radius of the hole in the neighborhood of the plate. Extending this arrangement, as shown in Figs. 21(b) and (c) and Fig. (22), leads to a structure of stacked disks perforated with holes that are aligned on common cylinder axes. The anode wires are strung axially through the holes. The entire assembly may be compared to a bundle of counters, the effective diameter of each counter being appreciably greater than the hole diameter because of the penetration of the fringing field between the plates. Again, Hare cited the following figures: If the cathode plate was 1 inch in diameter, the hole 5/16 inch, and the plate spacing 0.1 inch, the same number of counts was obtained as with a conventional counter of $1\frac{3}{8}$ inches diameter.

DuMond[46] described a form of multicellular counter in which the cathode structure was a stack of die-cast lead-alloy disks, each disk having a round hole at the center. As shown in Fig. 23, four anode wires are spread out in the form of a spider between each pair of plates, from a common supporting rod extending through the holes in the centers of the disks. This type of tube was used to receive the converging beam of gamma rays from a bent crystal spectrometer designed to measure wavelengths up to 1 Mev. At 0.5 Mev, the counter detected about 8 per cent of the incident quanta.

Another multisection counter, recently described by Beyster and Wiedenbeck,[47] was based upon a simple unit cell, any number of which could be stacked up to produce the

[46] J. W. M. DuMond, "High resolving power, curved-crystal focusing spectrometer for short wavelength X-rays and gamma rays," *Rev. Sci. Instr.*, vol. 18, pp. 626–639; September, 1947.

[47] J. B. Beyster and M. L. Wiedenbeck, "Cell-type gamma counter," *Rev. Sci. Instr.*, vol. 19, p. 819; November, 1948.

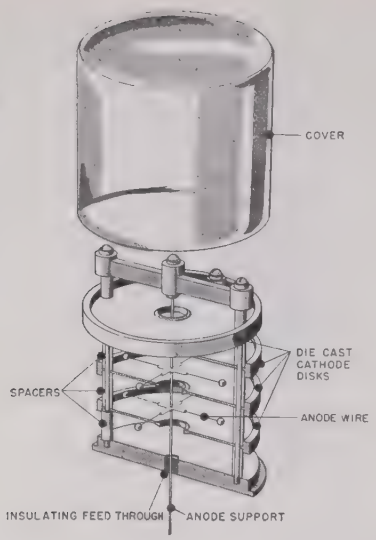

Fig. 23—Multicell gamma-ray counter. (See Du Mond, footnote reference 46.)

desired increase in efficiency. Each cell resembled a flat cylindrical cheesebox, made of brass, 4 inches in diameter and ½ inch deep. The anode was a circular loop of 10-mil wire 2 inches in diameter, supported midway between the two faces of the box by glass-insulated "feed-throughs," waxed into the cylindrical wall of the box.

Beta-Ray Counters

The specific ionization of beta rays is high enough so that any particle traversing the interelectrode space of a Geiger counter is almost certain to trigger a discharge. The major problem in designing a beta-ray counter is, therefore, one of providing a suitable window for the particles to penetrate from outside. Alternatively, a demountable counter tube may be used, which can be assembled with the sample inside the envelope of the tube, and then filled with the counting gas mixture.

The simplest type of beta-ray counter closely resembles the ordinary gamma-ray counter except that the cathode wall and envelope are thinned down to the extreme permitted by requirements of mechanical strength. Most familiar of this type is the thin glass-wall tube, about 30 mg/cm², coated with a thin conductive layer of silver, copper, or colloidal graphite (Fig. 24(c)). Because of the fragility of the thin blown-glass portion, attempts have been made to achieve equivalent transparency in metal-wall tubes. Two such tubes have been offered commercially, one fabricated of aluminum with a 0.005-inch wall, and the other of chrome iron with a 0.002-inch wall. The wall thickness of 30 mg/cm² is generally considered to be the minimum compatible with requirements of mechanical strength and vacuum tightness, so that tubes of the thin-wall type are unsuited for use with the softer beta-ray emitters.

The thin-walled counter has been used extensively to measure the artificially induced activities in foils which could be wrapped around the counter and measured

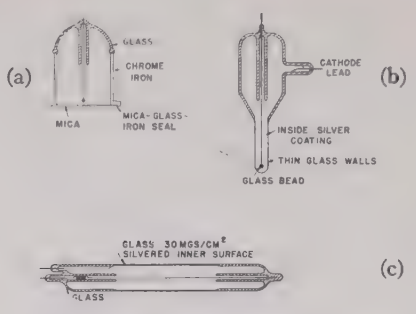

Fig. 24—(a) End-window beta-ray counter. (b) Thin-walled dipping counter. (c) Thin-walled beta counter.

after activation. Larger tubes of the same form are well suited to filter-paper measurements, where again the paper is wrapped around the counter, exposing a relatively large surface to the cylindrical beta-ray window. Fig. 24(b) illustrates an adaptation[48] of the thin-walled tube for the measurement of beta activity in liquids. The thin-walled, thimble-shaped end may be dipped directly into the liquid. In still another arrangement, the thin-walled portion of the tube is surrounded by a jacket with provision for admitting the active liquid into one end of the jacket, circulating it about the thin-walled portion, and finally passing it out the opposite end.

The most popular type of beta-ray counter is the end-window tube intended for use with small, flat disks of radioactive deposits. Mechanically, such a tube is identical with the X-ray counters of Fig. 15, but the length of the cylinder is reduced to the minimum consistent with maintaining a flat plateau (Fig. 24(a)). The dimensions are chosen with the intention of providing the maximum solid angle of collection and the minimum response to gamma rays and cosmic-ray background. Reducing the length of the tube relative to its diameter creates end effects which increase the slope of the plateau and decrease its length. Most tubes compromise at a ratio of length to diameter between 3/2 and 2.

A more effective approach to the problem of increasing window area relative to cathode area is to construct a shallow counter bounded by two plane-parallel cathode surfaces. One of these faces is the mica window, conductively coated on the inner surface. The anode wire is mounted parallel to the plane of the window. An approach to such a construction was implicit in the early type of beta counter shown in Fig. 25. The usual cathode cylinder was replaced by a half cylinder with its concave side open toward a thin window. In the tube illustrated, the window was an aluminum foil mounted on a supporting grid. The half cylinder was later succeeded by a multiplicity of half cylinders (Fig. 26(a)), and finally by a flat plate,[49] producing the shallow box form of counter (Fig. 26(b), (c)), one

[48] W. F. Bale, F. L. Haven, and M. L. LeFevre, "Apparatus for the rapid determination of β-ray activity in solutions," *Rev. Sci. Instr.*, vol. 10, p. 193; June, 1939.

[49] R. Thompson and B. Diven, "The multiple wire proportional counter," MDDC Report 99, declassified, July 30, 1946.

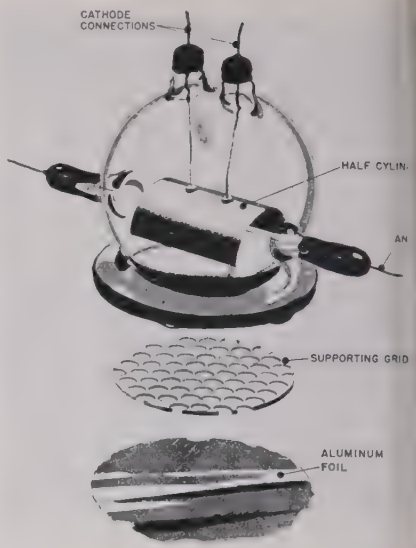

Fig. 25—Beta-ray counter with hemicylindrical cathode.

large face of which was the thin window. On or more anode wires were strung parallel t the cathode planes depending on the widt of the box. Large counters of this type ar widely used as air-proportional counter by laboratories of the Atomic Energy Com mission, with a thin nylon film coated wit colloidal graphite serving both as the win dow and one of the cathode plates.[50] I principle, such an arrangement is well suite to beta-ray counting when a vacuum-tigh window is provided and the counter is fille with a Geiger counting gas.

Another way of accomplishing the sam result was suggested by Beyster and Wieden-

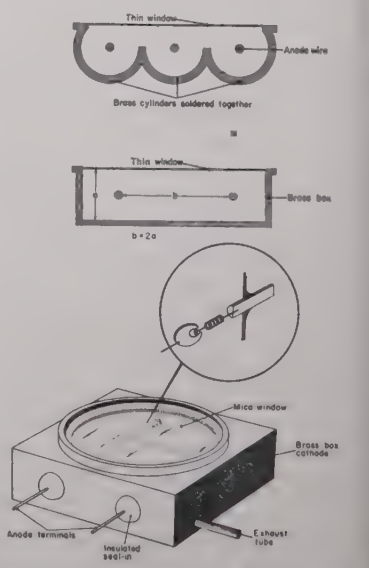

Fig. 26—Development of the flat-box form of beta counter from hemicylindrical cathode structure.

[50] J. A. Simpson, Jr., "Air proportional counters," *Rev. Sci. Instr.*, vol. 19, pp. 733–744; November, 1948.

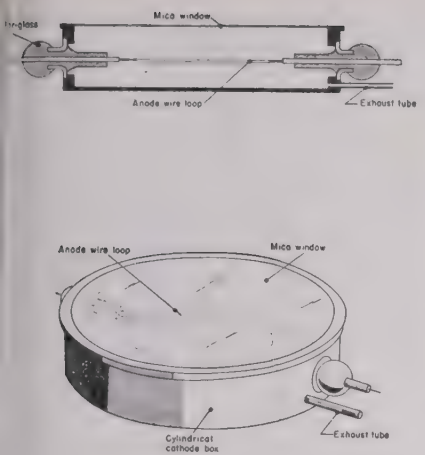

Fig. 27—Low-background beta-ray counter with loop form of anode.

eck[47] in connection with the high-efficiency amma-ray construction described above. Replacing one face of the shallow cylindrical ox with a thin window (Fig. 27) produces a at-box counter with the same counting eometry as the ordinary end-window ounter, but with a minimum of volume and athode surface.

Mica is the most suitable window for eta-ray counters. It can be split in very thin ayers which are strong enough to withtand atmospheric pressure over relatively arge areas. The best grade of material for hin windows is imported from Africa. Perhaps the most notable recent advance in he technique of constructing beta-ray ounters is the use of powdered glass as the ealing medium for joining mica to soft lass or to chrome iron. In the past, mica indows were attached by methods involvng compression seals and lead gaskets, wax oints, or the use of special cements such as elenium. None of these produce satisactory permanent seals, the tightness of the oints being affected by aging, temperature hanges, and reactions between the sealing ompounds and the gas of the counter. The owdered-glass technique employs a fine owder of lead-borosilicate glass which has temperature coefficient of expansion very lose to those of soft glass, chrome iron, and nica. The glass is used as a thick water aste, applied with a brush around the rim f the mica and the seating flange of the lass or chrome-iron-tube body. With the nica window in place, the seal is heated to he fusing point of the glass powder, producng a vacuum-tight, inert, and permanent eal.

A common difficulty with mica windows a tendency to acquire a charge, thereby ntroducing spurious counts and a hysteresis the response of the tube to changes in ntensity. This effect is minimized in tubes lled with gas mixtures containing electroegative components such as the halogens. Ordinarily, it can be eliminated by making he inner surface of the mica slightly conuctive.

One-inch mica windows of 1.5 mg/cm² hickness are supplied in commercial tubes. uch windows are adequate for measurements of S^{35} (167 kev) and C^{14} (145 kev), but are not thin enough for tritium, H^3, whose beta rays have a maximum energy under 15 kev. Extremely thin films of materials such as nitrocellulose, formvar, and evaporated silica can transmit electrons with energies as low as 1,000 or 2,000 electron volts. These films are sufficiently vacuum tight and strong enough, when mounted on a fine supporting grid, that semipermanent fillings can be made, which retain satisfactory counting characteristics for a day or longer.

In working with tritium, it is generally desirable to admit the radioactivity directly into the counter as part of the counting gas.[51] The tritium can be converted to HTO water, which may be introduced into the counting mixture as water vapor at a pressure of 1 or 2 mm Hg without seriously damaging the counting characteristics. Alternatively, tritium gas may be electrolyzed from tritium water and used in the same manner as inactive hydrogen as a counter gas. If C^{14} is carried in CO_2, it may be used as the counting gas[52,53] in combination with CS_2 vapor and the aid of an electronic quenching circuit. About 2 cm Hg of CS_2 is used with anywhere from 10 to 50 cm Hg of CO_2, providing thresholds from about 2,000 to 5,000 volts, depending on the tube dimensions.

The screen-wall counter[54] shown in Fig. 28(b) is illustrative of a demountable type in which the source is placed inside the envelope, so as to eliminate the need for a window. Radioactive material to be measured is coated on the inside of the metal sample cylinder. This cylinder can be made of nickel, so that it may be moved within the tube by means of an external magnet. The active volume of the counter is defined by the wire-mesh cathode in the center of the tube. When the sample holder is in alignment with the screen cylinder, as shown in the figure, the counter presents a large solid angle to the source and accommodates a relatively large area of sample. Background count is determined with the sample cylinder drawn to one end of the tube, out of the sensitive region. Any suitable gas mixture may be used. It is recommended that the tube be operated with "drag-in" voltage between the screen and the sample cylinder or outer wall, so as to sweep out positive ions which drift outside the gauze. The disadvantage of this type of counting is, of course, the need for disassembling the tube every time a sample must be changed, a procedure which may consume about 20 minutes between sample measurements.

An apparatus, known as a "gas-flow" counter[55] which provides for quick sample changes and eliminates the inconvenience

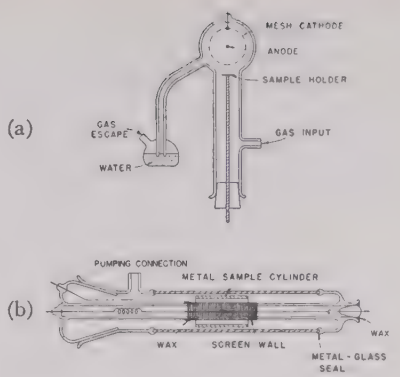

Fig. 28—(a) Demountable windowless beta counters. "Gas flow" beta-ray counter for internal samples.
(b) Demountable beta-ray counter for internal samples.

of disassembling and reassembling the counter tube, and evacuating before refilling, is shown in Fig. 28(a). The sample is brought up close to the mesh cathode through a side tube. Methane, helium, or a mixture of helium and a quenching gas stored in a high pressure tank, is admitted through the input sidearm. The incoming gas flushes the air out of the tube through a bubbling bottle. By maintaining a continuous flow of gas at atmospheric pressure, it is unnecessary to have a perfectly vacuum-tight system. The operating voltages need not exceed 2,500 volts with methane, and are much lower with helium mixtures. The arrangement illustrated in Fig. 28(a) is relatively crude compared to some more recent versions of gas-flow counters which permit the use of larger samples and more efficient geometries.

Size Limitations

There are many problems, particularly in medical physics and in nuclear physics, which call for the use of small-sized probes for gamma- and beta-ray detection. For example, in medical tracer work it may be desirable to determine the location of a radioisotope within the tissue of an animal or human "in vivo." The limitations on the extent to which the dimensions of a Geiger counter may be scaled down have thus far been entirely mechanical. Curtis described[56] what is perhaps the smallest counter yet built. The glass envelope was coated with aquadag on the inner wall to form a cathode cylinder only 0.8 mm inside diameter and a length of 3 mm. The anode was a tungsten wire 0.005 m in diameter. Curtis compared the size of the tube to a number 2 sewing needle, as shown in Fig. 29. The tube was filled with the usual amyl-acetate and argon mixture at 4 cm Hg total pressure, and gave a background count of 20 per hour. Pulse size in such small tubes is comparable to, or greater than, that obtained in larger tubes. Because of the small volume of the tube, it is natural to expect the life to be shorter than in larger tubes, where the number of

[51] R. Cornog and W. F. Libby, "Production of radioactive hydrogen by neutron bombardment of boron and nitrogen," *Phys. Rev.*, vol. 59, pp. 1046; June 15, 1941.
[52] W. F. Libby, "Measurement of radioactive tracers," *Anal. Chem.*, vol. 19, pp. 2–6; January, 1947.
[53] W. W. Miller, "High efficiency counting of long-lived radioactive carbon as CO_2," *Science*, vol. 105, pp. 123–125; January 31, 1947.
[54] W. F. Libby and D. D. Lee, "Energies of the soft beta radiations of rubidium and other bodies. Method for their determination," *Phys. Rev.*, vol. 55, pp. 245–251; February 1, 1939.
[55] S. C. Brown, "Beta ray energy of H^3," *Phys. Rev.*, vol. 59, pp. 954–956; June 15, 1941.
[56] L. F. Curtis, "Miniature Geiger-Müller counter," *Jour. Res. Nat. Bur. Stand.*, vol. 30, pp. 157–158; February, 1943.

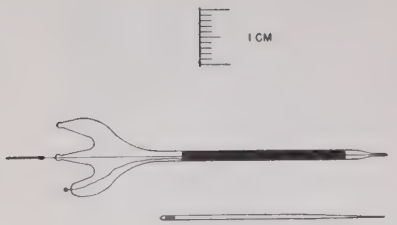

Fig. 29—Miniature Geiger counter. (See Curtiss, footnote reference 55).

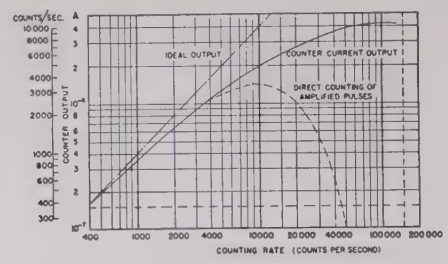

Fig. 30—Counting losses due to dead time. The amplifier responded to pulses as small as half normal amplitude. (See Trost, footnote reference 56.)

molecules dissociated per pulse constitute a smaller percentage of the total number originally present.

At the other extreme, unusually large counters offer no constructional difficulties, but they are inherently slow, have relatively high background rates, and a greater percentage of delayed and spurious counts. To avoid excessively high operating voltages, the anode diameter is ordinarily kept small, while the cathode diameter is increased. The field throughout most of the counter volume is, therefore, relatively weak. As a result, the electron collection time is longer and the positive-ion sheath must cover most of the enlarged distance from wire to cylinder in a weak field, with a consequent increase in the dead time. In the enlarged weak-field part of the counter volume there is also a greater probability for negative ion formation, and delayed counts. Finally, the increased capacitance slows up the recovery of the wire potential and broadens the pulse.

Reduction of Dead Time

Stever's experiments[5] demonstrated the existence of a natural dead time of 10^{-3} to 10^{-4} second. The dead time explained the choking of Geiger counters at rates of a few thousand counts per second, when used with low-sensitivity amplifiers. Trost[57] found that the integrated current flowing through a counter tube increased well beyond the "choking rate," as shown in Fig. 30. The conclusion to be drawn from Trost's experiment was that pulses appeared within the dead time which were reduced in amplitude below the detection level of the amplifier. They were then not counted, but contributed a reduced charge per pulse to the flow of current through the tube. Muehlhouse and Friedman,[58] using a sensitive wide-band amplifier, measured counting rates as high as 100,000 per second in a Geiger tube whose resolving time at low rates appeared to be 10,000 per second. The dead time decreased with counting rate above 10,000 per second in such a manner that a constant 40 per cent of the counts were lost at any rate up to 100,000 counts per second.

Baldinger and Huber[59] recently studied the behavior of counters at rates higher than the "Stever dead time." At very high rates almost all pulses fell into the "recovery period," and the average pulse height became a small fraction of normal. These smaller pulses were followed by shorter dead times. The dependence of dead time on pulse height was linear down to pulses of about one-fifth normal amplitude, which was the range covered by the experiment. Increasing the amplifier sensitivity is, therefore, effective in raising the maximum counting rate, but does not materially improve the resolution at low rates.

Attempts have been made to reduce the dead time by reversing the collecting field immediately after formation of the positive ion sheath so as to return the positive ions to the wire. The recovery time, instead of being governed by the time required for the positive ions to cross the diameter of the counter, would then be reduced to the time required to cover the very small distance from the initial radius of the sheath to the wire. Simpson's[60] original circuit for this purpose applied a high and adjustable negative pulse of a few microseconds duration to the wire. The pulse was derived from a fast one-shot multivibrator, triggered by the amplified initial pulse of the Geiger discharge. Simpson estimated that the improvement in speed of ion collection obtained this way could reduce the dead time by almost a factor of ten.

Other reversing circuits have since been described by Hodson[61] and by Smith[62] but they attributed most of the dead-time reduction which they obtained to limitation of the discharge spread, rather than to positive-ion collection. Before the discharge could propagate the full length of the tube, the wire potential dropped below threshold, bringing the discharge to a stop and leaving the remaining length of the counter still sensitive. Since the rate of spread of the discharge is about 10 centimeters per microsecond, this effect is most readily observed in a long counter. Extremely fast circuitry would be required to limit the discharge spread appreciably in a short counter. Smith estimated that ion collection alone reduced the dead time by only a factor of two, and cautioned against the possibility of interpreting spurious pulses which arise from secondary emission at the wire during the positive ion collection period, as evidence of dead-time reduction.

An effective way to reduce the dead time is to limit the discharge spread along the wire by the use of glass beads. If, for example, the counter wire were divided into two equal lengths by a bead at the center it would behave as two separate counters connected in parallel. The effective dead time of the combination would then be half the dead time of either section alone. Because the positive-ion sheath is only half as long, normal pulse amplitude must, of course, be only half that of the same counter minus the bead on the wire.

Substituting a bundle of small counters for the equivalent volume of a single large counter will increase the resolution by more than simply the number of counters in the bundle, since each counter of the bundle will itself have a shorter dead time than the single large counter. Multi-element structures of the types illustrated in Figs. 19–23 show similar gains in resolving power. The parallel-plate and wire structure is particularly effective, because the small spacing of individual plates in itself produces a short dead time per element. In open structures such as the tube of Fig. 21, only a few per cent of the discharges can spread from one wire to another because of the strong absorption of ultraviolet light in fillings of rare gases in combination with polyatomic quenching admixtures. The effect on resolution is almost equivalent, therefore, to operation of independent counters in parallel. If such a tube is filled with simple gases, or the rare gases with halogen admixtures, the discharges spread throughout the entire structure, and the effect of limiting each discharge to a single wire is lost.

Background Reduction

When measuring weak activities, the ultimate sensitivity of the counting method is controlled by the background count against which the sample activity must be distinguished. This background consists of cosmic radiation, gamma rays from natural radioactivity in the surroundings, and, in many laboratories, stray radiation from near-by accelerators. A rough figure for the cosmic radiation is about 1.5 cosmic rays per minute per square centimeter of horizontal surface at sea level. The larger the background, the more difficult it becomes to detect a small increase in counting rate. For example, if the background is equal to the counting rate being measured, then six times as many counts are needed to achieve a given statistical accuracy compared to the number required in the absence of background. If the ratio of sample count to background is as low as one tenth, then 121 times as many counts are required as in the absence of background. The advantage to be gained by any technique which reduces background is obvious.

In discussing the construction of Geiger counters for beta-ray measurements, consideration was given to designs in which the ratio of sensitive volume to window area was minimized, thereby improving the ratio of beta count to background. It is customary to surround a counter and the sample to be

[57] A. Trost, "A method for measuring high radiation intensities using a counter tube," *Zeit. für Phys.*, vol. 117, pp. 257–264; 1941.

[58] C. O. Muehlhause and H. Friedman, "Measurement of high intensities with the Geiger-Mueller counter," *Rev. Sci. Instr.*, vol. 17, pp. 506–511; November, 1946.

[59] E. Baldinger and P. Huber, "On the resolving power of self-quenching counter tubes at high rates," *Helv. Phys. Acta*, vol. 20, pp. 470–475; November 6, 1947.

[60] J. A. Simpson, "Reduction of the natural insensitive time in Geiger-Mueller counters," *Phys. Rev.*, vol. 66, pp. 39–47; August, 1944.

[61] A. L. Hodson, "Reduction of insensitive time in Geiger-Mueller counters," *Jour. Sci. Instr.*, vol. 25, pp. 11–13; January, 1948.

[62] P. B. Smith, "Dead-time reduction in self-quenching counters," *Rev. Sci. Instr.*, vol. 19, pp. 453–458; July, 1948.

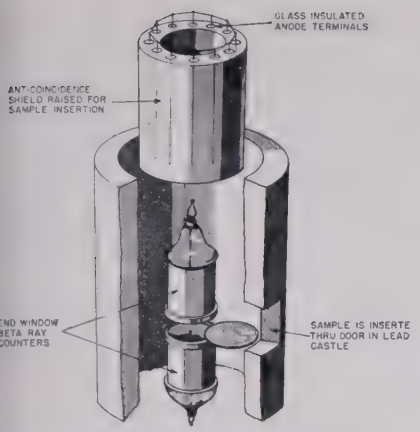

Fig. 31—Schematic arrangement for background reduction.

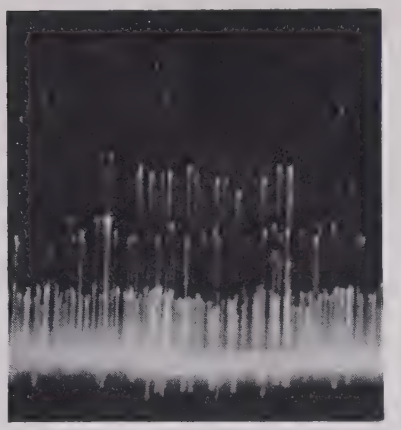

Fig. 32—Variety of pulse amplitudes obtained from tube of Fig. 22.

neasured by a lead shield which effectively eliminates the gamma-ray background, but does not stop the penetrating cosmic-ray particles. However, because the efficiency of cosmic-ray particle detection with Geiger counters is close to 100 per cent, it is a simple matter to screen out the counts due to penetrating cosmic-ray particles by anticoincidence circuitry.

Fig. 31 illustrates an arrangement of high geometry for beta-ray detection combined with an anticoincidence shield. Two end-window beta-ray counters are mounted face to face with a sufficient gap between them to accommodate a flat sample. The sample material may be supported on a thin aluminum foil or plastic film which is capable of transmitting almost all the beta rays emitted by the radioactive atoms in the sample. With a small source, this arrangement collects nearly every particle emitted over the entire solid angle or presents what is ordinarily referred to as a 4π geometry. The circuitry is so arranged that single random firings of the two counters are transmitted to the scaling circuit, but coincident pulses, excited by the passage of the same cosmic-ray particle through both tubes, are rejected. The cosmic ray shield is completed by slipping the anticoincidence guard counter down around the two beta counters. The guard counter as illustrated is equivalent to a cylindrical ring of counters connected in parallel. Any coincidence between this shield counter and either of the two beta counters is rejected by the electronic circuit. The net result achieved by this arrangement for rejecting coincidence counts is to reduce the background, after shielding in lead, by still another factor of five, without loss of beta-ray counts. Fig. 31 illustrates a system employing two conventional end-window counters. It is immediately apparent that shallow counters of the type shown in Figs. 26 and 27 are still better suited to anticoincidence counting. If the depth of each Geiger counter is much less than its window diameter, then it is possible to dispense with the outer cylindrical shield and rely entirely on rejection of coincidences between the two beta-ray counters.

Gamma-ray counters of the multiple-element types illustrated in Figs. 19–23 are well suited to the application of anticoincidence counting. Fig. 32 is a photograph showing the variety of pulse amplitudes observed on an oscilloscope with the counter of Fig. 22 exposed to gamma rays. Since the anodes and cathodes are connected in parallel, coincidence pulses on more than one wire appear with double, triple, quadruple, etc., amplitudes, depending on whether two, three, four, etc., wires are fired by the passage of a single particle. The great majority of the pulses are single counts typical of gamma rays. Occasionally, the Compton electron ejected by a gamma ray traverses the fields of two wires, and a few per cent of the discharges spread from one wire to another, leading to double-amplitude counts. Triple-amplitude pulses from gamma rays are very infrequent. On the other hand, all wires whose sensitive regions are cut by the trajectory of a cosmic-ray particle fire in coincidence. The largest pulses are, therefore, produced by a cosmic-ray particle penetrating the tube along a plane through its axis. If the cosmic ray penetrates fewer elements of the tube, pulses of lesser amplitude result. By selecting the proper pulse-amplitude discrimination level, it is possible to reject pulses above a given level so as to eliminate almost all background from penetrating cosmic rays.

Directional Counters

The production of a preferred directional sensitivity in a gamma-ray counter, without the benefit of external shielding by means of lead or other high density absorbers, is rather difficult to achieve in any high degree. Since the efficiency of counting depends on the material of the cathode wall, its thickness, and distribution in the path of the beam, it is possible to construct a tube so as to present a higher counting efficiency to a source in one direction than in others. Also, since gamma rays are detected mainly by virtue of the ejected Compton electrons, which have a predominantly forward distribution, a tube that is responsive to electrons moving in a particular direction should, therefore, be directional in response to the primary gamma rays.

Rajewski[63] described a bimetallic cathode for a gamma-ray counter consisting of two hemicylinders of lead and aluminum. Because of the different efficiencies of the two metals, the counting rate for rays entering lead and leaving aluminum was greater than for rays traveling in the reverse direction. Craggs and his coworkers[64] recently determined the contrast in sensitivity obtainable by such tubes with the aid of a parallel-plate and wire form of counter. Diametrically opposed windows were cut in the glass envelope of the tube at positions orthogonal to the planes of the plates. These windows were covered with aluminum foil 0.002 inch thick. The response of this counter to a collimated beam of gamma rays was 32 per cent lower when the beam passed through the windows than when it was directed perpendicularly to the surfaces of the plates. This experiment indicates the extreme of contrast obtainable in a bimetallic form of directional counter.

The experiments of Stever showed that it was possible to localize the discharge in a Geiger counter by placing glass beads on the anode wire. If the beads were opaque to ultraviolet light, the spreading of the discharge by photoelectric effect in the gas was blocked at the bead. Stever suggested the use of the beaded-wire counter as a directional detector of energetic particles. For example, if the wire were partitioned into three sections by glass beads, a particle traversing the tube in a direction normal to the axis would fire only one section, whereas a particle traversing the counter parallel to the axis would fire all three sections. Since the pulse amplitude developed by the counter is proportional to the length of the discharge along the wire, a circuit which discriminates against smaller pulses arising from the firing of one or two sections rather than all three will register only those counts arising from the triggering of all three sections by a primary particle traveling essentially parallel to the axis of the counter.

Since high-energy gamma rays produce a distribution of recoil electrons with a maximum in the forward direction, a Stever type of beaded-wire counter should have directional properties for gamma-ray detection. However, because of the angular distribution of recoil electrons, the directionality of response is not very pronounced, and the counting rate is corresponding low.

The most satisfactory arrangements for obtaining directional sensitivity with gamma counters are those which simply employ shielding with lead or other high-density absorbers. When the gamma rays are emitted from a point source, it is advantageous to use two counters separated by a lead barrier and coupled to a differential-counting-rate meter.

Photon Counters

The photon counter combines the principle of the photocell with the amplification mechanism of the G-M counter. Rajewski[65] and Locher[66] described the behavior of such

[63] B. Rajewsky, "The use of the Geiger-Mueller counter in mining," *Zeit. für Phys.*, vol. 120, pp. 627–638; March, 1943.

[64] J. D. Craggs, P. W. Bosley, and A. A. Jaffe, "Some experiments with Geiger-Mueller counters," *Jour. Sci. Instr.*, vol. 25, pp. 67–71; March, 1948.

[65] B. Rajewsky, "On the sensitivity of photon counters," *Phys. Zeit.*, vol. 32, pp. 121–124; February, 1931.

[66] G. L. Locher, "Photoelectric quantum counters for visible and ultraviolet light," part I, *Phys. Rev.*, vol. 43, pp. 525–546; November 15, 1932.

tubes in 1931. Much of the work since then has been confined to ultraviolet counters operating in the region below 3,000 Å, although Locher achieved considerable success in the preparation of blue-sensitive (threshold, 4,000 Å) tubes. So little effort appears to have been expended on the production of photon counters with long-wavelength sensitivities that it is difficult to evaluate their possibilities. Of all detectors, the photon counter has inherently the maximum sensitivity for measuring the photocurrent; i.e., it counts every photoelectron. To date, however, it has not been possible to duplicate in gas-filled tubes the quantum yields obtained with photo surfaces in vacuum in the spectral range from 3,000 to 5,000 Å. Surfaces that are highly photosensitive in vacuo when exposed to visible light are invariably poisoned and desensitized by contact with the gas in a counter. At shorter wavelengths in the ultraviolet, however, quantum efficiencies between 10^{-4} and 10^{-3} counts per quantum are commonly obtained[67] in photon counters. These yields are comparable to those observed for most photosurfaces in vacuum in that region of the spectrum.

[67] O. S. Duffendack and W. E. Morriss, "An investigation of the properties and applications of the Geiger-Mueller photoelectron counter," *Jour. Opt. Soc. Amer.*, vol. 32, pp. 8–24; January, 1942.

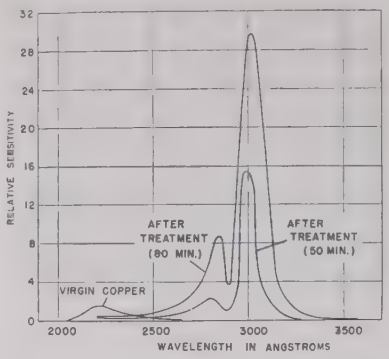

Fig. 33—Ultraviolet sensitivity of activated photon counter tube. (See Scherb, footnote reference 58.)

Locher described many surface coatings and treatments which produced enhanced quantum yields in photon counters operating in the blue and ultraviolet portions of the spectrum. Since Locher's experiments, very little has been published on photon counters. More recently, Scherb[68] described unusual spectral sensitivities obtained by glow-discharging an argon-butane-filled copper-cathode counter at liquid-air temperature. Fig. 33 illustrates the results of this treatment which produced a peak at about 3,000 Å with a quantum yield about 15 times as great as that of the untreated copper surface between 2,000 and 2,500 Å. It seems reasonable to expect that many similar improvements would develop out of research on photon counters if an effort were made to continue such investigations. There are interesting possibilities for the application of such tubes to spectroscopic instruments and in connection with scintillation counting.

[68] M. V. Scherb, "Photoelectric effect in self-quenching Geiger-Mueller counters," *Phys. Rev.*, vol. 73, pp. 86–87; January 1, 1948.

Conclusion

The writer has limited the contents of this paper to a discussion of Geiger-counter tubes for the detection of cosmic rays, X rays, gamma rays, beta particles, and ultraviolet light. Neutrons, protons, and alpha particles are ordinarily detected by means of proportional counters and pulse ionization chambers, which do not fall within the scope of this paper.[69]

[69] The references cited here represent only a small portion of the published literature on Geiger counter tubes.

Microwave Phase Front Measurements for Overwater Paths of 12 and 32 Miles*

A. W. STRAITON†, MEMBER, IRE

Summary—**This paper presents the results of microwave measurements at a wavelength of 3.2 cm for overwater paths of 12 and 32 miles near Galveston, Texas. Continuous curves of phase and signal strength for a range of transmitter and receiver heights between 10 and 55 feet mean sea level are shown. Comparison of the two radio paths is made, and deviations of the results from those commonly expected for overwater propagation are pointed out.**

I. Introduction

THE UNUSUAL characteristics of microwave propagation over water at low elevations have been discussed in numerous papers.[1,2] When the air along the radio path used in this study has traveled a considerable distance over water, radio ducts are produced in which microwave signals may be trapped. This trapping produces signal strengths beyond the optical horizon much greater than would occur under standard conditions.

This paper describes the measurement of phase and signal strength as functions of transmitter and receiver heights at a wavelength of 3.2 cm for overwater paths of 12 and 32 miles. It is believed that these are the first microwave vertical phase measurements which have been made for overwater paths.

II. Radio Path

The radio path was adjacent to the shoreline along Bolivar Peninsula near Galveston, Texas. A curve in the shoreline permitted completely overwater paths as shown in Fig. 1. The receiving tower was located on a projection of land near the west end of the peninsula.

The transmitting tower was set up at two points on the shoreline at distances of 12.3 and 31.6 miles from the receiver. A few measurements were made for other distances with the transmitter mounted on top of a truck.

III. Receiving Equipment

The receiving equipment measured the phase difference between two antennas spaced 10 feet apart

* Decimal classification: R248. Original manuscript received by the Institute, June 10, 1948; revised manuscript received, September 13, 1948. Presented, joint meeting, American Section, URSI and Washington Section, IRE, Washington, D. C., May 3, 1948. This work was sponsored by the Office of Naval Research, under contract N5 ori-136.

† Electrical Engineering Research Laboratory, The University of Texas, Austin 12, Texas.

[1] P. A. Anderson, K. E. Fitzsimmons, G. M. Grover, and S. T. Stephenson, "Results of low level atmospheric sounding in the southwest and central Pacific oceanic areas," Department of Physics, Washington State College, Report No. 9, February 27, 1945.

[2] Katzin, Martin, Robert W. Buchman, and William Binnian, "Three and nine centimeter propagation in low ocean ducts," PROC. I.R.E., vol. 35, pp. 891–906; September 1, 1947.

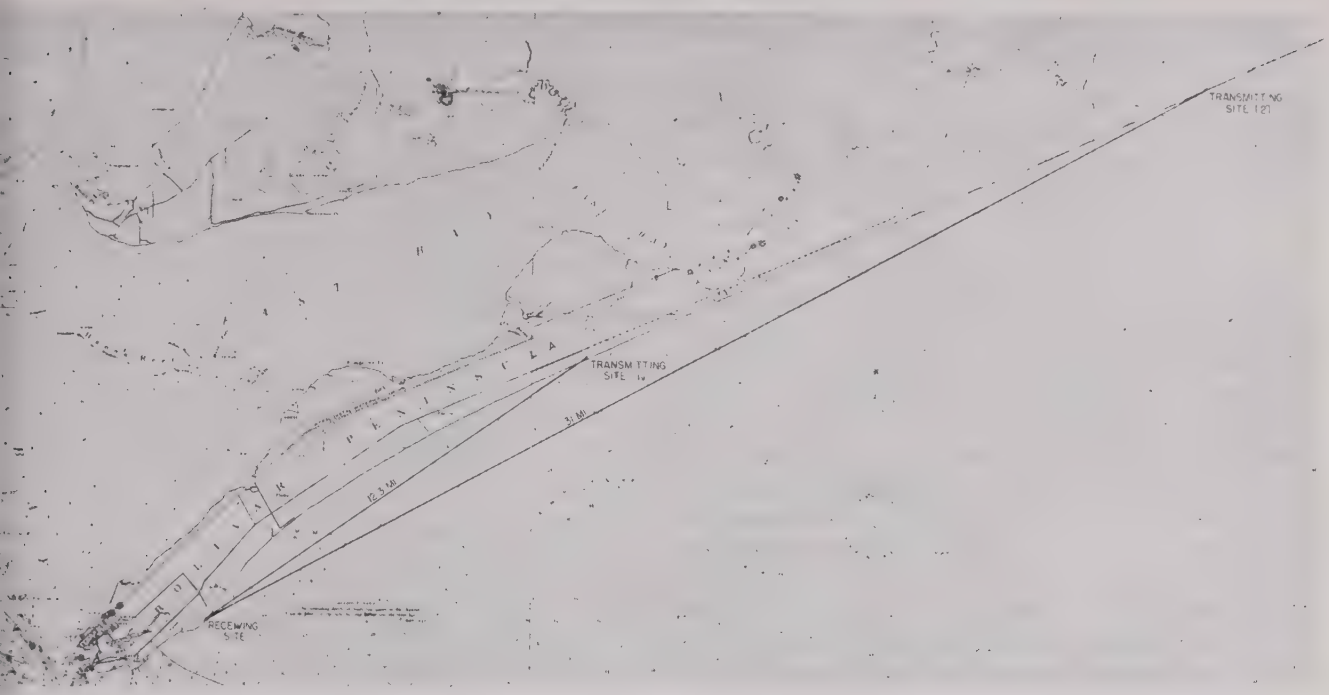

Fig. 1—Radio path.

ertically and the signal strength at the two antennas. 'his equipment was developed by the Electrical Engineering Research Laboratory of The University of 'exas, and is described elsewhere.[3] The receiving antennas were mounted on an elevator on the face of the 0-foot receiving tower as shown in Fig. 2. Deviations n the alignment of the antennas from a vertical plane ere recorded, and appropriate corrections were applied to the phase measurements. The center point between the antennas was raised continuously from 10 to 5 feet mean sea level in an interval of approximately hree minutes.

IV. Transmitting Equipment

The transmitting equipment was mounted on the levator of a fifty-foot tower. The elevator was raised om 10 to 55 feet mean sea level in approximately two inutes.

The transmitter employed a 2K39 reflex klystron with cw output of 200 milliwatts.

V. Procedure for Taking Data

The general procedure for taking data was to take six ets of phase-difference and signal-strength variations ith height in an interval of approximately 20 minutes. he receiver was moved through its complete height ange with the transmitter fixed successively at elevaons of 10, 30, and 54 feet mean sea level. The transitter was then moved through its complete height ange with the receiver fixed successively at 11, 31, and 5 feet mean sea level. Fifteen complete sets or ninety height runs were made for the 12.3-mile path and 18 complete sets or 108 runs were made for the 31.6-mile path. With the transmitter height fixed, two receiver runs were made for a 40-mile path and eight receiver runs for a 47-mile path.

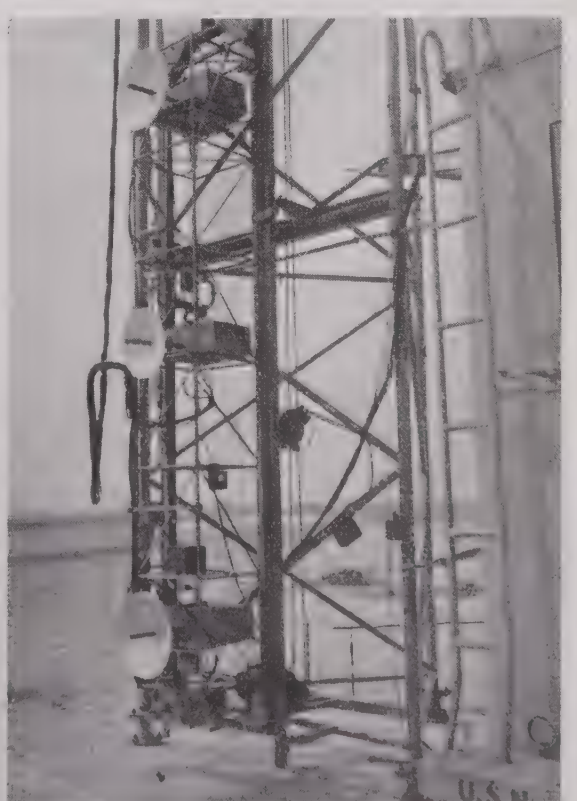

Fig. 2—Receiving equipment.

[3] F. E. Brooks, Jr., et al., "Operating manual for phase difference quipment," The University of Texas, Electrical Engineering Research Laboratory, Report No. 8, May 1, 1948.

All phase differences were measured with reference to that for a ray coming in horizontally. This was obtained by use of a reference transmitter several hundred feet along the path from the receiver. This reference transmitter was removed when the distant signals were being recorded.

VI. Modified Index of Refraction

In studying the variation of index of refraction with height, the modified index was used instead of the actual index.[4] This use permits treating the sea surface as plane, taking account of the curvature in the modified index of refraction.

The meteorological data taken in connection with the radio measurements are described elsewhere.[5] Measurements of the modified index of refraction were made at the receiving site and on board a ship which cruised adjacent to the radio path.

It was found that the variation of the modified index of refraction with height could be made to approximate the linear-exponential curve suggested by Pekeris[6] above the first few feet by the proper choice of equation constants. The general form of the height variation was always the same, and since only minor variations existed in the necessary values of the constants, it was possible to represent the prevailing meteorological condition by a single curve of modified index of refraction M as a function of height h, above the sea surface. This curve is shown in Fig. 3 and is expressed by

$$M - M_0 = 0.04h + 10.5e^{-0.14h} - 10.5.$$

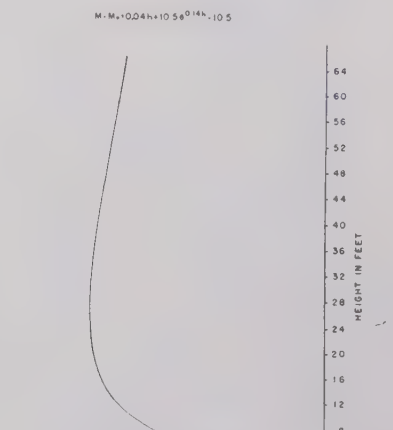

Fig. 3—Modified index of refraction.

[4] J. C. Schelleng, C. R. Burrows, and E. B. Ferrell, "Ultra-short-wave propagation," Proc. I.R.E., vol. 21, pp. 427–463; March, 1933.

[5] John R. Gerhardt, "Summary of meteorological measurements in the vicinity of Galveston, Texas, during July and August, 1947," The University of Texas, Electrical Engineering Research Laboratory, Report No. 18, March 1, 1948.

[6] C. L. Pekeris, "Wave theoretical interpretation of propagation of 10-centimeter and 3-centimeter waves in low level ocean duct," Proc. I.R.E., vol. 35, pp. 453–462; May, 1947.

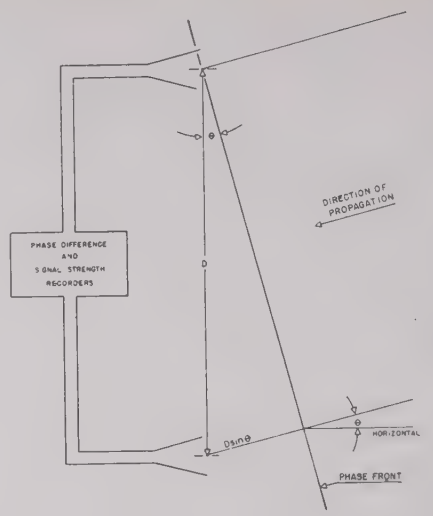

Fig. 4—Principle of angle-of-arrival measurements.

VII. Principle of Angle-of-Arrival and Phase Front Determinations

The angle-of-arrival equipment measured the phase difference between two points 10 feet apart vertically. For a phase front which is approximately plane in this interval, the phase difference may be used to obtain the angle of arrival of the phase front. If the phase front has an angle of arrival of θ above the horizontal, as shown in Fig. 4, the phase front will travel an extra distance in reaching the lower antenna after reaching the upper antenna given by

$$D \sin \theta.$$

The phase delay ϕ at the lower antenna will then be given approximately by

$$\phi = 2\pi D\theta/\lambda.$$

For a separation D of 10 feet and a wavelength λ of 0.105 feet (3.2 cm), this becomes

$$\phi = 600\theta.$$

The angle of arrival of the phase front is then obtained by dividing the phase difference by 600.

The shape of the phase front may be obtained from the phase difference measurements.[7] Since the phase difference is known between any two points 10 feet apart in the height range of the receiver, the phase with reference to a particular point may be obtained at 10-foot intervals above that point by adding the successive differences. This phase front determination can only be applied to the data for which the receiver was moving, and cannot be applied to the data for which the transmitter was moving.

VIII. Consistency of Data

For each of the radio paths used, the general characteristics of all of the signal strength and phase dif-

[7] A. H. LaGrone, E. W. Hamlin, and A. W. Straiton, "The indicated angle-of-arrival by phase front analysis," The University of Texas, Electrical Engineering Research Laboratory, Report No. 12, June 15, 1948.

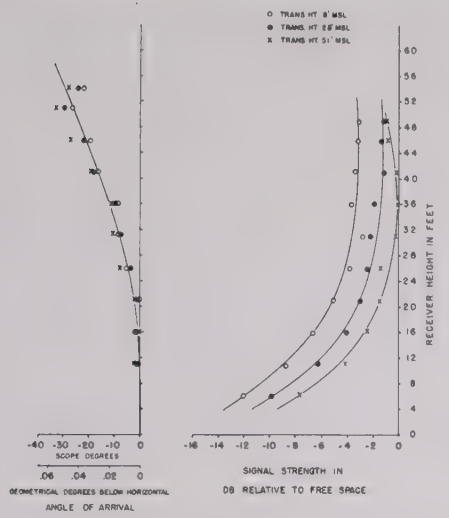

Fig. 5—Angle-of-arrival and signal-strength curves for 12.3-mile path with the receiver moving.

erence curves were the same, and only minor variations ccurred in the details of the curves. Therefore, it eemed desirable to use average data instead of indi- idual curves in presenting the results of the measure- nents. Accordingly, all of the data for corresponding eight runs were averaged to obtain the curves shown ater.

IX. General Characteristics of Data

The signal strength and angle-of-arrival curves for he average data of the 12.3-mile path are shown in ig. 5 for the receiver moving and in Fig. 6 for the ransmitter moving. The corresponding curves for the 1.6-mile path are shown in Figs. 7 and 8, respectively. he general characteristics of these curves are as follows:

1. The phase difference at the receiver is independent f transmitter height.
2. The phase front angle of arrival was negative below horizontal).

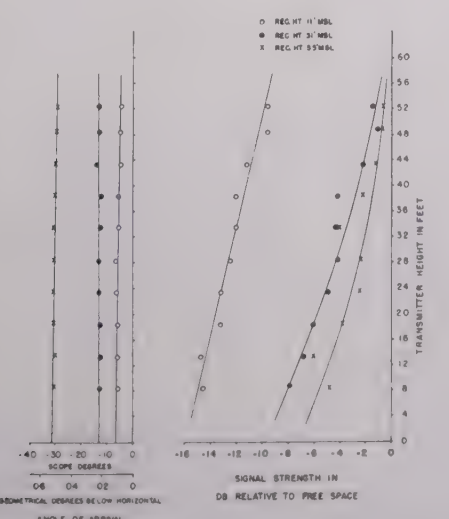

Fig. 6—Angle-of-arrival and signal-strength curves for 12.3-mile path with transmitter moving.

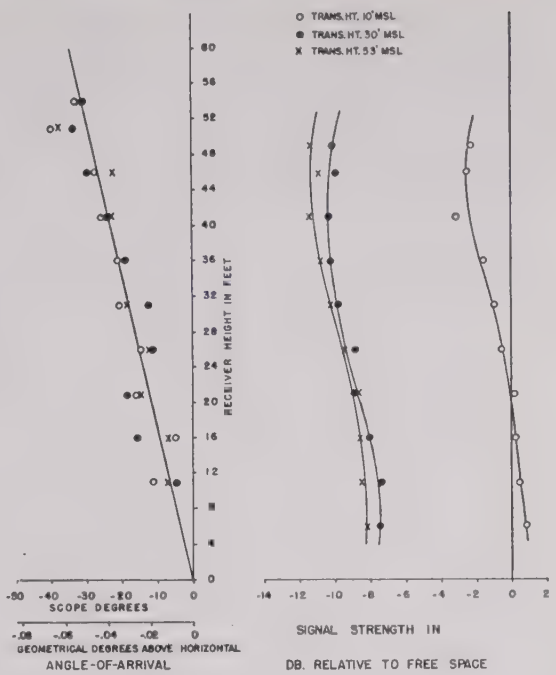

Fig. 7—Angle-of-arrival and signal-strength curves for 31.6-mile path with the receiver moving.

3. The signal strength increased with height for the 12-mile path and decreased with height for the 32-mile path.
4. The same signal strength does not result when the transmitter and receiver heights are interchanged.

A few receiver runs were made for 40- and 47-mile paths with the transmitter placed on a truck. The data for these paths show characteristics similar to those of the 12- and 32-mile path.

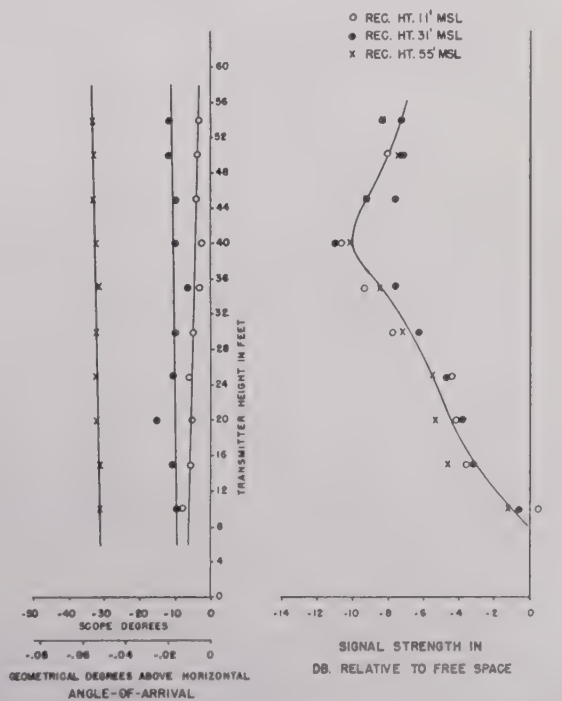

Fig. 8—Angle-of-arrival and signal-strength curves for 31.6-mile path with the transmitter moving.

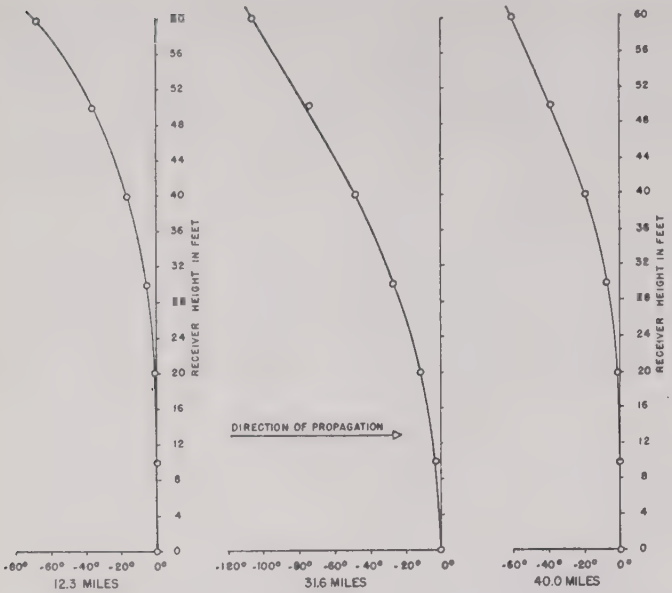

Fig. 9—Phase fronts.

The shape of the phase fronts for the various path lengths is shown in Fig. 9. It is seen to be divergent.

X. Normal Mode Solution of Wave Equation

1. General Solution

The problem of calculating the phase front and the field strength from the modified index of refraction distribution may be handled by ray tracing methods for relatively short distances.[8] However, for greater distance, the solution is given in terms of a sum of a number of normal modes.[9] Thus,

$$\psi = e^{i\omega t - i\pi/4}\sqrt{\frac{2\pi}{KR}}\sum_m e^{-\delta_m R}U_m(h_t)U_m(h_r) \qquad (1)$$

where

R is the distance along the earth surface, K is 2π divided by the wavelength, δ_m is the propagation function of the m mode, and $U_m(h_t)$ and $U_m(h_r)$ are the height-gain relationships as functions of transmitter and receiver heights, respectively. It is convenient to express δ_m in terms of a characteristic function such that

$$\delta_m^2 = -k^2(1 - \Lambda_m).$$

2. First Mode

For the modified index of refraction curve shown in Fig. 3, the first mode is found to fall in the transition region between complete trapping in the duct and considerable leakage from the duct. By use of the charts prepared by Pekeris and Ament[10] for asymptotic solution for transition modes, the value of Λ is given as

$\Lambda = 15 + 0.18\ i$ where distances are in natural units (1 natural unit of height = 15.1 feet and 1 natural unit of horizontal distance = 5.22 miles).

From the value of Λ, the attenuation of the first mode with reference to the inverse square root decrease is found to be 0.3 db per mile.

The characteristic height-gain function for the trapped mode is one which increases to a maximum at a height slightly less than the modified index of refraction minimum, and decreases for somewhat greater heights. The phase front to be expected is one which is constant for height changes in the duct, and decreases for values above the duct.

3. Second Mode

By the phase-integral method of footnote reference 9 the attenuation of the second mode is found to be 4.2 dbs per mile below the inverse square root value. It then appears that the second mode will not be significant, except possibly for the 12.3-mile path.

XI. Discussion

1. Phase Difference as a Function of Transmitter Height

For the 12.3-mile and 31.6-mile paths, the phase difference was found to be independent of the position of the transmitter. This condition indicates that only one mode is present for each of these paths. This follows from (1) since a change in transmitter height for one mode will produce the same change in phase at all receiver heights. The phase difference and the shape of the phase front are then independent of transmitter height for a single mode. For more than one mode, the changes in the signal strengths of the various modes with transmitter height would normally cause the resulting phase angle to change.

2. Phase Difference as a Function of Receiver Height

The direction of the angle of arrival of the phase front was found to be negative and the phase front was found to be divergent.

For a completely trapped mode, the phase would remain constant below the track width, and become negative above the track width. For the slightly leaky first mode, the phase would decrease consistently with height, giving a divergent phase front. It would normally be expected that the agreement would be better for the longer paths.

3. Signal Strength as a Function of Receiver and Transmitter Heights

The field equation solution for a single mode indicates that the shape of the height-gain curve is independent

[8] W. E. Gordon, and A. T. Waterman, Jr., "Angle-of-arrival aspects of radio meteorology," The University of Texas, Electrical Engineering Research Laboratory, Report No. 1, Appendix, March 23, 1946.

[9] W. H. Furry, "Theory of characteristic functions in problems of anomalous propagation," Radiation Laboratory Report No. 680.

[10] C. L. Pekeris, and W. S. Ament, "Characteristic value of the first normal mode in the propagation of microwaves through an atmosphere with a linear-exponential modified index of refraction, Naval Research Laboratory MPG-5.

distance, except for changes in magnitude. With ther the transmitter or receiver increasing in height, e single mode solution would give a signal strength creasing in magnitude up to a maximum at slightly ss than 25 feet.

Deviation Between Receiver and Transmitter Signal-rength Height Curves

As pointed out previously, the signal-strength curves a function of receiver heights were distinctly different om the curves as a function of transmitter height. The ld equation (1) indicates, however, that the trans-itter and receiver height may be interchanged without anging the signal strength. No satisfactory explana-on has been made for the deviation in the shape of e signal-strength curves, although several suggestions ve been advanced. These will be discussed in the fol-wing sections.

a. One explanation is the possibility that the index refraction varies with horizontal distance. However, e meteorological measurements indicated no measur-le variation of index with distance.

b. A second suggestion is that the differences in the transmitter and receiver antenna sizes may have caused the deviation. A 30-inch paraboloidal dish was used at the transmitter and 18-inch dishes were used at the receiver. However, the effective transmission angles were so small compared to the antenna beam angles that it is felt that the effect of the difference in antenna size is negligible.

c. A third possibility is that the horizontal distances and heights used were too great for the use of ray treatment and too short for the use of the wave theory. Even though the mode theory indicates that the higher mode would be negligible, the ranges used may not have been sufficiently long to establish the phase front predicted by the mode theory.

Phase and signal strength measurements for a large number of distances appear to be desirable. In addition, it seems desirable to obtain data with the receiver and transmitter interchanged. It is hoped that it will be possible for the Electrical Engineering Research Laboratory to take these additional data in the not too distant future.

Predetermined Electronic Counter*

B. R. GOSSICK†

Summary—**Proof is given that any integral scaling e can be obtained using binary counters with ropriate feedback connections. As examples, two ferent sets of feedback connections are given for h integer between 2^{n-1} and 2^n.**

ONSIDER n multivibrators connected in cascade. The two positions of stable equilibrium will be designated as 0 d 1. Connections are made so that the tial position for each multivibrator is zero. is arrangement is shown in Fig. 1.

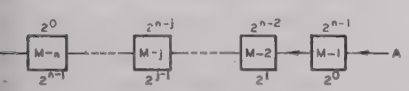

Fig. 1

The 2's underneath the multivibrators ve the number of input pulses required at to make the associated multivibrator shift sition. Thus, if a pulse is fed into the j^{th} ultivibrator it has the same effect as 2^{j-1} lses fed into the first multivibrator at A. ne 2's above each multivibrator represent e number of times their associated multi-brator makes the shift 0–1 per cycle of the ain, i.e., per output pulse produced at B. rosdoff[1] has shown how to make a connec-on between the k^{th} and j^{th} multivibrators, so that each time the k^{th} makes the shift 0–1, it transmits a pulse to the input of the j^{th} multivibrator. In general, $k>j$. Then, each time the k^{th} multivibrator shifts 0–1, it has the effect of 2^{j-1} pulses applied at A. Furthermore, as the k^{th} multivibrator makes 2^{n-k} shifts 0–1 for each complete cycle of the chain, it is evident that the feedback connection k–j has the same effect as $2^{n-k+j-1}$ pulses applied at A. Thus, the natural count 2^n has been reduced by this number, so that there are now only $2^n-2^{n-k+j-1}$ input pulses per cycle of the chain.

It follows that, by making other feedback connections in the chain, the count C (i.e., the number of input pulses per cycle) is given by

$$C = 2^n - \sum_{k=2}^{n} 2^{n-k-1} \sum_{j=1}^{k-1} 2^j \delta_j^k \tag{1}$$

$$\delta_j^k = \left.\begin{array}{l} 1, \text{ if } k \text{ and } j \text{ are connected.} \\ 0, \text{ if } k \text{ and } j \text{ are not connected} \end{array}\right\}. \tag{2}$$

Consequently, it is clear that the natural count can be changed to any integral number of input pulses per cycle; because any integer can be expressed in the binary system, and in that system the symbol for the number h is the sequence of coefficients a_i, where a_i equals either unity or zero, and

$$h = \sum_i a_i 2^i, \; i = 0, 1, 2, 3, \cdots . \tag{3}$$

Two examples follow. As the natural counts 2^n and 2^{n-1} are produced by chains of n and $n-1$ multivibrators, respectively, it only remains to show how to fill the gap between 2^n and 2^{n-1}. The first example is a circuit where feedback connections are from the k^{th} to the first multivibrator. Thus, by (1),

$$C = 2^n - \sum_{k=2}^{n} 2^{n-k} \delta_1^k \tag{4}$$

$$= 2^{n-1} + 1, (k = 2, 3, 4, \cdots , n) \tag{5}$$

$$= 2^{n-1} + 2, (k = 2, 3, 4, \cdots , n-1) \tag{6}$$

$$= 2^{n-1} + 3, (k = 2, 3, 4, \cdots , n-2, n) \tag{7}$$

$$= 2^{n-1} + 4, (k = 2, 3, 4, \cdots , n-2) \tag{8}$$

$$\vdots \qquad \vdots$$

$$= 2^n - 4, (k = n-2) \tag{9}$$

$$= 2^n - 3, (k = n-1, n) \tag{10}$$

$$= 2^n - 2, (k = n-1) \tag{11}$$

$$= 2^n - 1, (k = n). \tag{12}$$

The second example is a circuit where feedback connections are from the n^{th} to the j^{th} multivibrators. Thus, again by (1),

$$C = 2^n - \sum_{j=1}^{n-1} 2^{j-1} \delta_j^n \tag{13}$$

$$= 2^{n-1} + 1, (j = 1, 2, 3, \cdots , n-1) \tag{14}$$

$$= 2^{n-1} + 2, (j = 2, 3, 4, \cdots , n-1) \tag{15}$$

$$= 2^{n-1} + 3, (j = 1, 3, 4, \cdots , n-1) \tag{16}$$

$$= 2^{n-1} + 4, (j = 3, 4, 5, \cdots , n-1) \tag{17}$$

$$\vdots \qquad \vdots$$

$$= 2^n - 4, (j = 3) \tag{18}$$

$$= 2^n - 3, (j = 1, 2) \tag{19}$$

$$= 2^n - 2, (j = 2) \tag{20}$$

$$= 2^n - 1, (j = 1). \tag{21}$$

To prevent interaction it is, of course, necessary to provide isolation in the case of multiple feedback connections.

* Decimal classification: 621.375.2. Original manu-ipt received by the Institute, July 22, 1948; ab-act received, February 16, 1949. The solutions dis-sed by the author in this paper were developed and mpleted by him in the course of his employment by e Radio Corporation of America, RCA Victor Divi-n, Camden, N. J.

† Nepa Division, Fairchild Engine and Airplane rporation, Oak Ridge, Tenn.

[1] I. E. Grosdoff, "Electronic counters," *RCA ., vol. 7, pp. 438–448; September, 1946.*

Carrier Current Pulsing over Toll Telephone Circuits*

IMRE MOLNAR†, SENIOR MEMBER, IRE

Summary—**Recently developed multichannel carrier telephone systems, where calls are extended through automatic switching equipment, are described, together with performance data and application in commercial telephone service. Connections are established and dial pulses extended, utilizing the carriers associated with the various voice transmission channels.**

Introduction

NO MATTER what medium is used to transmit intelligence between two points—whether it consists of writing a letter, sending a telegram, or making a telephone call—two fundamental objectives are common to all such methods. One is that the "addressee" of the message must be sought out and reached; the other is that the message itself must be intelligibly transmitted.

In line with this dual aim, communication engineering concerns itself with two distinct kinds of techniques. There are, first, the techniques by which the path to the "addressee" is selected and made ready to receive the message; second, there are the techniques by which the message is transmitted over that path. In the following discussion we are concerned only with the former techniques, and specifically with their application to carrier telephone channels.

Generally speaking, a telephone connection can be established by the intermediary of one or more operators, by the substitution of remotely controlled switching equipment for the operators, or by a combination of the two methods. Since telephone connections now extend over unlimited distances and increasingly complex routes, the individual path chosen can no longer be identified. Accordingly, universal operating procedures are necessary; the same standard procedure must apply in all cases, irrespective of the transmission medium—open wire, cable, carrier, or radio—which is employed.

Because of their advantages in line plant economy and in quality of transmission, carrier systems today form the backbone of the nation's long-distance telephone network, as well as of a large number of systems used by service organizations such as railroads, power utilities, and pipelines. Consequently, the problem of signaling through, and switching of, carrier circuits is of the greatest importance.

Pulsing Methods in Toll Operation

Whenever connections are established by automatic switching equipment, there exists the problem of transmitting certain signals over whatever type of circuit employed. Although it is often believed that all conditions for automatic operation are fulfilled simply by assuring that pulses can be satisfactorily transmitted, it is in addition necessary at times to transmit a large number of signals in one direction or the other. There are a number of satisfactory toll dialing systems in operation, although this paper will mention only two of them.

The first method is called "voice-frequency signaling," because the signals used consist of short applications of voice-frequency current to the voice-frequency terminals of the talking channel. In a telephone circuit because a speech path exists from one end to the other, a signal path is provided automatically as long as voice frequencies are used for signaling. And, since speech transmission is maintained at a satisfactory level and quality over unlimited circuit lengths, a satisfactory signal level and quality is automatically maintained without additional provisions. The various signals are distinguished from one another by their sequence, direction of transmission, frequency, timing, and modulation.

Although its theory is sound and attractive, voice-frequency pulsing possesses inherent difficulties which make it about the most intricate problem in the whole art of automatic control. While most of these difficulties may be eliminated by proper circuit design, every such step results in a considerable increase in cost.

Voice-frequency pulsing is useful on long and complex circuits, which include one or more carrier links (not necessarily of the same system), and which are operated from end to end on a voice-frequency signaling basis. In many instances, however, inexpensive carrier systems are installed because of their economy on relatively short-haul toll lines. Since a properly designed terminal for voice-frequency signaling is quite costly, its use may defeat the economy of carrier installation on such circuits. Although voice-frequency dialing is widely and effectively used over all types of circuits, a much simpler, less costly, and even more efficient system for carrier operation has been developed jointly by Automatic Electric Company and Lenkurt Electric Company.

The second system of long-distance pulsing employs direct current exclusively. There are several types in operation, probably the most useful of which is known as "composite" pulsing. With suitable networks of chokes and capacitors it is possible to send dc signals independently over each wire of a pair, without mutual interference with speech simultaneously present on the same pair. It is possible, furthermore, to arrange these composite circuits for duplex operation, that is, for signaling simultaneously in both directions over the

* Decimal classification: 621.385. Original manuscript received by the Institute, April 7, 1947; revised manuscript received, October 27, 1948. Presented, 1947 IRE National Convention, New York, N. Y., March 3, 1947.

† Automatic Electric Co., Chicago, Ill.

me conductor. In spite of its excellent performance, wever, composite pulsing also has its limitations. One that dc signals must have a dc path, which is seldom ailable in carrier operation, and never on radio cir-its. Furthermore, a three-channel carrier system pro-des four speech circuits (including the physical one) er one pair of wires, while the maximum in dc opera-n is two duplex composite signaling channels on the ir, leaving two speech channels without means for naling.

From the standpoint of circuit technique, nothing uld be simpler and more straightforward than dc naling. Practically all signals for toll or straight auto-atic operation can be provided by the application and moval of a dc potential. This becomes particularly nple if a reliable duplex system or separate signaling annels are available for either direction. With a few ceptions the signals are independent of any timing or quence, and the marginal conditions are even less ingent than in ordinary local operation. This makes it parent that the most suitable pulsing method in car-r operation is one which duplicates dc signaling by eans which permits the passage of signals through car-r circuits. For instance, two independent frequencies, e for each direction within the transmission band of e system, can be applied, exactly as the dc operation. the signal frequencies are located within the trans-ssion band of the carrier system, but outside of the in-ligence sidebands, they will travel the whole dis-nce together with speech transmission without being bjected to mutual interference in the final demodula-n process. The boundary conditions are particularly nple; there is a 1:1 correspondence of direct to al-rnating current at the sending terminal, and back ain at the receiver.

There are several ways to provide such a circuit. If ere is a surplus frequency band beyond what is needed the speech channels, it can be divided into a number narrow bands, with two of these assigned to each annel for signaling in either direction. While this is a actical method and is used to some extent, it is also steful, because the signaling channels extend the total ndwidth upwards, and the surplus frequency spec-um could be more usefully employed for additional eech channels.

A far more efficient method is to exploit the channel rrier frequency for signaling purposes, since it is sup-essed in single-sideband operation, as far as voice nsmission is concerned. In the system frequency ectrum there is a separation between sidebands com-ising adjacent channels varying between 600 and 1300 s, and also a 250-cps separation between each side-nd and its associated carrier. This space can now be ilized for signal transmission. The signal channels us take advantage of the frequency bands which ould otherwise be wasted, and make use of the existing rrier frequency supply instead of separate signal fre-ency oscillators.

Establishing a Toll Connection over Carrier Circuits

As a typical example, let us consider a connection between a manually operated toll center and a distant automatic network.

Fig. 1 shows a schematic layout of a carrier toll connection. The carrier terminal (left) is connected to the toll board jacks through a special manual-to-automatic trunk circuit. The interconnection between the trunk circuit and the carrier terminal apparatus consists of a

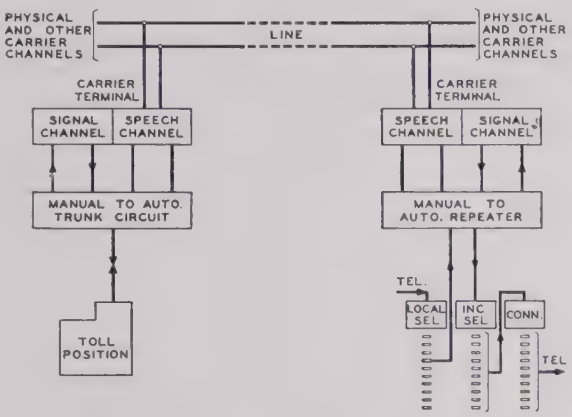

Fig. 1—Signaling system schematic diagram

pair of talking conductors and two signaling leads—one for each direction. A Strowger Automatic telephone exchange (right) is tied to the carrier system by a manual-to-automatic two-way repeater through a like number of conductors. A block diagram of the carrier signaling channel, and curves showing its transmission performance, appear in Fig. 2.

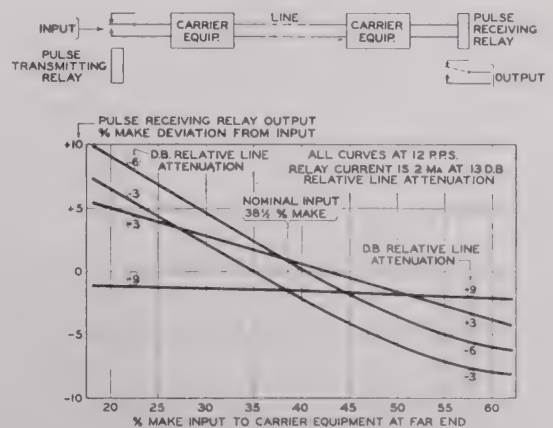

Fig. 2—Pulsing characteristics.

To reach a subscriber at the automatic exchange, the toll operator first inserts a plug into the jack of an idle carrier channel, placing a dc potential on the signaling lead in the direction of the automatic exchange. This

causes the carrier frequency signal to be transmitted. At the receiving end the carrier frequency signal is selected, amplified and detected, which establishes a dc circuit to the manual-to-automatic repeater, ready for seizure of the automatic equipment.

The operator now sends several series of dial pulses corresponding to the requested number. These pulses, consisting of interruptions of the steady potential, are set at an approximately rate of 10 per second, one interruption occupying 61½ per cent of each pulse cycle. In the automatic exchange these pulses, after being reconverted into direct current, alternately energize and deenergize ratchet-driven devices (switches) which extend the circuit step by step to a set of contacts to which the called subscriber's telephone line is connected.

The line is now tested. If it is free, it is automatically signaled by ringing current; if it is engaged, the operator receives a busy signal. When the called subscriber answers, a dc potential is placed on the signaling lead in the direction of the toll board. Upon receipt and detection it causes the carrier-frequency signal to be transmitted, which extinguishes the called-end supervisory lamp in the cord circuit. When the called subscriber hangs up, this dc potential is removed and the supervisory lamp again glows. If the operator's local subscriber has disconnected in the meantime, the operator removes the plug, thereby removing the potential from the signaling lead. The corresponding potential at the automatic terminal also disappears, and all switches there return to their normal position.

When a call originates at the automatic exchange, the calling subscriber dials the number of the distant toll board. The switches in the local office operate under the subscriber's control and automatically seize an idle carrier circuit through its manual-to-automatic repeater. The same dc potential as before is placed on the signal lead, and carrier-frequency current is transmitted. After being selected, amplified, and detected, the carrier signals appear as dc signals, and the line lamp associated with the carrier trunk glows at the toll switchboard. An operator plugs in, extinguishing the line lamp, and places a dc potential on the signal lead towards the automatic exchange. After receiving the number request, the operator completes the connection locally.

When the calling subscriber hangs up, the signaling potential is removed, and the calling-end supervisory lamp in the cord circuit glows. When the operator removes the plug from the carrier-circuit jack, the potential towards the automatic exchange is removed, and the toll circuit is again available for a new call in either direction. Whether the local equipment in the automatic exchange is held operated during the period between the calling subscriber's disconnnect and the operator's taking down of the connection, or is released as soon as the calling subscriber hangs up, is optional; each practice has points in its favor. These are typical procedures for the simplest connections.

Three-Channel Carrier System

Fig. 3 is a schematic diagram of the Lenkurt type 3 three-channel carrier telephone system, which is widely used in automatic toll operation. The meeting point between the carrier equipment and the individual local voice-frequency physical circuits is the hybrid network. The transmitting branch of the four-wire circuit consists of the transmitting low-pass filter for attenuating the voice frequencies above the desired pass band, the modulator, the output filter for passing the selected sideband only, and the transmitting amplifier. The receiving branch includes the demodulator, the receiving low-pass filter and the receiving amplifier.

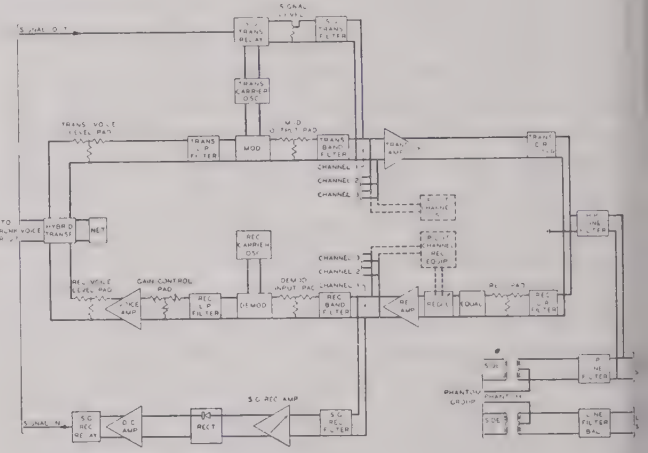

Fig. 3—Carrier terminal schematic diagram.

Disregarding for the time being the associated signaling equipment, the three transmitting branches are grouped together through their receiving band filters. Each group is amplified by the transmitting and receiving amplifiers, respectively, and further combined by the directional filters. The high-low-pass filter at the toll line entrance segregates the carrier band from the physical circuit.

The line current is a complex mixture of frequencies. It includes the voice-frequency of the physical circuit, the side-bands of the three carrier channels, and the carrier frequencies proper when employed for signaling. About 30 kc is the highest transmitted frequency on a three-channel system. Each repeater section may have up to 43 db line attenuation at 27 kc, and can furnish a 0-db loss circuit between the voice frequency terminals with the usual transmitting input level of 18 db above the transmitting switchboard. This attenuation would limit a repeater section of 114-mil copper wire to a distance of between 125 and 300 miles under adverse weather conditions. However, the distance can be somewhat increased if automatic gain regulating equipment is employed. The transmission range, of course, can be further extended to almost any distance by intermediate carrier repeaters.

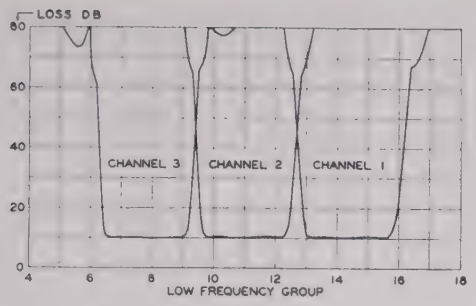

(a)

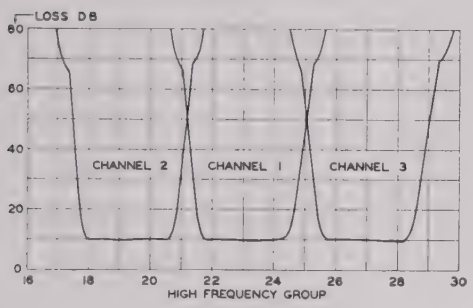

(b)

Fig. 4—Band filter attenuation characteristics.

The success of carrier dialing depends entirely on success in reproducing sharp pass-band filters which (1) keep the speech sidebands out of the signal channels; (2) keep the carrier frequency out of the speech channel; and (3) reproduce with little distortion important sidebands of the signal current. In addition, systems having filters of such well-defined characteristics also required well-balanced modulators, and stable oscillators for permanent centering of the carrier frequency inside the filter pass band. A 10-cps deviation between modulating and demodulating frequencies is about the limit of tolerance; during system lineup these frequencies can be adjusted to within ± 2 cps. The components which meet these requirements must be economical to manufacture, since low cost frequently determines the installation of carrier systems.

Fig. 4 shows the characteristics of typical transmitting and receiving band filters. They are substantially flat in the pass band, and in every case the attenuation is better than 60 db between adjacent channels in one

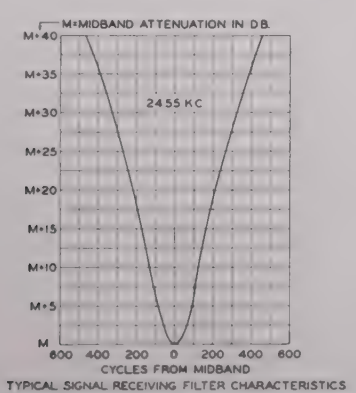

Fig. 5—Signal filter characteristics.

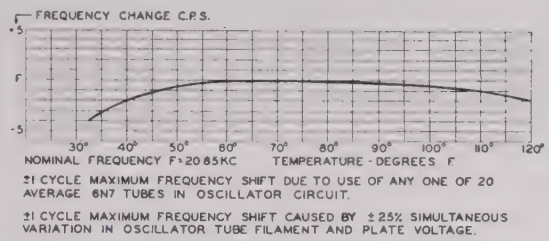

Fig. 6—Oscillator stability characteristics.

terminal. The amount is actually doubled, since there are identical transmitting and receiving pass-band filters at both ends of the circuit. Although there may be a difference of 43 db in the levels of the transmitting and receiving paths, cross talk between them at the same terminal is negligible. Their wide frequency separation and the directional filters between the transmitting and receiving amplifiers also help prevent cross talk. The net result is equivalent to what is known as "near-end cross talk" in physical circuits.

Fig. 5 shows the characteristics of typical signal receiving and transmitting filters. Sharp signal receiving filters are essential for satisfactory pulsing performance, because the selectivity of the signal receivers against the arriving complex frequency mixture depends entirely upon them.

Fig. 6 shows the stability of a typical carrier oscillator over a temperature range of 30 to 120°F. Within this range there may be a variation of $\pm 1\frac{1}{2}$ cps. If the filament and plate voltages applied to the oscillator tube circuit change simultaneously by 25 per cent, the frequency will not change more than ± 1 cps. There may be a like amount of random variation upon inserting any one of twenty commercial 6N7 tubes in the oscillator circuit.

Carrier Pulsing Circuit Operation

Fig. 7 is a circuit diagram showing one version of a signaling terminal. The dc potential which is placed on the signaling lead at the switching equipment operates the pulse-transmitting relay in the terminal. The contacts of this relay apply the carrier frequency source, through a signal-transmitting pad and the narrow-band signal transmitting filter, to the transmitting circuit common to all speech and signal channels. The carrier frequency signal is interrupted by the pulse-transmitting relay contacts while dial pulses are sent, at the rate and ratio specified below.

At the distant terminal the incoming signaling frequencies enter the signal receiving channel unit through the narrow-band signal receiving filter. This selects the proper signaling frequency for its particular channel out of the complex mixture of several carrier signals and speech sidebands. The signal then passes through a two-stage resistance-coupled amplifier, the output of which is transformer-coupled to a germanium diode. The recti-

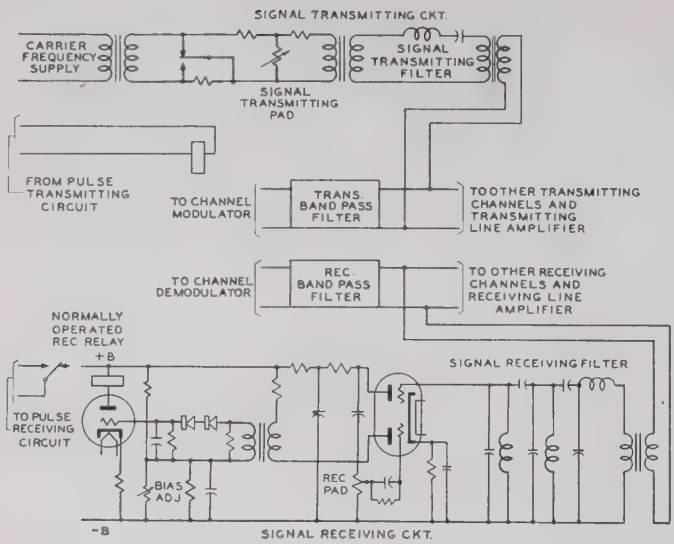

Fig. 7—Signaling circuit diagram.

fied signal voltage is connected to the grid of a relay tube. Since the rectified voltage is negative with respect to the cathode, the plate current of the relay tube is reduced on receipt of carrier signal, causing the normally energized receiving relay to release and to connect a marking potential through its contacts to the signaling lead to the switching equipment. The signal receiving relay follows the interruptions of the carrier signal during dialing, and reproduces these pulses in the form of interrupted direct current over the signal lead and the manual-to-automatic repeater to the switching equipment. The operation of the signal receiver is further discussed in the sections on signaling range and interference.

Dialing Performance

Specifications for automatic telephone equipment call for a pulsing speed of 8 to 12 pulses per second, and an exchange voltage held within ± 10 per cent of its nominal value. The limits in the ratio between "on" and "off" periods of the pulse are less explicit; it is customary instead to specify the extreme line conditions which can be tolerated. While the nominal value of the "off" pulse is $38\frac{1}{2}$ per cent of the cycle, satisfactory performance can generally be obtained between 30 to 50 per cent, and in many cases somewhat beyond this range.

The permissible deviation from the nominal pulse ratio must be apportioned among the several successive stages which are required to build up a complex connection. The local switching plant of a telephone system uses so many units of apparatus that they must be produced in the most economical manner: in other words, the tolerances in their performance should be as wide as feasible. Conversely, since there is only a comparatively small number of toll circuits having access to local equipment, it is sound economy to keep distortion over the toll signaling circuit as low as possible.

A further reason why the pulse tolerances should b apportioned to the local plant as far as feasible is tha most of these plants were installed long before toll dia ing entered the picture, and thus have already taken u a considerable portion of the permissible pulse distor tion.

Carrier toll dialing circuits are subject to distortio from several sources, including (1) pulse-repeating fror the outgoing trunk circuit; (2) pulsing conductor be tween trunk circuit and carrier terminal; (3) pulse repeating by the pulse-transmitting relay in the carrie equipment; (4) characteristic performance and attenua tion of the carrier signaling channel, and interferenc with it; (5) pulse-repeating by the pulse-receiving rela at the carrier terminal; (6) pulsing conductor betwee carrier terminal and repeater; and (7) pulse-repeatin by the automatic repeater.

The above causes of distortion (except for (3), (4) an (5)) are not confined to carrier systems, they are genera problems in the design of relay-type pulse-repeatin equipment over certain voltage, lines, and input ranges With suitable adjustment and circuit design, the dis tortion can be kept within practically any desired limits Actually, standard telephone-type relays are used unde (1), (3), and (7), with standard adjustments and circui arrangements. Their performance, therefore, corre sponds to that of pulse-repeating circuits over physica lines.

It is obvious that the performance of carrier dialing circuits depends almost entirely on the quality of items (3), (4), and (5). Fig. 2 shows the over-all signal distortion of a carrier circuit as a function of input pulse ratio, for various line attenuations, relative to their nominal value. It is apparent from the diagram that the carrier dialing circuit as a whole has a certain compensating tendency on signals already distorted at the input, pulses which were short are stretched, normal ones are reproduced with negligible distortion, and those which were long at the input are shortened.

Signaling Range

With a given sending power and channel attenuation, the performance of the signaling circuit depends on the sensitivity of the receiver and on the amount of interference. The sending power is specified to be between $+2$ and $+6$ dbm, measured at the transmitting amplifier output. The signal is amplified by the receiving amplifier to about the same level. This level is considered throughout the paper as the normal operating level of the signal receiver, and the system is adjusted to this level during its initial lineup. Subsequently, there will be some variation from this normal operating level due to changes of line attenuation. Although these variations can be offset by manual or automatic gain regulators, the usefulness of the signaling system is greatly enhanced if the signal receiver responds reliably over a fairly broad range of signal levels. On a 200-mile circuit without intermediate repeater, for example, the signal

receiver should perform satisfactorily between a 4-db reduction and an 8-db increase from normal line attenuation.

With reference again to the signal receiver, Fig. 8 shows the amount of plate current of the relay tube

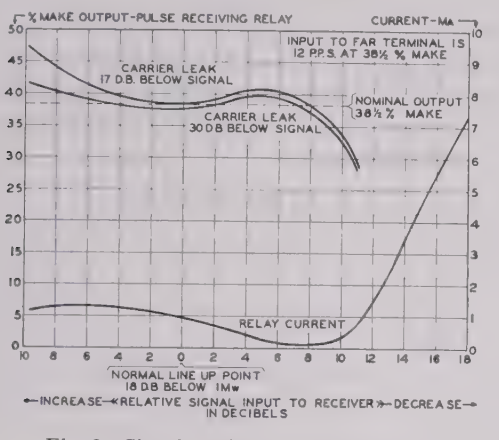

Fig. 8—Signal receiver characteristics.

over the signal input range to the receiver—0 being the normal operating level, as defined above. When a certain channel is not in use, the corresponding carrier is absent, and the relay tube is biased to about −4 volts, passing 13 ma plate current through the pulse receiving relay, which is thus held operated. When the toll circuit is seized, the received carrier signal, upon being amplified and rectified, increases the bias and reduces the plate current to a value insufficient to hold the relay, which therefore restores. Plate current cut-off is at about −8 volts.

During pulsing the carrier is alternately interrupted and reintroduced. Plate current flows and is shut off, while the receiving relay operates and releases accordingly. While carrier signal is received, dc potential is extended through the back contact of the released pulse receiving relay to the auomatic equipment. Conversely, during interruptions of the dial and the carrier, the dc potential is removed by the operated pulse receiving relay. Fig. 8 shows the output from the back contacts of the signal receiving relay, covering the period (nominal value 38½ per cent) corresponding to the closed condition of the dial. The diagram is prepared for 12 pulses per second with the standard input pulse ratio, and is representative of the over-all performance of the channel, including the signal transmitting relay. The total output pulse ratio variation over a 12-db range is about ½ per cent—only a fraction of the distortion that the automatic equipment can tolerate. The 12-db range itself is much wider than that occurring on a day-to-day basis in most practical applications.

The consistent pulsing output over such a wide variation of input level is achieved by a special circuit arrangement of the signal receiving amplifier. The latter is normally operated with current flowing in the grid circuit. However, a variable back-bias voltage, proportional to the input signal level to the receiver, is developed across a capacitance-resistance combination. The output of this amplifier, therefore, remains substantially steady over a considerable variation in signal input level.

Interference

The next problem involves investigating possible sources of interference with the signaling channel. The principal ones are: (1) noise induced on the line from external sources; (2) interference caused by the associated or electrically adjacent speech channel; and (3) carrier leak.

External interference is even more detrimental to signaling than to voice transmission. Fortunately, there are several methods available for controlling this interference, such as suitable transposing of wires or, in case of severe power disturbances, shortened repeater sections. If the interference has the same frequency as the signal carrier, its effect is similar to that caused by carrier leak; if it has a frequency some distance away from that of the carrier, the effect is comparable to speech-channel interference.

Should interference cause trouble in signal transmission, there is one remedy which always works: improving the signal-to-noise ratio by raising the signal level. There are, unfortunately, certain objections to this practice. As mentioned before, the signal power is specified at 2 to 6 db above 1 milliwatt. This is considerably lower than the level at which speech is transmitted, the latter being 18 db above the audio input level at the switchboard. Such a comparison may prove misleading. While a 1-milliwatt reference level for speech is generally accepted as a convenience and reflects at least the order of magnitude of the power content of speech, the major portion of a conversation has considerably less power, because the frequencies under 200 to 250 cps with high energy content are effectively eliminated.

Peak values of several decibels above 1 milliwatt are rare, and of comparatively short duration. On the other hand, the signal frequency is present at a constant level during conversation, and it may leak through the band-pass filter of the adjacent channel and demodulate there to a high-frequency tone—between 3,200 and 3,900 cycles, depending on the channel in question.

The signal frequency must therefore be limited to a safe compromise value, lest it cause interference with speech during periods of low energy level. Inspection of the band pass and demodulator low-pass filter characteristics reveals that the residual tone will be from 65 to 90 db below 1 milliwatt, with the specified signal transmitting level and on a 0-net-loss circuit. The value is perfectly satisfactory and barely detectable on a listening test, but it also indicates the limitation in signal power.

The second source of interference comes from the speech channels. Two must be considered: the lower frequencies of the associated voice band and the higher frequencies of the next channel. It will be recalled that

the signal receiving relay is normally energized, and releases upon receipt of carrier frequency. This relay is adjusted to release when the plate current falls below 1.8 ma. The plate current versus signal level curve of Fig. 7 shows that this value is reached when the carrier is 12 db below the nominal setting of the signal receiver, or stronger. This means that the interference must be kept below this value to maintain proper operation.

Fig. 4 shows the attenuation characteristics of a signal-receiving filter. Since frequencies under 300 cycles are substantially attenuated in the audio channel, and those under 200 cps effectively cut off, the signal filter attenuation—18 db at 200 cps, and 28 db at 300 cps off the carrier—is sufficient for reliable operation. There is an even greater margin against interference by the upper frequencies of the adjacent channel.

Interference may also be caused by carrier leak which is the residual carrier frequency which passes from the voice channel modulator, through the transmitting channel band filter, onto the line. Since the carrier leak and the signal current have identical frequencies, the "leak" current will pass through the signal-receiving filter with a minimum of attenuation. If it is sufficiently strong it will cause a false signal to the switching equipment by releasing the signal-receiving relay. Although the carrier frequency is adequately suppressed, as a rule, by the balanced circuit arrangement of the modulator, imperfect balance may nevertheless permit a small amount to be present. This will be further attenuated by the transmitting band pass filter.

As mentioned above, a maximum carrier leak of −15 dbm is specified—in other words, 17 db below signal level. It was also mentioned that the release value of the signal-receiving relay is 1.8 ma, and that (see Fig. 8) no signal less than 12 db below the nominal adjustment of the receiver would bring the relay current under this value. Since the carrier leak is at least 17 db below the normal signaling power, the line attenuation could drop 5 db before false operation occurs. Such a drop in attenuation is hardly permissible, because the associated four-wire-to-two-wire terminations of the voice channels would become unstable. A reduction of channel loss of such magnitude is almost impossible, and is not permitted in practice.

In this connection the efficiency of the automatic bias control in the signal-receiving amplifier can be strikingly demonstrated. Fig. 8 shows that the current through the receiving relay is 1.3 ma when the signal level is 5 db above that for which the nominal adjustment of the receiver was made. The same amount of relay current is also obtained for a signal power 12 db below the nominal adjustment point. Since 1.3 ma is below the value at which the relay holds, it releases.

The significance of this is that with the maximum permissible carrier leak of 17 db under the signal power and the line attenuation reduced to 5 db below its normal value, the receiving relay is in its released position, regardless of whether there is a signal current present or not. On the other hand, also according to Fig. 8, actua tests indicate that under the same conditions the re ceiving relay is pulsing satisfactorily with only 2 pe cent loss from the standard pulse ratio. The explanatio of this apparent contradiction can be found in the tim constant of the bias adjustment. The bias is always de termined by the combined signal current plus carrie leak level. It is maintained at this point by the tim constant of the bias circuit during subsequent short period interruptions of the signal current, even with th carrier leak still present.

Applications of Toll Dialing Systems

The link between the carrier terminal and the automatic or toll equipment is a trunk circuit or repeater. Its function is to convert the simple on-and-off conditions of dc potential on the signal "in" and "out" leads into the various conditions required by the associated switching equipment. Conversely, it translates the various signals used in telephone switching into these on-and-off potentials to the carrier terminal.

Four conductors are used between terminal and switching equipment. Two of them are for voice transmission and two for signaling, one in each direction. Terminal and switching equipment may be in the same location or some distance apart, since a conductor resistance of up to 300 ohms is permissible without special provisions.

There are many different types of trunk circuits and repeaters, since there are many different methods of operating telephone systems. All consist, however, of relays, retardation coils, capacitors, and resistors. Some of the circuits are simple, employing only three relays. Others are of varying complexity, depending on how they are used and what they have to do. The toll circuit between an automatic exchange and a toll board, discussed above, is an example.

On an incoming call, the following procedure must take place: seizure of the local equipment, busying of the repeater against attempted outgoing calls, transference of dial pulses from the signal leads to the talking loop, return of supervision to the operator when the called subscriber answers, flashes his switchhook or disconnects, and release of the connection from the distant end. On an outgoing call to toll, on the other hand, this sequence must occur; seizure of the carrier circuit and signaling of the distant operator, return of ring-back tone to the calling subscriber, signaling of the automatic equipment when the operator answers, forwarding of identification to the operator if the call originates from a pay station (a repeat identification on challenge), forwarding of a disconnect signal when the calling subscriber hangs up, and release of the connection when both the operator and the calling subscriber disconnect.

The same general method of operation described above can be applied to many other types of telephone traffic—such as intertoll dialing between remote toll centers, or interconnection of several automatic tele-

hone centers by carrier dialing circuits which permit ubscribers to complete connections themselves without he assistance of an operator. The problem of sub-criber dialing in toll traffic has become increasingly nportant, and a simple carrier-dialing system contrib-tes a great deal to its solution.

Public toll dialing, employing the normally sup-ressed speech carrier as a signaling channel, was first sed in commercial traffic by the Interstate Telegraph Company between Bishop and Leevening, Calif. The ialing equipment was designed and manufactured by utomatic Electric Company of Chicago, and the arrier system by Lenkurt Electric Company of San rancisco. Several similar systems have since been laced in service.

A typical example is a Director network of several idely separated Strowger Automatic exchanges in Venezuela. All calls between offices are completed by the subscribers themselves, without the assistance of an operator. Some of the offices are interconnected by carrier dialing circuits.

In all these applications the carrier equipment and signal terminals are identical, with the trunk circuits and repeaters, custom-made for the purpose, accomplishing the special functions.

Carrier dialing also solves the problem of automatic operation over radio links. Carrier telephone channels are superimposed on the radio carrier, and dialing or signaling is performed through the telephone carrier signaling channel exactly as described for wire communications. The first public use of automatic impulsing over radio links was when the Mutual Telephone Company of Hawaii installed Automatic Electric and Lenkurt equipment for dialing inter-island connections.

Nomograms for Ionosphere Control Points*

JAMES C. W. SCOTT†, MEMBER, IRE

Summary—Knowing the length of a radio circuit and the lati-des of its terminals, nomograms are given which permit rapid erivation of the latitudes of the ionospheric control points. The se of world charts of maximum usable frequency is thus facilitated.

THE PROVISIONAL FREQUENCY BOARD (PFB) of the International Telecommunications Union now meeting in Geneva, Switzerland, has he difficult problem of preparing a new international adio-frequency list that will satisfy the growing require-ents of all countries for space in the radio spectrum. n order to accomplish this task, the spectrum must be tilized with maximum efficiency. The PFB is, there-ore, attempting to elaborate rules for the assignment f those frequencies to each circuit which will give op-mum results over the whole period of a sunspot cycle or all seasons and all times of the day.

In this undertaking, the measurements of over 60 nosphere recording stations situated all over the orld are being fused to predict the maximum usable equencies that should be used at any time on a circuit f given length with terminals at given latitudes. From hese ionospheric measurements, contour charts of aximum usable frequency are prepared by a number f radio-propagation laboratories such as the Central adio Propagation Laboratory, Washington, D. C. hese charts give the muf as a function of latitude and local time for a given month and a given period of the cycle of solar activity.

In applying these charts to find the optimum frequencies for a particular circuit, it is necessary to know the latitude of the control points in the ionosphere for the great circle path of propagation between transmitter and receiver. It is the conditions in the ionosphere at the latitude of these control points which determine transmission over the circuit and not the conditions directly over the transmitter and the receiver. Consequently, we must be able to trace out the great circle path of propagation and locate the control points upon it.

It is well known that for paths under 4,000 km, propagation is chiefly by refraction at the midpoint of the path so that conditions at the midpoint control transmission. For such circuits, the midpoint of the path is the control point. For paths longer than 4,000 km, single-hop propagation is impossible because the curvature of the earth cuts off the ray path. For such circuits, propagation is by two or more reflections back and forth between the earth's surface and the ionosphere so that, in effect, transmission is guided between the earth's surface and the ionosphere. Under these conditions, in practice, the effective control points are found to be 2,000 km from each end.

The two following nomograms (Figs. 1 and 2) were developed for use by the PFB to permit rapid derivation of the latitude of circuit control points from the positions of the terminals. It is thought that they may be of value

* Decimal classification: R082×R115.1. Original manuscript received by the Institute, June 24, 1948; revised manuscript received, ptember 29, 1948.

† Radio Propagation Laboratory, Ottawa, Ontario, Canada.

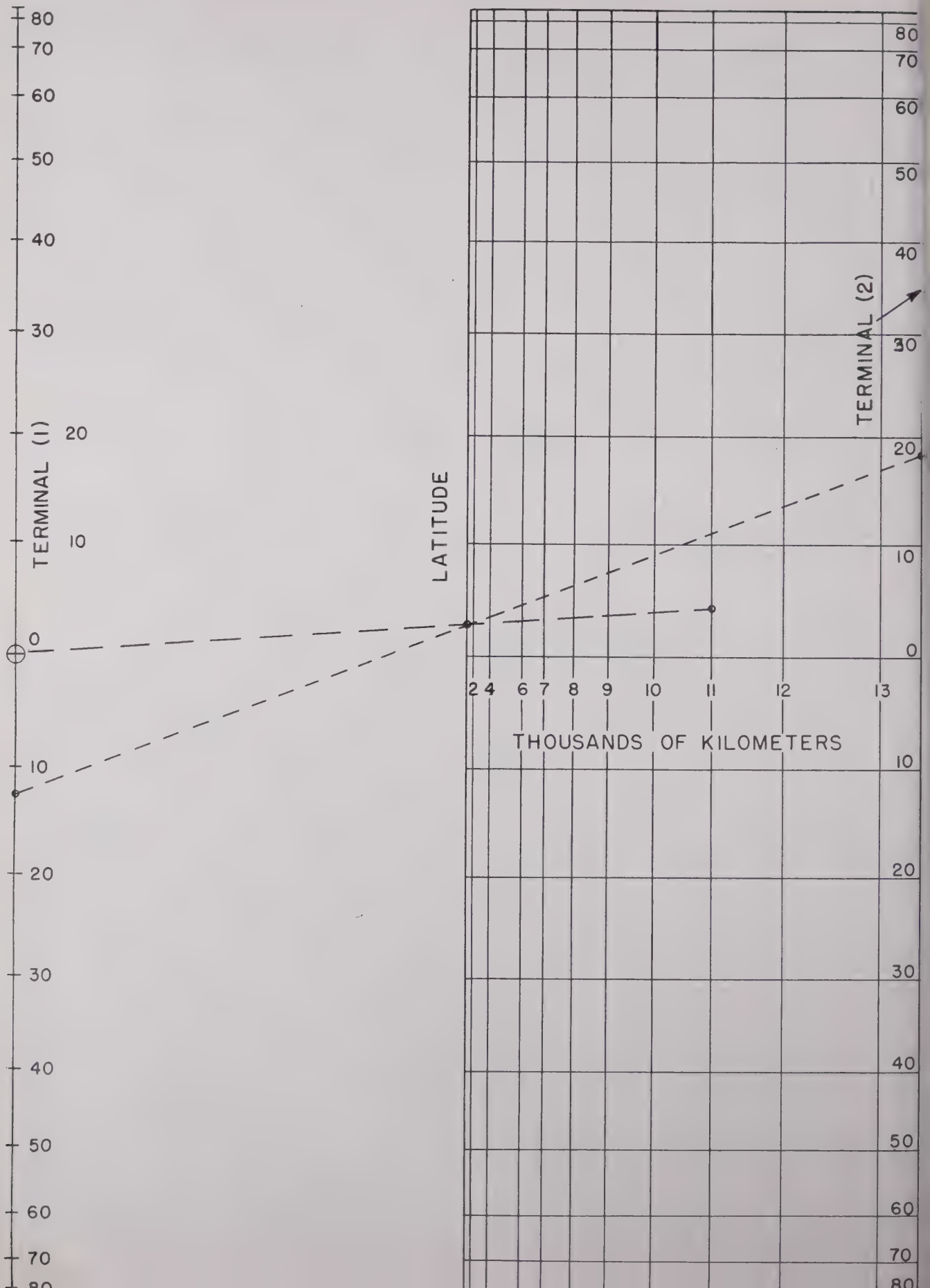
80
70
60
50
40
30
20
10
0
10
20
30
40
50
60
70
80
TERMINAL (1)
LATITUDE
TERMINAL (2)
2 4 6 7 8 9 10 11 12 13
THOUSANDS OF KILOMETERS

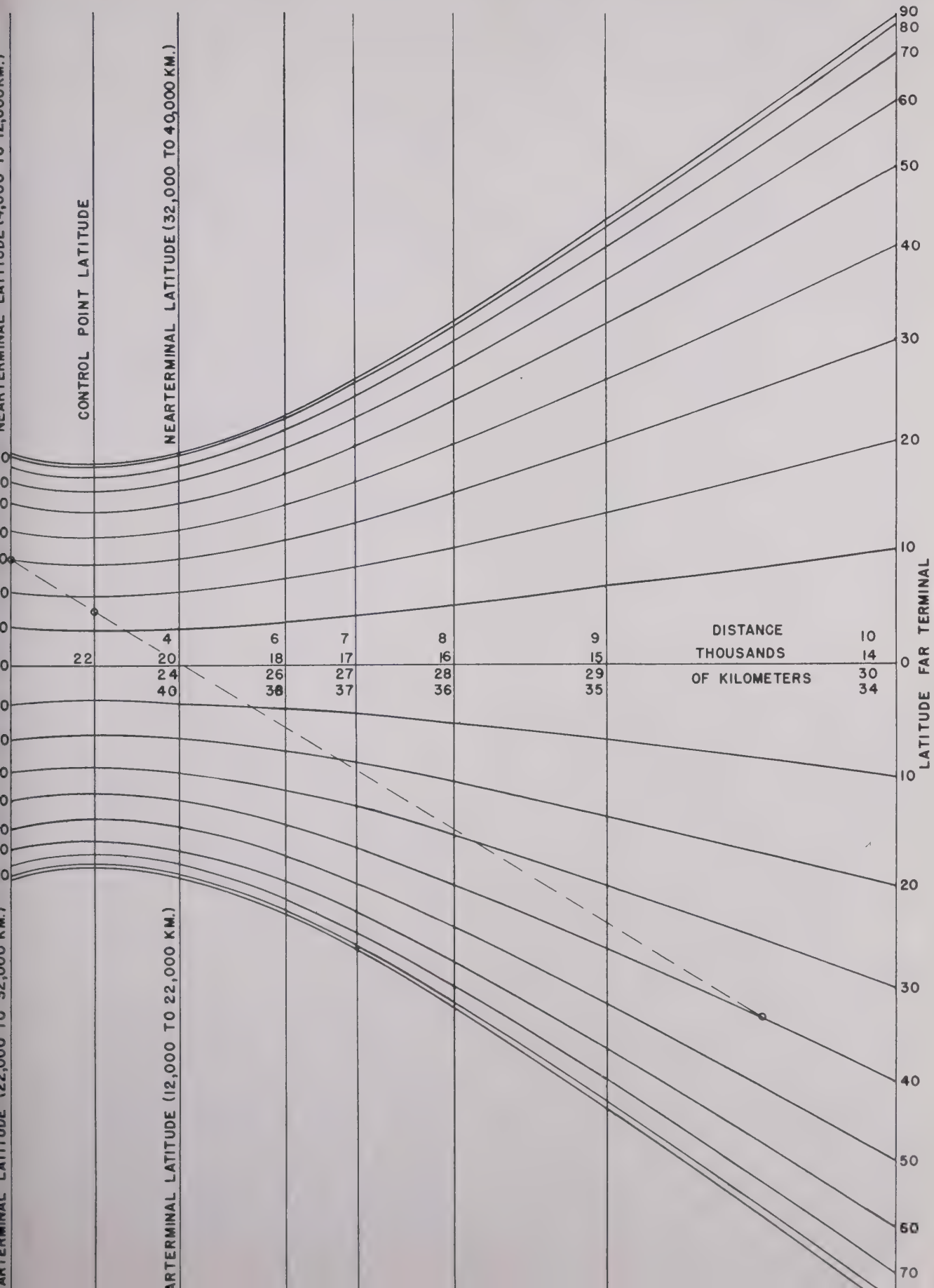

Fig. 2—Nomogram for latitudes of 2,000-km control points.

to other radio engineers concerned with propagation problems.

The construction of nomograms is based on the well-known condition for collinearity:[1]

$$\begin{vmatrix} x_a & y_a & 1 \\ x_b & y_b & 1 \\ x_c & y_c & 1 \end{vmatrix} = 0.$$

In this determinant, x_a, y_a; x_b, y_b; x_c, y_c are the cartesian co-ordinates of three points a, b, and c. Its vanishing is the condition that these three points be on the same straight line. Consequently, if a, b, and c are points on three curves determined by three parameters u, v, and w so that the determinant may be written

$$\begin{vmatrix} f_1(u) & f_2(u) & 1 \\ f_3(v) & f_4(v) & 1 \\ f_5(w) & f_6(w) & 1 \end{vmatrix} = 0.$$

The vanishing of this determinant insures that corresponding values of u, v, and w on the three curves are collinear. Thus, to construct a nomogram for an equation $f(u, v, w) = 0$, it is only necessary that this equation can be written in the above determinant form.

The relations of spherical trigonometry give the latitude L_K of the midpoint of a great circle path in terms of its length d and the latitudes of its terminals L_R and L_T.

$$\sin L_K = \frac{\sin L_R + \sin L_T}{2 \cos d/2}.$$

This equation may be put into the required determinant form to represent a nomogram for L_K in terms of d and the sum of sin L_R and sin L_T

Midpoint Nomogram Equations

$$\begin{vmatrix} 1 & \frac{1}{2}(\sin L_R + \sin L_T) & 1 \\ \sec \frac{d}{2} & \sin L_K & 1 \\ 0 & 0 & 1 \end{vmatrix} = 0.$$

Now, if we also write the identity sin L_R+sin L_T = (sin L_R+sin L_T) in the form

$$\begin{vmatrix} 1 & \frac{1}{2}(\sin L_R + \sin L_T) & 1 \\ 2 & \sin L_R & 1 \\ 0 & \sin L_T & 1 \end{vmatrix} = 0$$

we obtain a combined nomogram for L_K in terms of d, L_R, and L_T. This is the nomogram drawn for the midpoint latitude.

Its use is illustrated by the example. If the path is shorter than 2,000 km it is necessary only to draw a line from the transmitter latitude on the left-hand scale to the receiver latitude on the right-hand scale, and then read the midpoint latitude off the middle, zero range, scale. If the circuit is longer, a second line must be drawn through the point just found and through zero on the left-hand scale. This line will intersect the required midpoint latitude at the distance ordinate corresponding to the path length.

Further considerations of spherical trigonometry lead to the following equation for the latitude of the control point 2,000 km from one end of the path.

$$\frac{\sin L_T}{\sin 18^\circ} + \frac{\sin L_R}{\sin (d - 18^\circ)} = \sin L_{KT}(\cot 18^\circ + \cot (d - 18^\circ))$$

Here L_{KT} is the latitude of the control point 2,000 km from the transmitter and 18° is the angular distance equal to 2,000 km on the earth.

This equation may be transformed into the following equivalent determinant form which defines the nomogram drawn for the 2,000-km control points.

2,000-km Control-Point Nomogram

$$\begin{vmatrix} \frac{\sin L_T}{\cos 18^\circ} & -\tan 18^\circ & 1 \\ \sin L_{KT} & 0 & 1 \\ \frac{\sin L_R}{\cos (d - 18^\circ)} & \tan (d - 18^\circ) & 1 \end{vmatrix} = 0.$$

The use of this nomogram is as follows:

The latitude of the terminal nearest the control point is read off the ordinate to the left or right of the control-point ordinate for the ranges as marked. However, when the range is marked below the equatorial line, it is necessary to change the sign of the far terminal latitude. Thus for ranges between 12,000 and 32,000 km, if the far terminal is in the northern hemisphere, the equivalent southern latitude must be used in the nomogram and vice versa. The example gives a control-point latitude of 16° north when the near terminal is at 30° north. The circuit is either 29,600 km long with the far terminal at 40° north or is 9,600 km long with the far terminal at 40° south.

It is interesting to note that, for the critical ranges of 12,000 or 32,000 km, which on the chart are at an infinite distance to the right, the nomogram can be used quite easily by remembering that parallel lines meet at infinity. In this case, it is merely necessary to line up the latitude of the near terminal, at the proper ordinate, with the straight edge parallel at the extreme right to the curve corresponding to the far terminal latitude.

Since these nomograms together give the latitudes of the midpoint and of the control points 2,000 km from each end, propagation conditions along the path which depend on latitude can be quickly determined.

[1] S. Brodetsky, "First Course in Nomography," G. Bell and Sons, London, England; 1925.

Experimental Determination of the Distribution of Current and Charge along Cylindrical Antennas*

GIORGIO BARZILAI†

Summary—**This paper describes an experimental arrangement to determine the distributions of current and density of charge along cylindrical antennas.**

Using a wavelength of 1.90 meters, the distributions are determined for center-fed straight cylindrical antennas of a diameter of 29 mm, and lengths of 1.25 λ, 1.00 λ, 0.50 λ. For the first two cases, the measurements are repeated when a center self-tuned parasitic antenna, of the same length and diameter as the driven antenna, is situated at a distance of 0.30 λ and 0.15 λ. The distributions are determined also on the parasite.

To test the accuracy of the measurements and to relate the relative values of the current with the relative values of the density of charge, the distributions are determined on a coaxial line, having the inner conductor of the same diameter as the antenna under experiment, and fed at the same frequency as the antenna.

A few comparisons with theoretical results are made.

Introduction

THE PROBLEM of determining the distribution of current along an antenna is of the utmost importance, since the knowledge of this distribution allows the input impedance, and the spatial distribution of the radiated field, to be calculated. The hypothesis of the sinusoidal current distribution is acceptable when the antenna is very thin and short (not much longer than $\lambda/2$ for center-fed antennas), but for thick and long antennas, such as those used in microwave technique, this hypothesis leads to results that very often are not even a rough approximation.

In recent years, the theoretical determination of the distribution of current along an antenna has been studied by many authors,[1–5] and very interesting results have been obtained. However, the numerical calculations are invariably difficult and laborious even in the simplest cases. The majority of the investigations on this subject are theoretical and few are experimental, and the experimental results usually refer to the input impedance.

This paper describes an experimental arrangement to determine the distributions of the moduli of current and density of charge along thick cylindrical antennas. The distributions determined are relative, but it is possible, by measurements on a coaxial line, to refer both distributions to only one reference value of current or charge so that, once this reference value is supposed to be known, from the relative distributions, the absolute distributions can be obtained. In this way, using the equation of continuity, it is possible to calculate the phase of the current and the phase of the density of charge at every point of the antenna. It will be noted, however, that, since the equation of continuity is a differential relation and graphical procedure must be used, great accuracy cannot be expected in the estimates of the phases.

Some experimental results, relating to a wavelength of 1.90 meters, were recorded in diagrams. They refer to center-fed straight cylindrical antennas of a diameter of 29 mm, and lengths of 1.25λ, 1.00λ, and 0.50λ. It was considered of interest to carry out measurements on antennas with a parasitic element. The experiments with the parasitic antenna were carried out with a center self-tuned parasite of the same length and diameter as the driven antenna, situated at distances of 0.30λ and 0.15λ. The distributions of current and charge were determined also on the parasite.

The Experimental Equipment

Consider Fig. 1, a hollow cylindrical conductor maintained in a state of forced electrical oscillation of a very high frequency. Suppose this conductor to be longitudinally slotted, and a small loop or probe to be situated as indicated in Figs. 1(a) and 1(b). If the projections Δr and $\Delta' r$ of the loop and probe above the metallic surface are sufficiently small, it can be assumed that the emf induced on the loop is essentially due to the magnetic field **H** associated with the conductive current **I**, while the emf induced on the linear probe is due to the electric field **E** arising out of surface charge ρ. We can, therefore, write

$$\mathbf{I} = K_{AB} \cdot \mathbf{V}_{AB} \tag{1}$$

$$\rho = K_{A'B'} \cdot \mathbf{V}_{A'B'} \tag{2}$$

where

I = the conductive current, in amperes,

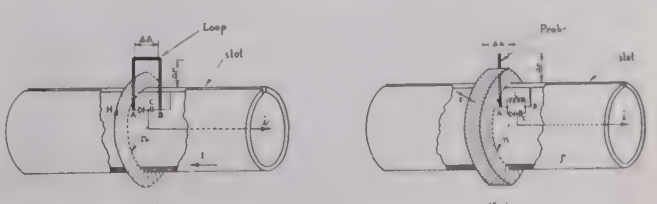

(a) (b)

Fig. 1—Sketch to explain the method used to determine the distributions of current and density of charge along the antenna.

* Decimal classification: R221×R326.611. Original manuscript received by the Institute, August 30, 1948; revised manuscript received, November 29, 1948.

† Compagnia Generale Elettronica, Electronics Park, Syracuse, N. Y.

[1] S. A. Schelkunoff, "Theory of antennas of arbitrary size and shape," Proc. I.R.E., vol. 21, pp. 493–521; September, 1941.

[2] C. J. Boukamp, "Hallen's theory for a straight perfectly conducting wire," *Physics*, vol. 9, p. 609; July, 1942.

[3] R. King and C. W. Harrison, "The distribution of current along a symmetrical center-driven antenna," Proc. I.R.E., vol. 31, pp. 548–567; October, 1943.

[4] Marion C. Gray, "A modification of Hallen's solution of antenna problem," *Jour. Appl. Phys.*, vol. 15, pp. 61–65; January, 1944.

[5] R. King and D. Middleton, "The cylindrical antenna," *Quart. Appl. Math.*, vol. 3, pp. 302–335; January, 1946.

flowing through that section of the conductor on which the center of the loop is situated ($\Delta a \ll \lambda$)

ρ = the linear density of charge, in coulombs per meter, at that section of the conductor on which the probe is situated ($\rho \Delta' a$ = total charge existing on that portion of conductor of length $\Delta' a \ll \lambda$)

$\mathbf{V}_{AB}$ and $\mathbf{V}_{A'B'}$ = the voltages measured across the terminals A–B and A'–B'

K_{AB} and $K_{A'B'}$ = two constants independent of the position of the loop or probe along the conductor.

Measurements of the phases of $\mathbf{V}_{AB}$ and $\mathbf{V}_{A'B'}$ are possible but difficult, and the equipment was designed to measure only the moduli of those voltages. For this purpose a small crystal, of the type used in microwave receivers, was used. The rectifiers circuits for the loop and probe are shown in Fig. 1(a) and Fig. 1(b).

The practical realization of the system sketched in Fig. 1 is shown in Fig. 2, where the slotted conductor, the carrier which slides inside the conductor and contains the rectifier crystal, capacitor C, and choke L, the loop that can be inserted in the carrier instead of the probe, and the flat end of the antenna removed, are clearly visible. It was assumed $\Delta a = \Delta r = \Delta' r = 1$ cm.

The whole experimental arrangement is sketched in Fig. 3. The oscillator *10*, employing a push-pull of 4,304 Ca/F (834), feeds the driven antenna *0* through the line *8*. The stub *7* is a matching device. The wire, carrying the rectified current i, runs inside one of the brass tubes of the lines *8* and *9*, and it is connected at the reflection galvanometer *4*, situated inside the screened box *3*. The purpose of line *9* is to remove the operator to a reasonable distance from the antennas. Line *9* is a short-circuited at the end and its length is $7/4\lambda$.

The parasitic antenna *1* is slotted in the same way as the driven antenna, so that the distributions can also be

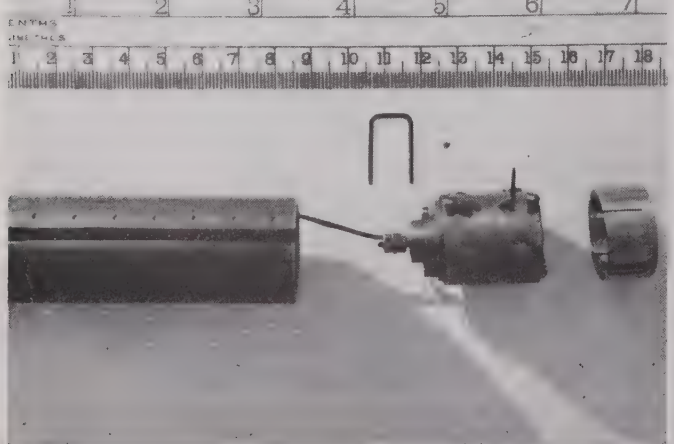

Fig. 2—View of the practical layout of the system used to measure the distributions of current and charge.

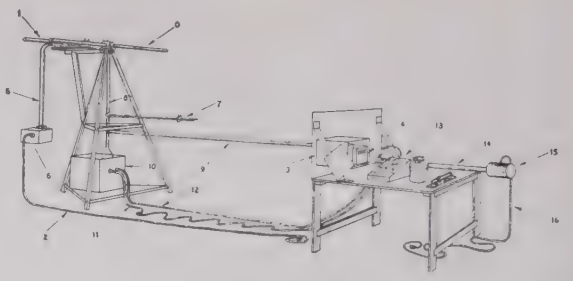

Fig. 3—Perspective sketch of the whole experimental arrangement.

determined on the parasite, using the same carrier used for the driven antenna. The wire, carrying the current i, runs inside one of the tubes of line *5* and it is connected to an insulated socket on the screened box *6*. The screened cable *2* is plugged into the above said socket and the other end can be connected to the galvanometer *4*, when the measurement on the parasite is carried out. To tune the parasitic antenna, after it was removed at a distance of about 2 wavelengths from the driven antenna, a short-circuit bridge on line *5*, and the indication of the galvanometer *4*, were used.

The oscillator *10* also feeds, through the coaxial cables *11* and *12* (polyethylene cables), the coaxial line *14*, air insulated and short-circuited at the end. Line *14* has a length of about 1.60 meters, the inner conductor has the same diameter as the antennas and it is slotted in the same way, so that the same carrier used for the antennas can be employed, and the internal diameter of its outer conductor is 68 mm. The vacuum-tube voltmeter *13* (General Radio 726 A) indicates the input voltage of line *14*. The screened box *15* and the cable *16* have the same purpose as *6* and *2*.

By inspection of Fig. 3, it is clear that all the wires carrying the rectified current i are screened.

In the operation of the equipment, I and ρ are the absolute values of the moduli of current and linear density of charge, and I_r and ρ_r are the relative values of current and linear density of charge, referred to the reference values I_{ref} and ρ_{ref} ($I_r = I/I_{\text{ref}}$ and $\rho_r = \rho/\rho_{\text{ref}}$). When particular reference is made to the values relating to the coaxial line, to the driven antenna, or to the parasite, we shall add the indexes l, 0 and 1, respectively to those symbols. For instance, we shall indicate with I_{1r} the relative value of the current on the parasite.

To determine the relative distributions of current and charge, the current i was always reset to a certain value i_c, by varying the output of the oscillator. The output of the oscillator was controlled by varying the plate voltage. Tests, which will be reported later, were made to check that the variations of the plate voltage of the oscillator did not affect the measurements appreciably.

By using the above procedure, the quantity under measurement is inversely proportional to the voltage indicated by the vacuum-tube voltmeter *13* and, therefore, we can write

$$I = K_I \frac{1}{V_I} \tag{3}$$

$$\rho = K_\rho \frac{1}{V_\rho} \tag{4}$$

here K_I and K_ρ are two constants, independent from ne position of the carrier along the conductor and V_I nd V_ρ are the voltages indicated by the vacuum-tube oltmeter *13*, when the current i is set at the value i_c. In ne following, we shall indicate the voltages appearing (3) and (4) by a capital V having the quantity to hich that voltage refers for index.

Now, it is possible to show how to refer both distribuons of current and charge to only one reference value current or charge. For the coaxial line *14*, the follow-g relation holds

$$\frac{E_{l\max}}{H_{l\max}} = 377\Omega \tag{5}$$

here $E_{l\max}$ and $H_{l\max}$ are the moduli of the maximum ectric and magnetic field at the surface of the inner onductor of the coaxial line. Now, if we indicate with $_{\max}$ and $\rho_{l\max}$ the maximum current and density of harge on the coaxial line, we can write:

$$\frac{K_\rho}{K_I} = \epsilon_0 377 \frac{V_{\rho l\max}}{V_{Il\max}} \tag{6}$$

here $\epsilon_0 = 8.85.10^{-12}$ F/m.

We can also write the following relations, which hold respectively if they refer to the coaxial line, to the riven antenna, or to the parasite

$$\rho = \frac{K_\rho}{K_I} \frac{V_{I\,\mathrm{ref}}}{V_{\rho\,\mathrm{ref}}} I_{\mathrm{ref}}\rho_r \tag{7}$$

$$I = \frac{K_I}{K_\rho} \frac{V_{\rho\,\mathrm{ref}}}{V_{I\,\mathrm{ref}}} \rho_{\mathrm{ref}} I_r. \tag{8}$$

From (7) and (8) it can be seen that, once the ratio $_\rho/K_I$ has been determined from (6), through measrements on the coaxial line, both distributions ρ_r nd I_r can be referred to a unique reference value I_{ref} ρ_{ref}. If, for instance, we suppose I_{ref} to be known, om (7) we can obtain the absolute distribution of harge.

Experimental Results

The measurements were made indoors. The antennas ere situated at a height of about one wavelength (2 etres) from the floor, and all the reflecting obstacles ere removed within a radius of about 2 wavelengths. ests were made to insure that all the wires, carrying the ctified current i, were completely screened. To do that was only necessary to remove the loop or the probe and observe if any indication was recorded by the galanometer when the system was excited. No appreciable dications were observed in those conditions. People alking around the antennas, even at a considerable disnce, produced variations on the indications of the alvanometer. In order to appreciate the order of magitude, these spurious effects and also the effect of the floor, a half-wavelength tuned antenna was placed in different positions, at a distance of about 2 wavelengths. Absolute variations of the order of 2 per cent were observed in the absolute values of current and charge, but the relative distributions were not appreciably affected.

A first set of measurements was carried out on the coaxial line, both to test the accuracy of the measurements and to determine the ratio K_ρ/K_I from (6). From these measurements, it can be concluded that the approximation that can be expected is satisfactory, as the experimental curves were quite near to the theoretical sinusoidal ones, and the errors did not exceed a few per cent of the maxima values. The chief source of errors was probably the harmonics of the oscillator. The minimum current was about 4 per cent of the maximum value instead of zero, while the minimum value of the density of charge was practically zero. This indicates presence of harmonics. The wavelength on the coaxial line was 1.90 meters for any one of the plate voltages used, and difference of 2 or 3 mm could be appreciated. The curves of current and charge were somewhat displaced with respect to one another. Differences of about 2°, with respect to the theoretical value of 90°, were found.

For

$$i_c = 30\mu \text{ amp}$$

$$V_{I\max} = 7.9 \text{ volts}, \qquad V_{\rho\max} = 9 \text{ volts}$$

and, therefore, from (6)

$$\frac{K_\rho}{K_I} \approx 3.8.10^{-9} \text{ seconds per meter.}$$

The ratio K_ρ/K_I was measured several times and under different conditions of operation of the oscillator, and no appreciable differences were found.

Both arms of the antenna and parasite were slotted in the same way, so that it was possible to test whether or not the system was balanced. This test was made before starting the measurements and, when necessary, the system was readjusted.

The results obtained with antennas of a half length $l = 0.625\lambda$ ($l \approx 1.19$ meters) are recorded in Fig. 4. $I_{0\,\mathrm{ref}}$ is the maximum value of the current on the driven antenna and $\rho_{0\,\mathrm{ref}}$ is the value of the linear density of charge at $x = 1.15$ meters ($x = 0$ at the center of the antenna). The values recorded in Fig. 4(a) refer to the antenna without the parasitic element, and two sets of measurements, corresponding to two different values of the current i_c, were recorded. The black circles refer to $i_c = 30\mu$ amp, except for those points for which it was impossible to reach that value of i_c. In these cases, the current i_c was set at a value lower than 30μ amp, and the calibration curve of the rectifying system used. The white circles refer to $i_c = 3\mu$ amp. Small differences, of about 1 to 2 per cent, were found between the two sets of measurements, despite the very different conditions of operation of the oscillator. For instance, for the set cor-

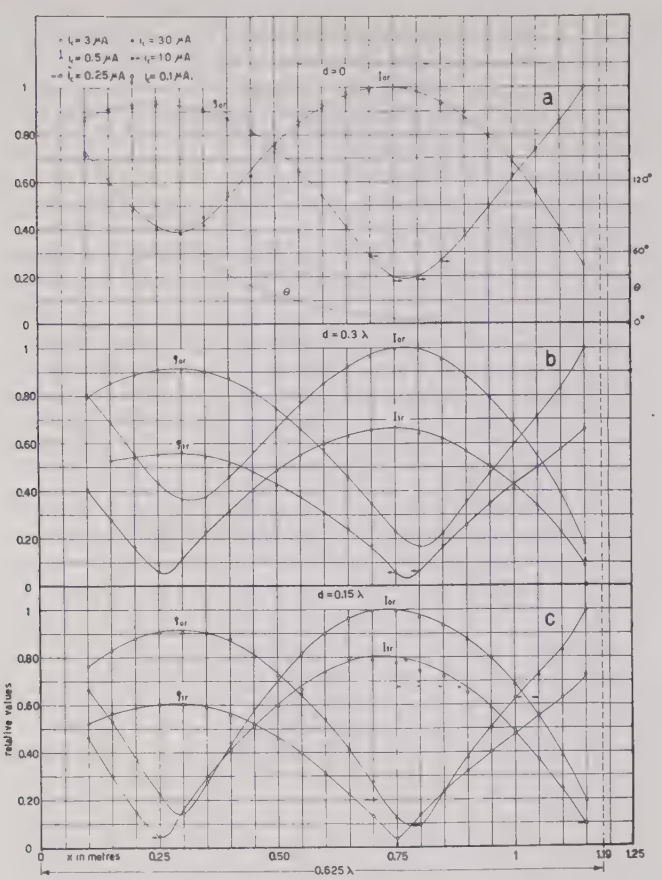

Fig. 4—Experimental relative distributions of the moduli of current and density of charge, along the driven antenna and the center self-tuned parasite, for $\lambda = 1.90$ m, $l = 0.625\lambda$, and distances between the two antennas $d = 0$, 0.15λ, and 0.30λ.

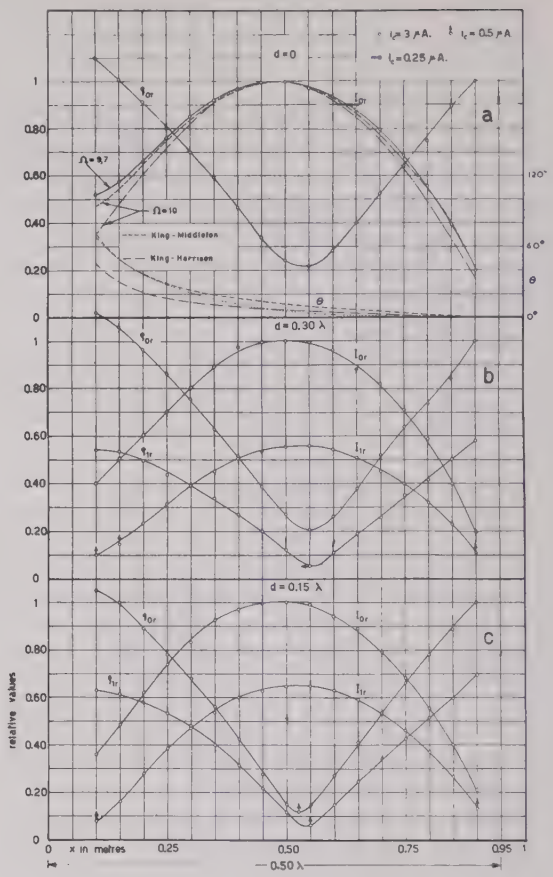

Fig. 5—The same as Fig. 4 but for $l = 0.50\lambda$.

responding to the black circles, the plate voltage of the oscillator varied from 400 to 1,050 volts in the measurements with the loop, and from 360 to 1,300 volts in those with the probe, while for the white circles, the corresponding values of the plate voltage of the oscillator were 220 to 760 volts and 210 to 850 volts. This test was made to ensure that the procedure of varying the plate voltage of the oscillator did not appreciably affect the measurements.

The curves of Figs. 4(b) and 4(c) refer to antennas with a center self-tuned parasitic element, of the same length and diameter as the driven antenna, situated at a distance $d = 0.3\lambda$ and $d = 0.15\lambda$. For both values of the distance d, it was assumed $I_{1\,\mathrm{ref}} = I_{0\,\mathrm{ref}}$ and $\rho_{1\,\mathrm{ref}} = \rho_{0\,\mathrm{ref}}$.

The curves of Fig. 5 are similar to those of Fig. 4, except that they refer to a value of $l = 0.5\lambda$ ($l = 0.95$ meter). In these diagrams, $I_{0\,\mathrm{ref}}$ is equal to the value of the maximum current on the driven antenna, and $\rho_{0\,\mathrm{ref}}$ is equal to the value of the linear density of charge on the driven antenna for $x = 0.90$ meter. For both values of the distance d, it was assumed $I_{1\,\mathrm{ref}} = I_{0\,\mathrm{ref}}$ and $\rho_{1\,\mathrm{ref}} = \rho_{0\,\mathrm{ref}}$.

Fig. 6 shows the measurements for an antenna of half length $l = 0.25\lambda$ ($l = 0.475$ meter) without parasitic element. $I_{0\,\mathrm{ref}}$ is the value of I_0 for $x = 0.10$ meter, and $\rho_{0\,\mathrm{ref}}$ is the value of ρ_0 for $x = 0.425$ meter.

In all the measurements recorded in Figs. 4, 5, and 6, the minimum value of x was $x = 10$ cm, because the holders, clamping the heavy tubes constituting the antennas, did not permit the smaller value of x to be reached.

TABLE I

l/λ	d/λ	$V_{I_{0\,\mathrm{ref}}}$	$V_{\rho 0\,\mathrm{ref}}$	$K_\rho V_{I_{0\,\mathrm{ref}}}/K_I V_{\rho 0\,\mathrm{ref}}$
0.625	0 (black circles)	35 volts	37 volts	3.6×10^{-9} seconds per meter
0.625	0 (white circles)	18 volts	19 volts	3.6×10^{-9} seconds per meter
0.625	0.30	17 volts	17.5 volts	3.7×10^{-9} seconds per meter
0.625	0.15	14 volts	14.5 volts	3.7×10^{-9} seconds per meter
0.50	0	17.4 volts	19.1 volts	3.5×10^{-9} seconds per meter
0.50	0.30	18.5 volts	18.5 volts	3.8×10^{-9} seconds per meter
0.50	0.15	15 volts	16 volts	3.6×10^{-9} seconds per meter
0.25	0	10.5 volts	11.5 volts	3.5×10^{-9} seconds per meter

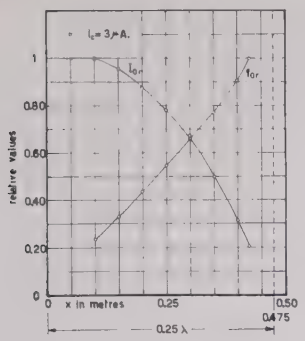

Fig. 6—The same as Fig. 4 except that the measurements were carried out without parasite, and for $l=0.25\lambda$.

Table I gives the values of $V_{I_0\,\mathrm{ref}}$ and $V_{\rho 0\,\mathrm{ref}}$ found in the different cases, and the corresponding values of the constant appearing in (7).

The distributions of the phases of current and density of charge can be obtained, with a reasonable approximation, using the equation of continuity which, in our case, can be written as follows:

$$\frac{d\mathbf{I}}{dx} = -j\omega\rho \tag{9}$$

where $\omega = 2\pi f$.

Now, dividing the antenna in m equal parts of length Δm, we can apply (9), written in an approximate finite form, to each element of length Δm, using (7) and the experimental values recorded in the last column of Table I. The above procedure can be easily understood by inspection of Figs. 7(a) and 7(b), which refer to the cases of Figs. 4(a) and 5(a), respectively. Each triangle drawn in Fig. 7 has one side which represents the vector $j\rho_{(n)}$, where $\rho_{(n)}(n=1, 2, \cdots, m)$ is the density of charge at the center of the nth element. The other two sides represent the vectors $\mathbf{I}_{(n)}/\omega\Delta_m$ and $\mathbf{I}_{(n+1)}/\omega\Delta_m$, where $\mathbf{I}_{(n)}$ and $\mathbf{I}_{(n+1)}$ are the currents at the two ends of the nth element.

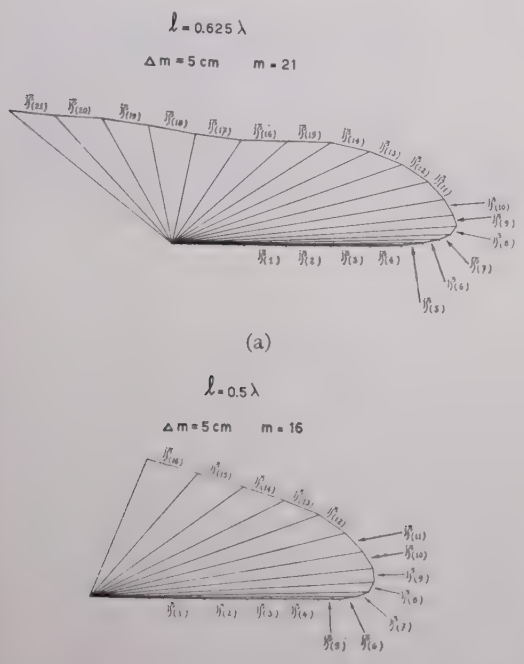

Fig. 7—Geometrical construction, based on (9), to find out the distribution of the phase of the current along the antenna.

In Figs. 4(a) and 5(a) are recorded the distributions of the phase θ of the current (dotted lines) obtained from Figs. 7(a) and 7(b). θ was assumed equal zero at the open end of the antenna.

It was thought interesting to compare some of the experimental results with theoretical calculations. Unfortunately, the distributions calculated refer to a few cases, and they were carried out only for the current, as this quantity allows the input impedance to be calculated. No theoretical calculations seem to be available for the distribution of the charge.

In Fig. 5(a) we have recorded the theoretical results obtained by King and Harrison[3] and by King and Middleton,[5] assuming 1 equal to the modulus of the maximum current. The calculations refer to the case of $l=0.50\lambda$ and $\Omega = 2 \ln 2l/r_0 = 10$, and the experimental results to $l=0.50\lambda$ and $\Omega = 9.7$. As it can be seen from Fig. 5(a), the results of King and Middleton seem to agree better with the experiments than those of King and Harrison. It is well known, in fact, that these last calculations are less approximate than the first ones.

For $l=0.625\lambda$ and $\Omega=10$, King and Harrison calculated the distribution of current, but unfortunately the more approximate solution obtained by King and Middleton has not been used. Peroni[6] calculated the distribution of current for $l=0.625\lambda$ and $\Omega=11.1$, using his own graphical method. The experimental results recorded in Fig. 4(a) refer to $l=0.625\lambda$ and $\Omega=10.2$. In this case also, the values of Ω do not differ much, and therefore, it is interesting to compare these results. We shall compare the most characteristic quantities; i.e. the ratio of the maximum current $I_{0\,\max}$ to the minimum current $I_{0\,\min}$, and the total variation of the phase θ along the antenna from $x=10$ cm to $x=119$ cm. The theoretical and experimental results are shown in Table II.

TABLE II

	$I_{0\,\max}/I_{0\,\min}$	Variation of θ from $x=10$ cm to $x=119$ cm
King and Harrison	6.2	162°
Peroni	2.9	130°
Experimental	2.6	142°

ACKNOWLEDGMENT

The author wishes to thank L. G. H. Huxley of the University of Birmingham, England, who suggested the use of slotted antennas, for his kind help in obtaining from the electrical department of the University of Birmingham the necessary mechanical and electrical facilities for preparing this paper.

[6] B. Peroni, "Antenne e Propagazione delle Onde Elettromagnetiche," Michele Dell'Aira, Roma, 1945.

The Course-Line Computer for Radio Navigation of Aircraft*

F. J. GROSS†, ASSOCIATE, IRE

Summary—**This paper describes an experimental model of a course-line computer which accepts bearing information from a vhf omnirange receiver and distance information from distance-measuring equipment and converts it to simple track-guidance directions for the pilot of an aircraft. Results of flight tests over eight parallel tracks are presented in map form. Theoretical relations between computer errors and errors in the bearing and distance information are also presented.**

Introduction

THE COURSE-LINE computer is a recent development in a group of aircraft navigation aids which already includes the CAA instrument-landing system,[1] the vhf omnirange,[2] and distance-measuring equipment.[3]

The vhf omnirange system consists of a ground station and an airborne receiver. In the airborne omnirange receiver, the phase angle between two 30-cps voltages is a measure of the magnetic bearing of the line between the aircraft position and the ground station. These voltages are used to position a bearing indicator in the aircraft. The distance-measuring equipment (DME) system consists of an airborne transmitter and receiver and a ground transmitter and receiver. A pulse initiated in the airborne transmitter is received on the ground and retransmitted to the aircraft. A circuit in the airborne equipment measures the round-trip travel time of the pulse and develops a dc voltage which is proportional to the distance. This dc voltage is hereafter referred to as the range voltage.

The course-line computer is an analogue-type computer that uses this bearing and distance information to continuously calculate the deviation of the aircraft from a straight-line course selected by the pilot. The result is presented on a course-line deviation indicator such as that shown in the lower left-hand corner of Fig. 3. If the vertical pointer of this indicator is centered, the pilot knows that the aircraft is on the course line that he has selected. Furthermore, if the aircraft heading is within 90° of the bearing of the intended course, then a pointer deflection to the right indicates the course is to the pilot's right, and a left deflection indicates the course is to the left. This deviation indicator is the same one that is connected to the localizer receiver when the aircraft is using the CAA instrument-landing system. The computer also calculates the distance along the course between the aircraft and a selected destination and presents this information on a dial calibrated in miles.

Because there had been a great deal of theoretical and speculative discussion about computers, the CAA Office of Technical Development contracted with the Minneapolis-Honeywell Regulator Company to construct an experimental computer suitable for making flight tests with the bearing-distance facilities available at the Experimental Station at Indianapolis. To expedite delivery, weight and space limitations were excluded from the specifications. Also, the manufacturer was permitted to mount all but one of the indicator dials and controls in one unit which was to be mounted in the radio compartment of a DC-3 aircraft. The exception was the course-deviation indicator, which was to be mounted on the pilot's instrument panel. The computer is illustrated in Fig. 1. In future models, all essential controls and indicators will be available to the pilot, and it is estimated that the amplifier unit will be compressed to the size of a standard one-half ATR.

Fig. 1—Experimental model of course-line computer.

Operation

The method of operating the computer can be best described with the aid of the trigonometric diagram of Fig. 2. In setting the computer dials for a particular course, the following operations are performed:

(1) Draw the selected course line on the chart such as the heavy line through the destination in Fig. 2.

(2) Measure the bearing of the course with respect to magnetic north. In Fig. 2 this is the angle *C*.

(3) Set the course angle into the computer by adjusting dial *C* in upper-left center of Fig. 1.

(4) Locate the desired station on the chart and measure the course-line offset distance, which is the shortest distance between the station and the course.

* Decimal classification: R526. Original manuscript received by the Institute, June 6, 1948; revised manuscript received, December 28, 1948. Presented, 1948 IRE National Convention, New York, N. Y., March 22, 1948.

† Civil Aeronautics Administration, Experimental Station, Indianapolis, Ind.

[1] Peter Caporale, "The CAA instrument landing system," *Electronics*, Part I, vol. 18, pp. 116–124; February, 1945. Also Part II, vol. 18, pp. 128–135; March, 1945.

[2] Peter Caporale, "Status of vhf facilities for aviation," *Electronics*, vol. 20, pp. 90–95; October, 1947.

[3] Publication entitled, "Radio Pulse Distance Measuring Equipment," available from Aviation Information, Civil Aeronautics Administration, U. S. Department of Commerce, Washington 25, D. C.

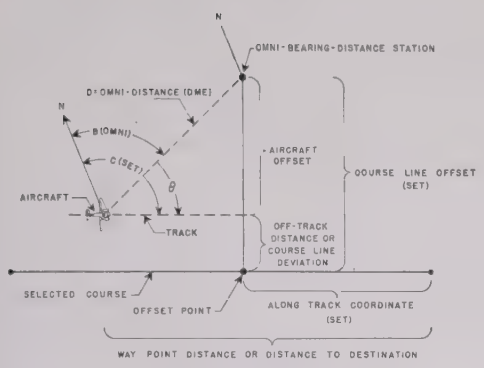

Fig. 2—Trigonometry of computer operation.

(5) Adjust offset dial at upper left of Fig. 1. Offset is o the left on the dial if station is to the left in passing as n Fig. 2. If station is going to be to the right in passing, hen the offset dial is set to the right.

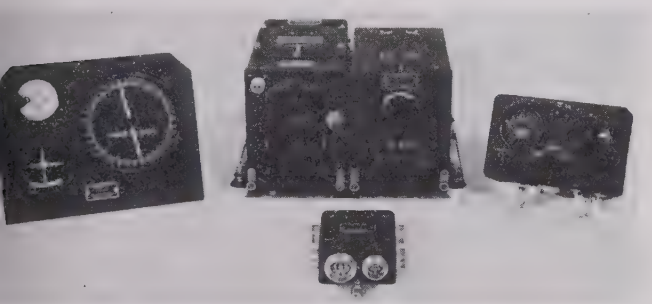

Fig. 3—Omnirange receiver used in computer tests.

(6) On the chart, locate the desired destination on the ourse and measure the along-track co-ordinate. This is ne distance between the destination and the point earest the omni station on the course, which is also the ot of the perpendicular from station to course.

(7) Adjust along track dial at upper right of Fig. 1. long track co-ordinate is the distance from the foot of ne perpendicular to the destination. If the destination beyond the offset point in Fig. 2, the dial is set to the ft, and if the destination precedes the offset point, the ial is set to the right.

(8) Tune in the selected station and switch course-eviation indicator to computer.

(9) Fly course-deviation indicator (cross-pointer in-trument) to place aircraft on course and keep it there. The course-deviation indicator has the same right or ft sensing as when flying omnirange or the instrument-nding-system localizer. However, the deflection of the ourse-deviation indicator is proportional to course-line eviation in miles in the computer, whereas it is propor-onal to angular deviation in localizer and omnirange quipments.

If the pilot wishes to fly another track parallel to the ne which he has already set up on the computer, he ay do so by setting the track selector either right or ft the desired number of indicated miles. For example, if he sets the track selector 10 miles right and flies the deviation indicator, the aircraft will travel a course 10 miles to the right of the course set up but parallel to it. Also, as one would expect, the destination will be displaced 10 miles right.

Installation

The panel of the computer is shown in Fig. 1. It was installed in CAA aircraft NC-182 and connected to the Aircraft Radio Corporation Model 15 variable-tuned omnirange receiver, shown in Fig. 3, and to a radar distance-measuring equipment shown in Fig. 4, which was constructed at the U. S. Naval Research Laboratory. The connections to the omni receiver were such that a servo-driven bearing selector in the computer was substituted electrically for the manual-bearing selector, and the omni leads normally connected to the course-deviation indicator were transferred to the input of the servo controlling the computer bearing dial. This servo positions the cylindrical dial in Fig. 1 so that it indicates bearing from aircraft to the omni station. The DME range voltage is supplied from a cathode-follower tube in the DME. The plate voltage of the cathode-follower tube, as well as the range voltage, is supplied to the computer. The ratio of these two voltages actuates a servo motor, so that it properly positions the dial labeled "Distance in Miles" at the lower-left center of Fig. 1.

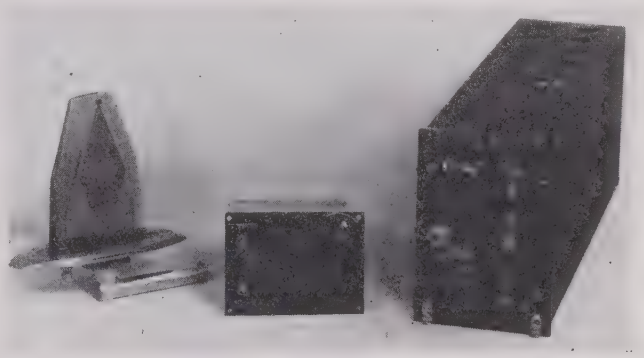

Fig. 4—Experimental distance measuring.

Circuitry of Experimental Computer

Fig. 5 is a simplified schematic diagram of the computer.

The distance-measuring-equipment range voltage acts through the distance servo motor in Fig. 5 to position the dual-distance potentiometer so that each of its output voltages are proportional to the distance D in Fig. 2. These voltages are applied to the resolver potentiometer whose left-hand wiper in Fig. 5 thereby develops a voltage proportional to the "aircraft-offset" of Fig. 2. The remainder of the circuit on the left side of Fig. 5 completes the calculation by subtracting voltage $D \sin (C-B)$ from the voltage set up by the "offset" dial and applies the difference to the course-deviation

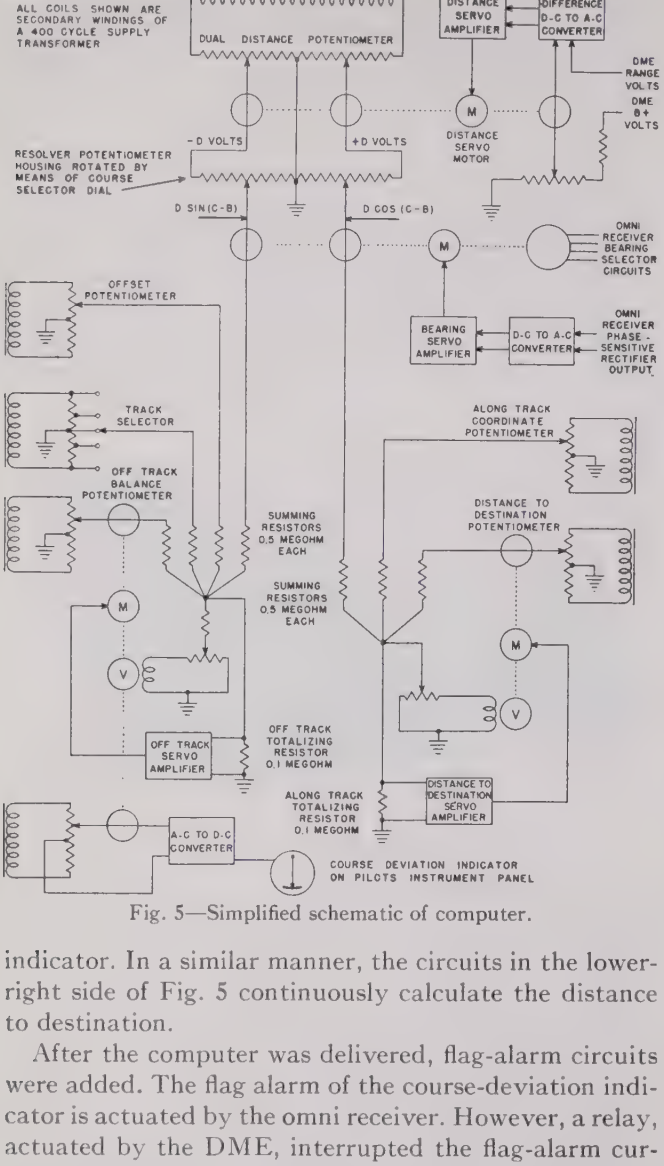

Fig. 5—Simplified schematic of computer.

indicator. In a similar manner, the circuits in the lower-right side of Fig. 5 continuously calculate the distance to destination.

After the computer was delivered, flag-alarm circuits were added. The flag alarm of the course-deviation indicator is actuated by the omni receiver. However, a relay, actuated by the DME, interrupted the flag-alarm current whenever the DME signal failed. Future development of more adequate flag-alarm circuits is contemplated.

Theory of Off-Track Errors

Given errors in bearing and distance information produce off-track errors of different magnitude at different points on a track. Since the omnirange errors are less than 3° and distance-measuring-equipment errors are less than 3 per cent, the following equation can be used to calculate the off-track error introduce by errors in the omni-bearing and the distance-measuring equipment:

$$\begin{bmatrix}\text{off-track error}\\ \text{caused by bearing}\\ \text{and distance errors}\end{bmatrix} = 0.017bD\cos(C-B) - d\sin(C-B)$$

where

b = the omni-bearing error in degrees (assumed less than 4°)

d = the DME distance error in miles (assumed le than 3 miles)

D, B, and C are defined in Fig. 2.

Note that, in this equation, the bearing error makes negligible contribution to the off-track error when th $\cos(C-B)$ is zero, namely when $(C-B)$ is 90°. Th condition exists when the aircraft is at the offset poin which is the point nearest the station for any trac Conversely, the bearing error has its greatest effect o the off-track error at the extremes of the track whe the angle $(C-B)$ is small and, therefore, $\cos(C-B)$ very nearly unity. As shown in Fig. 6, the off-trac error component for a given bearing error is proportion to the distance between the aircraft and the offset poin

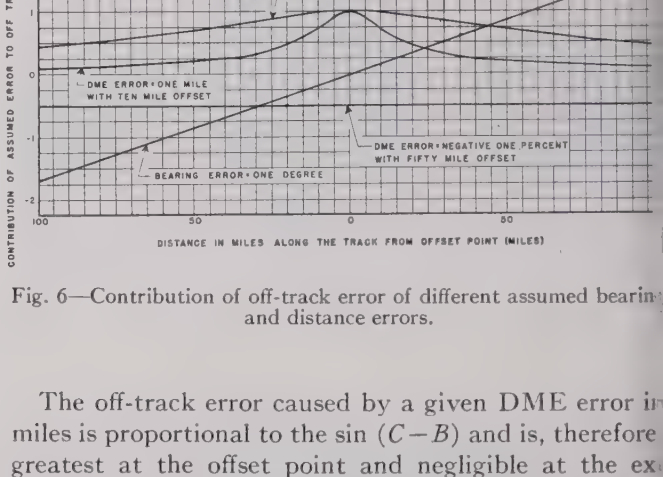

Fig. 6—Contribution of off-track error of different assumed bearin and distance errors.

The off-track error caused by a given DME error i miles is proportional to the sin $(C-B)$ and is, therefore greatest at the offset point and negligible at the ex treme ends of any track. When the component is plotte against distance along the track, as in Fig. 6, its effec is also a function of the offset distance.

Another condition of interest is that in which th error in the DME distance information is a fixed per centage of the distance. Such a given fixed per cen error produces a constant off-track error, which is pro portional to the offset distance for any track as is show graphically in Fig. 6.

The errors introduced by the computer itself were determined by a bench test in the laboratory. The computer was energized but the DME and bearing servo mechanisms were disconnected. The bearing and distance dials were positioned manually to the nearest even division for several calculated values on various tracks. The calculated off-track error was then subtracted from the observed off-track indication to obtain the computer error. For offsets up to and including 30 miles, the computer circuits introduced off-track errors of less than 1 mile right or left.

One possible source of off-track error was discovered in a bench check for accuracy made after the off-track servo motor was changed. It was found that the induc-

on-type velocity generator used for feedback in the ervo mechanism had a voltage output at standstill hich introduced a 1-mile off-track error. This was liminated by carefully selecting another servo-motor ssembly.

Theory of Distance-to-Destination Errors

Components of the distance-to-destination errors can e separated in a manner similar to that used for the ff-track errors.

The following equation can be used to calculate the istance-to-destination error introduced by errors in ie bearing and distance information:

$$\begin{bmatrix}\text{Distance-to-destination}\\ \text{error caused by bearing}\\ \text{and distance errors}\end{bmatrix} = d\cos(C-B) - 0.017bD\sin(C-B).$$

In this case, the DME errors have the greatest effect t the extremes of the track, while the effect of a given earing error is the same along any one track but is roportional to the offset distance $D \sin (C-B)$ which practically constant for a given track.

Distance-to-destination errors introduced by the mputer were determined by bench test and found to e less than plus or minus 3 miles.

Results of Flight Tests over Parallel Courses

In Fig. 7 is reproduced a simplified map of test flights i this computer. The triangular symbol in the center presents the station. The number near the center of ch track represents the offset in miles, for example, ie track numbered *N 10* is offset 10 miles to the north

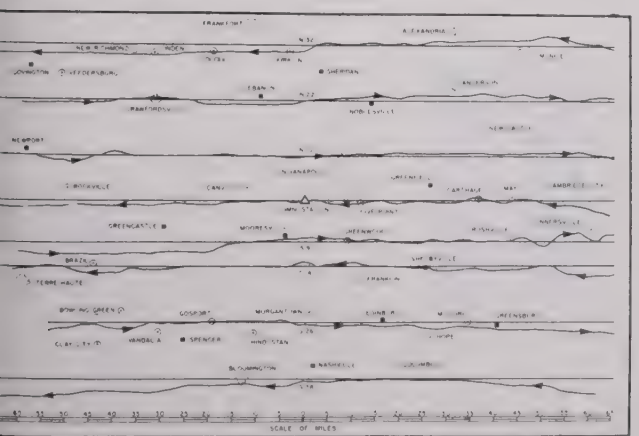

g. 7—Simplified map presentation of the data from flight tests over parallel courses.

the station. The straight lines represent the intended urses and the lines with arrow heads represent the tual tracks of the aircraft, the arrow head indicating e direction of flight. The deviation in miles of the air- aft track from the intended courses can be readily esti- ated by noting the proportion between deviation and urse spacing. Spacing for two courses is, of course, the fference between offset distances.

The average observed off-track error without regard to algebraic sign was $\frac{3}{4}$ mile. The service area of the station is expected to be within 45 miles of the offset point. The greatest single observed error within that service area was 2.5 miles. The greatest single error observed in these tests were 3 miles at the extreme ends of track S 38. A portion of this latter error is known to have been caused by a percentage change in the calibration of the distance-measuring equipment during this series of tests.

The method of plotting these computer tracks may be of interest. During the flights, the pilot endeavored to keep the needle centered while either the copilot or an engineer sat in the copilot's seat and plotted the path of the aircraft on detailed county maps having a scale of $\frac{1}{2}$ inch per mile. At the beginning of these tests, the observer's accuracy was tested by comparing his observation of the aircraft's position with that observed through an Army Type B-3 gyro-stabilized drift sight. The two observations were found to agree to better than 0.2 mile up to an altitude of 5,000 feet. The maps used were also compared with the sectional aeronautical charts and found to be in excellent agreement.

Although distance-to-destination readings were made during the flights illustrated in Fig. 7, it was not practical to precisely correlate these readings with the map. All that was done on these flights was to determine that distance-to-destination indications were reasonably accurate. However, one flight was repeated over track *N 10* of Fig. 7 in an east-to-west direction taking the data in a different manner. Some of the tracks, such as *N 10*, are township lines of the U. S. Land Survey and are visible from the air as straight continuous lines clearly marked by roads and farm boundaries. In making this flight over track *N 10*, the pilot ignored the course-deviation indicator and flew the aircraft on a straight track along this township line. Check points were selected in advance at intervals of approximately 5 miles. All the computer dials were read whenever the aircraft passed over one of these check points. True bearings and true distances for each point were determined from the detailed county maps having a scale of one-half inch per mile. The resulting data is contained in Table I.

Results of Flight Tests over Circular Orbits Around the Station

In the lower-right center of Fig. 1 is a switch labeled "orbit or line." If this switch is thrown to the "orbit" position, and the offset dial is set to a distance such as 20 miles to the left, then the pilot can fly a left-hand circular pattern about the station by flying the deviation indicator with normal sensing. The flight paths shown in Fig. 8 were made in a manner similar to those of Fig. 7 except that the orbiting function of the computer was used. The perfect circles are the intended orbital tracks, and the adjacent tracks are those made by the aircraft. Bench tests of the computer indicated that, of the errors shown in Fig. 8, 1 mile was con-

TABLE I

RESULTS OF STRAIGHT-LINE COMPUTER FLIGHT OVER COURSES N10

Computer settings: Offset—Left 9.7 miles
Course—268.5°
Along-track co-ordinate—0 miles

Check Point	Omni Distance Dial	Omni Distance From Map	Omni Bearing Dial	Omni Bearing From Map	Off-track Indication	Distance-to-Destination Dial	Distance-to-Offset Point From Map	Distance-to-Destination Correction
	(miles)	(miles)	(°)	(°)	(miles)*	(miles)	(miles)	(miles)†
80	62.6	62.5	259	259.6	0.8 L	L 62.0	61.8	−0.2
79	57.4	56.7	258	258.7	0.6 L	L 56.5	55.9	−0.6
78	53.3	52.3	258	257.8	0.6 L	L 52.8	51.4	−1.4
65	51.5	49.4	257.5	257.2	0.4 L	L 50.5	48.4	−2.1
64	43.5	42.6	255	254.7	0.1 L	L 42.3	41.5	−0.8
63	37.1	36.4	252	253.1	0.7 L	L 35.5	35.1	−0.4
62	33.0	32.1	253	250.5	1.2 R	L 31.3	30.4	−0.9
61	27.1	26.2	249	247.2	1.1 R	L 25.0	24.4	−0.6
60	23.4	23.0	246	243.8	0.8 R	L 22.0	21.0	−1.0
59	19.6	18.9	240	238.0	0.3 R	L 17.0	16.3	−0.7
58	14.3	13.8	226.5	224.6	0.3 L	L 9.5	10.1	+0.6
57	12.5	11.8	216	215.0	0.3 L	L 8.0	10.0	+2.0
56	10.3	9.6	186	183.0	1.0 L	L 1.5	0.9	−0.6
55	10.2	9.6	172.5	168.3	1.0 L	R 2.0	1.5	−0.5
53	13.5	13.0	138.5	135.3	0.8 L	R 10.0	8.8	−1.2
52	18.5	18.0	121.5	120.6	0.6 L	R 17.0	15.2	−1.8
51	20.5	20.3	118.0	117.0	0.6 L	R 19.0	17.6	−1.4
49	27.8	27.3	110.5	109.4	0.7 L	R 26.0	25.5	−0.5
48	32.7	32.2	106.0	106.1	0.4 L	R 32.0	30.7	−1.3
47	36.4	36.2	104.5	104.1	0.6 L	R 36.0	34.9	−1.1
46	44.1	45.9	103.0	100.5	2.2 L	R 44.0	44.9	+0.9
84	49.4	50.5	99.0	99.7	0.6 R	R 49.0	49.6	+0.6
85	55.0	57.3	99.0	98.3	0.5 R	R 55.0	56.5	+1.5

* Note—Right and left deflection of course-deviation indicator is indicated by R and L, respectively.
† Note—Correction is to be added algebraically to distance-to-destination dial reading.

tributed by the computer at 20 miles radius, 0.6 mile at a 10-mile radius, and 0.5 mile at a 5-mile radius.

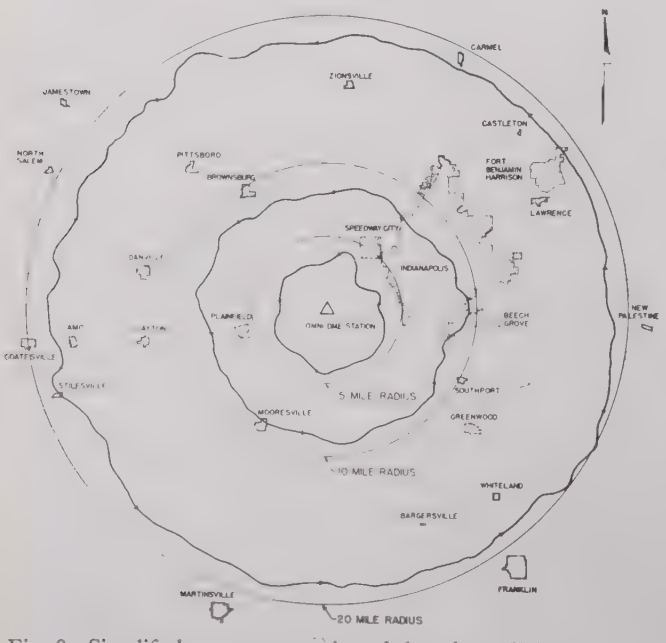

Fig. 8—Simplified map presentation of data from flight tests over circular orbits about the station.

CONCLUSIONS

Flight tests of the experimental computer show that it has an average off-track error of $\frac{3}{4}$ mile and a maximum error of 2.5 miles within the expected service range of the station. Errors in the distance-to-destination or way point are found to be of the same order of magnitude. These errors are well within the limits recommended by the January, 1947, Report of the Special Radio Technical Division of ICAO. There will soon be available navigation receivers and distance-measuring equipments built to more rigid specifications than those used in these tests, and as a consequence, the errors of computer flying will be reduced to less than those shown in this report.

In procuring the experimental computer, size and weight limitations were waived to obtain prompt delivery. With the precision potentiometers and autosyn units of compact design now available, it is believed that the size can be reduced to that of a one-half ATR unit, and the weight to approximately 20 pounds.

Off-track errors of the magnitude found in these tests would permit the use of 10-mile track separation with safety. Occasionally, the use of right- and left-hand prefixes for off-track and along-track settings was found to cause confusion in converting map measurements to computer settings. For this reason the settings to be made in future computers will be course angle, distance from omni station to destination, and bearing of destination from omni station. Additional circuits will convert the last two settings to voltages which are proportional to "offset" and "along-track" distances.

Contributors to Waves and Electrons Section

G. Barzilai was born in Rome, Italy, on e 23, 1911, and obtained the B.Sc. de- in industrial engineering from the University of Rome in 1935. For two years, he worked at the radio laboratory of the Italian Ministry of Communications on rf measurements. He was appointed vice-director of the Experimental Centre G. Marconi of the Italian National Council of Research and did e research work on antennas and propaion of radio waves. In 1941 he was sent the radio laboratory of the Italian Air ce for research work on radar equipment. remained on the technical staff of the lian Air Force until the end of 1946 when, h a British Council scholarship, he went he University of Birmingham, England, eleven months and did research work on ennas, obtaining his M.Sc. degree.

IORGIO BARZILAI

In 1948 Mr. Barzilai was granted, from Italian Ministry of Education, the "Li- a Docenza in Radiotecnica" which is an demic degree for teaching radio engineer- at an Italian University.

Mr. Barzilai is, at present, in the United tes as technical liaison between General ctric Co. and Compagnia Generale ttronica, licensee for General Electric tronic equipment in Italy.

❖

Herbert Friedman (A'45) was born in w York, N. Y., on June 21, 1916. He re- ed the A.B. degree from Brooklyn College in 1936 and the Ph.D. degree in physics from the Johns Hopkins University in 1940. He joined the Physical Metallurgy Division of the Naval Research Laboratory in 1941. In 1943, he transferred to the Optics Division of the same institution as Head of the Electron Optics Section, where has conducted research in electron miscopy, X-ray and electron diffraction, l gaseous discharge tubes.

ERBERT FRIEDMAN

Dr. Friedman is a member of the Ameri- Physical Society, the American Society X-ray and Electron Diffraction, the shington Philosophical Society, and ma Xi.

Francis J. Gross (A'46) was born at Seattle, Wash., on October 15, 1911. In 1933 he received the B.S. degree in electrical engineering from the University of Washington. He was with the meter testing department of the Puget Sound Power and Light Company from 1934 to 1937, and with the U. S. Patent Office as a patent examiner from 1937 to 1938. From 1938 to 1945 he served as an engineer and physicist in the electrical instrument section of the National Bureau of Standards. He joined the staff of the Technical Development, Civil Aeronautics Administration, as electronic engineer in 1945.

FRANCIS J. GROSS

From 1941 to 1945 Mr. Gross also served on the faculty of George Washington University in Washington, D.C., as an instructor in electrical engineering. He is a member of Tau Beta Pi and the American Institute of Electrical Engineers.

❖

Imre Molnar (SM'46) was born in 1906, and studied communication engineering at the University and Institute of Technology in Berlin, Germany, completing his studies there at the Master level in 1930. He has subsequently studied chemistry at the Illinois Institute of Technology in Chicago, and at the present is doing graduate work towards a Ph.D. degree at Northwestern University, Evanston, Ill.

IMRE MOLNAR

Mr. Molnar's first experience in telephone work was received between 1921 and 1925, with the International Telephone and Telegraph Corp., as an apprentice and installer. Since 1930 he has been associated with the Automatic Electric Company, engaged in circuit design, transmission engineering, and installation. He has also represented the Company as resident engineer in several foreign countries. In his present position as project engineer, he is concerned with general developments in the Company's laboratories. Mr. Molnar has been responsible for a number of major developments in practically all phases of the electrical communication field, which include manual, automatic, and long-distance telephony; voice frequency systems; carrier current systems; power supervisory; remote control; radio switching; airport traffic control; and automatic reservation systems.

Mr. Molnar has published numerous major papers and several hundred abstracts in electrical communications, as well as several other publications in various fields. He is a life member of the American Numismatic Association and a member of Sigma Xi.

❖

James C. W. Scott (M'47) was born at le Havre, France, on March 1, 1904. He graduated from the University of Washington with the degree of B.Sc. in physics. In 1930 he was employed by Bell Telephone Laboratories, where he did research work on copper-oxide rectifiers. In 1933 he returned to the University of Washington with a teaching fellowship to do graduate work in physics.

J. C. W. SCOTT

During the war, he joined the Royal Canadian Air Force and served overseas as a radar officer. He later was in charge of the Canadian east-coast chain of radar sections and started the radio propagation prediction section of the RCAF. At the end of the war, Mr. Scott retired from the Air Force with the rank of Squadron Leader to join the staff of the National Research Council of Canada. He transferred to his present position with the Defense Research Board in 1947 to take part in the organization of the new Radio Propagation Laboratory.

He has been secretary of the Canadian Radio Wave Propagation Committee, and is a member of the American Physical Society.

❖

For a photograph and biography of A. W. STRAITON, see page 931 of the July, 1948, issue of the PROCEEDINGS OF THE I.R.E.

Abstracts and References

Prepared by the National Physical Laboratory, Teddington, England, Published by Arrangement with the Department of Scientific and Industrial Research, England, and *Wireless Engineer*, London, England

NOTE: The Institute of Radio Engineers does not have available copies of the publications mentioned in these pages, nor does it have reprints of the articles abstracted. Correspondence regarding these articles and requests for their procurement should be addressed to the individual publications and not to the IRE.

The number in heavy type at the upper left of each Abstract is its Universal Decimal Classification number and is not to be confused with the Decimal Classification used by the United States National Bureau of Standards. The number in heavy type at the top right is the serial number of the Abstract. DC numbers marked with a dagger (†) must be regarded as provisional.

The Institute of Radio Engineers has made arrangements to have these Abstracts and References reprinted on suitable paper, on one side of the sheet only. This makes it possible for subscribers to this special service to cut and mount the individual Abstracts for cataloging or otherwise to file and refer to them. Subscriptions to this special edition will be accepted only from members of the IRE and subscribers to the PROC. I.R.E. at $15.00 per year. The Annual Index to these Abstracts and References, covering those published from February, 1948, through January, 1949, may be obtained for 2s. 8d. postage included from the *Wireless Engineer*, Dorset House, Stamford St., London S. E., England.

ACOUSTICS AND AUDIO FREQUENCIES

534+621.395.6 1563

1949 IRE National Convention Program—(PROC. I.R.E., vol. 37, pp. 160–178; February, 1949.) Abstracts are given of the following papers read at the convention:—18. The Reproduction of Sound, by H. F. Olson. 19. New Developments in Studio Design in Europe, by L. L. Beranek. 20. The Technique of Television Sound, by R. H. Tanner. Titles of other papers are given in other sections.

534.13 1564

Study, to the Second Approximation, of the Acoustic Transparency of a Rectangular Plate—T. Vogel. (*Ann. Phys.* (Paris), vol. 2, pp. 502–516; September and October, 1947.) The discussion of the case of an elastic plate forming a window in an infinite rigid wall and subjected to plane sound waves incident normally (2728 of 1947) is here extended to oblique incidence and vibrations of finite amplitude. The results are applied to the vibration of aircraft structures.

534.21 1565

Waves in Compressible Media—W. Weibull. (*Kungl. Tekn. Högsk. Handl.* (Stockholm), no. 18, 38 pp.; 1948. In English.) General equations of motion are derived and applied to plane, cylindrical, and spherical waves. Boundary conditions involving fixed and moving surfaces are considered.

534.232:621.313.12:538.652 1566

Magnetostriction Generators—Osborn. (*See* 1802.)

534.321.9 1567

Propagation of Ultrasonic Waves in Solid Rods—T. Hüter. (*Z. Angew. Phys.*, vol. 1, pp. 274–289; January, 1949.) Discussion with special reference to the transmission of ultrasonic energy along rods for medical purposes. Various theories are reviewed. Dispersion and resonance effects are considered and a graphical method of solution of the frequency equation is described. Determination of the cross-sectional distribution of the amplitude of axial displacement affords a new experimental method for velocity measurement.

Experiments showed that in Al rods of diameter 1.5 cm and 1.0 cm respectively, harmonics up to the order 40 could be detected. The use of an initial solid cone to concentrate the energy transmitted along a rod 20 cm long and 1.5 cm diameter, at a frequency of 780 kc, increased the energy density in the rod from 4 watts/cm² to 7.4 watts/cm².

534.7 1568

Determinations of Ear Fatigue with the Automatic Audiometer—G. G. Sacerdote. (*Alta Frequenza*, vol. 17, pp. 257–264; December, 1948. In Italian, with English, French, and German summaries.) An account of results obtained with an instrument of the type described by G. von Békésy (*Arch. Elek.* (Übertragung), no. 1, p. 13; 1947.)

534.845 1569

Absorption of Sound by Porous Materials: Part 5—C. Zwikker, J. van den Eijk, and C. W. Kosten. (*Physica, 's Grav.*, vol. 10, pp. 239–247; April, 1943. In English.) An account of further measurements using a system of glass tubes or a porous wall, the structure factors of which could be calculated as well as measured. Results confirmed the theory given in part 2. For parts 1 to 4 see 3322 of 1948.

534.851:621.395.813 1570

A Study of Frequency Fluctuations in Sound Recording and Reproducing Systems—P. E. Axon and H. Davies. (PROC. I.R.E., part III, vol. 96, pp. 65–75; January, 1949.) Discussion of the imperfections arising in the manufacture of phonographs and disks, causing wow. An instrument for measuring total wow is described. By statistical analysis of the results the sources of wow can be identified and appropriate corrections made.

534.86:621.396.61/.62:621.395.623.7 1571

Fundamental Electroacoustic Principles for the Transmission of a Wide Band of Audio Frequencies—Furrer, Lauber, and Werner. (*See* 1787.)

534.861:534.76 1572

Duplication of Concerts—R. Vermuelen. (*Philips Tech. Rev.*, vol. 10, pp. 169–177; December, 1948.) Stereophonic reproduction, with or without intermediate recording, enables the audience in an overflow auditorium to hear what is claimed to be an exact reproduction of the original music.

621.395.623.7 15

Voigt Permanent-Magnet Loudspeaker (*Wireless World*, vol. 55, p. 103; March, 194 The speaker has a flux density of 18,000 lin per cm² in a 1½-mm gap. The magnetomoti force is supplied by a massive center block Ticonal, with two parallel return paths of lar cross section. Difficulties of alignment or due inaccurate machining of the gap are overcon by making the pole tip assembly a separa unit. The speech coil impedance is 15 Ω and t total weight 30 lb.

681.85:534.43:621.395.813 15

High-Fidelity Response from Phonograp Pickup—E. J. O'Brien. (*Electronics*, vol. 22, p 118–120; March, 1949.) The main causes poor performance are briefly considered. Fo mulas for voltage gain and input admittan with results for feedback circuits, are given. I put circuits and response curves for sever pickups using feedback, and typical respon curves for different feedback networks, are i lustrated.

534 15

Vibration and Sound. [Book Review]—P. M. Morse. McGraw-Hill, London, 2nd ed tion, 468 pp., 33s. (*Wireless Eng.*, vol. 26, 38; January, 1949.) Intended primarily as textbook on the mathematical theory of vibra tion, for students of physics and communica tion engineering. The first edition (noted i 3023 of 1937) has been extensively revised t include discussion of modern techniques used i acoustics and a comprehensive treatment c transient phenomena. A sound knowledge c the calculus is assumed.

534.321.9 15

Supersonics—The Science of Inaudibl Sounds [Book Review]—R. W. Wood, Brow University, Providence, R. I., 1939, 162 pp $2.00. (*Jour. Frank. Inst.*, vol. 247, p. 84; Janu ary, 1949.) An historical review of superson research. Investigations in the last 15 years ar not reported, but the 1939 edition is reprinte with a supplementary bibliography which i "probably the most complete one ever pub lished in this field."

621.395.625.2 15

Practical Disk Recording [Book Review]—R. H. Dorf. Gernsback Library No. 39; Rad craft Publications Inc., New York, N. Y., 9 pp., 75c. (*Electronic Eng.* (London), vol. 2 p. 69; February, 1949.) " . . . should prove c great interest and usefulness to beginners an

ateur enthusiasts in the sound recording rld, to whom it is recommended."

ANTENNAS AND TRANSMISSION LINES

1.315+621.392+621.396.67 1578
1949 IRE National Convention Program—roc. I.R.E., vol. 37, pp. 160–178; February, 49.) Abstracts are given of the following pa-rs read at the convention:—7. Elliptically larized Radiation from Inclined Slots on linders, by G. Sinclair. 8. Some Properties of diation from Rectangular Waveguides by T. Bolljahn. 9. Theory of End-Fire Helical tennas, by A. E. Marston and M. D. Ad-k. 10. A Broad-Band Transition from Coax Helix, by C. O. Lund. 11. Equivalent Cir-ts for Coupling of Waveguides by Aper-es, by N. Marcuvitz. 22. Wide-Angle Metal-ite Optics, by J. Ruze. 23. Diffraction Pat-n from an Elliptical Aperture, by R. J. Ad-s and K. S. Kelleher. 24. The Measurement of rrent and Charge Distributions on Trans-tting and Receiving Antennas, by T. Mo-a. 25. Antenna Systems for Multichannel obile Telephony, by W. C. Babcock and W. Nylund. 26. A Low-Drag Aircraft An-na for Reception on Omnidirectional Range nals in the 108- to 122-Mc Band, by J. P anklin. 63. A Unidirectional Reversible-Beam tenna for Twelve-Channel Reception of Tel-sion Signals, by O. M. Woodward, Jr. 75. A gnetostrictive Delay Line, by E. Bradburd. les of other papers are given in other sec-ns.

1.315 1579
High-Frequency Polyphase Transmission e—C. T. Tai. (Proc. I.R.E., vol. 37, p. 58· uary, 1949.) Correction to 637 of April.

1.315.2:621.3.09 1580
Diagram for Determining the Propagation nstant [for a cable]—E. B. B. di Sambuy. *ta Frequenza*, vol. 17, pp. 274–279; Decem-, 1948. In Italian.)

1.315.212:621.397.743 1581
Coaxial Cable Joins East and Mid-West Networks—R. Hertzberg. (*Tele-Tech*, vol. pp. 18–20, 55; February, 1949.) The cable ks Philadelphia, Pittsburgh, and Cleveland. ch cable has 8 individual lines, four being for phone services; each television circuit has lines, one being a spare.

1.315.65 1582
A Coaxial-Line Support for 0 to 4,000 Mc—W. Cornes. (Proc. I.R.E., vol. 37, pp. 94–January, 1949.) The design of a broad-band dercut support is discussed, based on a slowly nging image impedance of the bead, so that s differs only slightly from the line imped-e up to some maximum frequency. A typical rowave application is described which has tage SWR less than 1,025 up to 4,000 Mc.

1.392.2:621.385 1583
Study of the Propagation of an Electromag-ic Wave in the Presence of Two Electron ms of Neighbouring Velocities—P. Laposs-e. (*Compt. Rend. Acad. Sci.* (Paris), vol. 228, 753–754; February 28, 1949.) Theory is en for an arrangement consisting of a trans-sion line, in which the propagation velocity y have any value whatever, and two concen-electron beams of neighboring velocities. beam, e.g. the external one, permits the pagation of waves whose velocity is near t of the electrons; the other beam, starting with the velocity of one of the preceding es, causes the appearance of another wave ch increases exponentially.

1.392.26† 1584
Wave Guides for Slow Waves—L. Bril-n. (*Jour. Appl. Phys.*, vol. 19, pp. 1023–1; November, 1948.) "Boundary conditions obtained for structures with very narrow slots, either closed or open, and a general method of solution of the wave equations is discussed. Fields in the free region and in the slot region are expanded in convenient Fourier series and these series joined along the border of both regions. In doing this, it can be proven that the field contains a dominant term, completed by corrections that represent the field distortion near the open end of the slots. Under favorable conditions, and for very narrow slots, the dominant terms are by far the most important. This allows for a simplified discussion of variety of examples." See also 1253 of 1948 (Chu and Hansen).

621.392.26† 1585
Diffraction and Perturbation in a Waveguide due to an Electromagnetic Wave—T. Kahan. (*Jour. Phys. Radium*, vol. 6, pp. 300–301; November, 1945.) Formulas are derived, in the form of series, for the electric field within a cylindrical waveguide and for the diffraction field outside it produced by an external plane wave incident normally to the waveguide axis.

621.392.26†:621.396.67 1586
Laterally Displaced Slot in Rectangular Waveguide—A. L. Cullen. (*Wireless Eng.*, vol. 26, pp. 3–10; January, 1949.) The admittance presented by a resonant slot cut in the top face of a rectangular waveguide and offset from the center of the face is calculated by a simple application of transmission-line theory. The Q of such a slot is calculated and it is shown that slots designed for a broad-band system should be as wide as possible. The phase of the radiation from the slot at resonance is independent of the amount of offset and bears a fixed relation to the phase of the field in the waveguide at the center of the slot. The effect of a small deviation from resonance is considered. Experimental results agree very well with the theory.

621.396.67 1587
Physical Limitations of Omni-Directional Antennas—L. J. Chu. (*Jour. Appl. Phys.*, vol. 19, pp. 1163–1175; December, 1948.) The directivity gain G and the Q of such antennas are calculated in terms of spherical wave functions under idealized conditions. Alternative criteria for optimum performance are (a) maximum G for a given complexity of the antenna structure (b) minimum Q, and (c) maximum G/Q. An antenna of maximum dimension $2a$ can have broad bandwidth provided that $G \leqq 4a/\lambda$. As G increased beyond this value, Q increases rapidly. The antenna which has potentially the broadest bandwidth has a radiation pattern corresponding to that of an infinitesimally small dipole.

621.396.67 1588
On the Theory of Biconical Antennas—C. T. Tai. (*Jour. Appl. Phys.*, vol. 19, pp. 1155–1160; December, 1948.) Discussion of the work of Schelkunoff (1049 of 1941 and 852 of 1946) and Smith (644 of April). Smith's expressions are extended to derive, for small-angle cones, an expression for the effective load admittance which is the same as that which Schelkunoff derived by other methods. Smith's results are not valid for large-angle cones. The advantages of the method over Schelkunoff's are demonstrated by deriving the characteristics of a biconical antenna where the space between the cones is filled with a dielectric other than air.

621.396.67 1589
Properties of a Long Antenna—E. Hallén. (*Jour. Appl. Phys.*, vol. 19, pp. 1140–1147; December, 1948.) Well-known integral expressions for the outgoing current waves are transformed into series expansions valid for all distances from the feeding point; results thus obtained are shown graphically.

621.396.67 1590
The Received Power of a Receiving Antenna and the Criteria for its Design—Yung-Ching Yeh. (Proc. I.R.E., vol. 37, pp. 155–158; February, 1949.) A general formula for the received power is derived. Two theorems which can be used as design criteria are deduced.

621.396.67:517.54(083.5) 1591
Iterated Sine and Cosine Integrals—Hallén. (*See* 1702.)

621.396.67:538.569 1592
Surface Currents on a Conducting Sphere Excited by a Dipole.—C. H. Papas and R. King. (*Jour. Appl. Phys.*, vol. 19, pp. 808–816; September, 1948.) Curves of the real and imaginary parts of the surface currents are given for the case of a $\lambda/2$ dipole erected on the surface of the sphere and various radii of the sphere.

621.396.67:621.396.9 1593
A Solution of the Problem of Rapid Scanning for Radar Antennas—R. F. Rinehart. (*Jour. Appl. Phys.*, vol. 19, pp. 860–862; September, 1948.) The theory of parallel plate waveguides was used by Myers (2679 of 1947) to design an antenna for rapid scanning, but the illumination properties of this antenna were unsatisfactory. A plane optical system with variable index of refraction can satisfy the requirements. By a suitable transformation, a surface of revolution of constant refractive index can be found whose optical properties are the same as those of the plane system. This surface provides an apparently practicable solution of the scanning problem. The diameter of the feed circle can be made arbitrarily small by judicious use of an ellipsoidal reflector.

621.396.67:621.396.931 1594
Flush-Mounted Antenna for Mobile Application—D. R. Rhodes. (*Electronics*, vol. 22, pp. 115–117; March, 1949.) A small annular-slot antenna with the same radiation pattern as a dipole, and which can be used in the metal roof of a car. Theory and performance are discussed.

621.396.67:621.396.97 1595
Multi-V Antenna for F.M. Broadcasting—M. W. Scheldorf. (*Electronics*, vol. 22, pp. 94–96; March, 1949.) Folded dipoles are bent into V-shape to form a light-weight array that can be mounted on top of existing AM antennas. The array is tuned by extensions on each arm, without seriously changing the impedance match and radiation pattern.

621.396.67.029.63:621.392.43 1596
The Design of Wide-Band Aerial Elements or 500–600 Mc/s Ground Radar—C. H. Westcott and F. K. Goward. *Proc. IEE* (London), part III, vol. 96, pp. 41–51; January, 1949.) Smith's circle diagrams are used to enable the matching of antennas with parabolic reflectors to feeders to be effected by means of a system of series and parallel stubs. Systems are described in which impedance changes in the stubs compensate for the impedance changes in the antenna system as the frequency is varied.

621.396.671 1597
On Antenna Impedances—E. Hallén. (*Kungl. Tekn. Högsk. Handl.* (Stockholm), no. 13, 18 pp.; 1947. In English.) Formulas given for the current in and impedance of a straight, symmetrical, center-fed antenna contain asymptotic series, and the importance of the smaller terms of these series is discussed. Coefficients of the second-order terms are expressed in a new form and are tabulated as functions of the antenna length.

621.396.671 1598
Radiation Impedance and Aerial Shortening of the Transmitter Dipole—J. Müller-Strobel. (*Bull. Schweiz. Elektrotech. Ver.*, vol. 37, pp. 710–714; November 30, 1946. In German, with French summary.) The theory of forced oscillations is applied to the case of the transmitter dipole (a) neglecting and (b) taking account of

antenna losses. Derivation of the formulas used is given in papers mentioned in the references and is omitted here. Calculated values are in good agreement with the results of measurements on a bronze wire supported by a balloon.

621.396.671 1599

An Experimental Investigation of Formulas for the Prediction of Horn Radiator Patterns—G. A. Woonton, D. R. Hay, and E. L. Vogan. (*Jour. Appl. Phys.*, vol. 20, pp. 71–78; January, 1949.) Measured *E*-plane radiation patterns give satisfactory agreement with the well-known Kirchhoff formula for angles up to 20° and distances as short as 1 foot from the horn mouth; *H*-plane measurements agree less well. Distant patterns are compared with the Stratton and Chu corrected formula (3875 of 1939).

621.396.671 1600

Gains and Effective Areas of Horn Antennas—R. B. Watson and C. M. McKinney. (*Jour. Appl. Phys.*, vol. 19, pp. 871–876; October, 1948.) A reciprocity method is described for determining absolute gain. An alternative method is used to obtain both gain and effective area by comparison of experimental and theoretical radiation patterns; results thus obtained are in satisfactory agreement with values obtained by the reciprocity method.

621.396.671 1601

Parasitic-Array Patterns—J. L. Gillson. (*QST*, vol. 33, pp. 11–15, 104; March, 1949.) Patterns determined experimentally are presented for a 3-element array adjusted both for maximum forward and minimum rear radiation at several heights, and for a 2-element array at a height of $5\lambda/4$ with various lengths of the parasitic element.

621.396.671 1602

On the Calculation of Radiation Patterns of Dielectric Rods—R. B. Watson and C. W. Horton. (*Jour. Appl. Phys.*, vol. 19, pp. 836–837; September, 1948.) Continuation of 1297 of June. The equivalent currents may be expressed, in terms of traveling waves without appreciably changing the computed radiation patterns.

621.396.677 1603

Design of Yagi Aerials—R. M. Fishenden and E. R. Wiblin. (*Proc. IEE* (London), part III, vol. 96, pp. 5–12; January, 1949.) An account of work done at the Telecommunications Research Establishment between 1938 and 1942. Discussion of: (a) advantages and limitations of multiple arrays, (b) the mode of operation of a Yagi antenna and (c) the effect on the polar diagram of changing parameters. Only antennas of length $>\lambda$ are considered; these normally consist of 3 or more directors in addition to an exciter and a reflector. Sufficient information is tabulated for approximate design of an antenna of given characteristics. See also 1348 of 1947 (Walkinshaw) and 1349 of 1947 (Reid).

621.396.677 1604

Dielectric Directive Radiators—P. Mallach. (*Fernmeldetech. Z.*, vol. 2, pp. 33–39; February, 1949.) Discussion of the polar diagrams of uniform and tapered dielectric rods and of arrays of such rods. Design theory is presented; experimental results are in excellent agreement.

621.396.677.029.54 1605

Design Considerations for Directive Antennae-Arrays at Medium-Wave Broadcast Frequencies, taking into account the Final Radio-Frequency Amplifier Circuits—J. C. Nonnekens. (*HF* (Brussels), no. 1, pp. 26–31; 1949. In English.) The horizontal directivity of broadcasting arrays is briefly reviewed and the power distribution, as determined from the impedance at the base of the antenna, is calculated. The general case of vertical antennas of unequal heights, with mutual inductance, is analyzed and measurement methods are outlined. The practical design of 4-terminal networks for matching and power distribution is considered. Difficulties due to parallel capacitance in the case of towers with high base impedance are discussed, and possible antiparasitic devices for inclusion in the final amplifier are mentioned.

CIRCUITS AND CIRCUIT ELEMENTS

621.3.018.7 1606

Pulse-Sinewave Converter—W. M. Cameron. (*Electronics*, vol. 22, pp. 174, 180; March, 1949.) A pulse input produces a positive and a negative exponential wave which are folded to produce a wave of approximately sinusoidal characteristics. Design and performance are discussed and a typical 2-tube circuit illustrated, in which a 30-volt pulse input provides a 17-volt peak-to-peak sinusoidal output of low harmonic content.

621.314.2.029.3:621.317.784 1607

Audio Frequency Transformer Design—C. F. Brockelsby. (*Marconi Rev.*, vol. 12, pp. 1–11; January to March, 1949.) Analysis for the transformer of a wide-range af absorption wattmeter.

621.316.726.078.3:621.396.615.142.2:538.569.4 1608

Frequency Stabilization of Microwave Oscillators by Spectrum Lines: Part 2—J. L. G. de Quevedo and W. V. Smith. (*Jour. Appl. Phys.*, vol. 19, pp. 831–836; September, 1948.) "The design of both narrow-band high-stabilization and broad-band lower-stabilization spectrum line discriminators is developed in a generalized form applicable to various spectrum lines and cavity designs. Comparison with experiment is made for two broad-band discriminators utilizing the NH_3 3,3-absorption line at 23,870 Mc as the frequency determining element. These discriminators, used with an amplifier of 2,000 gain, reduce drifts by factors of 250 and 1,000 respectively, compared to an unstabilized tube." Part 1, 2180 of 1948.

621.318.572:518.5 1609

Rectifier Networks for Multiposition Switching—D. R. Brown and N. Rochester. (PROC. I.R.E., vol. 37, pp. 139–147; February, 1949.) 1948 IRE National Convention paper. For computers and other applications where switching times <1 microsecond are required. Various types of network, including that using the minimum number of rectifiers, are discussed. Generalized equivalent circuits are derived.

621.318.572:621.396.822 1610

Spurious Signals Caused by Noise in Triggered Circuits—Middleton. (*See* 1777.)

621.319.4:551.57:621.317.335 1611

The Effect of Humidity on the Calibration of Precision Air Capacitors—L. H. Ford. (PROC. I.R.E., part III, vol. 96, pp. 13–16; January, 1949.) See 978 of May.

621.39 1612

1949 IRE National Convention Program—(PROC. I.R.E., vol. 37, pp. 160–178; February, 1949.) Abstracts are given of the following papers read at the convention:—Symposium on Network Theory, comprising (a) Modern Developments in the Topology of Networks, by R. M. Foster, (b) A Survey on the Status of Linear Network Theory, by E. A. Guillemin, (c) Recent Developments in Broad-Band Active Networks, by J. G. Linvill, and (d) General Review of Linear Varying-Parameter and Nonlinear Circuit Analysis, by W. R. Bennett. 27. A Method of Synthesizing the Resistor-Capacitor Lattice Structure, by J. L. Bower, J. T. Fleck, and P. F. Ordung. 28. Exact Design of Bandpass Networks using n Coupled Finite-Q Resonant Circuits ($n=3$ and 4), by M. Dishal. 29. Network Approximation in the Time Domain, by W. H. Huggins. 30. The Design of Frequency-Compensating Matching Sections, by V. Rumsey. 31. Amplifier Synt sis through Conformal Transformations, D. L. Trautman, Jr., and J. M. Pettit. 47. pedance Curves for Two-Terminal Netwo by E. L. Michaels. 48. An Analysis of Tri Tuned Coupled Circuits, by N. W. Mather. The Bridged Parallel-Tee Network for S pressed-Carrier Servo Systems, by C. F. Wh 50. Transients Response of Linear Netwo with Amplitude Distortion, by M. J. Di To 52. Subminiaturization of IF Amplifiers, G. Shapiro and R. L. Henry. 53. New Appli tions of a Four-Terminal Titanate Capacit by A. A. Pascucci. 54. Frequency-Control Uni by A. E. Miller. 55. The Type 5811 and Ty 5807 Tubes—the Smallest Commercial Pento Amplifiers, by L. G. Hector and H. R. Jacob 68. *G* Curves as an Aid in Circuit Design, K. A. Pullen. 69. A Direct-Coupled Amplif Employing a Cross-Coupled Input Circuit, J. N. Van Scoyoc and G. F. Warnke. 70. A nular Circuits for High-Power Multiple-Tu Generators at VHF and UHF, by D. H. Prei 71. Considerations on Electronic Multico plers, by W. R. Aylward and E. G. Fubini. Speed of Electronic Switching Circuits, E. M. Williams and D. F. Aldrich. 76. An Ele tromechanical Strain-Gage Multiplier, C. H. Woods, E. St. George, L. Isenberg, a A. C. Hall. 86. A High-Efficiency Sweep C cuit, by B. M. Oliver. 93. High-Power Sa tooth Current Synthesis from Square Wav by H. E. Kallmann. 94. Comparison of the Toroidal Filter with the Parallel-Tee Feedbac Amplifier Filter, by A. J. Stecca. 95. A Pea Selector Circuit, by M. J. Parker. 96. A Lo Frequency Synchronized Sawtooth Generat Providing Constant Amplitude Sweep wit Aperiodic Synchronization Input, by P. Ya fee. 97. Regenerative Amplifiers, by Y. P. Y 98. A Rectifier Filter Chart, by R. Lee. 12 Aspects of Double-Stream Amplifiers, by J. Pierce; W. B. Hebenstreit; A. V. Hollenber 135. An Analysis of Oscillator Performance u der Varying Load Conditions and an Ele tronic System for Automatic Load Compens tion, by E. Mittelmann. 136. Low-Power Wid Tuning-Range VHF Oscillators, by F. Kamphoefner and J. M. Pettit. 137. React ance-Tube Modulation of Phase-Shift Oscilla tors, by F. R. Dennis and E. P. Felch. 138. Low-Distortion Audio-Frequency Oscillato by C. W. Clapp and C. L. Hackley. 139. A Automatic-Frequency-Control System for Me chanically Tuned Oscillators, by J. G. Stephen son. Titles of other papers are given in othe sections.

621.392 161

The Duality between Interlinked Electri and Magnetic Circuits and the Formation o Transformer Equivalent Circuits—E. C Cherry. (*Proc. Phys. Soc.*, vol. 62, pp. 101–111 February 1, 1949.) Discussion of the condition under which equivalent circuits exist for cir cuits containing impedances and transformers and of rules for the formation of equivalent cir cuits. A physically realizable equivalent circui does not exist if the given magnetic circuit i nonplanar. Under certain conditions, the proc ess may be reversed and the impedances in circuit may be coupled by a suitable trans former so that the various current and voltag constraints are unaltered.

621.392 161

Properties of some Wide-Band Phase Splitting Networks—D. G. C. Luck. (PROC I.R.E., vol. 37, pp. 147–151; February, 1949. Discussion of passive networks producin polyphase output from single-phase input. Th properties of simple branch circuits are consid ered, and an expression is derived for the phas difference produced between branches, as function of frequency. This expression facil tates direct circuit design from required per formance. General performance and desig curves are included.

.392 1615
Thévenin's Theorem—"Cathode Ray." *reless World*, vol. 55, pp. 109–112; March, 9.) A simple explanation, with applications various network calculations.

.392.43:621.396.67.029.63 1616
The Design of Wide-Band Aerial Elements 500–600 Mc/s Ground Radar—Westcott Goward. (*See* 1596.)

.392.52 1617
Transmission-Line Filters—E. K. Sande-n. (*Wireless Eng.*, vol. 26, pp. 11–25; Janu-, 1949.) The discussion is limited to filters ng transmission lines whose loss is negligible whose lateral dimensions are small com-ed with λ. The treatment is thus not nor-ly applicable to waveguides. Three general es of filter are considered: (a) lengths of shunt-loaded with short-circuited or open-uited stubs consisting of lengths of the same e of line, (b) lengths of line series-loaded h short-circuited or open-circuited stubs, and two electrically unequal lengths of the same e of line in parallel. Although the image im-ances are different, the pass bands of filter ions constituted by lines shunt-loaded with rted stubs are the same as those of lines se--loaded with open stubs. Similarly the pass ds of lines shunt-loaded with open stubs are same as those of lines series-loaded with rted stubs. The relevant formulas are de-oped, using matrix theory. Pass and attenu-ng bands are shown graphically.

.392.52 1618
Filters and Filter Problems—F. Locher. *ll. Schweiz. Elektrotech. Ver.*, vol. 37, pp. –568; September 21, 1946. In German, with nch summary.) General discussion of the sent state of the art.

.392.52:621.392.26† 1619
Paralleled-Resonator Filters—J. R. Pierce. *oc. I.R.E.*, vol. 37, pp. 152–155; February, 9.) Discussion of microwave filters in which ut and output waveguides are connected by umber of resonators, each coupled directly both waveguides. Signal components of dif-ent frequencies can pass from the input to output largely through different resonators. experimental filter is described.

.396.611.1 1620
Resonance Curves of Forced Oscillations ited by Disturbances with Frequency-De-ident Amplitude—M. Päsler. (*Ann. Phys.* z.), vol. 4, pp. 1–13; September 20, 1948.) cussion for a mechanical oscillatory system jected to a force whose amplitude is propor-nal to the nth power of the frequency. Re-ts are given for $n=0, 1 \ldots 4$. The analysis be applied to oscillations in an electrical cuit.

.396.611.4 1621
On the Excitation and Coupling of Cavity sonators—J. Bernier. (*Ann. Radioélec.*, vol. pp. 3–11; January, 1949.) Starting from xwell's equations, methods of exciting and coupling cavities by means of conduction rents in loops or probes are discussed, and the interaction of cavities with periodic vection currents due to electron beams tra-sing the cavities. The results of Bethe (706 1945) for diffraction by small holes are ap-d to (a) the excitation of a cavity by an tromotive field entering the cavity through rcular hole, and (b) the coupling of two cavi-s by a circular hole in their common wall. netical formulas are given which allow nu-rical calculation for cases in which the rela-e value of the electromotive field in an ideal ity, with neither loop, probe, hole, nor elec-n beam, is known in the neighborhood of the nt where the excitation or coupling device is be located.

621.396.611.4:621.317.336 1622
On the Measurement of Cavity Impedance—Hansen and Post. (*See* 1719.)

621.396.615:621.385.029.63/.64 1623
Travelling-Wave Valves as Oscillators with Wide-Band Electronic Tuning—Doehler, Klen, and Palluel. (*See* 1830.)

621.396.615.029.3 1624
Study of a *RC* Audio-Frequency Oscillation Generator—E. Divoire. (*HF* (Brussels), no. 1, pp. 5–15; 1949. In French.) Theory is given for the Wien-bridge oscillator with automatic regulation by means of a small incandescent lamp. If the components of the bridge and its associated amplifier are suitably chosen, such oscillators can have purity and stability characteristics at af comparable or even superior to those of resonant-circuit oscillators. Experimental results confirm the theoretical calculations.

621.396.615.17:621.317.755 1625
The Miller Time Base—B. H. Briggs. (*RSGB Bull.*, vol. 22, pp. 198–202; June, 1947.) Discussion of the basic circuit and various derivatives.

621.395.645 1626
Square-Wave Analysis of Compensated Amplifiers—P. M. Seal. (Proc. I.R.E., vol. 37, pp. 48–58; January, 1949.) The theoretical response of a single-stage compensated video amplifier to square-wave and sinusoidal inputs is found. High-frequency compensation is obtained by a shunt peaking coil, and low-frequency compensation by a *RC* network, in series with the anode load resistance. Output wave shapes for typical operating conditions are shown. Experimental verification has been obtained for a low-frequency amplifier.

621.396.645 1627
Theory of the Superregenerative Amplifier—L. Riebman. (Proc. I.R.E., vol. 37, pp. 29–33; January, 1949.) A very general solution is obtained mathematically for the superregenerative circuit, by regarding it as an oscillatory circuit which includes a resistance varying with time from a positive to a negative value. An ideal control-voltage wave form is deduced, approximations to which may be obtained in practice. For this wave form, the minimum realizable static bandwidth is 0.89 times the control frequency.

621.396.645 1628
Design of Resistance-Capacity Coupled Amplifiers—H. Mayr. (*Microtecnic* (Lausanne), vol. 2, pp. 245–248; December, 1948. In English.) Theoretical analysis using an equivalent circuit, applicable to such amplifiers of any bandwidth and center frequency. The impedance of by-pass capacitors is neglected; a correction for this can be made.

621.396.645 1629
Amplifier Problems for Ultra-Short Waves—W. Sigrist. (*Bull. Schweiz. Elektrotech. Ver.*, vol. 37, pp. 5–22; January 12, 1946. In German, with French summary.) A detailed examination of the relations between electron beam concentration and tube geometry and construction, as affecting amplification factor, limiting wavelength, and efficiency.

621.396.645:621.385.032.24 1630
Practical Notes on Grid Current and Neutralization—Dickson. (*See* 1838.)

621.396.645.029.62/.63:621.396.822 1631
On the Reduction of the Effect of Spontaneous Fluctuations in Amplifier Valves for Metre and Decimetre Waves—M. J. O. Strutt and A. van der Ziel. (*Physica. 's Grav.*, vol. 10, pp. 823–826; December, 1943. In German.) Further discussion, with special reference to the optimum detuning of the input circuit of an amplifier. For long abstract of main paper, see 749 of 1945.

621.396.662.029.64:621.315.61 1632
Attenuator Materials for Microwaves—Teal, Rigterink and Frosch. (*See* 1691.)

621.396.69+621.317.7 1633
Standardized Super High-Frequency Components and Instruments—(*Engineer* (London), vol. 187, pp. 143–144; February 4, 1949.) Special matching features are incorporated to prevent confusion; female types of connection are used for power outputs and male for power inputs. Wavemeters, attenuators, bolometers, matching stubs, crystal units, adjustable loop probes, fixed probes, tuning plungers, and connectors are all briefly discussed.

621.396.69 1634
1949 Components Exhibition, Paris—(*Radio Prof.* (Paris), vol. 18, pp. 16–23, 25; February, 1949. *Toute la Radio*, vol. 16, pp. 115–122; April, 1949. *TSF Pour Tous*, vol. 25, pp. 99–101 and 143–146; March and April, 1949.) Descriptions of novelties and exhibits of particular interest or merit.

621.397.645 1635
On the Design of Television Intermediate-Frequency Amplifiers—J. Sokolov. (*Bull. Schweiz. Elektrotech. Ver.*, vol. 37, pp. 509–514; August 24, 1946. In German, with French summary.) A very wide pass band is required and the phase variation of the signal with frequency should be as nearly linear as possible. Taking these conditions into account, the necessary formulas for complete design calculations are deduced; a numerical example is given.

621.392.029.64 1636
Principles of Microwave Circuits [Book Review]—C. G. Montgomery, R. H. Dicke, and E. M. Purcell (Eds.). McGraw-Hill, London, 486 pp., 36s. (*Wireless Eng.*, vol. 26, p. 37; January, 1949.) Vol. 8 of the MIT Radiation Laboratory series. The field equations of waveguides are discussed very generally; waveguide elements (irises etc.) and cavities are considered. Much space is given to the matrix algebra of the general network and to equivalent network theory. See also 1016 of May (Ragan).

621.396:518.3 1637
Technische Nomogramme [Book Review]—H. J. Schultze. Ingenieurbüro für Nomographie und Fernmeldetechnik, München, 1948, 71 nomograms, 26 DM. (*Elektron Wiss. Tech.*, vol. 3, p. 88; February, 1949.) Abacs for calculations relating to oscillatory circuits, filters, amplifiers, transformers, coils, tracking, etc.

621.396.645 1638
Vacuum Tube Amplifiers [Book Review]—G. E. Valley, Jr., and H. Wallman (Eds.). McGraw-Hill, London, 743 pp., £3. (*Wireless Eng.*, vol. 26, pp. 37–38; January, 1949.) Vol. 18 of the MIT Radiation Laboratory series. The book necessarily includes much well-known material, but also contains much not previously published, such as pulse-response curves of band-pass amplifiers and some items concerning dc amplifiers. The treatment is essentially practical.

GENERAL PHYSICS

53 1639
1949 IRE National Convention Program—(Proc. I.R.E., vol. 37, pp. 160–178; February, 1949.) Abstracts are given of the following papers read at the convention:—Symposium on Nuclear Science, comprising (a) The Fundamental Particles, by D. J. Hughes, (b) The Detection and Measurement of Nuclear Radiation, by H. L. Andrews, (c) The Effects of Ionizing Radiation on Tissue, by J. P. Cooney, and (d) The Application of Nuclear Radiation to Industry, by J. R. Menke. 90. Geometrical Representation of the Polarization of a Plane

Electromagnetic Wave, by G. A. Deschamps. 122. On the Theory of Axial Symmetric Electron Beams is an Axial Magnetic Field, by A. L. Samuel. 123. Electron Beams in Axial Symmetric Magnetic and Electric Fields, by C. C. Wang. Titles of other papers are given in other sections.

53.081+621.3.081 1640

Some Units in the Giorgi System and the C.G.S. System—E. Hallén. (*Kungl. Tekn. Högsk. Handl.* (Stockholm), no. 6, 44 pp.; 1947. In English.) In the Giorgi system, corresponding electric and magnetic quantities have dimensions differing by a velocity. All factors of conversion to the Summerfeld cgs system are powers of 10, and are tabulated.

537.521 1641

Electronic Interaction in Electrical Discharges in Gases—J. H. Cahn. (*Phys. Rev.*, vol. 75, pp. 293–300; January 15, 1949.

537.523.3:621.396.823 1642

Radio Influence from High-Voltage Corona—Slemon. (*See* 1780.)

537.523.4.029.64 1643

Oscillographic Observations on Ultra-High-Frequency Sparks—W. A. Prowse and W. Jasiński. (*Nature* (London), vol. 163, pp. 103–104; January 15, 1949.) Tracings show the collapse of field in a resonator energized at 2,800 Mc, during breakdown of irradiated hydrogen, nitrogen, and oxygen at atmospheric pressure in a 1.4-cm gap. With mid-gap irradiation, abruptness of breakdown is comparable to that with dc. Breakdown stress is independent of rate of voltage rise and location of irradiation. See also 361 of March (Cooper and Prowse).

537.525:538.551.25 1644

Plasma-Electron Oscillations—T. R. Neill. (*Nature* (London), vol. 163, pp. 59–60; January 8, 1949.) Experiments using a specially designed tube with a straight wire filament and movable probes confirm the existence of plasma-electron vibrations and v.m. of primary electron beams passing through a small volume close to the cathode, as suggested by Armstrong (2506 of 1948). The relationship between the bunching parameter $V^{3/2}\lambda/I$ and the bunching distance d has approximately the linearity predicted by Webster (968 of 1940) in a particular case, V being the tube voltage, λ the vacuum wavelength of the oscillations, and I the amplitude of response of the resonator with the probe at the bunching point.

538.3:517.54 1645

Application of Conformal Representation to Wave Fields—H. H. Meinke. (*Z. Angew. Phys.*, vol. 1, pp. 245–252; January, 1949.) By means of conformal representation, the inhomogeneous plane wave between two surfaces of relatively general form is transformed into a plane wave between two parallel planes with an intervening inhomogeneous dielectric. Maxwell's equations for this wave then give an infinite system of linear differential equations of the second order with an infinite number of unknown functions of a variable. Convergence considerations for these functions show that the problem can be treated with sufficient accuracy with only two functions. This makes it possible to develop a systematic step-by-step approximation method for the wave field of such inhomogeneous systems, starting from the electrostatic field, which, in most cases, is a satisfactory first approximation.

538.3:531.314.2 1646

An Extension of Lagrange's Equations to Electromagnetic Field Problems—P. D. Crout. (*Jour. Appl. Phys.*, vol. 19, pp. 1007–1019; November, 1948.) If, in a given problem, a sufficiently close approximation to the instantaneous electric field can be obtained by a linear combination of chosen "current modes," whose coefficients are functions of time and of generalized co-ordinates, then Lagrange's equations are satisfied if the kinetic and potential energies are replaced by the magnetic and electric energies respectively. In certain cases, the generalized co-ordinates can be considered as charges which have flowed around the various meshes of a lumped network whose Kirchhoff voltage equations are identical with the Lagrange equations. This lumped network is, therefore, an equivalent network whose accuracy depends on the current modes chosen. The method has been applied to the design of complex echo boxes; other high-frequency applications are indicated.

538.566.029.64:53.087.3 1647

Experiments in Electromagnetic Optics—N. Carrara, P. Checcucci, and M. Schaffner. (*Alta Frequenza*, vol. 17, pp. 243–256; December, 1948. In Italian, with English, French, and German summaries.) A description of apparatus and methods for observation of interference, circular polarization, and double refraction with centimeter waves.

549.211:537.533.8:537.525.92 1648

Space Charge Effects in Bombardment Conductivity through Diamond—R. R. Newton. (*Phys. Rev.*, vol. 75, pp. 234–246; January 15, 1949.) A tentative theory is given and found to agree reasonably well with experiment. Suggestions for future work are included.

621.39.001.11:621.396.822 1649

Communication in the Presence of Noise—C. E. Shannon. (Proc. I.R.E., vol. 37, pp. 10–21; January, 1949.) Messages and the corresponding signals are represented geometrically as points in two "function spaces." The modulation process is regarded as a mapping of one space into the other. Results concerning expansion and compression of bandwidth and the threshold effect are deduced. Formulas are found for the maximum rate of transmissoin of binary digits over a system subject to various types of noise. Ideal systems which transmit as this maximum rate are discussed. The number of binary digits necessary for satisfactory transmission of a continuous source is also calculated. See also 1361 of June.

621.396.029.64:43 1650

The Physical Applications of Microwaves—J. B. Birks. (*Jour. Brit. I.R.E.*, vol. 9, pp. 10–28; January, 1949.) Discussion of: (a) the principles and experimental methods used in the study of electromagnetic properties of materials at microwavelengths, (b) the dielectric properties of solids and liquids, including polar solutions, (c) the magnetic properties of solids, and (d) the absorption spectra of gases.

GEOPHYSICAL AND EXTRATERRESTRIAL PHENOMENA

523.7 1651

Recent Results of Solar Investigations—W. Menzel. (*Elektron Wiss. Tech.*, vol. 3, pp. 55–61; February, 1949.) Solar problems still unsolved include the origin of sunspots, their magnetic fields and relatively regular period, the general solar magnetic field, and solar rf radiation.

523.72 1652

1949 IRE National Convention Program—(Proc. I.R.E., vol. 37, pp. 160–178; February, 1949.) Abstracts are given of papers read at the convention, including:—89. On the Origin of Solar Radio Noise, by A. V. Haeff. Titles of other papers are given in other sections.

523.746+523.72 1653

Sunspots, Radio-Fading, and Radio-Noise—H. Spencer Jones. (*Not. Proc. Roy. Inst.*, vol. 33, no. 153, pp. 637–648; 1948.) Discussion of the nature and characteristics of sunspots, flares, etc., and their association with magnetic storms and rf solar radiation. The impor of the solar corona is emphasized.

523.746:550.385

Giant Sunspot and Geomagnetic Sto (*Nature* (London), vol. 163, pp. 203–204; ruary 5, 1949.) A bipolar group of sunspo size 2,300 millionths of the sun's hemis had central meridian passage on Januar 1949. A severe magnetic storm associated aurora began suddenly on January 24. Th so far little evidence of any large assoc solar flare.

538.12:521.15

Magnetic Fields of the Heavenly Bodi H. von Klüber. (*Elektron Wiss. Tech.*, v pp. 45–54; February, 1949.) General discus with special reference to the Zeeman e sunspot phenomena, magnetic field of th and of the fixed stars, and Blackett's th (3112 of 1947.)

550.38:521.15

Non-Uniformity of the Earth's Rotation Geomagnetism—W. M. Elsasser. (*N* (London), vol. 163, pp. 351–352; Marc 1949.) Study of the secular variation of earth's magnetic field suggests that the los and irregularities in, the angular momentu the earth are due to changes in the liquid rather than to the frictional effect of oce tides.

550.385:523.746.5

On the Variation, during the Solar Cycl the Period and Extent of the Recurrenc Magnetic Storms—É. Thellier and O. Thel (*Compt. Rend. Acad. Sci.* (Paris), vol. 228, 701–703; February 21, 1949.) Magnetic sto with sudden commencements show no evid of recurrence at 27-day intervals, whereas tl starting gradually show a definite tendenc recur. Study of 328 storms of the latter t show that variation of the recurrence perio certainly not great. The extent of the re rence is most strongly marked in the decrea phase of the cycle.

551.510.52:621.396.11

A Theory on Radar Reflections from Lower Atmosphere—Gordon. (*See* 1761.)

551.510.52:621.396.11

Theory and Practice of Tropospheric Sou ing by Radar—Friend. (*See* 1760.)

551.510.535

Comparison of Ionospheric Data from A podal Points—(*Jour. Frank. Inst.*, vol. 247, 64–65; January, 1949.) The two most suita existing stations for such comparison are Wa eroo, Western Australia, and Baton Rou Louisiana. A statistical comparison shows t Baton Rouge conditions can be predicted nea as efficiently from Watheroo data as fr Baton Rouge data. Watheroo data can be us to predict Brisbane conditions with similar ficiency; this is probably because the differe in longitude between Watheroo and Brisban nearly equal to that between Baton Rouge a the antipodal point of Watheroo.

551.510.535

The Ionosphere over Mid-Germany January 1949—Dieminger. (*Fernmeldetech.* vol. 2, p. 44; February, 1949.) An account features of special interest, with graphs of t diurnal variation of the monthly mean values the critical frequencies and heights of the ferent layers, as determined at the Institute Ionosphere Research, Lindau über Northei See also 1475 of June.

551.510.535

Note on Night-Time Phenomena in the Region at Brisbane—G. de V. Gipps, D. Gipps, and H. R. Venton. (*Jour. Coun. S Industr. Res.* (Australia), vol. 21, pp. 215-

gust, 1948.) (h', f) records made on the multrequency recorder at Indooroopilly reveal artures from normal F_2-layer formation at ht. Possible ionospheric configurations for ducing these abnormalities are discussed.

.510.535 1663
Evidence of Horizontal Motion in Region onization—W. J. G. Beynon. (*Nature* (Lon-), vol. 162, p. 887; December 4, 1948.) Irlarities in the F_2 layer near the midpoint of path, detected by means of signals received Slough from a transmitter at Zeesen, 990 km of Slough, were observed 60 to 75 minutes r overhead. A 70-minute delay would re- a horizontal motion of 430 km per hour. also 1664 below.

.510.535 1664
Short-Period Changes in the *F* Region of Ionosphere—G. H. Munro. (*Nature* (Lon-), vol. 162, pp. 886–887; December 4, 1948.) account of observations during the period vember, 1947 to May, 1948, to detect horital movements in the ionosphere. Signals n a group of three synchronized and suitaphased transmitters were received at one or e of three points, the locations being chosen provide eight possible combinations for cking uniformity of motion. Clearly defined nges in echoes from the *F* region showed e differences at the three receiving points cating a horizontal velocity of 3.9 miles per ute in a direction 60°E of N. Time differes also occurred in quasiperiodic variations ie "split" observed at one receiving point in echo records for the three transmitters. See 1663 above.

.510.535:525.624 1665
Lunar Variations in the Principal Ionoeric Regions—D. F. Martyn. (*Nature* (Lon-), vol. 163, pp. 34–36; January 1, 1949.) tical tidal air movements do not account the semidiurnal variations in ionosphere racteristics. From consideration of the elecynamic forces brought into play by horital air movements, a semidiurnal tilting ion about an axis corresponding to the llel of latitude at about 35° is deduced, with llations which are out of phase on opposite s of the axis. *E*-layer height measurements irm this. *F*-layer variations show no conent phase difference between high and low udes, but this can be explained by the elecl connection between the layers. In the *F* on, tidal air motions may be relatively k, so that ionospheric variations would be uenced by the stronger low-latitude effects ie *E* region, with results such as are found. ther support is also provided for the conion that the main seat of the lunar magnetic ations is below the *E* region. See also 1053 lay and back references.

.510.535:621.396.11 1666
The Radio Amateur and Upper Atmosphere earch—O. P. Ferrell. (*CQ*, vol. 5, pp. 25–27, February, 1949.) Discussion of sporadic-*E* ds and the part that radio amateurs, oping at frequencies in the 50-Mc band, can in locating them. Observations of marked adic-*E* clouds for two days in 1948 are dised in detail. See also 3117 of 1948 and 3410 948 (Revirieux:Lejay).

.551:621.396.11 1667
The Problem of Diffusion in the Lower Atphere—O. G. Sutton. (*Quart. Jour. R. Soc.*, vol. 73, pp. 257–276; July to October, 7. Discussion, pp. 276–281.) A detailed dision, including the conjugate power-law ory of eddy diffusion which was applied by ker to the problem of superrefraction (1159 lay and back references).

.553.11:621.396.11 1668
Sea Breeze Structure with Particular Refnce to Temperature and Water Vapour Gradients and Associated Radio Ducts—R. W. Hatcher and J. S. Sawyer. (*Quart. Jour. R. Met. Soc.*, vol. 73, pp. 391–406; July to October, 1947.) Marked superrefraction occurs when dry air is heated over land and drifts out over cooler sea. The program of observations here discussed was undertaken because lack of knowledge of sea breeze structure hindered the development of an adequate theory of such superrefraction. Hygrometer readings were taken at vertical intervals of a few hundred feet and horizontal intervals of a few miles near the coast in the Madras district. Results are shown graphically and discussed. The existence of a surface radio duct, as suggested by Booker, is confirmed, but the observations do not indicate any elevated radio duct. See also 1159 of May (Booker) and back references.

551.578.1:621.396.9 1669
Radar Observation of Heavy Rain—Whalley and Scoles. (*See* 1675.)

LOCATION AND AIDS TO NAVIGATION

534.88 1670
Use of Sonar in Harbor Defense and Amphibious Landing Operations—E. Klein and T. F. Jones. (*Elec. Eng.*, vol. 68, pp. 107–114; February, 1949.) Discussion of the development of ultrasonic ranging and direction-finding equipment. The "Herald" equipment comprised a station on the sea bed and a shore station. Remote control of the training and tilting mechanisms for the acoustic mirror was achieved with a step-by-step transmission. A common oscillator for receiver and transmitter, of frequency 175 kc above that of the sound beam, greatly simplified operation of the equipment. Ultrasonic beacons for guidance of assault craft transmitted for 12 hours in the band 17 to 25 kc and then automatically flooded and sank.

535.61-15:621.383 1671
Infra-Red Location of Objects with Lead Sulphide Cells—Ochmann. (*See* 1732.)

621.396.9 1672
1949 IRE National Convention Program—(Proc. I.R.E., vol. 37, pp. 160–178; February, 1949.) Abstracts are given of the following papers read at the convention:—Symposium on Radio Aids to Navigation, comprising (a) The Radio Technical Commission for Aeronautics—its Program and Influence, by J. H. Dellinger, (b) Frequency Allocations to the Aeronautical Services above 400 Mc, by V. I. Weihe, (c) Experimental Multiplexing of Functions in the 960 to 1,660-Mc Frequency Spectrum—its Influence on Weight and Complexity of Equipment, by P. C. Sandretto and R. I. Colin, (d) The Philosophy and Equivalence Aspects of Long-Range Radio Navigation Systems, by M. K. Goldstein, and (e) The Future in Approach and Landing Systems, by H. Davis. 92. A Forward-Transmission Echo-Ranging System, by D. B. Harris. 115. The Determination of Ground Speed of Aircraft using Pulse-Doppler Radar, by I. Wolff, S. W. Seeley, E. Anderson, and W. D. Hershberger. 116. The Dimeal Aircraft Approach and Landing System, by L. B Hallman, Jr. 117. Theoretical Aspects of Nonsynchronous Multiplex Systems, by W. D. White. 118. Band-Pass Circuit Design for Very-Narrow-Band, Very-Long Range Direction-Finder Receivers to minimize Bearing Error due to Receiver Mistuning, by M. Dishal and H. Morrow. 119. Crystal Control at 1,000 Mc for Aerial Navigation, by S. H. Dodington. 130. VHF Airborne Navigational Receiver and Antenna System, by A. G. Kandoian, R. T. Adams, and R. C. Davis. 131. Certain New Performance Criteria for Localizer and Glide-Slope Ground Installations, by P. R. Adams. 132. Phase and other Characteristics of 330-Mc Glide-Path Systems, by S. Pickles. 133. Principles of Volume Scan [for radar], by D. Levine. 134. The Control of Resonance Effects on the Radio Bearings of an Aircraft High-Frequency Direction Finder, by M. K.Goldstein. Titles of other papers are given in other sections.

621.396.9 1673
Principle of Constant Path-Time Difference and its Application in Radiolocation—W. Stanner. (*Elektron Wiss. Tech.*, vol. 3, pp. 70–78; February, 1949.) Discussion of systems using (a) elliptical, (b) hyperbolic-isodromes.

621.396.9 1674
Position-Finding by Radio: First Thoughts on the Classification of Systems—C. E. Strong. (*Jour. IEE* (London), part I, vol. 95, pp. 31–35; January, 1948. Reprinted in *Elec. Commun.*, vol. 25, pp. 278–285; September, 1948.) Full paper; long summary noted in 1039 of 1948.

621.396.9:551.578.1 1675
Radar Observation of Heavy Rain—H. Whalley and G. J. Scoles. (*Nature* (London), vol. 163, p. 372; March 5, 1949.) Photographs of a radar PPI screen showing a belt of heavy rain passing over the Manchester district are reproduced and briefly discussed.

621.396.9:551.594.6 1676
Location of Thunderstorms by Radio—(*Nature* (London), vol. 163, p. 75; January 8, 1949.) Brief discussion of the British Meteorological Office storm-location network. The apparatus used was described by Adcock and Clarke (2779 of 1947). See also 1056 of May (Ockenden).

621.396.932 1677
The Application of Radar to the Science and Art of Marine Navigation—P. G. Satow. (*Jour. Roy. Soc. A.*, vol. 97, pp. 221–234; February 25, 1949.) General discussion of the way in which marine radar, developed primarily for war purposes, has been adapted to assist navigation in harbors and narrow waters, collision prevention, position fixing, etc.

621.396.932 1678
The Decca Navigator System with Lane Identification—(*Engineer* (London), vol. 187, pp. 101–102; January 28, 1949.) The English and Danish chains cover an area of 500,000 square miles; other chains in Scotland and Western England are under construction. Lane identification enables navigators entering the area of coverage to determine a reference point. For this purpose, special transmissions take place at approximately one-minute intervals. The identification meter is then illuminated by the appropriate color (red, green, or purple), and the pointer takes up a position from which the corresponding decometer can be set. A vernier arrangement gives greater accuracy of setting, particularly at night.

621.396.933 1679
Developing an Indicator for H_2S Equipment—R. T. Croft. (*Jour. Brit. I.R.E.*, vol. 9, pp. 75–81; February, 1949.) Description of a rotating radial timebase for a PPI, with a particular attention to the design of deflection circuits for complete and sector display. The basic circuits for the deflection amplifiers, the cathode-ray-tube supplies, and the video amplifiers are also considered.

629.13.014.57:621-526 1680
Automatic Pilots—J. C. Owen. (*Elec. Eng.*, vol. 67, pp. 551–561; June, 1948.) Discussion of the application of servomechanisms to airplane control.

MATERIALS AND SUBSIDIARY TECHNIQUES

533.5+621.315.59+621.315.61 1681
1949 IRE National Convention Program—(Proc. I.R.E., vol. 37, pp. 160–178; February, 1949.) Abstracts are given of the following papers read at the convention:—Symposium on Germanium and Silicon Semiconductors, com-

prising (a) Electrical Properties of Germanium and Silicon, by K. Lark-Horovitz, (b) The Metallurgy of Germanium and Silicon Semiconductors, by J. H. Scaff, (c) Theory of Rectification, by F. Seitz, and (d) Physics of the Transistor, by W. H. Brattain. 56. Conductive Plastic Materials, by M. A. Coler; F. R. Barnet, A. Lightbody, and H. A. Perry. 79. A Critical Survey of Methods of making Ceramic-to-Metal Seals and their Use for Electron-Tube Construction, by R. P. Wellinger. 81. An Improved Method of testing for Residual Gas in Electron Tubes and Vacuum Systems, by E. W. Herold. Titles of other papers are given in other sections.

535.37 1682

Theory of the Extinction of Luminescence of Organic Phosphors—B. Ya. Sveshnikov. (*Zh. Eksp. Teor. Fiz.*, vol. 18, pp. 878–885; October, 1948. In Russian.)

535.37 1683

Dependence of the Intensity of the Luminescence of ZnO and ZnS-Zn on the Intensity of Excitation—F. I. Vergunas and F. F. Gavrilov. (*Zh. Eksp. Teor. Fiz.*, vol. 18, pp. 873–877; October, 1948. In Russian.)

535.37 1684

Contributions to the Study of the Photoluminescence of Zinc Sulphide—J. Saddy. (*Ann. Phys.* (Paris), vol. 2, pp. 414–455; July and August, 1947.) The suppressing or enhancing effect of traces of metals of the Fe group on the photo luminescence of Cu-activated ZnS is studied. The principal formulas proposed for the natural decay of the phosphorescence of ZnS-Cu are discussed theoretically and compared with experimental results.

537.228.1:549.514.51 1685

Calculation of the Piezo-Electric Constants of α-Quartz on Born's Theory—B. D. Saxena and K. G. Srivastava. (*Indian Jour. Phys.*, vol. 22, pp. 475–482; November, 1948.)

538.23:621.318.323.2 1686

Hysteresis and Eddy Currents in Coil-Core Stampings in Weak A.C. Fields—R. Feldtkeller. (*Fernmeldetech. Z.*, vol. 2, pp. 9–14; January, 1949.) Measurement results are presented graphically for various Si/Fe and Ni/Fe alloys of German manufacture.

546.287:621.315.61 1687

Silicones. Their Use in Electrical Technique—G. de Senarclens. (*Bull. Schweiz. Elektrotech. Ver.*, vol. 37, pp. 117–126; March 9, 1946. In French.) A general account of the preparation and properties of silicone liquids, greases, resins and varnishes, and their use for insulation or lubrication, particularly at relatively high temperatures.

546.289:621.315.591.1†:537.311.33 1688

Interpretation of Dependence of Resistivity of Germanium on Electric Field—E. J. Ryder and W. Shockley. (*Phys. Rev.*, vol. 75, p. 310; January 15, 1949.)

546.431.82:621.315.612 1689

Production and Investigation of $BaTiO_3$ Single Crystals—H. Blattner, W. Känzig, and W. Merz. (*Helv. Phys. Acta*, vol. 22, pp. 35–65; February 15, 1949. In German.) The investigations were concerned with the behavior of the dielectric constant, the specific heat, and the resonance frequency as functions of temperature. Results are shown graphically and discussed.

621.315.553 1690

On the Use of New Resistance Materials for Standard Resistors—A. Schulze. (*Elektrotechnik* (Berlin). vol. 3, pp. 23–28; January, 1949.) A detailed account of measurements, extending over a period of about 10 years, of the values of various resistors of the Cu/Mn group of materials, including manganin, novoconstant (82.5 per cent Cu, 12 per cent Mn, 1.5 per cent Fe, 4 per cent Al) and a Heusler alloy 306, and also of Au-Cr and Ag-Mn resistors. The alloy 306 contains some Zn and has a temperature coefficient of resistance of less than 1 part in 10^6 per 1°C. The coefficients of the Au-Cr and Ag-Mn resistors are of the same order. Curves and tables show the variations of the different resistors with time.

621.315.61:621.396.662.029.64 1691

Attenuator Materials for Microwaves—G. K. Teal, M. D. Rigterink, and C. J. Frosch. (*Elec. Eng.*, vol. 67, pp. 754–757; August, 1948.) Homogeneous dielectrics have serious drawbacks as attenuator materials. The dielectric properties of inhomogeneous solid lossydielectrics such as silicon carbide dispersed in porcelain, or graphite dispersed in phenol formaldehyde, are considered; methods of reducing unwanted reflections as the air versus solid interface are discussed. Resistor strips such as sprayed films of graphite pigmented acryloid or silicone can also be used.

621.315.612.011.5 1692

Electrical Properties of Ceramics—E. W. Lindsay and L. J. Berberich. (*Elec. Eng.*, vol. 67, p. 440; May, 1948.) Long summary of AIEE paper. If the logarithm of the resistivity, dielectric strength, or power factor be plotted against the reciprocal of the absolute temperature, the graph consists of two straight lines whose intersection determines a transition temperature. Below this temperature, current flow appears to be dominated by dielectric absorption; above, by electrolytic conduction.

621.315.614 1693

Thermal Aging Properties of Cellulose Insulation Materials—G. Malmlöw. (*Kungl. Tekn. Högsk. Handl.* (Stockholm), no. 19, 67 pp.; 1948. In English.) A general discussion with historical introduction and bibliography of 56 references.

621.315.615.011.5 1694

Dielectric Strength of Liquids for Short Pulses of Voltage—K. A. Macfadyen and W. D Edwards. (*Nature* (London), vol. 163, pp. 171–172; January 29, 1949.) Measurements on ethyl alcohol and benzene indicate an increase in their dielectric strength as the pulse duration is reduced. The breakdown, once started, becomes complete in about 10^{-9} second.

621.315.616.011.5 1695

The Electric Strength of some Synthetic Polymers—W. G. Oakes. (Proc. I.R.E., part I, vol. 96, pp. 37–43; January, 1949. Discussion, p. 43.) Results for the temperature range $-200°$ to $+110°$C are discussed in the light of Fröhlich's electronic theory of breakdown (2405 of 1947 and back references).

621.315.616.015.5 1696

A Note on Crystallite Size and Intrinsic Electric Strength of Polythene—D. W. Bird and H. Pelzer. (Proc. I.R.E., part I, vol. 96, pp. 44–45; January, 1949.) Continuation of 764 of 1947 (Austen and Pelzer). No significant difference is found between measurements on quenched and unquenched polythene. Crystallite size, therefore, appears to have little effect on electric strength.

621.316.99 1697

The Behaviour of Earth Connections Subjected to High Current Surges—K. Berger. (*Bull. Schweiz. Elektrotech. Ver.*, vol. 37, pp. 197–211; April 20, 1946. In German, with French summary.) The results of measurements with various types of earth connection, subjected to surges from 200 to 800 kv with currents ranging up to 11,000 amperes are shown graphically and tabulated.

621.318.22 1698

The Permanent Magnet Steel "Ticonal" and its Application in Loudspeakers—(*Phi Tech. Commun.* (Australia), pp. 3–14; A 1948.)

666.11:621.315.612.011.5:621.385 1

Contribution to the Study of the Electr Properties of Glasses used in the Construct of Radio Valves—P. Meunier. (*Ann. Ra élec.*, vol. 4, pp. 54–67; January, 1949.) M ods are described for investigating the va tions of resistivity, loss factor, dielectric c stant, and power dissipation with temperat and frequency. The results obtained have i mediate practical application in tube manuf ture.

621.315.59+621.314.6+621.396.622+621.3 17

German Research on Semi-Conducto Metal Rectifiers, Detectors and Photoce [Book Notice]—B.I.O.S. Final Report N 1751. H.M. Stationery Office, London, 46 p 5s. 6d.

MATHEMATICS

517.512.2 17

A Clear Representation of the Spectral D tribution of Periodic and Nonperiodic Pheno ena—F. A. Fischer. (*Fernmeldetech. Z.*, vol. pp. 21–23; January, 1949.) A direct derivati of the Fourier integral for nonperiodic pl nomena; for the periodic case, the integral tra forms into Fourier series.

517.65(083.5):621.396.67 17

Iterated Sine and Cosine Integrals—E. H lén. (*Kungl. Tekn. Högsk. Handl.* (Stockholn No. 12, 6 pp.; 1947. In English.) The followi functions relevant to antenna theory are tab lated:

$$L_{11}(x) = C_{11}(x) + iS_{11}(x) = \int_0^x \frac{L(\xi)}{\xi}\, d\xi$$

$$L_{21}(x) = C_{21}(x) + iS_{21}(x)$$

$$= \int_0^x \frac{e^{i\xi}}{\xi} L(2\xi) - L(\xi) d\xi$$

where

$$L(x) = \int_0^x \frac{(1 - e^{-i\xi})}{\xi}\, d\xi.$$

518.5 17

1949 IRE National Convention Program (Proc. I.R.E., vol. 37, pp. 160–178; February 1949.) Abstracts are given of the following pa pers read at the convention:—Symposium o Electronic Computing Machines, comprisin (a) Results of Tests on the Binac, by J. W Mauchly, (b) The Mark III Computer, b H. H. Aiken, (c) The IBM Type 604 Elec tronic Calculator, by R. Palmer, (d) Electro static Memory for a Binary Computer, by F. C Williams, (e) Counting Computers, by G. R Stibitz, and (f) Programming a Computer fo Playing Chess, by C. E. Shannon. 37. A Dy namically Regenerated Memory Tube, by J. P Eckert, Jr., H. Lukoff, and G. Smoliar. 38. A Electronic Differential Analyzer, by A. E Macnee. 39. An Analogue Computer for th Solution of Linear Simultaneous Equations, b R. M. Walker. 40. The Electronic Isograph fo a Rapid Analogue Solution of Algebraic Equa tions, by B. O. Marshall, Jr. 41. A Parametri Electronic Computer, by C. J. Hirsch. Titles o other papers are given in other sections.

518.5 17

Electronic Analog Computer—H. R. Heg bar. (*Electronics*, vol. 22, pp. 168, 174; Marc 1949.) Results are accurate within 0.1 per cen Sets of simultaneous differential equations wit constant coefficients can be solved.

518.5:512.39 17

An Electronic Method for Solving Simu taneous Equations—A. C. Hardy and E. C Dench. (*Jour. Opt. Soc. Amer.*, vol. 38, pp. 308

2; April, 1948.) For solving equations in 3 or variables arising in color printing. Each indidual variable is involved linearly, but the to- l degree equals the number of variables. Solu- ns are obtained at the rate of about 1,000 per cond.

8.5:517.944 1706
Electric Circuit Models of Partial Differen- l Equations—G. Kron. (*Elec. Eng.*, vol. 67, . 672–684; July, 1948.) Discussion of electri- l models developed to represent some of the sic linear partial differential equations of athematical physics. The models can be used r all orthogonal curvilinear co-ordinate sys- ms and can represent transient, sinusoidal, or atic fields. Particular equations thus repre- nted include: (a) Laplace's and Poisson's uations, (b) the general scalar-potential and ctor-potential equations, (c) compressible id flow equations, (d) Maxwell's equations, the wave equations of Schrödinger, and (f) e basic equations of elasticity. The models n be used to solve initial-value, boundary- lue, and characteristic-value problems. Ac- racy is within 1 to 5 per cent.

8.5:517.947.4 1707
An Electrical Potential Analyser—S. C. dshaw. (*Proc. Inst. Mech. Eng.* (London), l. 159, War Emergency Issue No. 38, pp. 55– ; 1948. Discussion, pp. 62–80.) The analyzer ovides, in effect, an electrical analogy to the lution of Poisson's and Laplace's equations ien expressed in finite difference form. It con- ts essentially of a square mesh, the nodal ints of which are interconnected by low-value re resistances, and a base. Corresponding ints on the mesh and base are connected rough high-value resistances. A mesh separa- n of 1/12 of the side length is satisfactory.

7.564.3(083.5) 1708
Tables of the Bessel Functions of the First nd [Book Review]—Harvard University ess, Cambridge, Mass.; Oxford University ess, London, 1948, 55s. each volume. (*Na- re* (London), vol. 163, p. 152; January 29, 49.) Vols. 7 to 10 of the tables compiled by e staff of the Computation Laboratory, Har- rd, covering orders 10 to 39. For orders above a uniform interval of 0.01 is used for the ar- ment. Vols. 3 to 6 were noted in 463 and1396 1948.

8.2 1709
Five-Figure Tables of Natural Trigonomet- al Functions [Book Review]—H. M. Nauti- Almanac Office. H. M. Stationery Office, ndon, 1947, 124 pp., 15s. (*Nature* (London), l. 163, p. 347; March 5, 1949.) An auxiliary ble gives values of the cotangent for every cond of arc up to 7: 30′. The main table gives lues of the sine, tangent, cotangent, and co- e at 10-second intervals.

MEASUREMENTS AND TEST GEAR

1.76:681.11 1710
A Watch Rate Recorder—H. G. M. Spratt. *lectronic Eng.*, vol. 21, pp. 39–44; February, 49.) The amplified ticks of the watch under t actuate a printing bar and are recorded on aper chart, which is driven at a constant own rate by a power source whose frequency lerived from a quartz oscillator. Circuit dia- ams are given, together with detailed ex- ples of the use of the instrument. See also 59 of 1948 (Mackay and Soule) and 2838 of 48 (van Suchtelen).

1.761 1711
Time Service Equipment at the Dominion bservatory—G. A. Eiby. (*N. Z. Jour. Sci. ch.*, vol. 29, pp. 296–308; May, 1948.) The ctrical wiring and relay system for this serv- is described, with photographs and circuit grams of certain parts of the equipment. The development, present capabilities, and possible extension of the service are considered.

621.3.018.4(083.74) 1712
Microwave Frequency Standards—B. F. Huston and H. Lyons. (*Elec. Eng.*, vol. 67, pp. 436–439; May, 1948.) Long summary of AIEE paper. Discussion of a new National Bureau of Standards service providing frequency measurements and calibrations of frequency meters or voltage sources. The standard frequencies are derived from a primary 100-kc standard, accurate to 1 part in 10^8, by frequency multiplication, conversion, and harmonic selection.

621.317 1713
1949 IRE National Convention Program—(Proc. I.R.E., vol. 37, pp. 160–178; February, 1949.) Abstracts are given of the following papers read at the convention:—12. Measuring the Efficiency of a Superheterodyne Converter by the Input-Impedance Circle Diagram, by H. A. Wheeler and D. Dettinger. 13. Electrolytic-Tank Measurements for Microwave Delay-Lens Media, by S. B. Cohn. 14. A Michelson-Type Interferometer for Microwave Measurements, by B. A. Lengyel. 15. Impedance Instrumentation for Microwave Transmission Lines, by P. A. Portmann. 16. A Broad-Band High-Power Microwave Attenuator, by H. J. Carlin. 17. An Absolute Method for Measuring Microwave Power of Low Intensity, by H. Herman. 21. The Measurement of Nonlinear Distortion, by A. P. G. Peterson. 32. An Impulse Generator-Electronic Switch for Visual Testing of Wide-Band Networks, by T. R. Finch. 33. A 50-Mc Wide-Band Oscilloscope, by A. M. Levine and M. Hoberman. 34. A Timing-Marker Generator of High Precision, by R. C. Palmer. 35. The Evaluation of Specifications for Cathode-Ray Oscillographs, by P. S. Christaldi. 51. Spectrum Analysis of Transient-Response Curves, by H. A. Samulon. 73. An AM Broadcast Station Monitor, by H. R. Summerhayes, Jr. 99. High-Impedance Millivolt Measurements above 5 Mc, by W. J. Volkers. 101. A Wide-Band Audio Phasemeter, by J. R. Ragazzini and L. A. Zadeh. 102. A Device for Admittance Measurements in the 50 to 500-Mc Range, by W. R. Thurston. 103. An Improved RF Capacitometer, by E. F. Travis and T. M. Wilson. Titles of other papers are given in other sections.

621.317.324†:621.396.615.141.2 1714
Rotating Probe Machine—G. L. Stambach. (*Electronics*, vol. 22, pp. 182, 189; March, 1949.) For investigating field patterns inside multi-cavity magnetrons. Brief details are given of construction and operation; measured and theoretical results are compared.

621.317.33(083.74) 1715
Radio Standards—L. Hartshorn and L. Essen. (Proc. I.R.E., part III, vol. 96, pp. 37–39; January, 1949.) The status and accuracy of the standards of capacitance, inductance, and frequency are briefly reviewed.

621.317.331:621.316.99 1716
The Measurement of Earth Resistance—H. Engel. (*Tech. Mitt. Schweiz. Telegr.-Teleph. Verw.*, vol. 27, pp. 14–20; February 1, 1949. In French and German.) An account of simple dc methods and also of a new method with particular advantages which uses the ac mains supply.

621.317.335.3†:621.315.611 1717
Dielectric Measurement Methods for Solids at Microwave Frequencies—W. H. Surber, Jr., and G. E. Crouch, Jr. (*Jour. Appl. Phys.*, vol. 19, pp. 1130–1139; December, 1948.) A high-loss dielectric sample is enclosed within a section of waveguide; the loss is then calculated from the SWR obtained with open-circuit and with short-circuit termination of the waveguide. Using the same apparatus, the loss of low-loss dielectrics can be measured by matching-in the sample and using a frequency-variation method.

621.317.336 1718
Impedance Measurements in Decimetre Wave Band—B. Josephson. (*Kungl. Tekn. Högsk. Handl.* (Stockholm), no. 23, 70 pp.; 1948. In English.) For relatively low impedances, a standing-wave method is described in which the distance between the probe and the inner conductor is varied so as to keep the line voltage constant. For high impedances, a resonant-circuit method analogous in principle to a Q meter is considered. A comprehensive practical and theoretical study of the two methods includes detailed discussion of apparatus and results.

621.317.336:621.396.611.4 1719
On the Measurement of Cavity Impedance—W. W. Hansen and R. F. Post. (*Jour. Appl. Phys.*, vol. 19, pp. 1059–1061; November, 1949.) The ratio R/Q is defined, where R is the shunt resistance. R/Q is measured by observing the change in resonant wavelength caused by introducing small conducting buttons into the cavity.

621.317.44 1720
An Arrangement for Maintaining a Constant Magnetic Field—H. Naumann. (*Z. Angew. Phys.*, vol. 1, pp. 260–264; January, 1949.) Apparatus using large Helmholtz coils for producing fields of the order of that of the earth is compensated for external disturbing effects, both as regards intensity and direction, by means of a variometer. This variometer is operated by photo cells whose currents are controlled by the motion of small magnetic needles suitably oriented at points on the axis of the system.

621.317.444† 1721
A Simple Direct-Reading Fluxmeter—J. H. Briggs and W. H. Mitchell. (*Jour. Sci. Instr.*, vol. 26, pp. 40–42; February, 1949.) Eccentric cylindrical vanes of aluminium are thinly coated with dust iron having negligible hysteresis. The large torque in a field of the order of 1,000 gauss enables strong control springs and ball-ended pivots to be used for robust instruments that can measure fluxes up to 7,500 gauss, for magnets of various shapes, to an accuracy within 2 per cent.

621.317.7+621.396.69 1722
Standardised Super-High-Frequency Components and Instruments—(*See* 1633.)

621.317.73 1723
An Automatic Impedance Meter—H. Werthén and B. Nilsson. (*Kungl. Tekn. Högsk. Handl.* (Stockholm), no. 8, 95 pp.; 1947. In English.) The meter includes a signal generator and alternative recording instruments for rough and accurate measurements respectively. Attenuation and phase can be determined for 2-terminal and 4-terminal networks, at frequencies from 10 to 500 kc.

621.317.73:621.315.2.029.6 1724
A Pulse Test Set for the Measurement of Small Impedance Irregularities in High-Frequency Cables—F. F. Roberts. (Proc. I.R.E. part III, vol. 96, pp. 17–23; January, 1949.) The impedance irregularities are measured in terms of the return loss (up to 90 db) of echo pulses reflected from the irregularities when 0.3-microsecond 20-Mc pulses are fed into the coaxial cable.

621.317.761 1725
Some Problems in the Accurate Measurement of Frequencies in the Region of Microwaves (1,500—40,000 Mc/s)—M. Denis and B. Epstein. (*Ann. Radioélec.*, vol. 4, pp. 12–25; January, 1949.) Standard-frequency generators of the type developed at the National Bureau of Standards are described and the possibility

is considered of using klystron frequency multipliers, associated if need be with traveling-wave tube amplifiers, in lieu of some of the crystal multipliers normally used at uhf. Methods of calibrating cavity-type frequency meters are described and block diagrams are given. A suitable klystron frequency multiplier is the X.M. 10; this has an input cavity whose resonance frequency is adjustable from 250 to 310 Mc, and an output cavity giving any harmonic of the input from the 8th to the 13th. A frequency band from 2,000 to 4,000 Mc can thus be covered with a useful power of about 250 mw, the high-frequency input power being about 5 watts. Crystal multipliers can then extend the range to frequencies of the order of 40,000 Mc.

621.317.772 1726

An Electronic Phasemeter—E. F. Florman and A. Tait. (PROC. I.R.E., vol. 37, pp. 207–210; February, 1949.) An instrument designed to read within 0.5° and record directly on calibrated scales the phase angle between two sinusoidal voltages for a voltage range of 1 to 30 volts and frequency range 100 to 5,000 cps. The voltages are converted to square waves through cascade amplifiers and limiters and applied to two separate phase indicators. One of these has a 180° ambiguity and records the average of the algebraic sum of the square waves. The second indicator is unambiguous; the square waves are differentiated and the proper resultant pulses are used to fire an Eccles-Jordan trigger circuit. The average trigger-tube anode current is proportional to the phase angle between the input voltages.

621.317.784 1727

Absolute Power Measurement at Microwave Frequencies—A. L. Cullen. (*Nature* (London), vol. 163, p. 403; March 12, 1949.) The technique is similar to that used for measuring light-radiation pressure with a torsion balance.

621.317.784:621.314.2.029.3 1728

Audio Frequency Transformer Design—Brockelsby. (*See* 1607.)

621.317.79:621.392.26† 1729

The Reflectometer—H. R. Allan and C. D. Curling. (PROC. I.R.E., part III, vol. 96, pp. 25–30; January, 1949.) General theory is given and a design suitable for waveguides using 10-cm waves is described. Applications to the monitoring of standing waves and transmitted power in a radar transmitter system and to the testing of radar receiver sensitivities are considered; reflectometer methods are shown to be superior to other methods. See also 3968 of 1947 (Parzen and Yalow).

621.396.662(083.74) 1730

Microwave Attenuation Standard—R. E. Grantham and J. J. Freeman. (*Elec. Eng.*, vol. 67, pp. 535–537; June, 1948.) Long summary of AIEE paper.) A standard has been established using the heterodyne or if substitution method of calibration. A preliminary model of the standard has been built and its accuracy is within 0.02 db and 0.02 per cent of measured attenuation in the 0 to 10 db and 10 to 50-db ranges respectively. Methods of eliminating unwanted modes are discussed.

OTHER APPLICATIONS OF RADIO AND ELECTRONICS

534.321.9.001.8:539.32 1731

Determination of the Elastic Constants of Solids by Ultrasonic Methods—W. C. Schneider and C. J. Burton. (*Jour. Appl. Phys.*, vol. 20, pp. 48–58; January, 1949.)

535.61-15:621.383 1732

Infra-Red Location [of objects] with Lead Sulphide Cells—W. Ochmann. (*Elektron Wiss. Tech.*, vol. 3, pp. 96–101; March, 1949.) A description of German equipment for the location of aircraft, ships, etc. A parabolic mirror 150 cm in diameter, with a special reflector system, concentrates the received radiation on the sensitive cell. A device using a rotating glow-lamp provides a visual indication of direction adjustment, a sector of light of increasing extent being seen as the mirror axis approaches the target, with a complete ring of light when on target. Under good conditions, the range for aircraft is of the order of 20 km and the accuracy of location within $\frac{1}{16}$ degree.

Optical apparatus, developed at a later date used lenses 8 cm in diameter made from a special material, principally lithium fluoride, with very good infrared transmission properties. With this apparatus, a bomber could be located at a distance of 3 km.

539.16.08+621.3 1733

1949 IRE National Convention Program—(PROC. I.R.E., vol. 37, pp. 160–178; February, 1949.) Abstracts are given of the following papers read at the convention:—57. The RF System for the University of Rochester 130-inch Synchrocyclotron, by W. W. Salisbury. 59. Design of a G-M Counter Tube for High Counting Rates, by W. W. Managan. 61. Proportional-Counter Equipment for Beta Detection, by W. Bernstein. 62. Industrial Thickness Gauges employing Radioisotopes, by J. R. Carlin. 77. Radar-Circuit-Powered X-Ray Movie Equipment for Operation at 150 Frames per Second, by D. C. Dickson, Jr., C. T. Zavales, and L. F. Ehrke. 104. A Radio-Frequency Gas-Discharge Phenomenon and its Application to Mechanical Measurements, by K. S. Lion and J. W. Sheetz. Titles of other papers are given in other sections.

550.838:538.71 1734

Canadian Aerial Magnetic Surveys (M.A.D.)—R. Bailey. (*Canad. Jour. Res.*, vol. 26, sec. F, pp. 523–539; December, 1948.) Tests with an airborne magnetic detector measuring the earth's total field indicate that it has a high degree of accuracy and speed for reconnaissance work over large areas and is cheap to operate.

551.508.1:621.396.9 1735

The Development of the Meteorological Office Radar Reflector, Mk. IIB—O. M. Ashford and H. J. Ferrer. (*Met. Mag.*, vol. 77, pp. 224–227; October, 1948.) The development and performance of a corner reflector, with planes of nylon mesh impregnated with silver, for use with 10-cm radar in the detection of upper winds. The reflector performs slightly better than a standard 3-foot paper reflector; it has less drag and requires less storage space.

621.317.39 1736

Electronic Gauges—J. Schwartz. (*Microtecnic* (Lausanne), vol. 2, pp. 199–206 and 267–274; October and December, 1948. In English.) Discussion of various devices for transforming mechanical quantities into electrical voltages, including (a) piezoelectric gauging heads for measuring large pressures or forces, (b) strain gauges of the resistance type, (c) gauges using variation of capacitance, magnetic flux or inductance, and (d) arrangements which transform dimension changes into variations of the illumination of photo cells. The relative merits of these various types for precision measurements are considered; methods using variations of capacitance or inductance are particularly suitable for precision measurements of length.

621.317.39:620.178.3 1737

Vibration Testing of Airplanes—A. R. Willson. (*Electronics*, vol. 22, pp. 86–91; March, 1949.) Fatigue and vibration test methods are described and the layout of equipment for a typical aircraft test is illustrated. Below 7 cps, motor-triggered thyratrons operate the electromotive source of vibration, while electronic equipment is used for higher frequencies. Measuring and recording techniques are described and the type of oscillograph record obtained is shown. See also 3217 of 1947 (Cogman) and 3218 of 1947 (Corke).

621.365.5+621.365.92

Radio-Frequency Heating—L. Hartsh... (*Not. Proc. Roy. Inst.*, vol. 33, no. 153, pp. 553; 1948.) Discussion of the underlying ... ciples of induction and dielectric heating, ... illustrative examples.

621.38.001.8

Design for a Brain—W. Grey Walter ... Summer, H. F. Sheppard, A. Greenwood-... son, P. T. Hobson, W. R. Ashby. (*Electr... Eng.* (London), vol. 21, pp. 62–63; Febru... 1949.) Discussion on 1144 of May.

621.38.001.8:061.3

Applications of Electronics to Research ... Industry—(*Nature* (London), vol. 163, pp. ... 297; February 19, 1949.) For another acc... see 1145 of May.

621.38.001.8:578.088.7

Electronic Mapping of the Activity of ... Heart and the Brain—S. Goldman, W. E. ... ian, Chi Kuang Chien, and H. N. Bowes. ... *ence*, vol. 108, pp. 720–723; December ... 1948.) Any point P of the surface of the c... or skull corresponds to a point P' on the fa... a cathode-ray tube. The brightness at P' is ... portional to the potential at P.

621.38.001.8:615.84

The Electromedical Significance of D... metre and Centimetre Waves—W. Re... (*Elektrotechnik* (Berlin), vol. 3, pp. 3–10; Ja... ary, 1949.) Review of capacitor, inductor, ... radiation methods of applying high-freque... energy in medicine, with discussion of the ... sorption of dm and cm waves by var... organic substances, selective effects, and m... ods of treatment.

621.384.611.1†

16-MeV Betatron at the Clarendon Lab... tory, Oxford—(*Engineering* (London), vol. ... pp. 55–58; January 21, 1949.) For an earlier ... count see 3482 of 1948 (Wilkinson, Tuck, ... Rettie).

621.384.62†

A Proposed New Form of Dielectric-Loa... Wave-Guide for Linear Electron Accelera...—R. B. R. S. Harvie. (*Nature* (London), ... 162, p. 890; December 4, 1948.) A cylindr... metal waveguide has dielectric loading in ... form of circular washers, whose thickness ... spacing are small compared with the wa... length in the waveguide. The washers hav... smaller dielectric constant in the direction ... the waveguide axis than in the transverse di... tions. This anisotropy reduces power los... The total losses compare favorably with th... for a corrugated waveguide. A numerical ... ample is discussed.

621.385.833

The Theoretical Resolution Limit of ... Electron Microscope—O. Scherzer. (*Jour. A... Phys.*, vol. 20, pp. 20–29; January, 1949.) ... resolving power of the electron microscope ... the contrast in the image are calculated for ... ferent conditions of focusing, illumination, ... aperture.

621.385.833

The Optical Properties of Electrost... Lenses, and the Proton Microscope—P. Ch... son. (*Ann. Phys.* (Paris), vol. 2, pp. 333–4 ... July and August, 1947.) A comprehens... treatment, including discussion of aberrat... and of the resolving power of the electron ... croscope. With the proton microscope, hig... resolution should be possible.

621.385.833

A New Horizontal Electron Microscope... N. N. Das Gupta, M. L. De, D. L. Bhatta... arya, and A. K. Chaudhury. (*Indian Jo...*

vs., vol. 22, pp. 497–513; November, 1948.) hnical details of construction, power sup- s, and operation of an instrument con- ıcted at the University College of Science, cutta. Capable of operating at a maximum tron energy of 80,000 eV, it is designed to e a magnification of 20,000 diameters. The izontal arrangement enables any part to be ly dismantled or adjusted. An historical ine of research in this field is also given.

.385.833 1748
Electron Microscopy—C. J. Burton. (*Anal. m.*, vol. 21, pp. 36–40; January, 1949.) A vey of progress in the last 10 years, with iography of 159 references.

.385.833:061.3 1749
Electron Microscopy Conference [Cam- lge, England, Sept. 1948]—V. E. Cosslett. *ature* (London), vol. 163, pp. 32–34; Janu- 1, 1949.) A general account of the proceed-

.385.833:621.316.722.1 1750
Stabilization of the Accelerating Voltage in Electron Microscope—van Dorsten. (*See* 5.)

.385.833:621.317.729:[537.291+538.691 1751
Plotting Electron Trajectories—K. F. der, C. W. Oatley, and J. G. Yates. (*Na-* (London), vol. 163, p. 403; March 12, 1949.) ew method for electron optical systems. ifferential analyzer is used to integrate the ations of motion of an electron, the com- ents of acceleration being determined by matic measurements in an electrolyte tank. ults obtained agree satisfactorily with the-

386.1:778.332:548.73 1752
An Improved X-Ray Diffraction Camera—Parrish and E. Cisney. (*Phillips Tech. Rev.*, 10, pp. 157–167; December, 1948.) Various ors involved in design and interrelated in r influence on the properties of diffraction erns are considered.

38.001.8 1753
ndustrial Electronics Reference Book k Review]—Westinghouse Electric Corp. iley, New York, N. Y.: Chapman and Hall, don, 1948, 680 pp., $7.50. (*Science*, vol. 109, 4; January 14, 1949.) A "digest embracing applications as well as the design data." ıy excellent graphs, tables, and illustrations erning materials and equipment are in- ed; theory is necessarily treated briefly. See *Electronics*, vol. 22, pp. 247, 248; March,

PROPAGATION OF WAVES

421:538.56 1754
On the Diffraction of Electromagnetic es at a Wire Grid—R. Honerjäger. (*Ann.* s. (Lpz.), vol. 4, pp. 25–45; September 20, .) The theory of Wessel (5 of 1940) for e waves incident normally on an unlimited e grid of parallel wires applied to wave- ths exceeding half the grid spacing. The ry is here extended to any angle of inci- e and any wavelength, and verified by ex- nents with waves in a rectangular wave- e.

566 1755
Study of the Wave obtained by Total eous Reflection in Media with Non-Zero netic Susceptance—H. Arzeliès. (*Ann.* s. (Paris), vol. 2, pp. 517–535; September October, 1947.) The classical formulas of nel only apply to nonmagnetic media. The esponding general formulas here derived symmetrical for the two principal waves are consequently, in spite of their general- easier to handle than the particular formu- las of Fresnel. Applications to the technique of centimeter and millimeter waves are discussed.

538.566 1756
On the Calculation of the Electromagnetic Energy Dissipated in a Medium with Selective Absorption—H. Arzeliès. (*Ann. Phys.* (Paris), vol. 2, pp. 536–544; September and October, 1947.)

621.396.11 1757
1949 IRE National Conventional Program—(Proc. I.R.E., vol. 37, pp. 160–178; February, 1949.) Abstracts are given of the following papers read at the convention:—42. VHF Television—Propagation Aspects, by E. W. Allen, Jr. 43. Propagation Variations at VHF and UHF, by K. Bullington. 44. Propagation Tests at UHF, by J. Fisher. 45. A Test of 450-Mc Urban-Area Transmission to a Mobile Receiver, by A. J. Aikens and L. Y. Lacy. 46. Echoes in Transmission at 450 Mc from Land-to-Car Radio Units, by W. R. Young and L. Y. Lacy. 88. An Analysis of Distortion resulting from Two-Path Propagation, by I. H. Gerks. 91. Propagation Conditions and Transmission Reliability in the Transitional Microwave Range, by T. F. Rogers. Titles of other papers are given in other sections.

621.396.11 1758
Ground-Wave Propagation over an Inhomogeneous Smooth Earth—G. Millington. (Proc. I.R.E., part III, vol. 96, pp. 53–64; January, 1949.) Assuming the inhomogeneity to consist of annulae of homogeneous earth, concentric with the transmitter, the terminal field strength for short waves is shown to be the geometric mean of the values it would have if the earth were homogeneous and of the type near (a) the transmitter and (b) the receiver. Energy considerations enable the result to be extended, approximately, for longer waves. A tentative solution at the boundary shows that there is a recovery of field strength before attenuation sets in, when the wave passes to a more highly conducting region. Stress is laid on the need for more experimental verification.

621.396.11 1759
Radiation Pressure of Centimetre Waves—N. Carrara and P. Lombardini. (*Nature* (London), vol. 163, p. 171; January 29, 1949.) The pressure was measured by the torque produced on a torsion balance in a rarefied atmosphere at a pressure of 10 mm Hg. The balance was placed near the mouth of a rectangular waveguide connected to a magnetron generating 50 watts mean power at $\lambda=3$ cm. The observed pressure was about 10^{-2} dyne/cm^2. Theoretical considerations suggest a reduction in radiation pressure inside a waveguide.

621.396.11:551.510.52 1760
Theory and Practice of Tropospheric Sounding by Radar—A. W. Friend. (Proc. I.R.E., vol. 37, pp. 116–138; February, 1949.) 1948 IRE National Convention paper. Soundings have been made (a) at medium-frequency between 1935 and 1942, (b) more recently, by means of a modified SCR-584 and AN/CPS-1 (MEW) microwave radar, with continuous photographic recording. The types of echo that can be received in each of these cases are discussed, with illustrative examples; they include, at medium frequencies, discrete echoes from air-mass boundaries or thick regions of relatively high dielectric-constant gradient and, with microwaves, scattering from raindrops, snowflakes, etc., and dot, line, and other unusual weak-echo signals. The origins of many microwave echoes appear from theory and experimental evidence to be in the fine structures of the dielectric transition layers of air-mass boundaries and turbulent regions. Much valuable information could be obtained by the use of 3 vertical beam systems for simultaneous and continuous sounding and recording, operating with high-gain antennas and the maximum power available at frequencies of say 400, 4,000 and 40,000 Mc.

621.396.11:551.510.52 1761
A Theory on Radar Reflections from the Lower Atmosphere—W. E. Gordon. (Proc. I.R.E., vol. 37, pp. 41–43; January, 1949.) "Angels" may be attributed to sharp changes in the dielectric constant produced by atmospheric turbulence.

621.396.11:551.510.535 1762
Predicting Maximum Usable Frequency from Long-Distance Scatter—A. H. Benner. (Proc. I.R.E., vol. 37, pp. 44–47; January, 1949.) From observations of long-distance scatter, it is concluded that *E*-layer clouds are responsible for the leading edge of the echo but that the maximum amplitude is returned from the ground. This is used as a basis for calculating the maximum usable frequency from the time delay of the scatter.

621.396.11:551.510.535 1763
Deviation at Vertical Incidence in the Ionosphere—G. Millington. (*Nature* (London), vol. 163, p. 213; February 5, 1949.) Even at vertical incidence, the reflection points of the ordinary and extraordinary rays can be separated by a horizontal distance of some 50 km if the frequency is near the ordinary-ray critical frequency. *P'f* records, therefore, need careful interpretation if a large horizontal gradient in ionization is likely.

621.396.11:551.510.535 1764
The Radio Amateur and Upper Atmosphere Research—Ferrell. (*See* 1666.)

621.396.11:551.551 1765
The Problem of Diffusion in the Lower Atmosphere—Sutton. (*See* 1667.)

621.396.11:551.553.11 1766
Sea Breeze Structure with Particular Reference to Temperature and Water Vapour Gradients and Associated Radio Ducts—Hatcher and Sawyer. (*See* 1668.)

621.396.812+538.566.3 1767
Photographic Record and Diagrams of Luxembourg Effect with Resonance (Gyro-Interaction)—M. Cutolo and R. Ferrero. (*Nature* (London), vol. 163, pp. 59–60; January 8, 1949.) Discussion of the results of observations carried out in May and June, 1948, to measure the depths of parasitic modulation obtained when using a disturbing wave whose frequency was equal to the local gyrofrequency. For earlier work, see 513 of 1947 (Cutolo, Carlevaro, and Ghergi), 2055 of 1948 (Cutolo), and 1477 of May.

RECEPTION

621.316.729:621.396.619.16:621.396.41 1768
Synchronization for the PCM Receiver—J. M. Manley. (*Bell. Lab. Rec.*, vol. 27, pp. 62–66; February, 1949.) The incoming pulse frame is automatically and continuously examined every 125 microseconds. Any errors of alignment are corrected in under 0.1 second by a switch system.

621.396.621 1769
1949 IRE National Convention Program—(Proc. I.R.E., vol. 37, pp. 160–178; February, 1949.) Abstracts are given of the following papers read at the convention:—100. Some Aspects of the Performance of Mixer Crystals, by P. D. Strum. 125. Design in Nature [for improved signal-to-noise ratio] as Exploited by the Communication Engineer, by L. A. de Rosa. 128. Signal-to-Noise Improvements through Integration in a Storage Tube, by J. V. Harrington and T. F. Rogers. 129. Theory of Receiver Noise Figure, by L. J. Cutrona. Titles of other papers are given in other sections.

621.396.621 1770
Panoramic Reception—S. A. W. Jolliffe and

J. D. Peat. (*Marconi Rev.*, vol. 12, pp. 27–33; January to March, 1949.) General design considerations are discussed and a panoramic adaptor for the Type CR. 100 communications receiver is described in detail.

621.396.621 1771

The Marconi Single Sideband Receiver Type CRD.150/20B-SSR-2.—C. P. Beanland. (*Marconi Rev.*, vol. 12, pp. 21–26; January to March, 1949.) Advantages of single-sideband working for short-wave radio links are discussed. The receiver is adapted for single-sideband working from a basic receiver unit Type CRD.150/20B which by itself is a triple-diversity commercial telephony receiver.

621.396.621:621.396.619.13 1772

The Demodulation of a F.M. Carrier and Random Noise by a Limiter and Discriminator—N. M. Blachman. (*Jour. Appl. Phys.*, vol. 20, pp. 38–47; January, 1949.) Analysis based on the statistics of random noise. When the degree of limiting is large, as the input signal-to-noise ratio s_1 increases from 0 to 6 db, the output signal-to-noise ratio increases sharply from a value far below s_1 to a value only 0.9 db below. As the limiting action is reduced, so the ratio of output versus input signal-to-noise ratio tends to increase to the values obtained with square-law detection of a carrier with 100 per cent AM.

621.396.621.53 1773

On the Mixing Properties of Non-Linear Condensers—A. van der Ziel. (*Jour. Appl. Phys.*, vol. 19, pp. 999–1006; November, 1948.) If the charge and voltage are assumed to be related by the equation

$$Q=\alpha_0 V+\alpha_1 V^2+\alpha_2 V^3+\cdots,$$

it is shown that the conversion transconductance is imaginary and the input and output impedances are capacitive. If the mixing oscillator frequency f_m is lower than the signal frequency f_i, the power gain is less than unity; if $f_m>f_i$, oscillations may occur; and if the if is f_m+f_i, frequency instability may result. Bandwidth and noise factor are discussed, and a few supporting experiments described. A brief comparison with Pound's work (2609 of 1948) on diodes is given.

621.396.622+621.315.59+621.314.6+621.383 1774

German Research on Semi-Conductors, Metal Rectifiers, Detectors and Photocells [Book Notice]—(*See* 1700.)

621.396.622.71 1775

A Study of the Operating Characteristics of the Radio Detector and its Place in Radio History—E. H. Armstrong. (*Proc. Radio Club Amer.*, vol. 25, no. 3, pp. 3–20; 1948.) An experimental investigation of the FM ratio detector, with circuit diagrams and oscillograms. See also 2346 of 1948 (Seeley) and back references.

621.396.822 1776

Some Notes on Noise Figures—H. Goldberg. (Proc. I.R.E., vol. 37, p. 40; January, 1949.) Corrections to 505 of March.

621.396.822:621.318.572 1777

Spurious Signals Caused by Noise in Triggered Circuits—D. Middleton. (*Jour. Appl. Phys.*, vol. 19, pp. 817–830; September, 1948.) The expected number of spurious peaks per second, caused by noise or by a triggering pulse in the presence of noise, above a given triggering level, is calculated. The effects of bandwidth, pulse shape, filter response-curve shape, and rectification are considered. Significantly improved rejection of spurious peaks by a circuit follows only when the maximum tolerable number of triggering peaks is of the same order of magnitude as the noise bandwidth. Results are summarized in tables and curves.

621.396.822:621.396.619.16 1778

Noise in a Pulse-Frequency-Modulation System—F. L. H. M. Stumpers. (*Philips Res. Rep.*, vol. 3, pp. 241–254; August, 1948.) The optimum filter for pulse-frequency modulation is derived for any given pulse form and large signal-to-noise ratio. For some special pulse forms, the signal-to-noise ratio is calculated and normal FM is shown to give a better result. A method of calculating the noise spectrum is given; it is valid for all signal-to-noise ratios but is intricate. The noise threshold is estimated and the suppression of the modulation by noise is considered.

621.396.823 1779

Radiation from Car Ignition Systems—B. G. Pressey and G. E. Ashwell. (*Wireless Eng.* vol. 26, pp. 31–36; January, 1949.) Field strength measurements on a typical car ignition system were made with a set having a bandwidth of 2.5 Mc and a cathode-ray indicator. The general level of the field was maintained throughout the frequency range of 40 to 650 Mc and its value was about 10 millivolts per meter at a distance of 9 meters, for either vertical or horizontal polarization. The effect of two resistive suppressor systems was examined; suppression ratios of the order of 20 db were obtained.

621.396.823:537.523.3 1780

Radio Influence from High-Voltage Corona—G. R. Slemon. (*Elec. Eng.*, vol. 68, pp. 139–143; February, 1949.) Experiments were conducted using a single conductor at high voltage mounted parallel to an earthed plane. Experimental verification of Peek's formula for corona threshold voltage was obtained. Noise threshold was independent of frequency, though increase of frequency produced increased noise. Noise from a smooth conductor was produced only during negative peaks of the applied ac voltage. Weathering and conductor-contamination usually reduced noise considerably, indicating a possible method of controlling corona interference. Water on the conductor caused severe noise with positive dc, but eliminated noise with negative dc. In all cases, the initiation of audible sound and light radiation was coincident with that of radio noise.

621.396.828 1781

The Measurement and Suppression of Radio Interference—J. H. Evans. (*Jour. Brit. I.R.E.*, vol. 9, pp. 46–59; February, 1949.) A survey of the nature of interference and the principles of its measurement, with particular reference to mains-borne noise and domestic appliances. A comprehensive measuring set and a simpler version for factory use are briefly described. Methods of suppression and the difficulties of application are discussed. The recommended limits of interference are considered and some of the anomalies arising from the specification of such limits are indicated.

621.396.828 1782

Heterodyne Eliminator—J. L. A. McLaughlin. (*Electronics*, vol. 22, pp. 83–85; March, 1949.) For high attenuation of interference at frequencies close to that of a continuous-wave or modulated carrier. There is no loss in transmitted intelligence.

STATIONS AND COMMUNICATION SYSTEMS

621.39:665.5 1783

Telecommunications in the Petroleum Industry—Z. Friedberg. (*Jour. Inst. Petroleum*, vol. 34, pp. 309–330; May, 1948.) A general description of systems used by oil companies. The basic principles essential for securing reliable communications under the conditions encountered are outlined.

621.39.001.11:621.396.822 1784

Communication in the Presence of Noise—Shannon. (*See* 1649.)

621.396 1

1949 IRE National Convention Progra
(Proc. I.R.E., vol. 37, pp. 160–178; Febru
1949.) Abstracts are given of the following
pers read at the convention:—1. Developr
of a High-Speed Communication System
D. S. Bond. 2. Distortion in a Pulse-Co
Modulation System with Nonuniform Spa
of Levels, by P. F. Panter and W. Dite. 3. C
Talk Considerations in Time-Division M
plex, by S. Moskowitz, L. Diven, and L. I
4. Experimental Verification of Various
tems of Multiplex Transmission, by D.
Crosby. 5. Interference Characteristics
Pulse-Time Modulation, by E. R. Kretzme
Factors Involved in the Design of an Impro
Frequency-Shift Receiving System [for N
facsimile], by C. C. Rae. 67. Television
Pulse-Code Modulation, by W. M. Goo
110. A Microwave System for Television
laying, by J. Z. Millar and W. B. Sullinger.
Intercity Television Radio Relays, by W.
Forster. 113. Video Design Considerations
Television Link, by M. Silver, H. French,
L. Staschover. 114. Six-Channel Urban Mc
System with 60-kc Spacing, by R. C. Sl
P. V. Dimock, W. Strack, and W. C. Hur
117. Theoretical Aspects of Nonsynchror
Multiplex Systems, by W. D. White. 126.
perimental Determination of Correlation Fu
tions and the Application of these Function
the Statistical Theory of Communications,
T. P. Cheatham, Jr. 127. The Transmissio
Information through Band-Limited Transı
sion Systems, by W. P. Boothroyd and E.
Creamer, Jr. Titles of other papers are give
other sections.

621.396.61/.62 1

Modifying the T.R.1143 for Amateur Us
G. L. Benbow. (*RSGB Bull.*, vol. 24, pp. 85–
October, 1948.) The T.R. 1143 covers frequ
cies from 100 to 125 Mc and is obtainable un
the Ministry of Supply disposals scheme. I
circuit details for the conversion are given, v
practical notes.

621.396.61/.62:534.86:621.395.623.7 1

Fundamental Electroacoustic Principles the Transmission of a Wide Band of Au Frequencies—W. Furrer, A. Lauber, and Werner. (*Tech. Mitt. Schweiz. Telegr.-Tele Verw.*, vol. 27, pp. 3–14; February 1, 1949. French and German.) Microphones, amplifi transmitter and receiver circuits, and the acc tic properties of studios are today all capabl meeting requirements for an af band extend up to about 15 kc. The outstanding problen that of loudspeakers, which are particula considered here. Some types of combinat coaxial loudspeakers give satisfactory resu For high-fidelity ultra-short-wave reception,s cial loudspeakers appear indispensable, eve this does increase the cost considerably.

621.396.619.16 1

Timing Control for PCM—A. E. Johans (*Bell. Lab. Rec.*, vol. 27, pp. 10–15; Janua 1949.) A detailed explanation, with block a wave-form diagrams.

621.396.619.16 1

The Spectrum of Modulated Pulses—Fitch. (*Proc. IEE* (London), part III, vol. p. 24; January, 1949.) Discussion on 2619 1948. See also 3752 of 1946 (Gladwin).

621.396.619.16:621.396.41 1

Multiplex Employing Pulse-Time a Pulsed-Frequency Modulation—H. Goldbe and C. C. Bath. (Proc. I.R.E., vol. 37, pp. 2 28; January, 1949.) Pulsed time-division tra mission channels may be effectively doubled number by adding FM bursts on the puls microwave carrier. Experimental studies in cate that crosstalk on either channel may kept 60 db below maximum output, in t worst case of a single pulse-time channel. E

imental transmitter and receiver circuits wave forms are described and illustrated.

.396.619.16:621.396.41:621.316.729 1791
Synchronization for the PCM Receiver—nley. (*See* 1768.)

.396.65:621.396.932 1792
The Great Lakes Radiotelephone System—H. Herrick. (*Elec. Eng.*, vol. 68, pp. 152–; February, 1949.) Description of the ship shore equipment and services provided. See 2432 of 1947.

.396.65.029.64 1793
A Broad-Band Microwave Relay System ween New York and Boston—G. N. Thayer, A. Roetken, R. W. Friis, and A. L. Durkee. oc. I.R.E., vol. 37, pp. 183–188; February, 9.) See 2920 of 1948 (Chaffee) and back refices.

.396.712 1794
The Skeleton Short-Wave Transmitting tion of the British Broadcasting Corporation *Engineering* (London), vol. 167, pp. 7–9 and 33; January 7 and 14, 1949.) A fuller acnt than that noted in 3521 of 1948.

.396.712.3+621.397.7 1795
Planning Radio and Television Studios—M. Nixon. (*Broadcast News*, pp. 58–69; Deber, 1948.) General discussion of requireits of space, shape, noise prevention, con- arrangements, etc.

.396.72 1796
Headquarters' Station GB1RS—(*RSGB L.*, vol. 24, pp. 26–27; August, 1948.) A short cription of the equipment, which is crystaltrolled on a frequency of 3,500.25 kc. This uency and its harmonics provide a series of its below which an amateur transmitter in 3. 5-, 7-, 14-, or 28-Mc bands cannot be cored "safely inside." Transmission, lasting a minutes, are made each hour from 0600 to 0G.M.T. (or B.S.T. if in force) in Morse code 2 words per minute.

.396.931 1797
V.H.F. Radio Equipment for Mobile Serv—D. H. Hughes. (*Jour. Brit. I.R.E.*, vol. p. 30–44; January, 1949.) The advantages he frequency band 30 to 180 Mc for local io-telephone services to vehicles and the ning of such systems are reviewed. The de of suitable transmitters and receivers for mobile and fixed stations is illustrated by a cription of a particular type of equipment. ure trends in development are discussed.

.396.932 1798
Single Sideband Radio-Telephony—D. B. Kirby. (*Wireless World*, vol. 55, pp. 91; March, 1949.) An outline of single-sided working is given, together with the block gram of a 300-watt transmitter installed on liner Caronia. Two af signals, together the output of a 100-kc oscillator, are fed balanced modulators. Crystal filters select upper sideband from one and the lower sided from the other. These are mixed with a tly reduced carrier and applied with the put of a 3-Mc oscillator to another balanced ulator. A 3.1-Mc filter selects the upper ulation product, which is mixed with a vari- frequency (7 to 19 Mc) to give the signal uency (4 to 22 Mc). See also *Engineer* (Lon-), vol. 187, p. 145; February 4, 1949.

.396.932 1799
Caronia Radio Equipment—(*Wireless World*, 55, pp. 91–92; March, 1949.) A few details he various telegraphy, telephony, direction ers, and radar sets installed in SS. Caronia.

SUBSIDIARY APPARATUS

-526+621.316.7+621.396.68 1800
1949 IRE National Convention Program—(Proc. I.R.E., vol. 37, pp. 160–178; February, 1949.) Abstracts are given of the following papers read at the convention:—36. Photographic Techniques in Cathode-Ray Oscillography, by C. Berkley and H. Mansberg. 60. High-Voltage Supplies for Radiation-Measuring Equipment, by R. Weissman and S. Fox. 72. Improved Degenerative Regulators, by Y. P. Yu. Titles of other papers are given in other sections.

621-526:629.13.014.57 1801
Automatic Pilots—Owen. (*See* 1680.)

621.313.12:538.652:534.232 1802
Magnetostriction Generators—J. A. Osborn. (*Elec. Eng.*, vol. 67, pp. 571–578; June, 1948.) A survey of fundamental magnetostriction phenomena and their application to the conversion of mechanical to electrical energy, and vice versa.

621.313.3:629.135 1803
A Rectified A.C. Electric System for Aircraft—L. M. Cobb, W. L. Kershaw, and Q. E. Erlandson. (*Elec. Eng.*, vol. 68, pp. 95–101; February, 1949.) A system using four 30-volt 3-phase engine-driven alternators, each output being rectified by means of a Se rectifier to 28 volts dc and connected to a common bus-bar. Two 34-ampere hour batteries provide initial field excitation and are permanently connected in parallel with the supply. Each rectifier, with suitable cooling arrangements, can supply 400 amperes. An estimated over-all efficiency of 72 per cent is obtained.

621.316.722 1804
Some Characteristics of Glow-Discharge Voltage Regulator Tubes—E. W. Titterton. (*Jour. Sci. Instr.*, vol. 26, pp. 33–36; February, 1949.) Measurements of samples of different tube types indicate that (a) the static characteristics show negative resistance discontinuities, (b) hysteresis voltage effects occur under dynamic conditions, and (c) characteristics of tubes of the same type differ widely. The input voltage with series resistor is calculated in terms of the load current and the permissible tube current.

621.316.722.1:621.385.833 1805
Stabilization of the Accelerating Voltage in an Electron Microscope—A. C. van Dorsten. (*Philips Tech. Rev.*, vol. 10, pp. 135–140; November, 1948.) Two regulating tubes are used in a feedback circuit to keep the voltage constant within 0.02 per cent for at least 30 seconds at any level between 50 and 150 kv.

621.362 1806
Thermoelectric Generator Designs—G. B. Ellis. (*Elec. Eng.*, vol. 67, pp. 657–660; July, 1948.) Theoretical and practical aspects of the design of thermocouples as sources of power are discussed and the required magnitude of some of the thermal and electrical characteristics is indicated. No efficient thermocouple has yet been developed; the best approach may be in the field of semiconductors. Characteristics of some materials are given.

621.396.68 1807
Some Additions to the Theory of Radio-Frequency High-Voltage Supplies—G. W. C. Mathers. (Proc. I.R.E., vol. 37, pp. 199–206; February, 1949.) The double-tuned overcoupled air transformer is represented by an equivalent primary circuit, which is used to develop the theory of the oscillator, including the two possible operating frequencies, the necessary conditions for oscillation and maximum efficiency, and the variation of operating frequency and load resistance with primary tuning. At the operating frequency, the load impedance is purely resistive. The various resistances in the circuit representing the power losses and the load resistance are included in the equivalent circuit resistance, which appears as the anode load of the class-C oscillator tube. Methods of designing a circuit to give any required power and voltage output are discussed.

621.396.68:621.397.62:535.88 1808
Projection-Television Receiver: Part 3—The 25-kV Anode Voltage Supply Unit—G. J. Siezen and F. Kerkhof. (*Philips Tech. Rev.*, vol. 10, pp. 125–134; November, 1948) Part 1: 1215 of May. Part 2: 1836 below. For another account see 2387 of 1948.

621.314.6+621.315.59+621.396.622+621.383 1809
German Research on Semi-Conductors, Metal Rectifiers, Detectors and Photocells [Book Notice]—(*See* 1700.)

TELEVISION AND PHOTOTELEGRAPHY

621.397 1810
1949 IRE National Convention Program—(Proc. I.R.E., vol. 37, pp. 160–178; February, 1949.) Abstracts are given of the following papers read at the convention:—6. Factors involved in the Design of an Improved Frequency-Shift Receiving System [for Naval facsimile] by C. C. Rae. 20. The Technique of Television Sound, by R. H. Tanner. 42. VHF Television—Propagation Aspects, by E. W. Allen, Jr. 64. A Method of Multiple Operation of Transmitter Tubes particularly adapted for Television Transmission in the UHF Band, by G. H. Brown, W. C. Morrison, W. L. Behrend, and J. G. Reddeck. 65. Transient-Response Tests on the WPTZ Television Transmitter, by R. C. Moore. 66. Television Transmitter Carrier Synchronization, by R. D. Kell. 67. Television by Pulse-Code Modulation, by W. M. Goodall. 83. The Measurement of the Modulation Depth of Television Signals, by R. P. Burr. 84. Development and Performance of Television Camera Tubes, by R. P. Janes, R. E. Johnson, and R. S. Moore, 85. An Anastigmatic Yoke for Television Deflection, by K. Schlesinger. 86. A High-Efficiency Sweep Circuit, by B. M. Oliver. 87. Current Developments in UHF Television, by T. T. Goldsmith, Jr. 112. Intercity Television Radio Relays, by W. H. Forster. 113. Video Design Considerations in a Television Link, by M. Silver, H. French, and L. Staschover. 140. The Graphechon—A Picture-Storage Tube, by L. Pensak. Titles of other papers are given in other sections.

621.397.62 1811
Superheterodyne Television Unit—(*Wireless World*, vol. 55, pp. 97–102; March, 1949.) Continuation of 1527 of June. Mechanical details and alignment are discussed.

621.397.62:535.88:621.385.832 1812
Projection-Television Receiver: Part 2—The Cathode-Ray Tube—de Gier. (*See* 1836.)

621.397.62:535.88:621.396.68 1813
Projection-Television Receiver: Part 3—The 25-kV Anode Voltage Supply Unit—Siezen and Kerkhof. (*See* 1808.)

621.397.62:656.22 1814
Train Television—F. R. Norton, C. G. McMullen, and G. L. Haugen. (*Electronics*, vol. 22, pp. 100–101; March, 1949.) Two sizes of folded dipole, with ends bent back, are used. This arrangement is more satisfactory than ring antennas. A normal type of 12-channel receiver has a special double-clamp agc circuit which improves synchronization considerably. Power-supply difficulties are mentioned.

621.397.645 1815
On the Design of Television Intermediate-Frequency Amplifiers—Sokolov. (*See* 1635.)

621.397.7+621.396.712.3 1816
Planning Radio and Television Studios—Nixon. (*See* 1795.)

621.397.7 1817
Practical Equipment Layouts for Television Stations—(*Broadcast News*, pp. 12–39; December, 1948.) Illustrated discussion of the requirements for stations of various types.

621.397.743:621.315.212 1818
Coaxial Cable Joins East and Mid-West TV Networks—Hertzberg. (*See* 1581.)

621.397.5 1819
Six Papers on Television (Translation) [Book Notice]—F.I.A.T. Final Report 865 (Supplement). H.M. Stationery Office, London, 74 pp., 7s. The papers are entitled: 1. New Scanning Method for Television. 2. Phase Modulation for Television. 3. Channeling by Time Division on a Wide-Band Carrier. 4. Apartment-House Television Distribution. 5. Code-Modulated Telephony. 6. Multiplex Code-Modulated Telephony. All these papers are by F. Schröter; they are preceded by a preface briefly describing recent advances in television techniques.

TRANSMISSION

621.396.61 1820
Broadcasting Transmitters at Villebon, Rennes and Lille—H. Campet. (*Ann. Radioélec.*, vol. 4, pp. 85–88; January, 1949.) The amplitude versus phase method of modulation used in these three reconditioned stations is described and performance figures for the Lille transmitter are given.

621.396.61 1821
Daily Routine of the Sottens [broadcasting] Transmitter—R. Pièce. (*Bull. Schweiz. Elektrotech. Ver.*, vol. 37, pp. 31–39; January 26, 1946. In French.) A short description of the quartz-controlled 100-kw 677-kc equipment with an outline of the functions of the staff and discussion of service faults due to external and internal causes.

621.396.619 1822
1949 IRE National Convention Program—(Proc. I.R.E., vol. 37, pp. 160–178; February, 1949.) Abstracts are given of papers read at the convention, including:—111. Synchrodyne Modulation of Klystrons, by V. Learned. Titles of other papers are given in other sections.

621.396.619.13 1823
Impedance Valves for Frequency Modulation—H. Klauser. (*Bull. Schweiz. Elektrotech. Ver.*, vol. 37, pp. 624–627; October 19, 1946. In German, with French summary.) The mode of operation of such devices, particularly for FM of transmitters, is explained and equivalent circuits are discussed, two of which give controllable capacitance and two controllable inductance, one of each pair being loss free. The conditions for distortionless modulation are considered for both capacitive and inductive impedance tubes. For a given frequency, it is possible, under certain conditions, to suppress the AM which is produced together with the FM.

VACUUM TUBES AND THERMIONICS

621.385+621.396.615 1824
1949 IRE National Convention Program—(Proc. I.R.E., vol. 37, pp. 160–178; February, 1949.) Abstracts are given of the following papers read at the convention:—10. A Broad-Band Transition from Coax to Helix, by C. O. Lund. 55. The Type 5811 and Type 5807 Tubes—the Smallest Commercial Pentode Amplifiers by L. G. Hector and H. R. Jacobus. 58. Electrometer Tubes and Circuits, by H. F. Starke. 78. Microphonism Investigation, by L. Feinstein. 79. A Critical Survey of Methods of Making Ceramic-to-Metal Seals and Their Use for Electron-Tube Construction, by R. P. Wellinger. 80. Rugged Tubes, by G. W. Baker. 81. An Improved Method of Testing for Residual Gas in Electron Tubes and Vacuum Systems, by E. W. Herold. 82. Design Factors, Processes, and Materials for the Envelope of a Metal Kinescope, by R. D. Faulkner and J. C. Turnbull. 105. The Effects of Various Barium Compounds with respect to Cold-Cathode Behavior as a function of Life in a Glow Discharge, by H. Jacobs and A. P. LaRocque. 106. Oxide-Cathode Properties and their Effects on Diode Operation at Small Signals, by G. C. Dalman. 107. Microanalysis of Gas in Cathode-Coating Assemblies, by H. Jacobs and B. Wolk. 108. Exposure of Secondary-Electron-Emitting Surfaces to the Evaporation from Oxide Cathodes, by C. W. Mueller. 109. The Use of Thoriated-Tungsten Filaments in High-Power Transmitting Tubes, by R. B. Ayer. 120. General Solution of the Two-Beam Electron Wave-Tube Equation, by A. V. Haeff, H. D. Arnett, and W. Stein. 124. Space-Charge Effects and Frequency Characteristics of CW Magnetrons relative to the problem of Frequency Modulation by H. W. Welch, Jr. 140. The Graphechon—A Picture-Storage Tube, by L. Pensak. 141. The Pencil-Type UHF Triode, by G. M. Rose and D. W. Power. 142. Practical Applications of the Resnatron in the High-Power Transmitter Field, by W. W. Salisbury. 143. The Electron Coupler—A Developmental Tube, Utilizing New Principles, for the Modulation and Control of Power at UHF, by C. L. Cuccia and J. S. Donal, Jr. 144. A Wide-Tuning-Range Low-Power CW Magnetron, by L. R. Bloom and W. W. Cannon. Titles of other papers are given in other sections.

621.385 1825
The Electron-Wave Tube—A Novel Method of Generation and Amplification of Microwave Energy—A. V. Haeff. (Proc. I.R.E., vol. 37, pp. 4–10; January, 1949.) Beams of electrons moving with different mean velocities are allowed to mix. Interchange of energy takes place, resulting in negative attenuation characteristics. Oscillators and amplifiers for microwave frequencies may thus be constructed without resonant structures of small dimensions.

The paper gives a mathematical analysis of the two-velocity case, and indicates how to extend the results to multiple and continuous velocity distributions. It is shown that amplification is obtained for a limited range of values of stream inhomogeneity.

Experimental tubes of two-velocity and space-charge types are described. A comparison of experimental and theoretical gain curves shows good agreement. Gains of the order of 80 db at 3,000 Mc and electronic bandwidths of over 30 per cent have been observed. The new method is likely to have important applications to tubes for millimeter waves. See also 1540 of June (Nergaard).

621.385 1826
The Development and Design of Cooled-Anode Valves—F. Smith. (*Proc. IEE* (London), part III, vol. 96, pp. 1–4; January, 1949.) Long summary of Radio Section Chairman's address.

621.385 1827
Trends in Electron Tube Design—W. C. White. (*Elec. Eng.*, vol. 67, pp. 517–530; June, 1948.) A comprehensive survey of modern practices and developments in the construction of all types of tube.

621.385:621.392.2 1828
Study of the Propagation of an Electromagnetic Wave in the Presence of Two Electron Beams of Neighbouring Velocities—Lapostolle. (*See* 1583.)

621.385:666.11:621.3.011 1829
Contribution to the Study of the Electrical Properties of Glasses used in the Constructi of Radio Valves—Meunier. (*See* 1699.)

621.385.029.63/.64:621.396.615 18
Traveling-Wave Valves as Oscillators w Wide-Band Electronic Tuning—O. Doehl W. Kleen, and P. Palluel. (*Ann. Radioélc* vol. 4, pp. 68–75; January, 1949.) Self-oscil tion due to internal feedback is discussed. F tubes in which the delay line gives an attenu tion sufficient to suppress all possibility of ternal feedback, external feedback may be a plied by means of a waveguide coupling t tube output to the input. In this case, the tu ing band is about double that obtained w internal feedback and may be of the order 10 per cent for a frequency of 3,000 Mc and per cent for 24,000 Mc. For traveling-wa tubes with a central conductor provided witl system of equidistant circular fins, and in whi the electron beam passes through the spa between the edges of the fins and the outer w of the tube, output power is high. At 3,000 this may be of the order of 20 watts, at 9,0 Mc about 1 to 2 watts, and at 24,000 Mc abo 0.1 to 0.2 watt.

621.385.032.24:621.396.645 18
Practical Notes on Grid Current and Ne tralization—F. Dickson. (*Philips Tech. Co mun.* (Australia), vol. 10, pp. 3–6; Septeml and October, 1948.)

621.385.2:621.396.822 18
The Behaviour of a Diode Noise Genera at Ultra High Frequencies—A. W. Love. (*Jo Inst. Eng.* (Australia), vol. 20, p. 201; Dece ber, 1948.) Discussion on 567 of March.

621.385.3.012 18
Factors Influencing the Perveance of Po er-Output Triodes—G. R. Partridge. (Pr I.R.E., vol. 37, pp. 87–94; January, 194 Perveance is a factor relating anode voltage a current. Several formulas for perveance and cathode current are listed and discussed.

621.385.38 18
A New Line of Thyratrons—A. W. Coolid Jr. (*Elec. Eng.*, vol. 67, p. 435; May, 194 Long summary of AIEE paper. Description the GL-5545 gasfilled thyratron, which claimed to have 10 times the life of other g filled thyratrons. The GL-5545 seldom requi a series *RC* circuit (snubber) for industrial a plications.

621.385.4.032.2 18
The Anode to Screen Grid Space in Bea Tetrode—Chai Yeh. (*Science Rec.* (Nankin vol. 2, pp. 57–62; October, 1947. In English

621.385.832:621.397.62:535.88 18
Projection-Television Receiver: Part 2 The Cathode-Ray Tube—J. de Gier. (*Philı Tech. Rev.*, vol. 10, pp. 97–104; October, 194 Part 1: 1215 of May. Part 3: 1808 above. F another account see 2387 of 1948.

621.383:621.315.59+621.314.6+621.396.622 18
German Research on Semi-Conducto Metal Rectifiers, Detectors and Photoce [Book Notice]—(*See* 1700.)

MISCELLANEOUS

621.396 18
Fundamentals of Electric Waves [Book R view]—H. H. Skilling. J. Wiley and Sons, N York: Chapman and Hall, London, 2nd editi 1948, 245 pp., $4.00. (*Jour. Frank. Inst.*, v 247, p. 80; January, 1949.) An elementary te on electromotive theory, illustrating its app cation to related items such as antennas a waveguides. Vector notation is explained a used. Considerable revision of the first editi (noted in 319 and 2027 of 1943) has taken pla